THE UNIVERSITY
of EDINBURGH

This thesis has been submitted in fulfilment of the requirements for a postgraduate degree (e.g. PhD, MPhil, DClinPsychol) at the University of Edinburgh. Please note the following terms and conditions of use:

This work is protected by copyright and other intellectual property rights, which are retained by the thesis author, unless otherwise stated.
A copy can be downloaded for personal non-commercial research or study, without prior permission or charge.
This thesis cannot be reproduced or quoted extensively from without first obtaining permission in writing from the author.
The content must not be changed in any way or sold commercially in any format or medium without the formal permission of the author.
When referring to this work, full bibliographic details including the author, title, awarding institution and date of the thesis must be given.

Programming of Cardiovascular Disease: An Exploration of Epigenetic Mechanisms

Catherine M. Rose

Thesis presented to The University of Edinburgh for the degree of Doctor of Philosophy

2015

Abstract

Fetal exposure to excess glucocorticoid is associated with low birth weight and increased cardiovascular disease risk in first generation offspring. Such phenotypes can be produced experimentally through the administration of the synthetic glucocorticoid dexamethasone (Dex) to pregnant rats during the last week of gestation. These 'programmed effects' can be transmitted to a second generation through both maternal and paternal lines. The overall hypothesis for this thesis was that the transmission of programmed effects through the male line may result from alterations in fetal germ cells, which form sperm in adulthood.

Epigenetic reprogramming of germ cells is characterised by the genome-wide erasure and subsequent re-establishment of 5-methylcytosine (5mC), however this process has not previously been described for the rat. Furthermore, the involvement of more recently identified cytosine modifications; 5-hydroxymethylcytosine (5hmC), 5-formylcytosine (5fC) and 5-carboxylcytosine (5caC), has not been characterised during germ cell ontogeny. Using immunofluorescence to study DNA modifications during late gestation I identified that 5hmC, 5fC and 5caC were present between e14.5 and e16.5 but absent thereafter. In contrast, 5mC was absent during this time but remethylation was noted from e19.5 onwards. Prenatal Dex exposure was associated with the presence of significantly more 5mC-positive germ cells at e19.5 relative to controls. This difference did not persist at e20.5 suggesting that Dex exposure promotes premature global remethylation. The mechanisms for this are unclear since there were no differences between groups in the localisation of the DNA methyltransferases DNMT3a and 3b, or in markers of normal testis maturation.

To enable the study of gene-specific changes in DNA methylation in the germline a colony of Germ Cell Specific-Enhanced Green Fluorescent Protein (GCS-EGFP) rats was established and characterised. GCS-EGFP rats had a transgenerational decrease in pup weight with Dex exposure, as in Wistar rats. The expression of both established and novel candidate genes was compared between strains. Multiple genes across different pathways had altered expression, with some affected in both Wistar and GCS-EGFP rats, whilst other differences were strain-specific. Enhanced

Reduced Representation Bisulfite Sequencing was performed on liver and fetal germ cells from males exposed to Dex *in utero* to explore effects on DNA methylation.

These studies confirm that epigenetic reprogramming occurs in the rat and that this process may be susceptible to modification by prenatal Dex exposure. GCS-EGFP rats also exhibited a Dex programming phenotype, with decreased pup weight and altered liver gene expression. The use of this unique strain of rats will permit dissection of the mechanisms for the transmission of programmed phenotypes across generations.

Table of Contents

Declaration of Authorship

I certify that this thesis is a result of my own work, and that the data it contains are my own, except where otherwise stated. This work has not been submitted for any other degree or professional qualification.

Catherine M. Rose, April 2015

Acknowledgements

There are many who have helped me greatly during my time at Edinburgh and to whom I now give very many thanks for what they have done:-

My primary supervisor Dr Mandy Drake for her help, encouragement and guidance during my PhD studies and whilst writing my thesis. Her enthusiasm for science and optimism in the face of setbacks was always evident. My second supervisor Prof Richard Meehan for his wisdom and oversight in my project, and his advice regarding my thesis. The British Heart Foundation for their excellent PhD programme, and generous funding of my research.

Some wonderful Post-Docs who have helped me throughout my studies. Dr Khulan Batbayar and Dr Jessy Cartier have provided lots of encouragement and advice during my time in Team Drake. Dr Sander van den Driesche has been invaluable in teaching me the art of microdissection and providing advice for the epigenetic reprogramming studies.

Prof Richard Sharpe and his lab group for generously allowing me to use their experimental tissues for one of my studies, and for teaching me everything I know about immunofluorescence, and in particular Sheila MacPherson for her patience and kindness, and Dr Tom Chambers, my epigenetics buddy.

The animal technicians, particularly the excellent Will Mungall for looking after my furry colleagues so well, and for going out of his way to help with my experiments. Dr Tom Smith (University of Oxford) for performing the bioinformatic analysis of sequencing data, and Dr Marcus Lyall for statistics advice.

MSc students Ashley Boyle and Marina Mitsikakou who worked hard and produced some lovely data - you were a pleasure to supervise! Everyone in Team Drake, both past and present, for all of their support, and for providing the most wonderful lab meeting cakes.

My fellow PhD students, in particular Barry, Charlotte, Cristina, Rachel, Mei and Holly for sharing this journey with me, feeding me chocolate and helping me to feel

better when things were hard. I have enjoyed all of our adventures, both here and abroad, and hope there will be many more to come!

My wonderful parents, and other students and members of staff not mentioned here have also supported me in diverse ways during my studies.

My thanks to you all, for all you have done to make this PhD possible.

Publications and Presentations

The following journal publications have resulted from the work of this thesis:

Rose CM, van den Driesche S, Sharpe RM, Meehan RR, Drake AJ (2014) Dynamic changes in DNA modification states during late gestation male germ line development in the rat. Epigenetics & Chromatin 7:1-15

Rose CM, van den Driesche S, Meehan RR, Drake AJ (2013) Epigenetic reprogramming: preparing the epigenome for the next generation. Biochem Soc Trans 41: 809-814

The following presentations were made of work contained within this thesis:

Rose CM, van den Driesche S, Boyle AK, Sharpe RM, Meehan RR, Drake AJ (2013) Glucocorticoid effects on germline epigenetic reprogramming in the rat – a mechanism for the transmission of programming effects across generations? 8th International Congress on the Developmental Origins of Health and Disease. ***Oral Presentation by Rose CM***. Singapore.

Rose CM, van den Driesche S, Boyle AK, Sharpe RM, Meehan RR, Drake AJ (2013) Glucocorticoid effects on germline epigenetic reprogramming in the rat – a mechanism for the transmission of programming effects across generations? Cardiovascular Science Symposium Day. ***Oral Presentation by Rose CM***. Edinburgh, UK.

Rose CM, van den Driesche S, Sharpe RM, Meehan RR, Drake AJ (2012) Investigating germ line epigenetic reprogramming in the rat. Biochemical Society Annual Symposium: Epigenetic Mechanisms in Development and Disease. ***Oral Presentation by Rose CM***. Leeds, UK.

Rose CM, van den Driesche S, Boyle AK, Chambers T, Sharpe RM, Meehan RR, Drake AJ (2014) Fetal glucocorticoid overexposure impacts on germline epigenetic reprogramming in the rat. European Society for Endocrinology Summer School. ***Poster Presentation by Rose CM***. Bregenz, Austria.

Rose CM, van den Driesche S, Boyle AK, Chambers T, Sharpe RM, Meehan RR, Drake AJ (2014) Fetal glucocorticoid overexposure impacts on germline epigenetic reprogramming in the rat. British Society for Endocrinology. ***Poster Presentation by Rose CM***. Liverpool, UK.

Rose CM, Boyle AK, van den Driesche S, Sharpe RM, Meehan RR, Drake AJ (2013) Germ line epigenetic reprogramming in the late gestation male rat. Scottish Society for Experimental Medicine. ***Poster Presentation by Rose CM***. Edinburgh, UK.

Rose CM, van den Driesche S, Boyle AK, Sharpe RM, Meehan RR, Drake AJ (2013) Altered germline epigenetic reprogramming in the rat: a mechanism for the intergenerational transmission of cardiovascular disease risk? British Heart Foundation: 3rd Fellows Meeting. ***Poster Presentation by Rose CM***. Cambridge, UK.

Rose CM, Boyle AK, van den Driesche S, Sharpe RM, Meehan RR, Drake AJ (2013) Germline epigenetic reprogramming in the rat and intergenerational cardiovascular disease transmission. British Heart Foundation PhD Programme Symposium. ***Poster Presentation by Rose CM***. Oxford, UK.

Abbreviations

11β-HSD	11β-hydroxysteroid dehydrogenase
5caC	5-carboxylcytosine
5fC	5-formylcytosine
5hmC	5-hydroxymethylcytosine
5hmU	5-hydroxymethyluracil
5mC	5-methylcytosine
ADH1	Alcohol Dehydrogenase 1
ADP	Adenosine Diphosphate
AGD	Ano-Genital-Distance
AID/APOBEC	Activation Induced Deaminase/ Apolipoprotein B mRNA Editing Enzyme, Catalytic Polypeptide-like
ANOVA	Analysis of Variance
ATP	Adenosine Triphosphate
AU	Arbitrary Units
BER	Base Excision Repair
BSA	Bovine Serum Albumin
CAP	Adenylate Cyclase-Associated Protein
CDK9	Cyclin-Dependent Kinase 9
CDKN1C	Cyclin-Dependent Kinase Inhibitor 1C
cDNA	Complementary DNA
CGAT	Computational Genomics Analysis and Training Programme

ChARP	Chicken anti-Rabbit Peroxidase
CIS	Carcinoma in-Situ
CpG	Cytosine-Phosphate-Guanine
CRH	Centre for Reproductive Health
CVS	Centre for Cardiovascular Science
DAB	Diaminobenzidine
DAPI	4',6-diamidino-2-phenylindole
DAZL	Deleted in Azoospermia-Like
DBP	Di(n-butyl) phthalate
Dex	Dexamethasone
DLK1/GTL2	Delta-like Homolog 1/ Gene Trap Locus 2
DMC	Differentially Methylated Cytosine
DMR	Differentially Methylated Region
DMRT1	Doublesex and Mab-3 Related Transcription Factor 1
DNA	Deoxyribonucleic Acid
DNMT	DNA Methyltransferase
DTT	Dithiothreitol
e	Embryonic Day
EDTA	Ethylenediaminetetraacetic Acid
EGFP	Enhanced Green Fluorescent Protein
ELISA	Enzyme-Linked Immunosorbent Assay
ERRBS	Enhanced Reduced Representation Bisulfite Sequencing

ERV	Endogenous Retrovirus
ES cell	Embryonic Stem Cell
F1	First Generation
F2	Second Generation
F3	Third Generation
FACS	Fluorescence-Activated Cell Sorting
FCS	Fetal Calf Serum
FISH	Fluorescent *in Situ* Hybridisation Analysis
FSH	Follicle-Stimulating Hormone
GAPDH	Glyceraldehyde 3-Phosphate Dehydrogenase
GARP	Goat anti-Rabbit Peroxidase-Conjugated Secondary Antibody
GCS-EGFP	Germ Cell Specific-Enhanced Green Fluorescent Protein
GDP	Guanosine Diphosphate
GLP	G9a-Like Protein
GR	Glucocorticoid Receptor
GRB10	Growth Factor Receptor-Bound Protein 10
GTP	Guanosine Triphosphate
GTPase	Guanosine Triphosphatase
GTT	Glucose Tolerance Test
H19	H19, Imprinted Maternally Expressed Transcript
HBSS	Hank's Balanced Salt Solution
HCl	Hydrochloric Acid

HDAC1	Histone Deacetylase Inhibitor 1
HMGB2	High Mobility Group Box 2
HPA	Hypothalamic-Pituitary-Adrenal
HPRT	Hypoxanthine-Guanine Phosphoribosyltransferase
HSP70	70kDa Heat Shock Protein
HSPA5	Heat Shock 70kDa Protein 5
IAP	Intracisternal A-Particle
IAPLTR1	Intracisternal A-particle Long Terminal Repeat 1
ICR	Imprinting Control Region
IGF	Insulin-Like Growth Factor
IGF2R	Insulin-Like Growth Factor 2 Receptor
IGFBP1	Insulin-Like Growth Factor Binding Protein 1
IL6	Interleukin 6
IRS1	Insulin Receptor Substrate 1
IUGR	Intra-Uterine Growth Restriction
IVF	*In Vitro* Fertilisation
LH	Luteinizing Hormone
LINE1	Long Interspersed Nuclear Element 1
LSD	Fisher's Least Significant Difference
LTR	Long-Terminal Repeat
LTR-ERV1	Long Terminal Repeat-Endogenous Retrovirus 1
MBD	Methyl-CpG Binding Domain Protein

MBD4	Methyl Binding Domain IV
MeCP2	Methyl-CpG-Binding Protein 2
MeDIP	Methylated DNA Immunoprecipitation
MEST	Mesoderm-Specific Transcript
Mili	Piwi-like RNA-mediated Gene Silencing 2
MINT	Msx2-Interacting Nuclear Target
miRNA	Micro RNA
MR	Mineralocorticoid Receptor
mRNA	Messenger RNA
MSP1	Microsomal Serine Proteinase 1
mTOR	Mammalian Target of Rapamycin
NaCl	Sodium Chloride
NAD	Nicotinamide Adenine Dinucleotide (oxidised)
NADH	Nicotinamide Adenine Dinucleotide (reduced)
NChS	Normal Chicken Serum
ncRNA	Non-coding RNA
NGS	Normal Goat Serum
NHS	Normal Horse Serum
NP95	Nuclear Protein 95
NRS	Normal Rabbit Serum
NTC	No-template Control
PBS	Phosphate Buffered Saline

PCR	Polymerase Chain Reaction
PDIA6	Protein Disulphide Isomerase Family A Member 6
PEPCK	Phosphoenolpyruvate Carboxykinase
PER1	Period Circadian Clock 1
PER3	Period Circadian Clock 3
PGC	Primordial Germ Cell
PI	Propidium Iodide
PND	Postnatal Day
PPIA	Peptidylprolyl Isomerase A
PRAME	Preferentially Expressed Antigen in Melanoma
PRAMEL1	Preferentially Expressed Antigen in Melanoma-like 1
qPCR	Quantitative Polymerase Chain Reaction
RAChP	Rabbit anti-Chicken Peroxidase-Conjugated Antibody
RALGAPB	Ral Guanosine Triphosphatase Activating Protein, Beta Subunit
RAS	Renin-Angiotensin System
RASGRF1	Ras Protein-Specific Guanine Nucleotide-Releasing Factor 1
RNA	Ribonucleic Acid
RPS6	Ribosomal Protein Serine 6
RPS6K1	Ribosomal Protein Serine 6 Kinase 1
RPS6K2	Ribosomal Protein Serine 6 Kinase 2
RRBS	Reduced Representation Bisulfite Sequencing
SDS	Sodium Dodecyl Sulfate

SINE	Short Interspersed Nuclear Element
SMUG1	Single-Strand Selective Monofunctional Uracil DNA Glycosylase
SMYD2	SET and MYND Domain-containing 2
sncRNA	Small Non-Coding RNA
SNRPN	Small Nuclear Ribonucleoprotein Polypeptide N
SOX9	SRY-Box 9
SPEN	Split Ends Family Transcriptional Repressor
SRY	Sex-Determining Region Y
SURF	Shared University Research Facilities
TBE	Tris-Borate-EDTA
TBP	TATA-Box Binding Protein
TBS	Tris Buffered Saline
TDG	Thymine DNA Glycosylase
TE	Tris/EDTA
TET	Ten-Eleven-Translocase
TEX19.1	Testis Expressed 19.1
TNFα	Tumour Necrosis Factor Alpha
TPT1	Tumour Protein, Translationally Controlled 1
TSS	Transcription Start Sites
UPL	Universal Probe Library
WTC	World Trade Centre

Xa	Active X Chromosome
Xi	Inactive X Chromosome
ZFP57	Zinc Finger Protein 57 Homolog
ZFP57/KAP1	Zinc Finger Protein 57/ Krüppel Associated Box-Associated Protein 1

Chapter 1 Introduction

Cardiovascular disease has a significant impact on the health and economy of society, and is the predominant cause of mortality within Europe [1]. It is therefore important to investigate the factors which might predispose an individual to this condition. Fetal programming is the concept that a change in the environment *in utero* can alter tissue structure and function, and lead to an increased risk of disease [2,3]. Evidence for programming has come from a range of epidemiological studies, exploring, for example, the relationships between maternal diet or stress levels in pregnancy with offspring birth weight and subsequent cardiovascular disease risk [2,4-7]. Such studies will be explored in depth later in this thesis, but characteristically indicate that an altered *in utero* environment correlates with a decrease in birth weight, and alteration of metabolic parameters, such as glucose intolerance, and increased blood pressure [2,4-7]. Laboratory models have been developed to investigate this phenomenon further, in a more controlled environment. Models of both undernutrition and over-exposure to glucocorticoids (a class of steroid hormones that bind to the Glucocorticoid Receptor (GR), present in almost every vertebrate animal cell) during pregnancy have been shown to correlate with low birth weight and increased cardiometabolic disease risk in offspring [8-10]. Intriguingly, these phenotypes can be transmitted to a subsequent generation without further intervention [10,11].

In our research group, the synthetic glucocorticoid Dexamethasone (Dex) is administered to pregnant Wistar rats during mid-late gestation, to generate a model of fetal programming. Their offspring have a lower birth weight and altered cardiometabolic parameters, and these effects are also seen in a subsequent generation [8,12]. The effects of Dex exposure have been extensively characterised in previous studies [8,10,12], however the mechanism of transmission across generations remains elusive. In investigating potential pathways for transmission, it should be considered that the Dex-programming phenotype can be evoked in a second (F2), but not third (F3) generation without further intervention. It can also be transmitted through both the maternal and the paternal lines [10]. As the father is not present with the mother or pups after fertilisation, we hypothesise that the

information for the transmission of the programming phenotype may be carried in his sperm.

During the period of Dex exposure, the fetal germ cells are present, and therefore potentially susceptible to effects of treatment. These stem cells form the progenitors of the spermatogenic pathway in the adult [13]. Therefore, we hypothesise that if these germ cells are affected by Dex exposure during their time *in utero*, this could give alterations in the sperm produced in adulthood, ultimately carrying an epi-phenotype to the next generation.

One mechanism by which this phenotype could be carried is through changes in epigenetic regulation. This confers a change in phenotype, without a permanent mutation of genotype, and this hypothesis is compatible with the observation that the effects of Dex-programming can be transmitted to a second, but not third generation [12]. DNA methylation has been shown to undergo dramatic genome-wide reprogramming during the development of the mouse fetal germ cell [14], and so we hypothesised that this process might be susceptible to alteration by Dex exposure. Thus, changes in DNA methylation might either carry the phenotype of increased cardiovascular risk to the next generation or be an indirect read-out of the transmissible agent.

1.1 Fetal Programming

A correlation between the prenatal environment and a predisposition to future cardiovascular disease was initially described with respect to low birth weight [2,3]. Lower birth weight was seen to be inversely proportional to systolic blood pressure and death rates from cardiovascular disease in adulthood [2,15]. This association has been found to be independent of factors such as smoking and alcohol consumption, and is identified within the normal range of birth weights [2,15]. It has therefore been suggested that in addition to genetic effects on growth and disease risk, the developing fetus may be permanently ‘programmed’ by the intrauterine environment for a specific adult phenotype [3,16]. In this way, the mother may transmit information about the external world to her unborn child, preparing it for the environment into which it will be born. This could be beneficial, for example, in

preparing offspring to cope with famine, yet if these cues are incorrect, or the external environment alters during the lifespan of the offspring, this may leave them physiologically less adapted for their surroundings, and therefore at greater risk of developing conditions such as cardiovascular disease [17]. Two main environmental factors have been proposed to induce fetal programming: fetal undernutrition; and exposure to glucocorticoid excess [4,8,10].

1.1.1 Nutrition and Fetal Programming

The effects of maternal undernutrition became apparent following the 'Dutch Hunger Winter' of 1944-1945. During this time, residents of the Western Netherlands experienced acute famine for a short period during World War Two. Later, research revealed that women who were pregnant during this time had babies with a lower birth weight and a greater risk of glucose intolerance, insulin resistance, obesity and cardiovascular disease in adulthood [4,5,18,19]. The exact outcome was shown to be dependent on the stage of gestation when exposure occurred [7,20].

Similarly, maternal obesity or over-nutrition has been shown to produce programming in offspring [21,22] It could be suggested that such an association simply reflects a transmission of genetic disposition between mother and child. However, in mothers that gained weight between pregnancies, the risk of having a baby that was large for gestational age was increased [23]. Conversely, offspring born to mothers after anti-obesity surgery had improved cardiometabolic parameters compared to siblings born before maternal weight loss [24].

An examination of the direct effects of maternal nutrition has also been achieved through animal studies. Maternal dietary restriction has been shown to produce offspring with lower birth weight, glucose intolerance, and cardiovascular dysfunction [9,25,26]. These phenotypes may also be transmitted to a second generation without further intervention [11]. Similar phenotypes were exhibited with maternal low-protein [27-30] or high-fat [31,32] diet in pregnancy. Intriguingly, offspring were reported to have increased preference for a high-fat diet following

either protein restriction or nutrient excess *in utero* [33-35], perpetuating a disposition to cardiometabolic disease.

1.1.2 Glucocorticoid Programming

A second potential stimulus for fetal programming is excessive exposure to glucocorticoids. These steroid hormones are crucial regulators of a diverse range of physiological pathways, including the stress response, metabolic pathways, response to infection and the maintenance of blood pressure and fluid homeostasis [36]. Glucocorticoids can act through two receptors: the GR and the Mineralocorticoid Receptor (MR). In humans GR is detectable in most tissues by 8-10 weeks gestation [37]. In mice, a more detailed profile of *Gr* expression in development has been obtained. At embryonic day (e) 9.5, *Gr* expression is low, however expression increases, with tissue-specific timing, as development progresses. Some tissues, such as liver show a rise in *Gr* expression by e12.5 [38]. This elevation in GR promotes fetal maturation, and exogenous glucocorticoids are frequently given to accelerate lung development in fetuses at risk of premature delivery [39].

The 11β-Hydroxysteroid Dehydrogenase (11β-HSD) enzymes regulate the action of glucocorticoids by catalysing the conversion between active and inactive forms (Figure 1.1). The Type 1 isoform acts as a reductase, converting inactive glucocorticoids to their active forms (cortisone to cortisol in humans, and 11-dehydrocorticosterone to corticosterone in rodents) [40-42]. Conversely, 11β-HSD2 converts active glucocorticoids into inactive metabolites, and is present in the placenta, serving to protect the fetus from the comparatively high levels of glucocorticoid in the maternal circulation. Inhibition of this second enzyme in pregnant rats has been shown to correspond to decreased weight at birth, with hyperglycemia and increased blood pressure in adult offspring [43,44]. *11β-Hsd2* knockout mice also produced progeny with a lower birth weight and which demonstrated greater anxiety in adulthood [45]. Although placental 11β-HSD2 acts as a barrier to maternal glucocorticoid, some active cortisol/corticosterone still passes to the fetus. Therefore elevated maternal cortisol, in periods of stress, can still have an impact upon the unborn child. For example, rats exposed to restraint stress during

pregnancy had offspring that had lower birth weight and hyperglycemia and glucose intolerance at 24 months (old age) [46]. This stress was also found to alter the placenta itself, reducing the expression of *11β-Hsd2*, and potentially augmenting fetal exposure to glucocorticoids [47]. Another study suggested that the effects of stress on 11β-HSD2 activity differ depending on the duration of the stimulus. In the short term, acute restraint stress for one day (e20) of pregnancy increased placental activity of 11β-HSD2, protecting the fetus from excess corticosterone. However in chronic stress (e14-e19), 11β-HSD2 activity was not altered, and could not subsequently be upregulated in response to acute stress [48]. Glycyrrhetinic acid, a component of liquorice, is known to be an inhibitor of 11β-HSD2 [49], and therefore studies have explored the outcome of pregnancies in Finland, where liquorice consumption is common [50]. Children of mothers who consumed high levels of liquorice were found to have greater circulating levels of cortisol than those whose mothers ate less or no liquorice during pregnancy [51]. Indeed, high liquorice consumption in pregnancy was associated with poorer cognitive performance in offspring at 8.1 years, constituting reduced visuospatial and verbal skills and impaired narrative memory compared to those whose mothers consumed no or low amounts of liquorice. A greater risk of behavioural issues in offspring was also reported, with increased tendency for rule-breaking and aggression [50]. It was not, however, found to induce changes in birth weight [52].

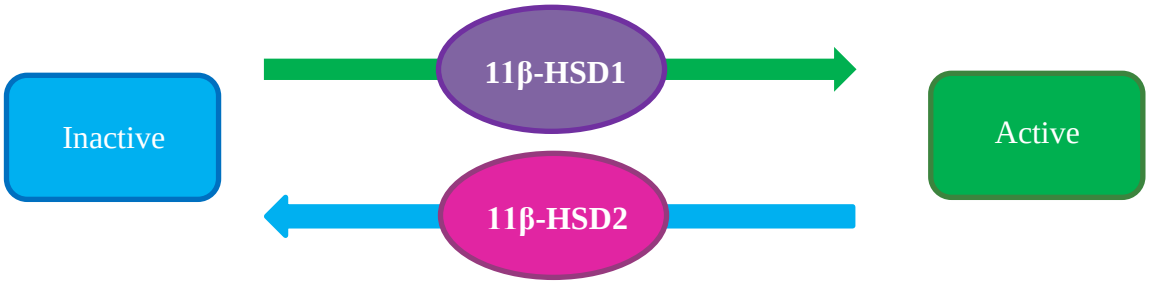

Figure 1.1. Action of the 11β-HSD enzymes. 11β-HSD enzymes catalyse the conversion between active and inactive forms of glucocorticoid. 11β-HSD1 acts as a reductase, converting inactive glucocorticoids to their active forms (cortisone to cortisol in humans, and 11-dehydrocorticosterone to corticosterone in rodents) [41,42]. Conversely, 11β-HSD2 inactivates these glucocorticoids [53].

Some insight into the effects of prenatal glucocorticoid overexposure may be gained from epidemiological studies examining the effects of the glucocorticoid cortisol on offspring, elevated due to maternal psychological stress [54], for example during war. Such studies however, can be complicated by co-existent factors such as exposure to food restriction, chemical pollutants, and ionizing radiation, which could also impact upon fetal development [55]. For example, babies born to pregnant women who were physically close to the World Trade Centre (WTC) during or shortly after the disaster of September 11, 2001 had a lower birth weight compared to those born to women living out with a 2 mile radius of the WTC. Potentially confounding variables such as infant sex and maternal pre-pregnancy weight were controlled for [6]. Similarly, offspring of mothers in proximity to the WTC disaster were found to have a greater risk of intra-uterine growth restriction (IUGR) than those delivered in a different area of New York, whose mothers had not been close to the WTC at the time of the disaster [56]. This change could result from mothers being closer to the air pollution generated by the disaster, compared to control mothers from other areas. However, mothers geographically closer may also have been more emotionally affected by the disaster. The causes of IUGR and decreased birth weight in this group are therefore likely to be complex. Such studies need to be

treated with caution as there are not perfect control populations with which to compare their results. However, taken together with other epidemiological studies and laboratory data, they do contribute to our understanding of the effects of glucocorticoid exposure on development.

It should also be noted that the time-point in pregnancy where maternal stress occurs may also influence the birth outcome. For example, Lederman *et al*. (2004) report that those in the first trimester of pregnancy during the World Trade Centre disaster had offspring with a shorter gestation, and smaller head circumference compared to those in second or third trimesters at that time [6]. However, no difference was seen in rates of IUGR [56]. Taken together, these studies support the conclusion that human maternal emotional stress can correlate with reduced fetal growth in offspring.

However, whilst maternal cortisol is elevated in response to psychological stress, activity of 11β-HSD2 may also be upregulated, protecting the fetus from some of this excess of glucocorticoid [54]. Further insight is gained from studies exploring the effects of synthetic glucocorticoid administration, such as Dex, which is a poor substrate for 11β-HSD2 [57]. Exogenous glucocorticoids are routinely given to accelerate lung maturation in fetuses at risk of premature delivery [39]. This reduces the incidence of respiratory distress syndrome, but repeated doses can also restrict intrauterine growth [39]. The metabolic effects of such administration have yet to be fully elucidated [39]. 30 years after prenatal glucocorticoid treatment, offspring had no change in weight, incidence of cardiovascular disease or diabetes, but did have higher insulin levels, indicating that diabetes could become more prevalent in later life [58]. Similarly, another study showed that prenatal glucocorticoid treatment was not associated with alterations in body composition, insulin resistance or blood pressure at 19 years of age, however a lower glomerular filtration rate was identified, which could give a greater risk of hypertension and renal failure with aging [59]. Furthermore, babies born at term, but whose mothers had received glucocorticoid treatment due to a threat of premature delivery had increased cortisol levels in response to pain, suggesting alterations in the Hypothalamic-Pituitary-Adrenal (HPA) axis [60].

Clearly, antenatal glucocorticoid treatment is important in improving outcomes for children born prematurely, and although research suggests there could be some risks to metabolic health in later life, further studies are required to properly inform the assessment of these risks. Currently, antenatal administration of glucocorticoid continues, as the benefits to health and survival outweigh the characterised risk in later development. However, the effects of glucocorticoid exposure have been more extensively investigated in animal models. They suggest that there could be detrimental effects of glucocorticoid exposure which may have yet to be elucidated in humans [8,10]. Crucially, they also provide a well-controlled model of fetal programming as a whole, potentially giving insights into the relationship between maternal environment, low birth weight and cardiovascular disease.

The effects of Dex administration have been studied in the developing fetus. When administered to pregnant rats, their offspring were shown to have a lower birth weight, and develop hyperinsulinemia and hyperglycemia in adulthood [8]. Expression and activity of Phosphoenolpyruvate Carboxykinase (PEPCK), involved in gluconeogenesis and upregulated in diabetes [61], was also increased in the liver [8]. Blood pressure was also found to be increased, along with levels of leptin, involved in regulating appetite and weight gain [62,63]. Dex exposure also changes gene expression in the livers of offspring. In late gestation, expression of Insulin-like Growth Factor 2 (*Igf2*), Cyclin-Dependent Kinase Inhibitor 1C (*Cdkn1c*), Growth Factor Receptor-Bound Protein 10 (*Grb10*) and *H19*, all important in the regulation of growth and development, were increased in livers of Dex-exposed fetuses [12]. Furthermore, when the Dex-exposed offspring were weaned on to a high-fat diet they had increased liver triglyceride content and increased expression of genes implicated in fatty acid esterification and triglyceride synthesis, compared to those exposed to Saline control in utero. This indicates that these animals have a greater risk of developing fatty liver disease [64]. Fatty acid uptake was also reduced in visceral adipose tissue, along with an increase in the expression of GR, which could promote insulin resistance [65].

Dex administration also alters the structure and function of the renal and cardiovascular systems, which could contribute towards the observed change in

blood pressure. In Dex-exposed female offspring, hypertension was concurrent with increased expression of liver angiotensinogen and renin activity. This suggests an activation of the Renin-Angiotensin System (RAS), which regulates fluid homeostasis and blood pressure [66]. Increased blood pressure could also be in part due to an increase in contractility of arteries [67].

Furthermore, some studies have shown the effects of exogenous prenatal glucocorticoid treatment in other mammals. In sheep, administration of glucocorticoid to pregnant ewes resulted in increased blood pressure in lambs [68,69]. This corresponded to altered renal function, with increased glomerular filtration rate and renal sodium reabsorption [68]. It was also seen to alter vascular responsiveness to stimuli in the fetus [69] and early postnatal period, which could promote the development of hypertension [70]. At 5 months however, there was no change in blood pressure between Dex and control offspring, which the authors propose is a result of compensatory mechanisms relaxing the vasculature [71]. Hepatic mRNA and protein levels of 11β-HSD1 were also found to be increased in the fetus, which could alter the expression of glucocorticoid-dependent genes in the liver and augment the effects of the initial exposure [72].

Programming effects of prenatal glucocorticoid exposure have also been reported in non-human primates. Glucocorticoid treatment increases the blood pressure of the unborn fetus in mid-late gestation [73]. Dex exposure was not found to alter the birth weight of offspring, but did impair growth postnatally. At 8 months, offspring had glucose intolerance and hyperinsulinemia, and by 12 months reduced numbers of insulin-producing β-cells were found in the pancreas, and blood pressure was increased [74]. Furthermore, 11β-HSD1 expression and activity was increased in the liver and pancreas of offspring, whilst *Gr* expression remained unchanged [75]. Such direct studies are clearly not possible in humans, for example the measurement of *11β-HSD1* expression in offspring liver. However the fact that the programming phenotype is conserved in other primates does support the conclusion that metabolic changes characterised in animal studies may be largely applicable to humans.

1.1.3 Intergenerational Programming

Research indicates that the effects of maternal nutrition or exposure to excess glucocorticoid may not only influence the first generation (*in utero* during the period of exposure), but may also be transmitted to a subsequent generation. In the Dex-programmed rat model, a reduction in birth weight following *in utero* Dex exposure was found to be carried to a second generation, without further intervention [10]. The phenotype of glucose intolerance and elevated hepatic PEPCK was also seen in second generation (F2) males whose mothers and fathers had both been exposed to Dex. Intriguingly, the effect on birth weight and PEPCK activity was also seen when Dex-exposed first generation (F1) males were mated with control females, and vice versa. Thus, the phenotype may be carried through both maternal and paternal lines [10].

Intergenerational transmission of the programming phenotype induced as a consequence of glucocorticoid programming has also recently been demonstrated in sheep. Dex exposure was found to result in reduced birth weight and glucose intolerance in both first and second generation lambs, when transmission was studied through the maternal line [76]. Similarly, in guinea pigs, a phenotype of altered HPA activity and behaviour was transmitted to a second generation through the maternal line [77].

Intergenerational effects have also been reported in models of nutritional programming. In a mouse model of prenatal undernutrition, the phenotype of low birth weight was transmitted to the F2 through the paternal line, obesity through the maternal line, and impaired glucose tolerance through both lines [11]. Grand-maternal protein restriction also corresponded to altered glucose and insulin metabolism in F2 rats [78]. Interestingly, a phenotype of impaired glucose metabolism in rats following maternal undernutrition was transmitted to both a second and third generation, through the maternal line [79]. This is in contrast to the Dex-programming model, where the phenotype had resolved by the third generation [10].

Intergenerational transmission of a phenotype through both maternal and paternal lines has also been seen in human studies. Many explore the effects of nutrition,

which are sometimes dependent on a calculated likelihood of food availability, based on historical knowledge and local community records. A greater availability of food to the paternal grandfather during his slow growth period correlated to an increased incidence of diabetes in grandsons [80]. Pembrey *et al*. (2006) show that food availability to the paternal grandfather is correlated with calculated mortality risk in grandsons exclusively. Conversely, the diet of the paternal grandmother was correlated with the granddaughter's mortality risk. This was based on diet exposure in the slow growth period of both grandparents, and the fetal life of the grandmother. Therefore a transgenerational effect was observed, with gender-specific phenotypes, which the authors conclude may be transmitted through the X and Y chromosomes [81]. Studies have also explored the effects of the Dutch Hunger Winter on grandchildren. Exposure to famine was not found to significantly alter the birth weight [20,82], or metabolic or cardiovascular disease incidence in grandchildren [82]. However F2 body length was decreased and adiposity increased at birth, and more ill-health was reported in adulthood, suggesting there were some effects of F1 maternal undernutrition, carried in the female line to the next generation [82].

1.1.4 Mechanisms of Programming

Fetal programming therefore has been seen to occur in animal models in response to aberrant nutrition or excess glucocorticoid exposure, and although less extensive, data suggest that these effects are also seen in humans. A phenotype of low birth weight and altered cardiometabolic parameters may be carried in both the maternal and paternal lines to subsequent generations [10]. The precise phenotype exhibited is seen to vary, with type and timing of exposure, however some patterns have emerged. Many studies report a change in birth weight in offspring, with adverse effects on glucose and insulin regulation. It has therefore been suggested that a common mechanism may underlie many of the examples of programming [36].

Clearly in some instances of intergenerational transmission, it is possible that the stimulus that promoted the phenotype in the first generation may still be present whilst the second generation is *in utero*. For example, a mother who eats a high-fat diet in pregnancy may subsequently raise children who will also eat a high-fat diet in

their own pregnancies. Indeed, even if such a trait is not transmitted by behaviour alone, animal studies have shown that exposure to a high-fat diet *in utero* increases the offspring's preference for unhealthy food in adulthood [34]. Therefore a phenotype could perpetuate across generations. For many studies, however, this is not a suitable explanation. Many of the studies above involve exposure to an isolated stimulus. For example, offspring were seen to be 'programmed' during the Dutch Hunger winter, which represented an isolated event which was not repeated during the pregnancies of the F1 generation.

It could also be suggested that changes in the F1 mother could alter the *in utero* environment of her children. Studies have shown that programming can change HPA axis regulation or insulin responses in the F1 mother during pregnancy, so that her children might themselves experience an adverse environment *in utero*, which could in turn induce the programming phenotype [8,74]. This could be a valid explanation for some studies which show programming through the maternal line.

It should however, be considered that a transmission of phenotype has also been shown through the male line, where there is no direct influence on the *in utero* environment [10]. In human studies, it could be suggested that there is some influence of paternal behaviour on the offspring either pre or post-natally. For example, an F1 father who experienced *in utero* malnourishment during the Dutch Hunger Winter could respond differently to stressful stimuli, promoting changes in the pregnant mother carrying his child. However, programming has been shown to be transmitted through the male line of laboratory rats, where the father has no interaction with the mother or offspring after mating [12]. A behavioural influence on the mother at this point cannot be ruled out, but seems less likely to produce a significant and reliable phenotype in the offspring born weeks later.

We therefore hypothesise that a programming phenotype may be transmitted to an F2 generation in the sperm of F1 males. It is interesting to note that in the Dex-programmed rat, the phenotype differs between first and second generations. Although both may have changes in birth weight and cardiometabolic parameters, changes in gene expression differ. For example, Dex exposure increased the expression of *Igf2* in F1 liver, whilst a decrease was seen in F2 [12]. One possible

explanation for these differences is that the mechanisms of programming induction are different between generations. The F1 fetus experiences the exposure whilst it is *in utero*, therefore the excess glucocorticoid can have a direct effect on its metabolic development. The second generation do not experience direct exposure, but may have an altered phenotype based on information carried in the germ cells (see Figure 1.2). Therefore a programming phenotype could be carried to a second, but not third generation, as observed in this model [10]. Whilst it is equally possible that a phenotype can be carried in both maternal and paternal germ cells, it is hard to isolate the effects of the maternal germline from those of the intra-uterine environment she provides.

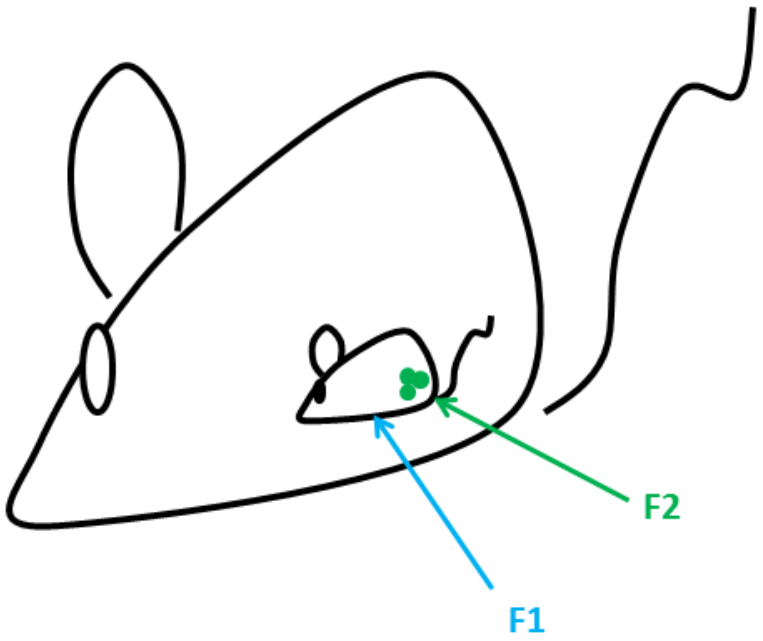

Figure 1.2. Intergenerational transmission of disease risk phenotype. Whilst the F1 generation are *in utero* during the period of Dex exposure in the programming model, their germ cells, which will one day contribute to the F2 generation are also present. If Dex exposure impacts upon these developing germ cells, this could be transmitted to the next generation.

When considering programming by *in utero* exposure to excess glucocorticoid or altered nutrition it is worth noting that the literature broadly presents three different routes for programming. There are studies which present the effects of intra-uterine exposure on the first generation, such as those of Painter *et al*. (2005) who report that maternal malnutrition during the Dutch Hunger Winter correlated with increased prevalence of coronary heart disease, glucose intolerance and obesity in adult offspring [7]. There are others which demonstrate the effects of an intra-uterine exposure on a second generation through maternal or paternal lines, such as Jimenez-Chillaron *et al.* (2009) who showed that maternal dietary restriction corresponded to reduced F2 birth weight, through the male line, and increased F2 adulthood obesity through the female line [11]. Here it could be suggested that there is some effect of the initial exposure on the developing germ cells. In a third type of study there is an effect demonstrated on a third generation, which has never been exposed to the initial insult, whether directly, whilst *in utero*, or indirectly, whilst the germ cells from which the F2 generation are formed are *in utero*, within the F1 pups. The effects on the F3 generation are less frequently reported in the literature, potentially due to the time and financial implications of such studies. However, for example, Benyshek *et al*. (2006) report that maternal protein restriction alters glucose metabolism in the third (F3) generation [79]. In the Dex programming model, there are observed effects on the F1 and the F2, but not the F3, thus there is no reported effect on pups which have had no direct or indirect exposure to Dex treatment [10]. We propose therefore that the effects seen in the F2 are carried in the germline of the F1 pups. If indeed the F2 phenotype results from germline exposure this effect is transgenerational, but not truly inherited, in the sense that there has been some exposure, in the form of F1 germ cells, to the initial insult.

I therefore sought to investigate the transmission of the programming phenotype in the Dex model. The male line was studied as it allowed the hypothesis of transmission in the germline to be studied, without the potential confounding factor of an altered intra-uterine environment.

1.2 Mechanism of Intergenerational Transmission – the Developing Germ Cell

Since sperm is not found in the fetal male, F1 *in utero* Dex exposure cannot directly affect the sperm itself, but could change the developing sperm progenitor cells, or germ cells. These germ cells will form the progenitors of the spermatogenic pathway in adulthood, so that if these germ cells are changed whilst they are *in utero* during F1 fetal exposure, this could later be transmitted through the spermatogenic pathway to a second generation.

The process of spermatogenesis allows around 300 million sperm to be produced in the testes daily from puberty [13]. This process occurs in the seminiferous tubules within the testis, which contains germ cells at different stages of maturation and somatic Sertoli cells, which serve to support germ cell development [83]. Fetal germ cells become the progenitor stem cells of the spermatogenic pathway, termed spermatogonia, and they exist around the basal circumference of the seminiferous cord. These cells undergo mitotic division, followed by two rounds of meiosis, progressing through various stages of maturation, and migrating towards the central lumen of the tubule as they do so (Figure 1.3) [84]. The process of spermatogenesis is cyclical, with different cell types being present within different sections of the tubule, depending on its corresponding cycle stage. Each stage has a defined duration, and the entire process is complete within 12.8 days in rats [13,85]. Mature spermatozoa are released into the seminiferous tubule lumen, and progress to the epididymis, where they undergo the final stages of maturation.

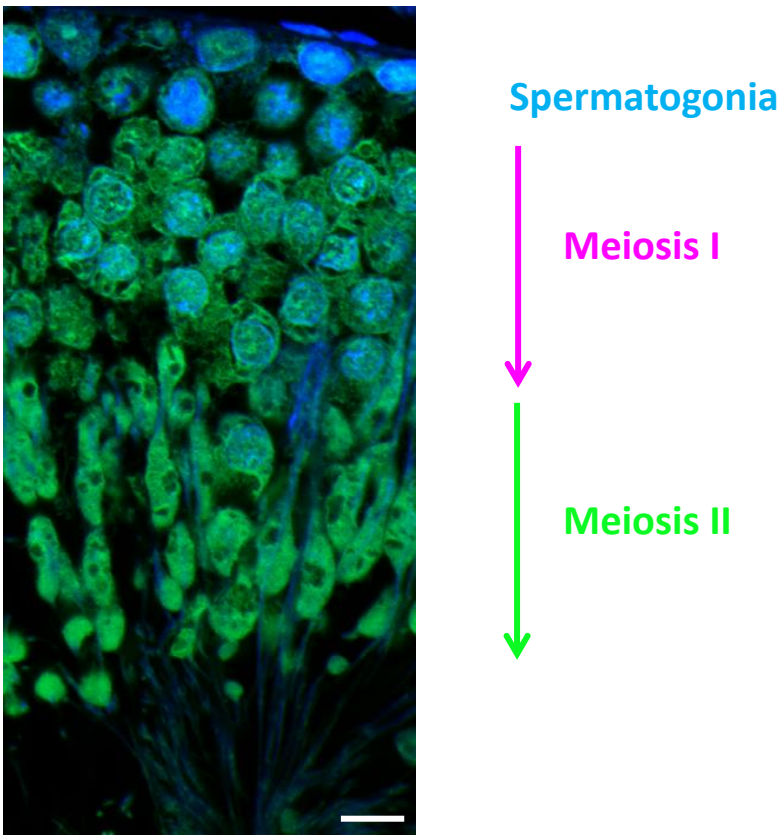

Image: Rose *et al*. Unpublished

Figure 1.3. Primordial germ cells form the progenitors for adult spermatogenesis. This process is initiated by the mitotic division of the spermatogonia, maintaining the progenitor population, before some are converted into sperm through two rounds of meiotic division [86]. Bar = 10µm.

Some studies have shown that programming stimuli can affect reproductive development in male offspring. For example, maternal protein restriction in rats produced male offspring with an increased Ano-Genital-Distance (AGD), indicating increased masculinisation, which may result from the increase in maternal serum testosterone levels, observed at e19. Testis descent was also delayed and testis weight decreased at all ages [87]. At 70 days of age, concentrations of luteinising hormone and testosterone were decreased, and sperm count and maturation was also decreased at maturity [87]. Furthermore, maternal restraint stress in late gestation was found to reduce the testis weight of male rats, corrected for body weight [47]. In contrast to the protein restriction model of Zambrano *et al.* (2005), AGD was found

to decrease, but this was not corrected for body length, and pups were of lower weight [47]. The authors suggest the change in testis weight could be due to effects on steroid production in development. Indeed maternal restraint stress was found to reduce plasma testosterone in pups in late gestation, and the authors suggest that this could alter sexual behaviour [88]. Prenatal stress was reported to feminise juvenile play behaviour in male offspring, and correlated with more feminine sexual behaviour [89]. A correlation between reported maternal stress and gender role was not found in human children [90].

Therefore environmental factors may influence the development of the testis as a whole in addition to mating behaviour of offspring. In the Dex-programmed rat, Dex exposure was not found to change intratesticular testosterone in fetuses at e17.5, nor the AGD or testis weight of adult offspring, although it did augment the detrimental effects of the endocrine disruptor Di(n-butyl) Phthalate (DBP) [91]. It cannot be ruled out that Dex may have an effect on plasma testosterone levels during the fetal surge between e17.5-e18.5 [88]. It has been observed that Dex-exposed F1 males appear less aggressive in mating, but do still mate shortly after being paired (Drake *et al*., unpublished observation). The Dex males are clearly still fertile, and produce as many pups per litter as control rats. It may therefore not be important that gross changes in the testis were not observed previously, as a phenotypically programmed offspring is still produced. I hypothesise that the sperm itself, and the germ cells from which it is derived, are of the most relevance.

Investigating this hypothesis is challenging, in that it is difficult to access pure populations of fetal germ cells, separating them from the surrounding somatic cells of the testis. We recently obtained Germ Cell Specific-Enhanced Green Fluorescent Protein (GCS-EGFP) rats that have EGFP expression specifically in the male and female germlines [92]. This allowed me to use Fluorescence-Activated Cell Sorting (FACS) to purify germ cells for study.

Recent studies have suggested that there may be some link between epigenetic regulation in the germ cell, the subsequent sperm and the resulting offspring [93], which will be reviewed later. Along with them, I hypothesise that one kind of

epigenetic regulation that could be changed in the germline with programming is DNA methylation.

1.3 Introduction to Epigenetics

Epigenetics was first defined as "the science concerned with the causal analysis of development" by Conrad Waddington in 1952 [94]. More recently Berger *et al*. (2009) proposed that "an epigenetic trait is a stably heritable phenotype resulting from changes in a chromosome without alterations in the DNA sequence" [95]. This may constitute modifications to DNA itself, or a change to the structure of chromatin, for example by histone modification. Histone proteins form the central core of a nucleosome, consisting of 146 base-pairs (bp) of DNA wound around an octomer of histone proteins, with two copies of histones H3, H4 and the dimer H2A-H2B [96-98]. Each core histone has an N-terminal tail which protrudes from the nucleosome, the amino acids of which are subject to post-translational modification, such as acetylation, phosphorylation or mono-, di- or tri-methylation [99]. Thus, H3K4me3 would constitute tri-methylation of lysine 4 of the tail of a H3 histone protein [98]. This in turn influences chromatin compaction, the interaction of transcription factors with DNA and ultimately regulates whether genes are expressed or silenced [100]. Non-coding RNA (ncRNA) sequences can also influence gene expression. For example micro RNA (miRNA), the most extensively characterised class of ncRNA, are around 22 nucleotides in length and can regulate expression at the level of translation. miRNA has sequence specificity for mRNAs and can either facilitate the binding of a silencing complex, or target mRNA for degradation [101].

1.3.1 DNA Methylation

One of the most extensively characterised forms of epigenetic regulation is DNA methylation. DNA methylation involves the addition of a methyl group to the 5' position of a cytosine base to form 5-methylcytosine (5mC). DNA methylation was first reported by Wheeler and Johnson in 1904 [102], but it was not until 1925 that it was demonstrated to exist in nature, in a study of the bacterium *Tubercle bacillus* [103]. Paper chromatography was then used to prove its existence in calf thymus

DNA in 1948, the first demonstration of methylation in mammalian cells [104]. A fundamental advance in the field of DNA methylation research was made in 1975 when Holliday and Pugh, and independently, Riggs proposed that this cytosine modification might be key in regulating gene expression [105,106]. 5mC is now recognised as a meiotically and mitotically heritable epigenetic modification with an important role in transcriptional regulation [95]. DNA methylation is found in bacterial, plant and mammalian cells, but is not ubiquitous, and is undetectable for example, in yeast. The degree of cytosine methylation was found to vary between species, with 14% of total cytosines methylated in *Arabidopsis thaliana*, 7.6% in mice, 2.3% in *Escherichia coli* and only 0.034% in *Drosophila melanogaster* [107].

One way in which DNA methylation mediates effects on gene expression is through altering the interaction of DNA with transcriptional elements, such as RNA polymerase II, reducing transcriptional efficiency within the gene body [108]. DNA methylation has also been found to recruit proteins such as the Methyl-CpG Binding Domain Proteins (MBDs), which subsequently promote the interaction of other factors which may, for example alter chromatin structure, and therefore DNA accessibility to transcriptional machinery [109]. For example, DNA methylation recruits the Methyl-CpG-Binding Protein 2 (MeCP2) which in turn recruits histone deacetylase, therefore inducing chromatin remodelling to produce a repressive state [109].

In mammals, this modified cytosine predominantly exists in a Cytosine-Phosphate-Guanine (CpG) dinucleotide, where a cytosine base is located next to a guanine in the DNA sequence [110]. Whilst most individual CpGs throughout the mammalian genome are methylated, regions of high CpG density are predominantly unmethylated; approximately 50% of these CpG islands occurring at annotated transcription start sites, with the remainder distributed equally between intra- and inter-genic regions in mice and humans [111,112]. Intriguingly, GpG islands out with known transcription start sites have a greater incidence of methylation during development, indicating that they may regulate the expression of developmentally relevant genes [112]. Methylation has also been demonstrated in CpG island ‘shores’ – regions up to 2kb from a CpG island, which were found to have differential

methylation in colon cancer [113]. Differential methylation at CpG island shores had a greater correlation with gene expression than that associated with CpG islands themselves [114]. Much less frequently, non-CpG methylation occurs, but its precise function remains elusive [115]. It has been reported to exist predominantly in pluripotent cells, with decreased identification upon cellular differentiation, and subsequent reappearance with induced pluripotency [115,116].

Cytosine modification contributes to the regulation of transcription, with promoter DNA methylation characteristically associated with gene silencing [117]. One such role of this regulation is in the inactivation of the paternally inherited X chromosome in females. This second X chromosome is inactivated (Xi) rendering the majority of genes transcriptionally silent in early embryogenesis, in a process that is yet undefined, but has very recently been suggested to involve the Long Interspersed Nuclear Element 1 (LINE1) retrotransposon [118,119]. DNA methylation then contributes to the maintenance of this silencing throughout development [118]. The active X (Xa) chromosome has approximately two times more allele-specific DNA methylation than the Xi, however this predominantly exists in gene bodies, with corresponding hypomethylation at gene promoters [120]. The majority of CpG islands on the Xi were found to have increased methylation, and were associated with transcriptionally silent genes, whilst 7% were found to have reduced methylation, and escaped inactivation [118].

DNA methylation also has an important role in the silencing of retrotransposons, mobile genetic elements capable of moving around the genome via RNA intermediates. Three classes exist in mammals; LINEs, Short Interspersed Nuclear Elements (SINEs) and Endogenous Retroviruses (ERVs), which are sometimes flanked by a Long-Terminal Repeat (LTR) region (reviewed in [121]). DNA methylation is thought to protect the genome from mutation through transposition, by silencing of these retrotransposons [122,123].

Imprinting confers the expression of genes in a parent of origin-specific manner [124]. One mechanism which can contribute to imprinting is DNA methylation, where one allele of the imprinted gene is unmethylated, whilst the other is methylated at key regulatory regions, the pattern of which is inherited from the

parental genome. Intriguingly, the pattern of methylation at imprinted genes may reflect the competing interests of the parent from which it originates, as first proposed in the study of flowering plant endosperm [125,126]. Therefore, it has been hypothesised that imprinting from the paternal line may promote the expression of growth factors, promoting the maximum growth of his offspring. Conversely, imprinting from the maternal line may promote the moderation of growth, balancing the need for fetal development, with the conservation of the mother's own resources [127,128]. Very recently, this theory was suggested to be overly simplistic, and that instead of conflict, imprinting may for example represent a benefit of offspring exhibiting a phenotype more similar to one parent [129].

The DNA Methyltransferase (DNMT) enzyme family catalyse *de novo* and maintenance methylation. DNMT1 is the key enzyme involved in maintaining DNA methylation, and imprinting. When DNA is replicated, DNMT1 methylates the newly replicated CpGs corresponding to methylated sites on the mother strand of DNA. It is attracted to these sites by the proliferating cell nuclear antigen-interacting binding partner Nuclear Protein 95 (NP95) and serves to methylate hemimethylated CpGs [130,131]. Loss of DNMT1 is associated with a reduction in levels of DNA methylation, and subsequent embryonic lethality [132]. A loss of NP95 was shown to have a similar effect [131]. DNMT1 and its ovarian isoform DNMT1o are involved in the maintenance of this imprinting in mice [133,134]. Partial loss of DNMT1 in transgenic mice therefore corresponded to a dysregulation of the imprinted genes *H19*, *Igf2* and the *Igf2* receptor (*Igf2r*) [135]. The DNMT3 family are involved in *de novo* methylation, and will be discussed in section 1.4.2.

1.3.2 Different forms of methylation

To date, four different types of methylation have been identified in mammalian and plant cells and it has been suggested that these variants may have different effects on gene expression.

The Ten-Eleven-Translocase (TET) dioxygenase enzyme family has been shown to oxidise 5mC to 5-hydroxymethylcytosine (5hmC) (Figure 1.4) [136,137]. 5hmC was first identified in a study of bacteriophages in 1952 [138], and in mammals in 1972

[139], however the latter was subsequently refuted by other researchers who failed to replicate this finding [140]. In 2009, 5hmC was identified in mouse brain, giving greater certainty of its existence, and reigniting interest in this form of methylation [141]. Some studies have also reported the presence of 5hmC in plants [142,143], whilst other data suggest that it is absent from the plant genome, at least in some species [144]. 5hmC has widespread distribution, with tissue-specific patterns of localisation. This modification is primarily associated with euchromatin and located in the body of transcribed genes, with 5hmC levels having a positive correlation with the level of gene transcription [145-147]. Intriguingly, however, this correlation is only relevant within a given tissue. Thus, the absolute level of 5hmC, corresponding to high levels of transcription may differ greatly between tissue types [145]. In contrast to 5mC, 5hmC is also enriched at some CpG-rich Transcription Start Sites (TSS) in Embryonic Stem (ES) cells [146,147]. Decreased levels of TET expression during differentiation is associated with a decrease in 5hmC at the gene promoters of ES cells, and a corresponding increase in 5mC levels and gene silencing [147]. TET 1 and 2 knockout mice also have decreased 5hmC, increased 5mC levels and abnormal imprinting. Mice are however viable, suggesting that TET 3 may be able to partially compensate for this knockout [148].

Two additional forms of methylation have been described, termed 5-formylcytosine (5fC) and 5-carboxylcytosine (5caC). 5fC can be produced from 5hmC by further oxidation by the TET enzyme family (Figure 1.4). In the same way, 5caC can then by produced from 5fC [149]. These additional methyl forms may form part of a demethylation pathway, where 5mC is progressively oxidised to 5fC and 5caC, which are then removed, giving unmodified cytosine. This has been referred to as active demethylation. For example, the base excision enzyme Thymine DNA Glycosylase (TDG) has been shown to recognise and act upon 5fC and 5caC, and depletion of TDG in mouse ES cells corresponds to an accumulation of 5caC [150,151]. Very recently this depletion was found to promote the accumulation of both 5fC and 5caC at many proximal and distal gene regulatory elements [152]. Conversely, overexpression of TDG results in depletion of 5fC and 5caC [153]. Resulting 5fC or 5caC may then be a target for the Base Excision Repair (BER) pathway, leaving unmethylated cytosine to complete the demethylation process.

Intriguingly, plants express DNA glycosylases that are able to act on 5mC directly, removing DNA methylation [154,155]. However animals do not have a form of DNA glycosylase that can act directly on 5mC, therefore TET enzyme conversion through 5hmC to 5fC and 5caC might be required for a TDG mediated demethylation [151]. Very recently, plants have also been shown to contain 5fC and 5caC, despite the ability to remove DNA methylation without progressive oxidation [155].

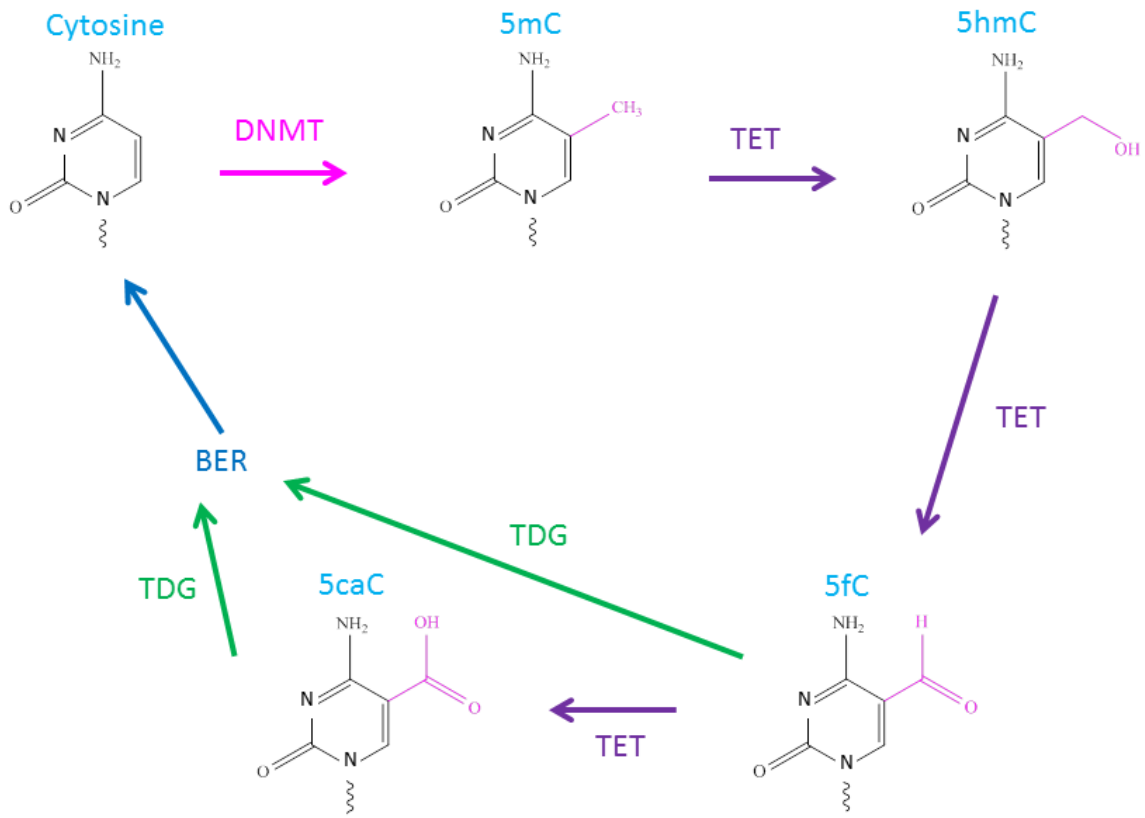

Adapted from a publication resulting from this thesis - Rose *et al*. (2013) [156].

Figure 1.4. The proposed conversion of 5mC to 5hmC, 5fC and 5caC. A cytosine base is converted to 5mC by the addition of a methyl group to its 5' position by the DNMT family. TET enzymes have been shown to produce each form of methylation by progressive conversion from 5mC [136,149]. 5fC and 5caC may then be targets for removal by TDG and the BER pathway. Research indicates that each form may have functionality [157], in addition to representing a pathway for the removal of 5mC.

Conversely, it has been suggested that the Activation Induced Deaminase/ Apolipoprotein B mRNA Editing Enzyme, Catalytic Polypeptide-Like (AID/APOBEC) enzyme may deaminate 5mC to produce Thymine (T). As the 5mC would originally have been paired with a guanine (G) base in the double helix, this would leave a T-G mispair [158-160]. This would then be recognised by TDG, or another glycosylase that recognises T-G mispairing – Methyl Binding Domain IV (MBD4). Both would remove the thymine from the mispair, preparing for the BER pathway to replace with a cytosine. This would reinstate a C-G pairing, meaning that ultimately an unmodified cytosine had replaced 5mC [151,160-163].

Another potential pathway could involve the TET-mediated conversion of 5mC to 5hmC, followed by deamination to 5-hydroxymethyluracil (5hmU) by AID/APOBEC [164]. 5hmU could then be excised by TDG [163], or another DNA glycosylase, Single-Strand Selective Monofunctional Uracil DNA Glycosylase 1 (SMUG1) [165]. More recently, however, Nabel *et al.* (2012) showed that AID/APOBEC has greatly reduced activity on templates containing 5mC compared to unmodified C, and no detectable activity on 5hmC *in vitro*. Furthermore, when AID/APOBEC was overexpressed, no deamination products of 5hmC were detected, but 5fC and 5caC were found [153]. This therefore makes the theory of demethylation by deamination of 5hmC less plausible. Whilst the primordial germ cells (PGCs) of AID deficient mice were found to have decreased demethylation relative to controls, the process did still occur. This suggests that if indeed demethylation occurs via AID, there must be additional AID-independent pathways involved [166] .

Some research has also suggested that the process of demethylation may occur by passive dilution of the oxidative products of 5mC, rather than active removal. Both 5fC and 5caC have a strong detection by immunofluorescence in the early stage zygote, with concentrations depleting gradually with increasing numbers of cellular division [157]. Similarly, 5hmC was found to undergo replication-dependent dilution [167]. This led the authors to conclude that 5hmC, 5fC and 5caC might have some functionality in the early stage zygote, due to their long-lasting presence. Indeed,

Iqbal *et al*. (2011) demonstrate that 5hmC persists in one- and two-cell and cleavage stage embryos, rather than being rapidly removed [168].

However, in a very recent study, Wang *et al.* (2014) sequenced methylated cytosines in the oocyte, sperm and four-cell embryo. They show that there is a rapid reduction in 5mC, 5hmC and 5fC between gametes and four-cell embryos, leading them to conclude that active demethylation occurs after fertilisation, independent of cellular replication [169]. They found that only ~10% of demethylated sites had a corresponding enrichment for 5hmC, with a similar distribution for 5fC. They did detect all known forms of methylation in the 2 stage embryo, but conclude that active demethylation occurs, rather than passive dilution. They also demonstrate the presence of 5hmC and 5fC on both maternal and paternal alleles [169]. This contradicts previous work indicating that oxidized 5mC derivatives are only present on the paternal genome in the early embryo. For example, Iqbal *et al*. (2011) indicate that in the early stage zygote, the paternal pronucleus has enriched 5hmC and little 5mC, whilst the converse was shown in the maternal pronucleus [168]. This is supported by other studies [170].

Wang *et al*. (2014) used more advanced, base-specific techniques that were not available when 5fC and 5caC were first discovered in 2011. Even though this work suggests that demethylation occurs rapidly, this may not negate the suggestion that 5hmC, 5fC and 5caC may have functionality in the early stage zygote. Their functionality could exist before the 2 cell stage, or indeed, the 5hmC, 5fC and 5caC that was detected at the 2 cell stage, even though not found at every site of demethylation, could still be functionally active. Furthermore, a very recent study identified that 5fC and 5caC is produced extensively across the genome, with accumulation at major satellite repeats in mouse ES cells [152]. Much has still to be investigated regarding this potential functionality, but the presence of 5fC has been shown to correlate with increased transcription in ES cells, suggesting a role in chromatin remodelling [171].

1.4 Epigenetic Reprogramming

DNA methylation has been shown to change throughout the development of the fetus. Germline epigenetic reprogramming corresponds to the genome-wide erasure and subsequent re-establishment of methylation during the development of the fetal germ cell [14]. This has been shown to occur at the majority of the genome, but certain key regions are thought to be resistant to reprogramming. For example, the maintenance of methylation of retrotransposons during the phase of reprogramming may protect the genome from their undirected activation and transposition [172]. This process of epigenetic reprogramming is crucial to remove epimutations, erase and re-establish parental imprints and promote the totipotency required in this cell lineage [14,173]. This ultimately ensures that the correct epigenetic marks are established in the germline, particularly as they may be transmitted to future generations. The vast majority of studies on epigenetic reprogramming have been conducted in mice.

1.4.1 Demethylation

In mouse studies, PGCs are first identified at e7.25 [174] and migrate into the genital ridges by e11.5 [175]. At e13.5 PGC replication is complete, and male germ cells exhibit mitotic arrest, whilst female germ cells enter meiotic prophase [173]. Many studies indicate that during this development, PGCs exhibit dramatic erasure of DNA methylation, despite the continued expression of the maintenance methyltransferase DNMT1 [14]. This demethylation occurs simultaneously in both male and female germ cells, at the majority of genes studied, although female-derived embryonic germ cell lines were found to have less methylation than those from males [176]. This could reflect changes in germ cell DNA methylation occurring after specification [176].

DNA demethylation is thought to occur rapidly between e11.5-e12.5 for the majority of genes (Figure 1.5) [14,177]. However, some studies suggest that the demethylation of some loci may occur before e11.5, potentially whilst PGCs are still migrating to the genital ridge [177,178]. Demethylation has been reported to be initiated as early as e8 at some genes, and at the majority of genes by e9.5, with

rapid, bulk demethylation around e11.5 [179-181]. By e13.5 global methylation is reduced by around 90 % [182]. Hackett *et al*. (2013) showed that some imprinted genes are demethylated by e10.5, whilst others remain hypermethylated until e11.5 [183].

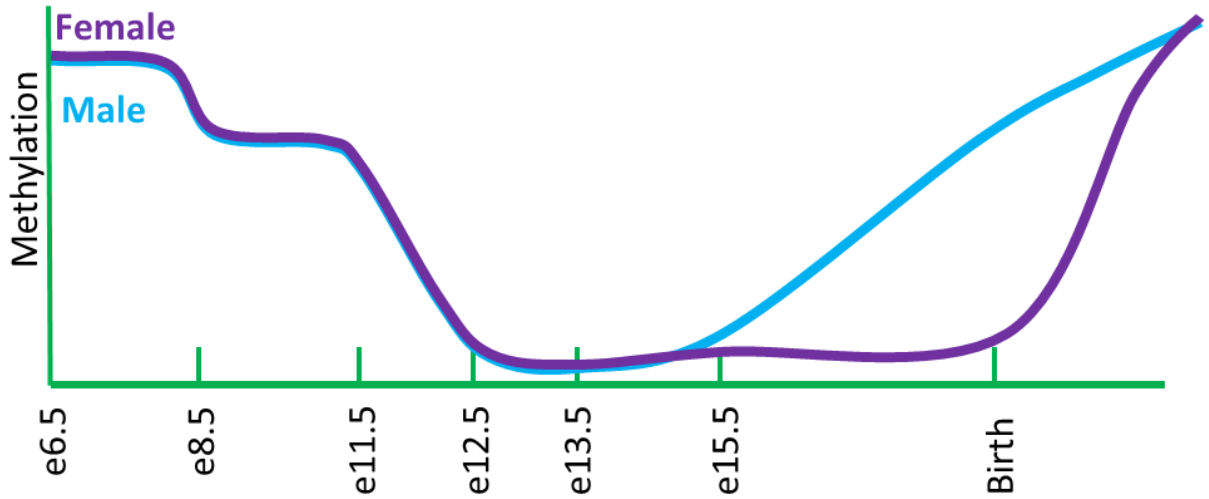

Adapted from a publication resulting from this thesis - Rose *et al*. (2013) [156].

Figure 1.5. Schematic of epigenetic reprogramming in the mouse. Bulk DNA demethylation may be initiated as early as e8 at some genes with bulk DNA demethylation occurring between e11.5 and e12.5 [14]. Demethylation occurs across the majority of the genome, whilst some regions remain resistant to reprogramming, particularly those corresponding to retrotransposons [179]. Remethylation predominantly occurs prenatally in male and postnatally in female germ cells [178,184].

This DNA demethylation phase could be mediated by any of the methods outlined above. In particular, the activity of TET enzymes may promote conversion of 5mC to its oxidative forms during PGC migration. TET1 has been shown to be expressed in PGC, along with components of the base excision pathway [182]. More recently TET1 and TET2 (but not TET3) were found to be expressed in PGC, peaking at e10.5-e11.5. A decrease in 5mC was associated with a corresponding increase in 5hmC. Intriguingly, 5hmC was seen to persist in germ cells between e11.5-e13.5, after 5mC concentrations had decreased, suggesting that 5hmC removal might be

replication-dependent [183]. The increase in TET1 expression and initiation of demethylation happened asynchronously between individual PGCs [183]. It should be noted, however, that no enrichment of 5fC or 5caC was seen in the PGCs in this study [183]. Furthermore, e11 germ cells isolated from TDG knockout mice show hypermethylation of both the maternal and paternal alleles of IGF2 Differentially Methylated Region (DMR) 2, in contrast to the wild-type control PCGs where the maternal allele is demethylated. This suggests that an absence of TDG disrupts PGC demethylation during epigenetic reprogramming [185]. Recent mRNA studies have also indicated that TDG is expressed in mouse germ cells from e9.5-e13.5, with concentrations depleting over this time period [186].

Kagiwada *et al*. (2013) also show that the PGC cell cycle is faster than previously suggested, and report rapid proliferation between e10.5-e12.5. This makes the involvement of partially passive mechanisms, dependent on cell replication, more plausible during epigenetic reprogramming [186]. Furthermore, based on this study, Hackett *et al*. (2013) calculate the rate at which a replication dependent removal of DNA methylation would occur, and find that the imprinted genes studied exhibited demethylation at that predicted rate [183]. Indeed RNA-sequencing results indicated that expression of NP95 was repressed at e11.5, and whilst immunofluorescence studies indicated that DNMT1 was found in germ cell nuclei at e13.5, NP95 had a solely cytoplasmic localisation. This suggests that during remethylation the actions of NP95 and DNMT1 have been physically uncoupled, meaning that DNMT1 is not targeted to methylate newly formed DNA strands during cellular division, facilitating passive demethylation [187]. Furthermore, DNMT3a and 3b were not expressed in PCGs at e11.5, preventing a remethylation of loci that have been demethylated, and a cyclical phase of demethylation/remethylation [182]. Additionally, the AID/APOBEC complex involved in active demethylation was shown to have a very low PGC expression during the period of demethylation in the mouse [182,186].

It has therefore been proposed unlikely that demethylation during epigenetic reprogramming is dependant exclusively on active mechanisms, partially because an active, genome-wide demethylation, which might involve DNA double strand breaks, would be very costly energetically [188]. Also, the lack of AID/APOBEC,

coupled with the presence of TDG and TETs 1 and 2 suggests that at least some demethylation occurs through the conversion of 5mC to oxidised states [183]. It has been suggested that the demethylation phase could involve a combination of both active and passive mechanisms [188]. Indeed Seisenberger *et al*. (2012) indicate that there is a second wave of demethylation during epigenetic reprogramming with certain genomic loci, particularly those conferring long-term methylation, such as imprints, remaining methylated until the later phase [187]. It is possible therefore that these regions are protected from passive demethylation, but are subject to a subsequent active demethylation [188]. As the late demethylating sites have an enrichment of binding sites for Zinc Finger Protein 57 homolog (ZFP57) [189], which is involved in the maintenance of methylation at certain imprinted regions during methylation loss in the embryo [190], this could be protecting some regions from early methylation loss during epigenetic reprogramming. Hackett *et al*. (2013) suggest that epigenetic reprogramming most likely involves multiple mechanisms, with some functional redundancy. This would account for the continued reprogramming and fertility that occurs in mice with knockouts in some of these components, for example TET1. It may also allow demethylation to occur so comprehensively across the genome [183].

Although this phase of demethylation is thought to occur across the majority of the genome [166,180], studies have suggested that certain regions, particularly those corresponding to transposable elements, are resistant to epigenetic reprogramming. During a bisulfite sequencing study LINE1 was found to be demethylated during epigenetic reprogramming in the mouse PGCs [172]. However Intracisternal A-Particle (IAP) retrotransposons, which exist as part of the ERV family, have been found to be more resistant to demethylation [14,172,180], although there is some demethylation at these loci, which is greater in female germ cells [184]. Very recently, a subset of IAP retrotransposons has been found to be significantly more methylated than other family members during reprogramming. IAP Long Terminal Repeat 1 (IAPLTR1) is the most active IAP subclass and therefore poses the greatest risk of undirected retrotransposition [183,191]. Furthermore, a subset of the Long Terminal Repeat-Endogenous Retrovirus 1 (LTR-ERV1) family of rare retroelements were found to be resistant to demethylation [180]. Interestingly, this

subset was longer, and had a greater CpG content than other members, suggesting that they had been more recently inserted into the genome. Methylation was also found at these genes at e14.5 and e15.5, suggesting that they do not simply show delayed demethylation. Similarly, some single-copy regions, a proportion of which were located next to IAPs in the genome, remained methylated at these time-points [180].

The expression of retrotransposons clearly has to be tightly controlled, due to their ability to move around the genome. The persistent methylation of these elements may therefore serve to protect against epimutations during the period of epigenetic reprogramming [172]. However, the DNA methylation state of LINE1 was not found to correlate directly with the degree of gene expression, indicating that transposable elements may be regulated by other mechanisms, in addition to methylation [187]. In mouse ES cells, retrotransposon expression was also found to be regulated by Histone Deacetylase Inhibitor 1 (HDAC1). Knockout of the polycomb repressor complexes was also shown to increase expression of some subsets of retrotransposons [192]. It is also interesting to consider that the phase of demethylation also reactivates the second X chromosome in female PGCs between e11.5-e13.5 [193]. Clearly it is important that the activation of such genes that are normally canonically silenced is tightly regulated.

Furthermore, during an epigenetic disruption and recovery screen, Hackett *et al*. (2012) identified a group of germline specific genes, the expression of which is exclusively regulated by promoter DNA methylation. This collection of genes, including Testis Expressed 19.1 (*Tex19.1*) and Piwi-like RNA-mediated Gene Silencing 2 (*Mili*) are termed germline-defence genes, and are thought to protect the genome from transposon activation during demethylation. They are transcribed as a result of demethylation during epigenetic reprogramming, and are therefore available to protect the genome from the potential side-effects of methylation loss, such as transposon-mediated epimutations [179].

Changes in histone modifications may also serve to protect the genome. In parallel with a loss of methylation during epigenetic reprogramming, chromatin remodelling has been shown to occur. Detection of H3-K9 dimethylation (H3K9me2), which is

associated with gene silencing, was significantly reduced at e8, as examined by immunohistochemistry in germ cells. Conversely, the levels of H3K27me3, also associated with transcriptional repression, were increased between e8.5 and e9, and found to be maintained at e12.5 [181]. Intriguingly, a loss of H3K9me3 occurred in parallel with a G2 arrest of cell cycle. RNA Polymerase II-dependent transcription was also repressed, until H3K27me3 levels were increased [194]. A loss of H3K9me2 is thought to correspond to a decrease in the G9a-Like Protein (GLP) methyltransferase, which is involved in H3K9 di-methylation. A mechanism for H3K27me3 upregulation remains elusive [195]. The reciprocal relationship between these histone modifications may serve to repress gene expression, and therefore provide another means of genome protection during epigenetic reprogramming [194].

1.4.2 Remethylation

The re-establishment of DNA methylation in germ cells has been much less extensively characterised. In mice, methylation has been shown to increase from e15.5 at some imprinted loci and repetitive elements, with global remethylation re-established by e18.5 [178,184,196]. Interestingly, whilst the imprinted genes *H19*, Ras Protein-Specific Guanine Nucleotide-Releasing Factor 1 (*Rasgrf1*), and Small Nuclear Ribonucleoprotein Polypeptide N (*Snrpn*) were found to be remethylated by e17.5, their DMRs were only fully methylated in mature sperm, indicating that methylation is augmented postnatally in male mice [196].

Whilst there is variability in the time-points studied, research does indicate that remethylation is at least initiated prenatally in male germ cells. Conversely, data suggests that remethylation occurs postnatally in females. Whilst remethylation of repetitive elements was seen between e15.5 and e17.5 in male germ cells, their female counterparts remained demethylated [184]. The remethylation of imprinted genes also occurs postnatally in females [197]. Interestingly, the timing of remethylation may also be dependent on the parent-of-origin. A bisulfite sequencing study in male germ cells revealed that remethylation of the paternal allele of *H19* is completed prenatally, whilst the maternal allele is remethylated postnatally [198].

Thus, the parental origin of unmethylated alleles can still be identified, although the mechanism by which this occurs remains elusive. This could, for example, involve the ZFP57/ Krüppel Associated Box-associated Protein-1 (ZFP57/KAP1) complex which interacts with imprinting control regions in a parent-of-origin dependent manner, and is involved in the recruitment of DNMT1, 3a and 3b [189].

The DNMT3 family mediate remethylation during the period of epigenetic reprogramming. The DNA methyltransferases DNMT3a and DNMT3b are both active in male and female germ cells during the period of remethylation [199]. Germline-specific DNMT3a knockout mice have disrupted paternal and maternal imprinting. Males have impaired spermatogenesis, and a lack of methylation at some paternally imprinted genes. Offspring of female knockouts had an embryonic lethal phenotype, with a lack of methylation at maternally imprinted alleles. However, germline-specific DNMT3b knockout mice had no detectable defects in imprinting or germ cell function [199]. Although its role appears less pivotal, DNMT3b is exclusively required for the remethylation of satellite repeats in male germ cells. DNMT3b works with DNMT3a in methylating the long interspersed repeats IAP and LINE1, and the DMR of the imprinted gene *Rasgrf1* [200].

Furthermore, a cofactor of the DNMT3 family, DNMT3L, can promote the activity of DNMT3a and 3b by around 15 fold [201]. DNMT3L interacts with DNMT3a to promote its binding to DNA, which may be mediated through a conformational change at the active site. After DNA has bound, DNMT3L will leave DNMT3a. DNMT3a then resumes a normal, closed structure, meaning that DNA is only released slowly from the complex, prolonging the interaction between DNA and DNMT3a [201]. Although catalytically inactive itself, DNMT3L-deficient prospermatogonia showed hypomethylation in imprinted genes and repetitive elements in germ cells. At postnatal day (PND) 0-2 in germline DNMT3L-deficient mice, the DMR of *Rasgrf1* was unmethylated, whilst the *H19* and Delta-like Homolog 1/ Gene Trap Locus 2 (*Dlk1/Gtl2*) DMRs were remethylated. This persisted at PND17 [200]. Kato *et al*. (2007) also report that DNMT3L-deficiency affected the remethylation of repetitive elements, including IAP and LINE1 at PND0-2. DNMT3L deficient germ cells had around 30% of the levels of DNA

methylation of wild-type controls at e16.5. However, by PND6, half of those sites that previously lacked methylation had been remethylated. Loci normally remethylated first were reported to be less susceptible to perturbation by DNMT3L deficiency, suggesting that other mechanisms might be more predominant in the remethylation of these sequences [202]. DNMT3a and 3L therefore have the greatest expression prenatally in male germ cells with DNMT3L deficiency impeding remethylation [202]. DNMT3b mRNA expression increases postnatally in both sexes, peaking at PND6 [203]. This represents different stages in PGC development, with remethylation occurring prenatally in male, and postnatally in female germ cells [184,197]. Therefore whilst a PND6 increase in DNMT3b may facilitate remethylation in females, in males this may work in conjunction with DNMT1 to maintain DNA methylation during rapid division of spermatogonia [203].

In females however, DNMT3a expression remains constant throughout development, and DNMT3L was found to have very high expression in the postnatal female germline, during the period of remethylation [203]. Levels of DNMT3a, 3b and 3L were found to accumulate with increasing oocyte diameter postnatally, during the period of remethylation [204]. When DNMT3a was knocked out in postnatal oocytes, maternal imprinting was disrupted, and this was then transmitted to the next generation. However, repetitive elements were remethylated between fertilisation and e9.5 [205]. Conversely, no effect of DNMT3b knockout was seen on remethylation of imprints or repetitive elements. DNMT3L deficiency corresponded to decreased methylation of IAP and LINE1 (45.8% and 16.1% methylation respectively), in comparison to wild-type controls (62.9% and 32.6% methylation respectively) [205]. Whilst Lucifero *et al*. (2007) also demonstrated aberrant methylation of imprinted genes in DNMT3L-deficient oocytes, they report normal remethylation of IAP and LINE1 [204]. This discrepancy could reflect the fact that Kaneda *et al*. (2010) studied fully mature oocytes (the exact time-point of which is not reported), as opposed to PND15 in Lucifero *et al*. (2007), so there could be a change in methylation state between these time-points. In either case it appears that at least some IAP and LINE1 remethylation can occur with depletion of DNMT3L. This is in contrast to male germ cells, where DNMT3L is required for the remethylation of these transposable elements [200], and suggests that the action of

DNMT3L at these elements is sex-specific [204]. Sex-specificity is also exhibited in the postnatal accumulation of the oocyte-specific DNMT1o. Furthermore, depletion of either this methyltransferase, or of DNMT3L corresponds to an increase in expression of DNMT3b, presumably as part of a compensatory mechanism [204].

1.4.3 Reprogramming in other Mammals

It is not known to what extent epigenetic reprogramming occurs in species other than the mouse. One study indicates that this process also occurs in the pig, and reports demethylation happening asynchronously between genes. For example, demethylation was shown to be complete at e22 for DMR2 of the IGF2 receptor (*Igf2r*), but found to occur gradually between e22-e42 in the *Igf2-H19* regulatory region, suggesting that it is not always a rapid process, and that there is variation between genes [206]. In the same study, global H3K9me2 was found to have a low level by e15, and be absent by e21 in PGCs, as analysed by immunofluorescence. Conversely, H3K27me3 was at a high level between e15-e21, suggesting that histone dynamics are comparable to the mouse. Cell cycle was also studied by introducing a fluorescent DNA stain into isolated PGCs, and analysing the relative amount of DNA in each cell by flow cytometry. As the amount of DNA in the cell varies depending on the stage of cell cycle, the proportion of cells at each stage of cell cycle could then be calculated. At e17, 44% of male germ cells were found to be in G2 cell cycle arrest [206]. Therefore the overall dynamics of epigenetic reprogramming seem comparable between mouse and pig.

Due to a lack of tissue availability there are few published studies in humans. One study used pre-invasive Carcinoma in-Situ (CIS) cells, which the authors report is a neoplastic equivalent of a male fetal germ cell [207]. In contrast to fetal germ cells, CIS cells were found to have low levels of DNA methylation, concurrent with a low expression of both H3K9me2 and H3K27me3 repressive histone modifications [207], the latter of which is increased globally in mouse germ cells to protect the genome during epigenetic reprogramming [181]. Conversely, high levels of H3K4 methylation, H3K9 acetylation and H2A.Z were detected, which are collectively associated with active transcription [207]. High levels of polymerase II activity were

also reported. Similar results were found in fetal testes from weeks 21-24, where global DNA methylation was undetected by immunohistochemistry. However, polymerase II activity was not studied in these tissues [207]. The authors also describe the detection of H3K4 methylation as being much more limited in fetal germ cells, compared to CIS cells, with only around 20% of germ cells having a positive detection for H3K4me2/3. They also report that at week 21-24 the fetal germ cells have finished migrating, but liken their epigenetic profile to that of migrating PGCs in mice [207]. Clearly this state of chromatin decondensation and active gene expression could promote chromatin instability and the subsequent malignant state that might be expected in CIS cells. It is however, intriguing that such a state would exist during the reprogramming of human fetal germ cells. Almstrup *et al*. (2010) suggest that these CIS cells should be reflective of the normal fetal state as previous studies have confirmed that they are derived from PGCs, and because they previously found them to have very similar gene expression profiles [208]. Furthermore, their studies in fetal testes do support the conclusion that they have a similar epigenetic profile at weeks 21-24, and that it differs to that reported in mice. Wermann *et al*. (2010) also identified hypomethylation in human male fetal germ cells at week 15, and suggest that remethylation occurs progressively from week 20 to term. Consistent with studies in mice, 5mC detection was low in pre- and post-natal germ cells in females [209].

Therefore epigenetic reprogramming appears to occur in species other than the mouse, but the mechanisms of reprogramming and of protecting the genome may vary. Clearly a great variation in the length of gestation necessitates that the time-points of epigenetic reprogramming will differ. This in itself might mean that different mechanisms are optimal for different species. In terms of human health, it should be considered that whilst the phase of epigenetic reprogramming may occur over a much longer time period than in the mouse, there is a greater window in which this process might be susceptible to disruption, for example, by environmental factors.

1.4.4 Potential for Alteration of Germline Methylation

As epigenetic reprogramming is clearly such a tightly regulated process, with the potential to influence the next generation, it is important that it is conducted correctly. The male germline may be particularly susceptible to disruption given that methylation is re-established during *in utero* development. Furthermore, the male germline also undergoes many rounds of mitosis after reprogramming, giving greater risk of methylation errors during replication [188].

In recent years there has been an increase in knowledge of the sperm methylome. Molaro *et al.* (2011) used bisulfite sequencing to demonstrate that the majority of promoters are unmethylated in human sperm [210]. Furthermore, Hammoud *et al.* (2014) explored DNA methylation in germline cells in different stages of spermatogenesis, and found that it remained strikingly conserved throughout this process. However, pluripotency genes were found to be 'poised' by DNA hypomethylation and the presence of bivalent chromatin, ready for expression after fertilization [211].

Some studies give an initial indication that *in utero* exposures may influence the germline methylome in offspring. Radford *et al*. (2014) explore the effects of maternal undernutrition during the period of germ cell remethylation in the mouse. As might be expected, the total amount of DNA methylation across the genome was not altered between groups in the sperm of offspring. However, some loci were found to be hypomethylated following maternal undernutrition [93]. Intriguingly, these loci were also found to be hypomethylated in male fetal germ cells at e16.5, suggesting aberrant remethylation in the mouse. This therefore supports the theory that alterations in epigenetic reprogramming of fetal germ cells could correspond to alterations in adult sperm. This is in keeping with Yamaguchi *et al*. (2013) who demonstrate that the methylation profiles of imprinted genes in the sperm of TET1 knockout mice correspond to those for the fetal germ cells at e13.5 [212].

Of the regions seen to be hypomethylated in F1 sperm in the undernutrition model, 43% are known to be resistant to whole embryo reprogramming, suggesting that these changes could influence the phenotype of the next generation [93]. Some of these DMRs corresponded to changes in gene expression of neighbouring genes in

offspring, whilst others did not. This study suggests that even the regions of hypomethylation that do not appear to correlate with changes in gene expression in offspring could ultimately influence the phenotype, for example by altering chromatin compaction [93].

A folate-deficient diet fed to male mice altered methylation of genes associated with development and diabetes [213]. Conversely, in another study in which adult male mice were fed a low-protein diet, there was a high correlation in methylation profiles of their sperm to that of controls, despite the fact that a low-protein diet correlated with altered liver gene expression in offspring [214]. This could be due to differences in the specific diet given, or more crucially, the point of exposure. In Radford *et al*. (2014), and indeed our programming model, the initial insult is given *in utero*, during epigenetic reprogramming, and not to the adult. Because this is a time-point of change in the DNA methylation profile, it could potentially be more susceptible to disruption [93].

Indeed, exposure of the rat fetus to the endocrine disruptors vinclozolin or methoxychlor was seen to alter DNA methylation in the sperm of the adult male. Sperm count and fertility were also decreased, and this phenotype was reported to be conserved in F2-F4 offspring [215]. Testis weight was not altered in adulthood, however there was a decrease in testis spermatid and epididymal sperm numbers, reduced sperm motility, and increased germ cell apoptosis [215,216]. This appeared to correlate with disease phenotype in subsequent offspring [217]. When studying the rat fetal testis directly, gene expression was found to be altered in the F1-F3 generation. The number of genes affected was dramatically reduced with each subsequent generation (F1 2071 genes, F2 1375 genes, F3 566 genes), with 196 genes similarly affected, across all 3 generations [218]. This is in keeping with the Dex-programmed rat, where changes in gene expression are seen to differ between generations, potentially as a reflection of differences in exposure to stimulus [12]. Although DNA methylation in the testis was not studied directly, the expression of DNMT3a was decreased in F1 and F2, and DNMT3L and DNMT1 decreased in F1-F3 testis following vinclozolin exposure. This suggests that there could be corresponding changes in DNA methylation [218]. Confusingly, however, Anway *et*

al. (2008) report that the vast majority (~90%) of genes had a decrease in expression of vinclozolin at e16, rather than the increase that might be expected from a lack of methylation [218]. This suggests that although DNA methylation may be affected, other factors are more dominant in regulating gene expression in this model. However, the authors subsequently went on to show changes in DNA methylation in sperm in the F1-F3 adult offspring of the vinclozolin model in rats [219] and mice [220]. In rats, differential methylation was reported at a wide variety of promoters, including transcriptional repressors, inflammatory mediators and olfactory receptors, whilst in mice, changes were reported in regulators of transcription and of the extracellular matrix and cytoskeleton. There was however no correlation between genes identified in rat and those in mice [219,220].

However, another group studied the vinclozolin model, and reported no effect on spermatid/sperm count or motility, or on germ cell apoptosis in F1-F3 offspring of the vinclozolin-exposed rat [221]. It should be considered that the route of vinclozolin administration is different between these studies, with Schneider *et al.* (2008) giving oral administration whilst Anway *et al*. give intraperitoneal injection. The exact timing of sacrifice of the adult males may also vary between the studies, with Anway *et al*. (2005) reporting sacrifice between PND 60-180, whereas the timeframe was much narrower (PND 127-134) for studies by Schneider *et al*. (2008). The former also used Sprague Dawley rats, whilst the latter conducted studies in Wistar [215,221]. It is therefore difficult to be sure exactly why these studies differ, and which reflects the most biologically relevant characterisation of the effects of vinclozolin exposure.

It should be considered that changes in DNA methylation in the germline may not be fully heritable, particularly as both the fetal germ cell and the early-stage zygote undergo epigenetic reprogramming. However, as discussed previously, imprinted genes may be resistant to this demethylation, and therefore represent key targets for epigenetic inheritance, particularly as they often confer growth and developmental regulation [188,190]. More recently, it has also been shown that other gene regions, particularly those corresponding to repeat regions, are resistant to reprogramming, and their methylation patterns could therefore be directly inherited [183]. It is also

intriguing that remethylation can occur in a parent-of-origin specific manner, suggesting that a 'memory' of origin, and potentially DNA methylation patterns remains, even in reprogramming [198]. Furthermore, if the period of exposure occurs during remethylation, after bulk erasure has taken place, there may be less potential for correcting any disruption.

Some studies have shown a phenotype resulting from changes in sperm DNA methylation. Pre-diabetic adult mice were found to have alterations in methylation in their sperm which correlated with methylation patterns in the pancreatic islets of their subsequent offspring. This supports the theory that inducing changes in the sperm methylome correlates with changes in the phenotype and methylome of offspring [222]. Neonatal stress in mice, by maternal separation, was found to alter methylation profiles at certain target genes in subsequent adult sperm, which had corresponding changes in the brains of their offspring [223].

Little is known about the effects of the Dex-programming model on germline methylation. The effects of Dex exposure on the fetal germ cell have not previously been studied and little is known about the effect on sperm. One study used a candidate gene approach to look at methylation of *Igf2* and *H19* in F1 sperm following fetal Dex exposure, but found no difference in methylation between groups [12]. However it may be that the specific target genes, or the regions within them, that were studied are not reflective of the genome as a whole. Indeed, a transgenerational effect of increased *H19* gene expression in F2 liver was subsequently only seen carried through the maternal line. My study therefore seeks to build on this work by giving a more global characterisation of the effects of Dex on the adult sperm.

Knowledge of such processes in humans is more limited. However male infertility has been shown to correspond to decreased methylation at the DMRs of *Igf2* and the *Igf2/H19* imprinting control region in sperm [224,225]. Conversely, methylation of the Mesoderm-Specific Transcript (*Mest*) imprinted gene was increased [225]. Two other studies have similarly reported hypomethylation of *H19* and hypermethylation of *Mest* in infertility [226,227]. Interestingly, a recent study showed that gestational diabetes produced offspring with decreased *Mest* methylation in cord blood and

placenta, and that *Mest* methylation negatively correlated with obesity in adulthood. [228]. *H19* hypomethylation has been associated with Silver-Russell Syndrome, conferring growth retardation both pre and post-natally, amongst other symptoms [229]. It therefore seems that the methylation of genes for growth and metabolism can be altered in sperm.

Research has also shown that there are other epigenetic marks which may be influenced in the germline. As previously discussed, histones undergo alteration during the period of epigenetic reprogramming in germ cell development. Therefore these modifications could also be susceptible to change during this critical period of development. Histones are removed and replaced with protamines during spermatogenesis, promoting the formation of highly compacted chromatin [230]. This may protect the paternal DNA from chemical and physical damage, and help sperm to have a hydrodynamic shape, facilitating swimming [231]. Nucleosomes containing histones are found in 1% of the paternal mouse genome [232], and 15% of the human genome in mature sperm [233]. This suggests the potential for inheritance of histone marks, which intriguingly, are particularly enriched in GpG-rich loci which lack DNA methylation [234]. Indeed, Hammoud *et al*. (2009) report that some histones, including H3K4me3 and H3K27me3 were found to be retained in mature sperm at some promoters, particularly those corresponding to developmental genes [235]. H3K4me3 levels were also increased at imprinted genes such as *Igf2* and *H19*, in comparison to other regions [235]. However, very recent studies have largely contradicted this work, suggesting that the majority of sperm histones are located in gene-poor regions, with few being associated with developmental regulators [236,237]. However, they were reported to associate with repetitive elements, including LINE1 in human sperm [237].

A low-protein diet corresponded to changes in levels of histone H3K27me3, although only at 2 gene loci [214]. Acetylated H3K9 was also increased in developing spermatids following diet-induced obesity in mice [238]. Folate deficiency also reduced H3K4 and H3K9 monomethylation and H3K9me3 levels in the sperm epigenome [213]. Although corresponding changes in offspring histone

levels were not examined, this suggests that there is a possibility for changes in histone levels to influence the next generation.

RNA is also found in mature sperm, some of which have relevance for embryonic development after fertilisation [239]. A high-throughput sequencing study indicated that sperm contain both mRNA and Small Non-Coding RNA (sncRNA) and two of the most highly expressed sncRNA were found not only in sperm, but also in embryos, at the one-cell and preimplantation stages [240,241]. This indicates that they may have some role in early development. Indeed, when transgenic mice expressed the miR-124 miRNA in sperm, or when this miRNA was injected directly into a fertilised mouse egg, pups had a 30% increase in birth weight [242]. Similarly injection of miRNA into a fertilised egg produced offspring with variations in tail colour [243] or cardiac function [244]. The latter phenotype was also found to be inducible by fertilisation of an egg with sperm containing the miR-1 miRNA, which correlated with decreased expression of the Cyclin-Dependent Kinase 9 (*Cdk9*) gene, involved in regulating cardiac growth [244].

Very recently, Gapp *et al.* (2014) explored the effects of traumatic stress in early postnatal life on the expression of sncRNA. An intergenerational phenotype was exhibited in this model, with the F2 generation having lower baseline plasma insulin and glucose, and reduced plasma glucose rise during a Glucose Tolerance Test (GTT), indicating insulin hypersensitivity [241]. Exposure to traumatic stress affected the expression of a range of sncRNA in F1 sperm, and in F2 plasma and hippocampus. RNA from sperm of stressed F1 males was then injected into control fertilised eggs, giving offspring with a similar phenotype to those exposed directly to the stressful stimulus. This adds weight to the suggestion that the phenotype was at least in part carried in the sperm RNA. However, whilst dysregulation of miRNA expression was resolved by the F3 generation, these animals still displayed a behavioural phenotype, and so the authors suggest this might be the involvement of other epigenetic mechanisms such as DNA methylation [241].

Thus, the transmission of the programming phenotype may involve a combination of epigenetic mechanisms. I decided to focus on DNA methylation because it undergoes dramatic remodelling in the fetal germ cell, during the period of Dex exposure, and it

has been hypothesised that it might be particularly susceptible to modification. The finding that DNA methylation is stable throughout spermatogenesis also indicates that patterns established in the fetal germ cells, which then become adult spermatogenic progenitor cells, may be maintained in sperm [211].

Although this area has not yet been studied extensively, taken together, these studies support the hypothesis that a) environmental factors may influence germ cell gene expression and DNA methylation b) fetal germ cell methylation can influence adult sperm methylation patterns and c) that adult sperm methylation can impact upon the methylation and phenotype of the next generation.

1.5 Aims and Hypotheses

The hypothesis of my PhD was therefore that the fetal programming of cardiovascular disease risk confers a change in DNA methylation within the developing germ cell. This would then ultimately allow the phenotype to be transmitted to the next generation through the germline.

To test this hypothesis there were four key aims:

1. To characterise baseline epigenetic reprogramming in the male rat fetal germ cell, confirming that this process previously studied in the mouse also occurs in the rat, giving a timeframe for the phase of remethylation and exploring the presence of all known forms of DNA methylation.
2. To explore the effects of Dex exposure on global methylation during the established timeline.
3. To characterise EGFP expression and fetal programming in GCS-EGFP rats, and to use them to study gene-specific changes in methylation in fetal germ cells and subsequent adult sperm of rats exposed to Dex *in utero*.
4. To explore gene expression and DNA methylation in the livers of Dex-programmed wild-type and GCS-EGFP rats.

Chapter 2 Materials and Methods

2.1 Materials

2.1.1 General Chemicals

All general chemicals were purchased from Sigma-Aldrich Ltd., UK, except the following:

Agarose	Bioline, UK
Bouins Fluid	Clin-Tech Ltd, UK
Ethanol	VWR International, UK
Hydrochloric Acid	VWR International, UK
Methanol	VWR International, UK
Xylene	Thermo Fisher Scientific, UK

2.1.2 Molecular Biology

Agilent RNA 6000 Nano Kit	Agilent, USA
DNeasy Blood and Tissue Kit	QIAGEN, USA
High Capacity cDNA Reverse Transcription Kit	Applied Biosystems, USA
LightCycler 480 Probes Master Mix	Roche Diagnostics Ltd, USA
Multiplex PCR Kit	QIAGEN, USA
Qubit DNA High Sensitivity Assay Kit	Life Technologies, USA
Qubit RNA Broad Range Assay Kit	Life Technologies, USA
RNeasy Micro Kit	QIAGEN, USA
RNeasy Mini Kit	QIAGEN, USA

SYBR Green Master Mix	Roche Diagnostics Ltd., USA
TaqMan Gene Expression Assays	Applied Biosystems, USA
100bp DNA ladder	Invitrogen, USA

2.1.3 Immunofluorescence

Alexa Fluor 488 Streptavidin	Invitrogen, UK
Chicken anti-Rabbit Peroxidase-Conjugated Secondary Antibody	DAKO Corp., USA
DAZL Antibody	AbD Serotec, UK
DMRT1 Antibody	A kind gift from Mark Murphy, Liverpool John Moores University
DNMT3a Antibody	Abcam, UK
DNMT3b Antibody	Abcam, UK
DNMT3L Antibody	Abcam, UK
EGFP Antibody	Invitrogen, USA
Fetal Calf Serum	Biosera, UK
Goat anti-Rabbit Alexa Fluor 555	Invitrogen, UK
Goat anti-Rabbit Peroxidase-Conjugated Secondary Antibody	DAKO Corp, USA
GR M20 Antibody	Santa Cruz Biotechnology, USA
ImmPress Diaminobenzidine (DAB)	Vector Laboratories, USA
ImmPress Ig (peroxidase) Polymer Detection Kit	Vector Laboratories, USA

Normal Sera (horse, goat, rabbit, chicken)	Biosera, UK
Perkin Elmer-TSA-Plus Cyanine 3 System	Perkin Elmer Life Sciences, USA
Perkin Elmer-TSA-Plus Cyanine 5 System	Perkin Elmer Life Sciences, USA
PermaFluor Aqueous Mounting Medium	Thermo Fisher Scientific, USA
Rabbit anti-Chicken Peroxidase -Conjugated Antibody	Sigma, USA
Surgipath APEX Superior Adhesive microscope slides	Leica Microsystems Ltd., UK
TDG Antibody	Sigma, USA
Vasa Antibody	Abcam, UK
Vimentin Antibody	Dako Corp., USA
5mC Antibody	Eurogentec, UK
5hmC Antibody	Active Motif, Belgium
5fC Antibody	Active Motif, Belgium
5caC Antibody	Active Motif, Belgium

2.1.4 Animals

GCS-EGFP Sprague Dawley Rats	Bob Hammer, University of Texas South Western, USA
Soya Free Diet (RM3 (E))	Special Diets Services, UK
Sprague Dawley Rats	Charles River, UK

Standard Laboratory Chow	Special Diets Services, UK
Wistar Rats	Charles River, UK

2.2 Equipment

Agilent 2100 Bioanalyzer System	Agilent, USA
BXT-20.M Transilluminator	Uvitec, UK
Cell strainer (70µm)	Becton Dickinson Falcon, USA
Comfort Thermomixer	Eppendorf, Germany
Decloaking Chamber	Biocare Medical, USA
DNA Speed Vac DNA 110	Savant Instruments Inc., USA
Electrophoresis PowerPac 300	Biorad Laboratories Inc., UK
Eppendorf Centrifuge 5415C	Eppendorf, Germany
FACSAria II Special Order System sorter	Becton Dickinson Falcon, USA
G-storm thermocycler	Gene Technologies, UK
Humidity Chamber	Fisher Scientific, UK
Labofuge 400R Centrifuge	Heraeus, UK
LSM 710 Meta confocal microscope	Carl Zeiss Ltd., UK
Microtome (RM2125RTF)	Leica, Germany
Nanodrop ND-1000 Spectrophotometer	ThermoScientific, USA
OPTImax Plate Reader	Molecular Devices, UK
pH Meter (3510)	Jenway, UK
PRO 200 homogeniser	PRO Scientific Inc., USA

Provis AX70 microscope	Olympus Optical, UK
Qubit 2.0 Fluorimeter	Life Technologies, USA
Roche 480 LightCycler	Roche Diagnostics Ltd., UK
Rotamixer Vortex	Hook and Tucker Instruments, UK
Rotary Microtome	Leica Microsystems Ltd., UK
Sub-cell 96 electrophoresis tank	Biorad Laboratories Inc., UK

2.3 Software

Image J	National Institute of Health, USA
Photoshop CS5.1	Adobe Systems Inc., USA
SPSS Statistics 21	International Business Machines Corporation (IBM), USA
Statistica 10	StatSoft, USA

2.4 Solutions

Agarose gel	1.2% (for RNA) or 2 % (for DNA) agarose (Bioline, UK) was dissolved in 0.5 X TBE whilst heating. 5-10 µl (depending on gel volume) of GelRed Nucleic Acid Stain (Biotium, USA) was then added to the solution.
0.5M EDTA	23.265g of EDTA (Ethylenediaminetetraacetic acid) was dissolved in MilliQ water (Millipore, USA) to give a final volume of 250ml. Solution was adjusted to pH 8.0 using HCl.
Orange G	30ml of glycerol and 0.25g of Orange G (Sigma) were combined, and made up to 100ml with Polymerase Chain Reaction (PCR)-grade H_2O.
PBS	1 Phosphate Buffered Saline (PBS) tablet was dissolved in 200ml MilliQ water, giving 0.01M phosphate buffer, 0.0027M Potassium Chloride, 0.137 M Sodium Chloride.
TBS	60.5g Tris and 87.6g NaCl were dissolved and made up to 1l in MilliQ water to give Tris Buffered Saline (TBS).
10 x TBE	108g of tris, 55g of boric acid and 40ml of 0.5M EDTA were combined, then made up to 1 litre with MilliQ water to give Tris/Borate/EDTA (TBE).
TE	2.5ml of 1M Tris (pH8) and 0.5ml of 0.5M EDTA was combined and made up to 250ml with MilliQ water to give Tris-EDTA.

2.5 Animals

All animals were maintained in an environment of controlled humidity, temperature (22°C), and lighting (artificial light between 7.00am-7.00pm), and had constant access to standard laboratory chow and water, except where indicated. All procedures were licenced by the UK Home Office, and completed in accordance with the UK Animals (Scientific Procedures) Act 1986.

2.5.1 Wistar Rats

2.5.1.1 F1 Metabolic Studies

Female Wistar rats with an initial mass of 200-250g were acclimatised to the research facility for two weeks before breeding. These animals were then individually housed with a stock Wistar male of similar age. Following expulsion of a vaginal plug (e0.5), females were housed individually for the duration of gestation (21-22 days), and body mass recorded daily. Subcutaneous injections were administered to pregnant females every morning, before 9.30am from e15.5-e22.5 inclusive. Dex (≥97% purity, Sigma) suspended in ethanol (4%) and normal Saline (0.9%) was given to the Dex treatment group (dosage of 100 µg Dex per kg of rat body mass), and an equivalent volume of ethanol (4%) and Saline (0.9%) to the Saline control group.

At e20.5, a proportion of mothers were sacrificed by cervical dislocation, and pups and placentas excised from the womb and weighed. Placental labyrinth and new-born liver were extracted from 6 pups, and snap frozen on dry ice.

The remaining dams were maintained until the end of gestation. Pups were delivered naturally between e21.5-e23.5, and weight recorded, before culling to 8 per litter, retaining similar numbers of both sexes. Livers were collected from supernumerary pups on the day of birth, and snap frozen on dry ice, before storage at -80°C.

At both the peripubertal stage (28 days) and at maturity (over 90 days) one quarter of males were sacrificed by decapitation, following CO_2 asphyxiation. Liver, kidney,

spleen, heart and retroperitoneal and mesenteric fats were harvested, snap frozen on dry ice, and stored at -80°C.

2.5.1.2 F1 Baseline Epigenetic Reprogramming Studies

Tissues for baseline epigenetic reprogramming studies were collected by Prof Richard Sharpe's Lab group, where all animals are maintained on Soya-free research diet (RM3(E) soya free, Special Diets Services, UK). Pregnant dams were killed by CO_2 asphyxiation and subsequent cervical dislocation at experimental time-points of e14.5-e19.5 and e21.5 (gestation is ~22 days in our colony). A further time-point (e20.5) was added as part of the current study. At e14.5-e19.5, pups were sexed by dissection, and at e20.5 and e21.5, by examining the AGD which is two-fold greater in males relative to females. Testes were removed from all male pups, and fixed for 1 hour in Bouins Fluid (Clin-Tech, UK). Tissues were then stored in 70% ethanol, before embedding in paraffin wax by the Shared University Research Facilities (SURF) histology group, The University of Edinburgh. Embedded tissues were then cut into 5µm thick sections using a microtome (Leica Microsystems, Germany), and mounted onto Surgipath APEX Superior Adhesive microscope slides (Leica Microsystems), before drying in the oven at 50 °C overnight.

2.5.1.3 F1 Methylation and Glucocorticoid Testis Time-line Studies

Virgin females were mated to males (both Wistar), and Dex and Saline solutions administered as outlined above. At time-points of e18.5, e19.5, e20.5 and e21.5 pregnant dams were sacrificed, and pups removed and weighed. Testes were removed by microdissection and processed as previously.

2.5.2 Sprague Dawley GCS-EGFP Rats

Sprague Dawley GCS-EGFP homozygous males, developed by Cronkhite *et al.* (2005) and supplied by Professor Bob Hammer (University of Texas Southwestern) [92], were crossed to wild-type females. Embryo transfer was performed into

recipient wild-type females to allow transfer into a clean animal facility. This was conducted by technical staff at the Biomedical Research Facility Animal Unit, The University of Edinburgh. Hemizygous offspring from these crosses were subsequently bred in order to establish a homozygous colony. Testis, Liver, heart, kidney and spleen were collected from founder males. Some tissue was snap frozen for RNA studies, and further samples were stored in formalin for 24 hours before storage in 70% ethanol. Tissues were then embedded in paraffin wax and microtomed to give 5µm sections, by SURF technicians.

2.5.2.1 F1 Fetal Germ Cell Studies

GCS-EGFP virgin females were mated with GCS-EGFP males, and sacrificed at e19.5, following the protocols above. Testes were extracted by microdissection and pooled to give one sample per litter. 100 µl of collagenase IV (Sigma) (1mg/ml in Hank's Balanced Salt Solution (HBSS, Life Technologies, USA)) was added to a 4-well plate, along with 6-8 fetal testes. Tissue was disaggregated using hypodermic needles, and the resulting suspension placed into a 1.5ml eppendorf. The well was then washed with 4 x 100µl of collagenase, subsequently added to the eppendorf. The resulting solution was placed on a Comfort Thermomixer (Eppendorf, Germany) at 37 °C and 650 rpm for 5 min to promote tissue disaggregation. Samples were then mixed before a further 2 x 5 min of thermomixing, yielding a single-cell suspension. Cells were then pelleted by centrifuging for 5 min at 1200 xg, and re-suspended in PBS to remove the collagenase. Cells were pelleted by further centrifugation before re-suspension in PBS supplemented with 2% fetal calf serum (FCS, Biosera, UK), inhibiting the action of residual collagenase. A further centrifugation step was performed before final re-suspension in 500 µl PBS/2% FCS. The solution was passed through a 70µm strainer (Becton Dickinson Falcon, USA) to remove any cell clumps that might damage the FACS machine. Germ cells were then isolated from the suspension by FACS sorting for EGFP using a BD FACSAria II Special Order System sorter (Becton Dickinson).

2.5.2.2 F1 Adult Sperm Studies

In order to generate pure sperm samples from first generation adult rats, GCS-EGFP virgin females were mated with GCS-EGFP males, and Dex and Saline solutions administered to pregnant dams from e15.5 as previously. Pups were delivered naturally between e21.5-e23.5, and weight recorded, before culling to 8 per litter, retaining similar numbers of both sexes. These pups were then weaned at PND 21-23, and subsequently maintained on standard laboratory chow.

Males were culled at 90 days, and epididymes removed. Each epididymis was nicked 4 times, evenly spaced along the length of the structure, and placed in a separate 15ml Falcon tube containing 5ml swim buffer (10% FCS, 2% Bovine Serum Albumin (BSA) in F12/DMEM (Life Technologies)). Samples were gently rocked for 45 min with occasional mixing, allowing the sperm to swim out of the epididymis. The epididymis was then removed from the tube, and sperm cells were pelleted by centrifugation for 7 min at 600 xg. The swim buffer was then removed, before the pellet was re-suspended in 2.5ml of 2% FCS/PBS. Sperm samples from both epididymes were combined, yielding 1 sample per animal. Resulting solutions were then passed through a cell strainer, and then kept on ice until FACS sorting. Pure populations of sperm were isolated from contaminants by sorting for EGFP expression as above.

2.5.2.3 Producing a Second Generation

In order to ensure that transgenerational effects on birth weight would be found in GCS-EGFP rats, as in studies of Wistar rats, a second generation were bred. In order to limit use of animals and resources, only 2 of the potential 4 crosses (shown in Figure 2.1) were bred. A Saline mother to Dex father cross (denoted SD) was chosen as this parentage was shown to have the greatest phenotypic effect in Wistar studies. This also allowed programming through the male line, a particular focus of this PhD, to be examined. Saline mothers were also mated with Saline fathers to give control offspring (denoted SS). Parents were mated as previously, and pregnancies allowed to progress without intervention. Pups were sexed and weighed at birth, before

animals were killed by decapitation, and livers from 3 males per litter extracted and snap frozen as previously.

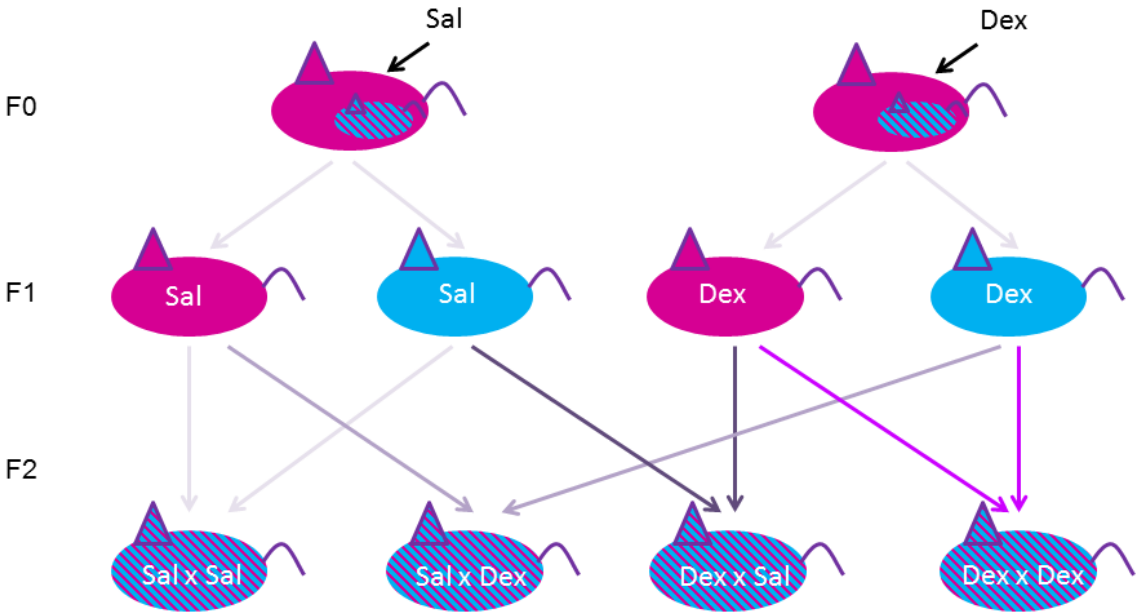

Figure 2.1. Producing a second generation. Pregnant dams (F0) were injected with either Dex or Saline (Sal) solutions from e15.5. Their offspring (F1) were then termed Dex or Saline based on this exposure in utero. They could be mated to produce 4 possible combinations of parentage for the 2nd generation (F2); Saline mother x Saline father, Saline mother x Dex father, Dex mother x Saline father, Dex mother x Dex father. This would give offspring denoted SS, SD, DS and DD respectively. For GCS-EGFP studies only SS and SD crosses were bred. Blue denotes male and red female offspring.

2.6 Genotyping

2.6.1 Sex-determining Region Y

Genotyping for the Sex-determining Region Y (*Sry*) was conducted to identify male pups from Wistar F1 and F2 metabolic studies. DNA was extracted from limb tissue, as outlined in section 2.14, and diluted 1:10 in PCR-Grade H_2O. Samples were then analysed using *Sry* primers (see Table 2.1) and the Multiplex PCR Kit (QIAGEN, USA), following manufacturer's instructions. Thermocycling was conducted on a G-Storm thermocycler (Gene Technologies, UK) with 10 min incubation at 95°C followed by 45 cycles of denaturation, annealing and extension (95°C, 58°C and 72°C respectively, for 20 seconds each) and then 7 min at 72°C. Products were then combined with 5 µl Orange G loading buffer (30% glycerol, 0.25% Orange G (Sigma)) (1:1 v/v) and run on a 2% agarose/0.5% TBE gel, submerged in 0.5% TBE in an Sub-Cell 96 tank (Biorad, UK), with attached Power Pac 300 (Biorad). DNA ladder (100 base pairs, Invitrogen, USA) was run in parallel, as a marker for band size. The gel was run at 100V for 45 min, before imaging using a BXT-20.M Transilluminator (Uvitec, UK). Product size was then compared to the DNA ladder, and a positive and negative control, taken from known males and females respectively (see Figure 2.2).

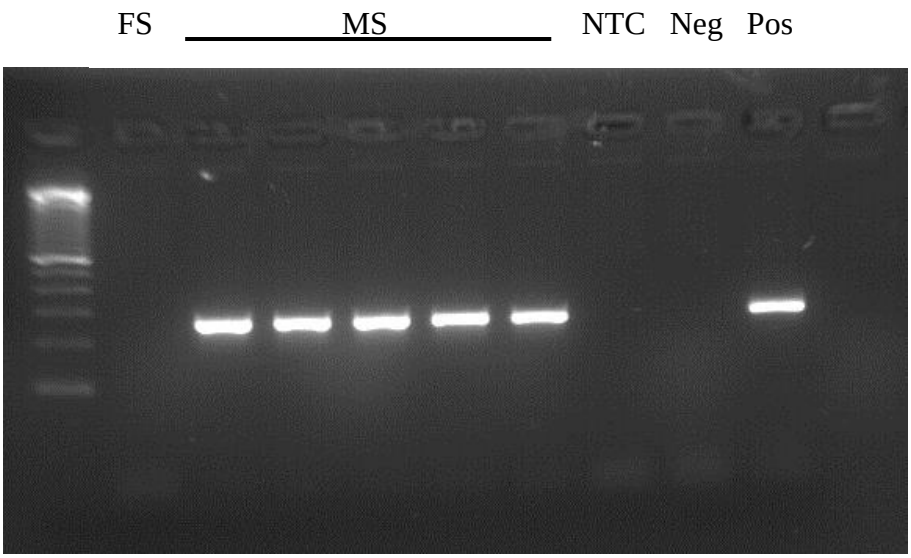

Figure 2.2. *Sry* genotyping. Samples from pups of unknown sex were genotyped, with a positive band for the *Sry* gene indicating male origin. Gel shows a female sample (FS), male samples (MS), a no-template PCR control (NTC), and controls of known female (Neg) and male (Pos) origin. Positive bands are seen for the male control, and not the female control, confirming that sex differences are being identified.

2.6.2 GCS-EGFP

DNA was extracted from ear clips as outlined in section 2.14, and diluted 1:10 with dH_2O. The presence of the EGFP insert was then determined using EGFP primers (see table 2.1) and the Multiplex PCR kit. Thermocycling was conducted and products run on a gel as above. Product size was compared to the DNA ladder and positive and negative controls, from rats known to be homozygous, or negative for the EGFP insert (Figure 2.3).

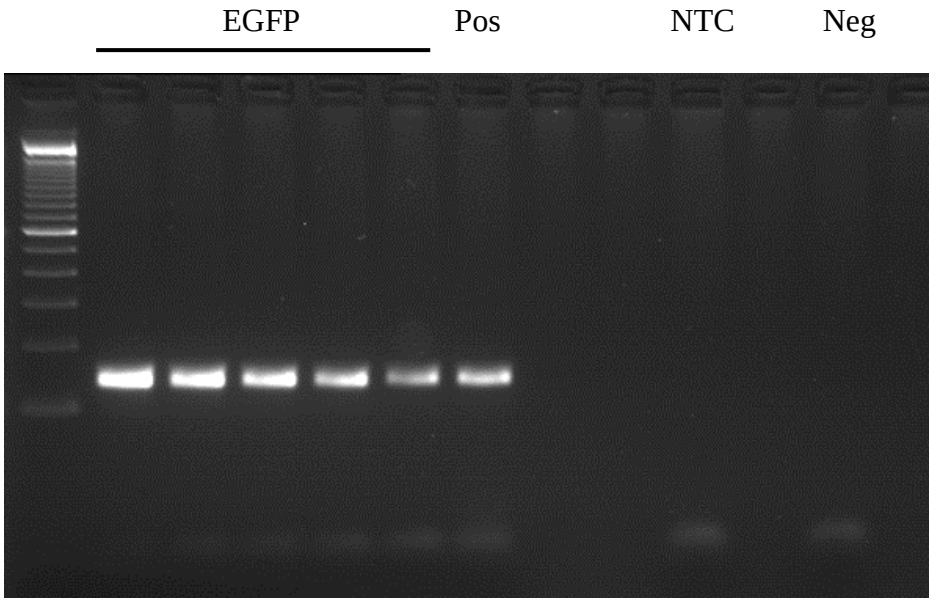

Figure 2.3. Genotyping for GCS-EGFP. Offspring of colony establishment process were genotyped to confirm the presence of the EGFP insert. A positive band was seen for a sample from a known homozygote positive control (Pos), but not from a Wistar rat (Neg). Samples from offspring (GFP) had a positive band, indicating the presence of the EGFP insert. A band was absent from the no-template PCR control (NTC) sample.

2.7 Immunohistochemistry

All tissue sections for immunohistochemistry were dewaxed in xylene, and rehydrated by incubation in progressively more dilute ethanol solutions (100%, 95%, and 70%). All washes were in TBS, and all antibody and reagent incubations performed at room temperature, in a humidity chamber, unless otherwise stated.

2.7.1 Preparation for Methylation Staining

The following procedures were conducted in preparation for all methylation immunohistochemistry protocols, unless otherwise stated. Following re-hydration, endogenous peroxidase activity was blocked by a 30 min treatment of incubating tissues in 3% (v/v) Hydrogen peroxide/methanol. Tissue was permeabilised, to allow

antibody access, with 1% Triton X-100 (Sigma, UK) in TBS for 30 min. DNA was then denatured to further increase antibody availability, by a 15 min incubation in 4M Hydrochloric Acid (HCl)/TBS, preheated to 37°C. Slides were washed with 0.1% Tween (Sigma) in TBS.

2.7.2 5mC and 5hmC Immunohistochemistry

Following preparation above, tissues were blocked with normal horse serum (NHS; Biosera) diluted 1:5 with 5% (w/v) BSA in TBS (NHS/TBS/BSA), before incubation with 5mC (1:300, mouse, Eurogentec, UK) or 5hmC (1:300, rabbit, Active Motif, Belgium) antibody overnight at 4°C. Slides were then washed and antibody detected using the ImmPress anti-mouse or anti-rabbit Ig (peroxidase) Polymer Detection Kit (Vector Laboratories, USA) and ImmPress Diaminobenzidine (DAB, Vector Laboratories) following manufacturers' instructions. Slides were counterstained with Surgipath Hematoxylin Harris (Leica), dehydrated in ethanol and mounted in Pertex media (Cell Path, UK).

2.7.3 5mC and 5hmC Double Immunofluorescence

Following preparation as above, tissues were blocked with Normal Goat Serum (NGS; Biosera) diluted 1:5 with 5% (w/v) BSA in TBS (NGS/TBS/BSA), before incubation with 5mC (1:100) antibody overnight at 4°C. Slides were washed before the addition of goat anti-mouse biotinylated secondary antibody (1:500, Dako Corp., USA), subsequently detected during a 60 minute incubation with Alexa Fluor 488 streptavidin (1:200, Invitrogen). Following further washing, slides were blocked with NGS/TBS/BSA and incubated with 5hmC (1:50) antibody overnight at 4°C. Goat anti-rabbit Alexa Fluor 555 (1:200, Invitrogen) was used to detect the primary antibody, before mounting in PermaFluor Aqueous Mounting Medium (Thermo Fisher Scientific, USA).

2.7.4 Seeking a Nuclear Counterstain

The HCl treatment required for antigen retrieval in these studies was found to prevent the specific binding of 4',6-diamidino-2-phenylindole (DAPI) to nuclei. Therefore, in order to optimise a method for nuclear counterstaining compatible with these protocols, some tissue sections were taken through the methylation staining preparation protocol, before incubation with Sytox Green (Invitrogen), TO-PRO (Invitrogen) or Propidium Iodide (Sigma) (all 1:500) for 45 min. Control slides were taken through the methylation staining preparation protocol, omitting incubation in HCl. All stains were found to be nuclear specific in control tissues, whilst neither Sytox Green nor TO-PRO was found to have nuclear specificity on tissue treated with HCl (see Figure 2.4). However, Propidium Iodide was found to be effective on these tissues, when imaged using maximum laser power.

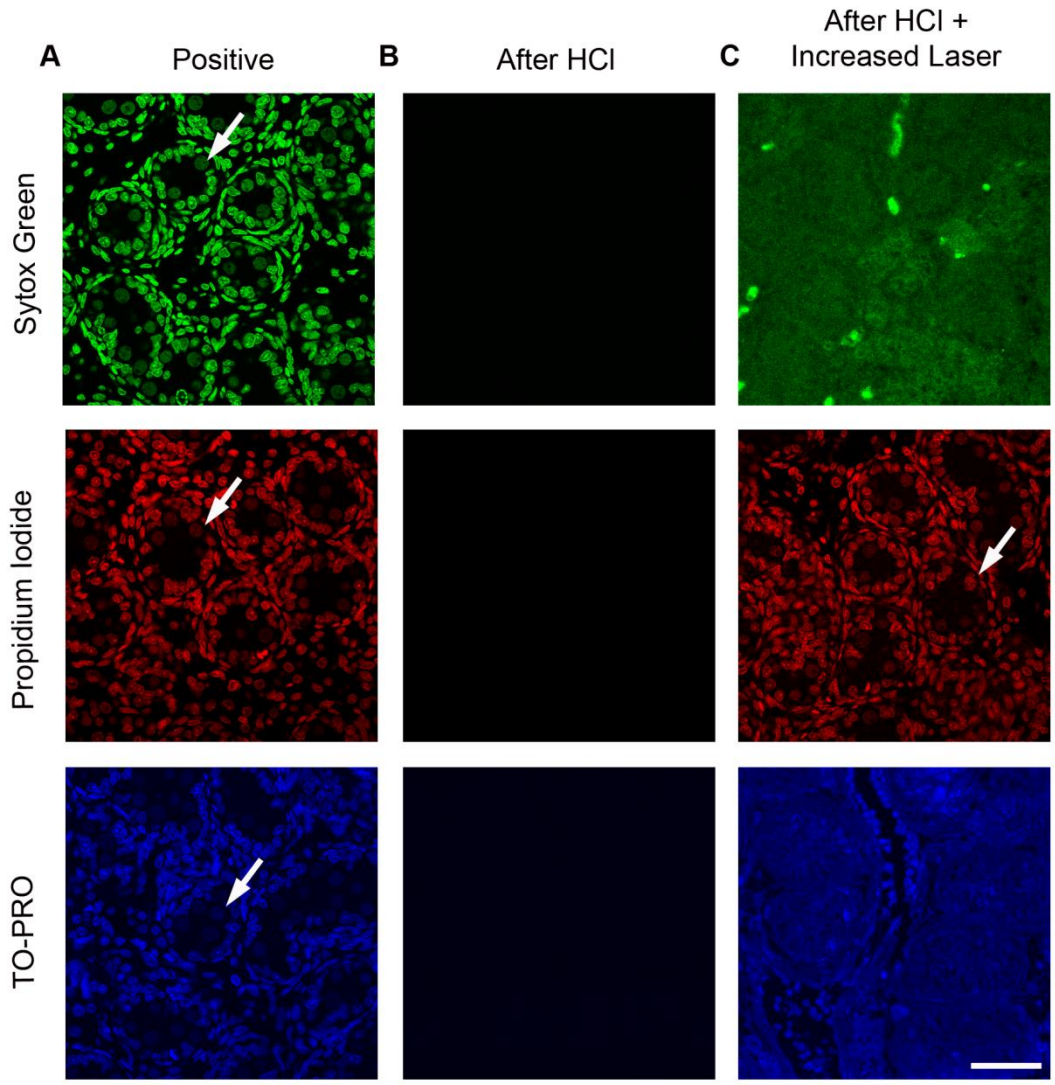

Figure 2.4. HCl treatment affects binding of nuclear stains. e21.5 fetal testis was prepared for immunohistochemistry, with or without incubation in HCl. (A) Sytox Green (Green), Propidium Iodide (red) and TO-PRO (Blue) staining for nuclei is seen in tissue without exposure to HCl (arrows). (B) Using the same confocal microscope settings, no staining is visualised in tissue treated with HCl. (C) Increasing laser power reveals that Sytox Green and TO-PRO staining is no longer nuclear-specific. Nuclei are visualised with Propidium Iodide (arrows). Bar = 50µm.

2.7.5 5fC and 5caC Immunofluorescence

Following tissue preparation as above, tissues were blocked with NGS/TBS/BSA and incubated with either 5fC or 5caC (1:200 or 1:1500 respectively, both Active Motif) overnight at 4°C. Antibodies were detected using goat anti-rabbit Alexa Fluor 555 (1:200) in TBS.

2.7.6 Seeking a Germ Cell Specific Marker

The HCl treatment required for antigen retrieval in these studies was found to prevent the binding of the germ cell marker Vasa. Therefore, another germ cell marker, Deleted in Azoospermia-like (DAZL), was selected, and protocols optimised for its use. Conditions of retrieval pH, detection method, permeabilisation and primary antibody concentration were all optimised, as highlighted in the summary diagram below (Figure 2.5).

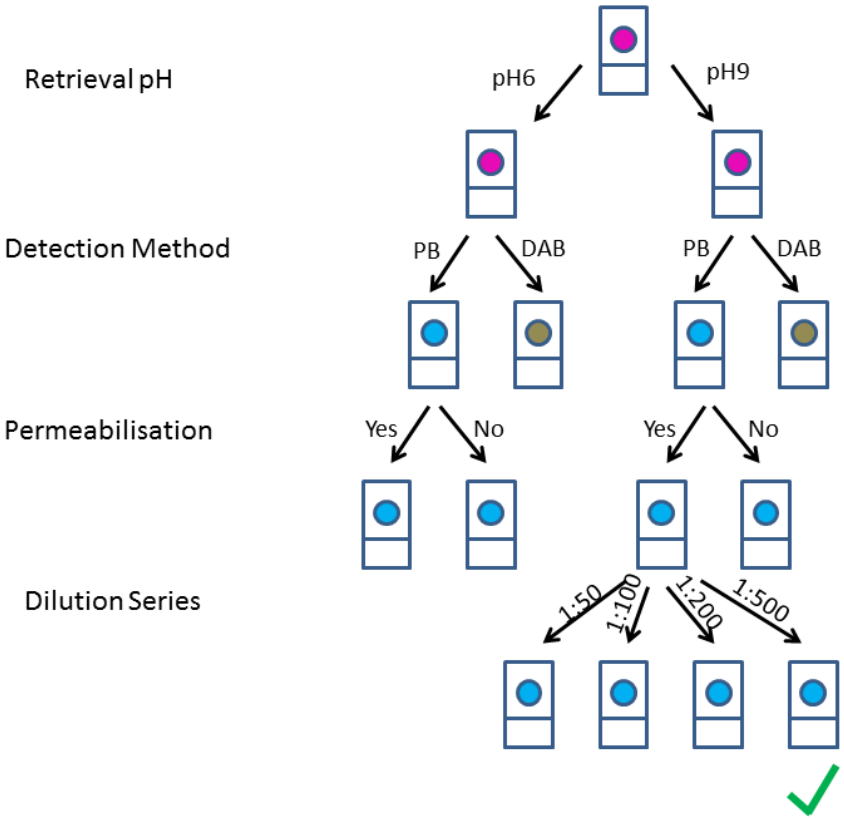

Figure 2.5. Optimisation of DAZL staining. Slides were exposed to different retrieval pH (pH6 and pH9), detection methods (PermaBlue (PB) or DAB), permeabilisation conditions (with (Yes) or without (No) 1% Triton) and antibody dilutions (1:50, 1:100, 1:200 or 1:500). The clearest staining, in conjunction with 5mC was found with antigen retrieval at pH9, PermaBlue detection, 1% Triton permeabilisation, and an antibody dilution of 1:500 (green tick). Pink dot represents pre-stained tissue. Blue dot indicates detection with PermaBlue and brown dot, with DAB.

2.7.6.1 Optimising DAZL Retrieval pH and Detection System

As incubation with HCl for methylation antibodies might alter the pH of tissue sections, it was decided that altering the retrieval pH for DAZL might buffer the effects of HCl and promote antibody binding. It was also hypothesised that different antibody detection systems might survive subsequent exposure to HCl and retain their colour. Therefore retrieval pH and detection systems were optimised.

Tissue sections were de-waxed and rehydrated as above, but not taken through the standard methylation staining preparation protocol. Tissues were then submerged in

either Novocastra Epitope Retrieval Solution (pH9, Leica) or 0.01M citric acid (pH 6, Sigma) and pressure cooked for 5 min at 125 °C in a Decloaking Chamber (Biocare Medical, USA). Endogenous peroxidase activity was then blocked by incubation in 3% (v/v) hydrogen peroxide/methanol. Tissues were blocked with NGS diluted 1:5 with 5% (w/v) BSA in TBS (NGS/TBS/BSA), before incubation with DAZL (1:50, mouse, AbD Serotec, UK) antibody overnight at 4°C.

Slides for PermaBlue end point were then washed and incubated with goat anti-mouse biotinylated (1:500) antibody for 30 min. Slides were washed before incubation with Streptavidin-Alkaline Phosphatase (1:200, Vector Laboratories) for 30 min. Following further washing, antibodies were detected using PermaBlue Plus/AP (Diagnostic Biosystems, USA) following manufacturer's instructions.

Slides for DAB end point were also washed and antibody detected using the ImmPress anti-mouse or anti-rabbit Ig (peroxidase) Polymer Detection Kit and ImmPress DAB following manufacturers' instructions.

Some germ cell-specific staining was seen in all slides. Sections were then incubated for 15 min in 4M hydrochloric acid (HCl)/TBS, preheated to 37°C, to test resilience of DAZL staining. Resulting staining appeared strongest with antigen retrieval at pH9, and PermaBlue end point (Figure 2.6 B).

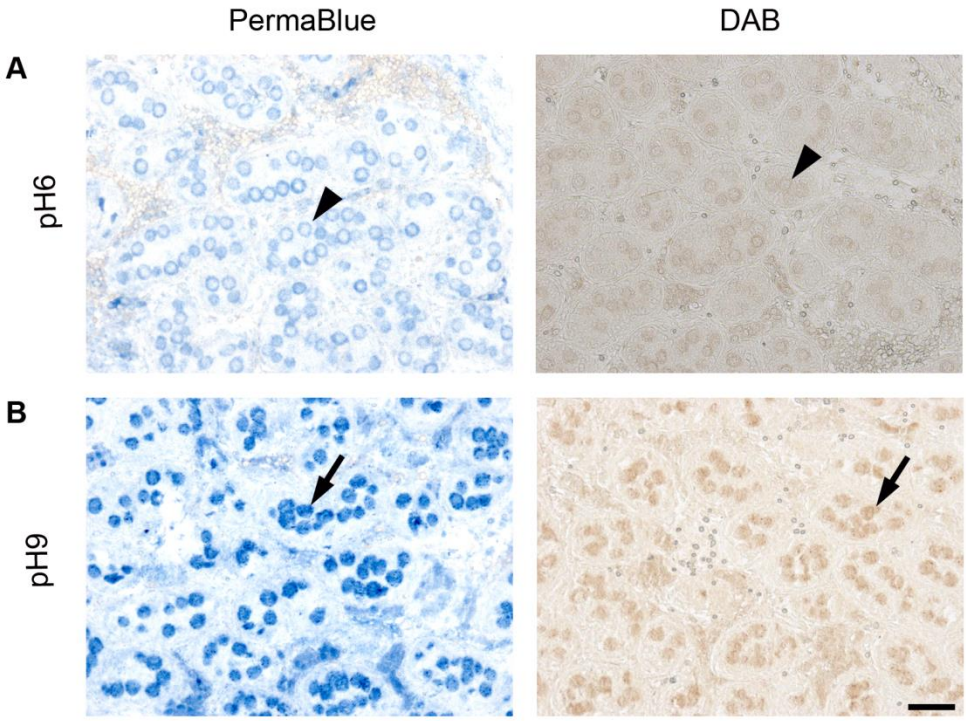

Figure 2.6. Optimising retrieval pH and detection system. Characteristic germ cell staining was seen following antigen retrieval at both pH6 (A, arrow heads) and pH9 (B, arrows) with either PermaBlue (blue) or DAB (brown) antibody detection. However, following incubation with HCl, required for subsequent methylation protocols, PermaBlue remained clearest, particularly following pH9 retrieval. Bar = 20µm.

2.7.6.2 Optimising Permeabilisation with Antigen Retrieval pH

It was hypothesised that PermaBlue staining might be affected by the subsequent exposure to 1% Triton normally used in 5mC staining protocols. To test this theory, slides were taken through all of the DAZL staining steps above, for a PermaBlue endpoint. Tissues were thereafter incubated for 15 min in 4M hydrochloric acid (HCl)/TBS at 37°C, and 50% of slides were incubated with 1% Triton/TBS for 30 min, whilst control slides remained in TBS (Figure 2.7). All slides were thereafter taken through standard DAB detection for 5mC. DAZL staining remained most distinct in pH9 retrieval slides (Figure 2.7B). 5mC staining was largely absent in pH6 retrieval slides (Figure 2.7A), but was clear in pH9 slides, appearing slightly sharper with Triton exposure. pH9 retrieval with Triton permeabilisation was therefore selected for DAZL/5mC protocols.

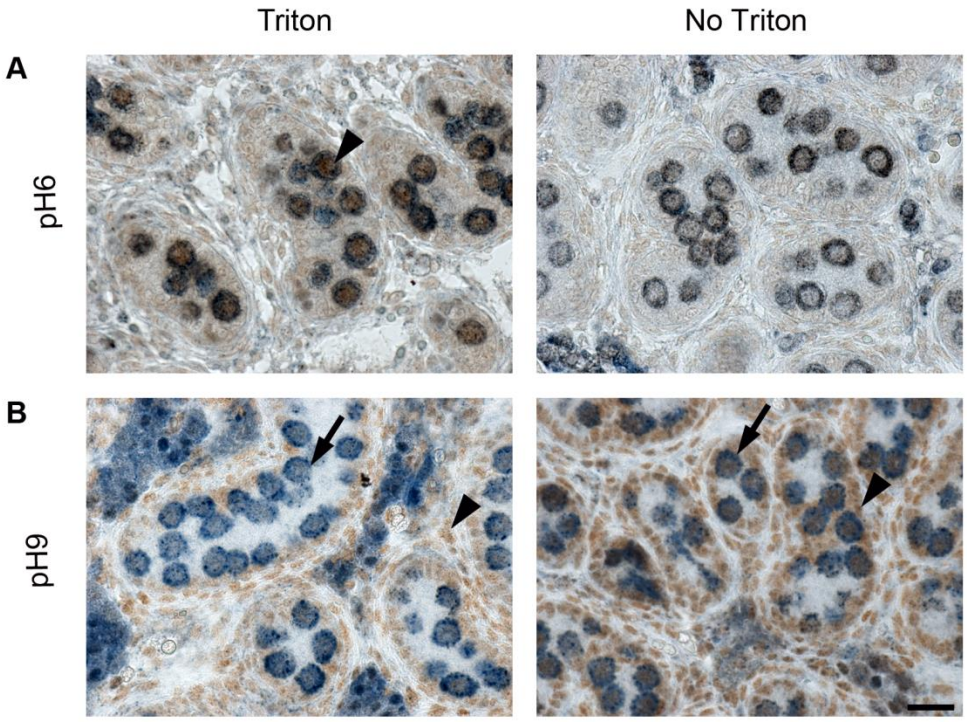

Figure 2.7. Optimising permeabilisation conditions. Following antigen retrieval at pH6 (A) or pH9 (B), tissues were incubated with TBS (No Triton), or TBS containing Triton before 5mC staining. DAZL staining (blue, arrows) remained clear after Triton exposure in pH9 retrieval slides. 5mC staining (brown, arrowheads) was detected in some nuclei following pH6 retrieval and Triton treatment (A) with clear detection in all nuclei following pH9 retrieval (B). Bar = 20µm.

2.7.6.3 Optimising Antibody Concentration

The primary DAZL antibody incubation step was performed at 1:50, 1:100, 1:200 and 1:500 concentrations (Figure 2.8). A concentration of 1:500 was found to give the greatest clarity of both DAZL and 5mC staining.

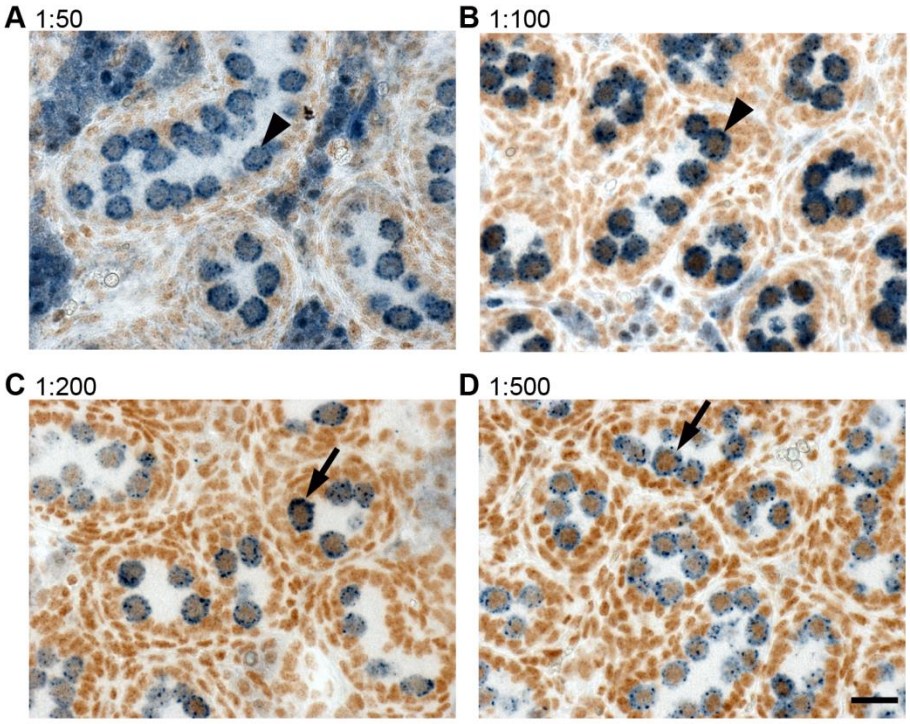

Figure 2.8. Optimising DAZL antibody concentration. Primary DAZL antibody was used at 1:50 (A), 1:100 (B), 1:200 (C), 1:500 (D). Clearest DAZL staining (blue, arrows) was seen at 1:500 dilution, and no inhibition of 5mC staining (brown) was indicated. Higher concentrations of DAZL (A,B) gave detection that prevented clear visualisation of 5mC in nuclei (blue, arrowheads). Bar = 20µm.

2.7.6.4 Final DAZL/5mC Protocol

The final protocol for 5mC and DAZL double immunohistochemistry was therefore as follows: Tissue sections were de-waxed and rehydrated as above, but not taken through the standard methylation staining preparation protocol. Tissues were then submerged in Novocastra Epitope Retrieval Solution (pH9) and pressure cooked for 5 min at 125 °C. Endogenous peroxidase activity was then blocked by incubation in 3% (v/v) hydrogen peroxide/methanol. All subsequent washes were in TBS, and antibody/serum incubations conducted in a humidity chamber (Thermo Fisher Scientific). Tissues were blocked with NGS diluted 1:5 with 5% (w/v) BSA in TBS (NGS/TBS/BSA), before incubation with DAZL (1:500) antibody overnight at 4°C.

Slides were then washed and incubated with goat anti-mouse biotinylated (1:500) antibody for 30 min. Slides were washed before incubation with Streptavidin-Alkaline Phosphatase (1:200) for 30 min. Following further washing, antibodies were detected using PermaBlue Plus/AP following manufacturer's instructions. Tissues were incubated for 15 min in 4M hydrochloric acid (HCl)/TBS, preheated to 37°C, then washed with 0.1% Tween in TBS. Tissue was permeabilised with 1% Triton X-100 in TBS for 30 min before blocking with NHS diluted 1:5 with 5% (w/v) BSA in TBS (NHS/TBS/BSA). Slides were incubated with 5mC (1:300) antibody overnight at 4°C. Slides were then washed and antibody detected using the ImmPress anti-mouse Ig (peroxidase) Polymer Detection Kit and ImmPress DAB following manufacturers' instructions. Mounting was conducted with PermaFluor Aqueous Mounting Medium.

2.7.7 GR Immunofluorescence

Following re-hydration, tissues were then submerged in citrate buffer (pH6) and pressure cooked for 5 min at 125 °C. Endogenous peroxidase activity was then blocked by incubation in 3% (v/v) hydrogen peroxide/methanol. Tissues were blocked with NGS diluted 1:5 with 5% (w/v) BSA in TBS (NGS/TBS/BSA), before incubation with anti-GR M20 (1:500, rabbit, Santa Cruz Biotechnology, USA) antibody overnight at 4°C. Following washing, tissues were incubated with goat anti-rabbit peroxidase-conjugated secondary antibody (GaRP, 1:200, DAKO Corp) in

NGS/TBS/BSA for 30 min. Following further washing, slides were incubated with Tyramide-Cy3 (Perkin Elmer-TSA-Plus Cyanine 3 System, Perkin Elmer Life Sciences, USA) (1:50 in kit diluent) for 10 minutes. Following further washing slides were counterstained with Sytox Green (1:500 in TBS) for 10 minutes, before mounting in PermaFluor.

2.7.8 DNMT3a and DNMT3b Immunofluorescence

In preparation to detect DNMT3a and DNMT3b antigens, antigen retrieval was conducted by pressure cooking, peroxidase activity blocked by hydrogen peroxide/methanol and non-specific binding blocked with NGS as for the GR antibody. Slides were then incubated with germ-cell-specific Vasa antibody (1:150, Abcam, UK) overnight at 4°C. Following washing, Vasa antibody was detected using GARP and Tyramide-Cy3 as previously. Antigen retrieval for DNMT3a and DNMT3b was conducted by boiling in 0.01M citrate buffer by microwaving for 2.5 min following by a 20 min cooling period. This lessened potential for cross reaction between antibodies raised in the same species. Slides for DNMT3a detection were blocked in Normal Rabbit Serum (NRS, Biosera) diluted 1:5 with 5% (w/v) BSA in TBS (NRS/TBS/BSA) for 30 min before incubation with primary DNMT3a (1:1500 in NRS/TBS/BSA, Abcam). For DNMT3b detection, slides were blocked in NGS/TBS/BSA before incubation with primary DNMT3b (1:1500 in NGS/TBS/BSA). Both incubations were conducted overnight at 4°C. Following washing, slides exposed to DNMT3a antibody were incubated with rabbit anti-chicken peroxidase-conjugated antibody (RAChP, 1:200 in NRS/TBS/BSA, Sigma) for 30 min. Slides for DNMT3b staining were incubated with GARP, as previously. Following further washing, all slides were incubated with Tyramide-Cy5 (Perkin Elmer-TSA-Plus Cyanine 5 System, Perkin Elmer Life Sciences) (1:50 in kit diluent) for 10 minutes. Slides were then counterstained with Sytox Green and mounted in PermaFluor as above.

2.7.9 DNMT3L Immunofluorescence

Slides were de-waxed and re-hydrated, and taken through 0.01M citrate buffer antigen retrieval, and hydrogen peroxide/methanol block as previously. Tissues were then blocked in Normal Chicken Serum (NChS, Biosera) diluted 1:5 with 5% (w/v) BSA in TBS (NChS/TBS/BSA) for 30 min before incubation with primary DNMT3L (1:900 in NChS/TBS/BSA, Abcam) overnight at 4°C. After washing, chicken anti-rabbit peroxidase (ChaRP, 1:200 in NChS/TBS/BSA, Sigma) was incubated with the slides for 30 min, before the addition of Tyramide-Cy3 as previously. Following further washing, slides were incubated with Sytox Green as previously before mounting in PermaFluor.

2.7.10 DMRT1 Immunofluorescence

Slides were taken through de-waxing, re-hydration, 0.01M citrate buffer antigen retrieval and hydrogen peroxide/methanol block as previously. Tissues were then blocked with NChS/TBS/BSA, before incubation with primary Doublesex and Mab-3 Related Transcription Factor 1 (DMRT1) antibody (1:750 in NChS/TBS/BSA, a kind gift from Mark Murphy, Liverpool John Moores University) overnight at 4°C. Slides were washed, and then incubated with ChaRP, then Tyramide-Cy3 as previously. Following further washing, tissues were exposed to Sytox Green and mounted in PermaFluor.

2.7.11 TDG Immunofluorescence

Slides were de-waxed, re-hydrated and exposed to antigen retrieval and hydrogen peroxide/methanol block before blocking in NChS/TBS/BSA, as previously. Tissues were exposed to primary anti-Thymine DNA Glycosylase (TDG, 1:500, rabbit, Sigma) antibody overnight at 4°C. Following washing, tissues were incubated with ChaRP in NChS/TBS/BSA, then Tyramide-Cy3 as previously. Following further washing slides were microwaved at full power for 2.5 min in boiling 0.01M citric acid, before further blocking in NGS/TBS/BSA, then incubation with anti-Vasa (1:150) antibody overnight at 4°C. Following further washing, tissue was incubated

with GARP in NGS/TBS/BSA for 30 min. Following further washing, slides were incubated with Tyramide-Cy5, counterstained with Sytox Green then mounted in PermaFluor as previously.

2.7.12 EGFP and Vimentin Immunofluorescence

Immunofluorescence for EGFP and Vimentin was performed by SURF. Slides were dewaxed and rehydrated as above, and immunofluorescence for EGFP (1:500, Invitrogen), Vimentin (1:1000, Dako) and DAPI (1:1000, Sigma) conducted using a BOND-MAX immunostaining machine (Leica).

2.7.13 Semi-Quantification of Immunofluorescence

2.7.13.1 5mC in Dex and Saline Studies

In order to give semi-quantification to a variation in 5mC staining visualised between Dex and Saline testes at e19.5, an intensity scale was devised (Figure 2.9). A grading of 1 corresponded to a weak, 2 a moderate, and 3 an intense positive stain for 5mC. 2 sections were taken from each testis, spaced 50 µm apart. Slides were then stained for 5mC, and counterstained with Propidium Iodide, following the protocols above. Tile scans were taken across the entire section using a LSM 710 Meta confocal microscope (Carl Zeiss Ltd., UK). The file names were then changed so that their treatment group could not be determined, and germ cells were counted blindly, using both Propidium Iodide, and 5mC stains. The grading scale was used when quantifying 5mC, and all results were expressed as number of germ cells in grading category, relative to total number of germ cells counted with counterstain.

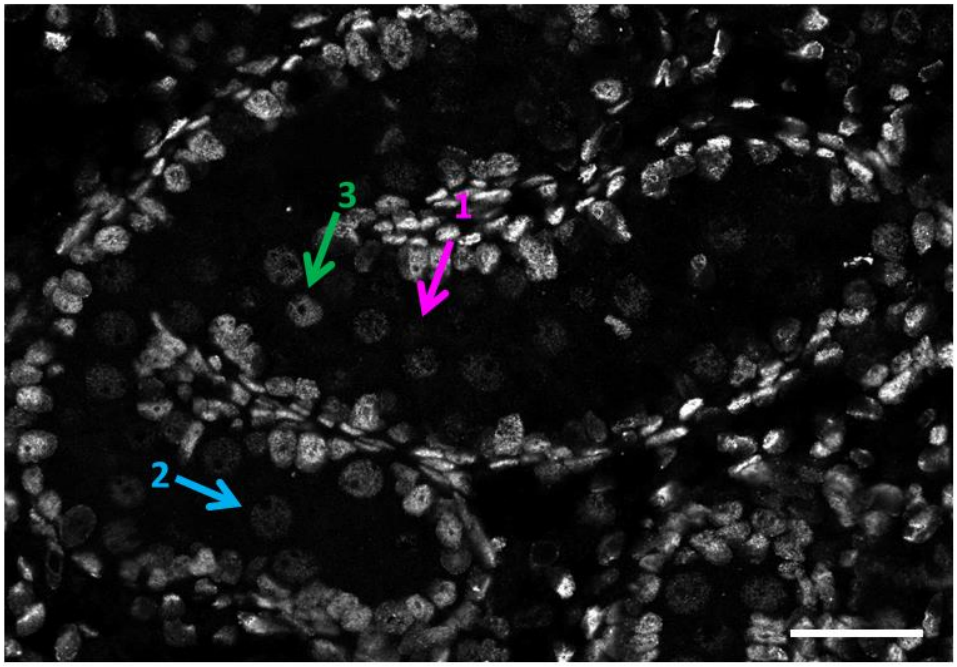

Figure 2.9. Semi-quantification scale for 5mC immunofluorescence. All images were counted blindly, and 5mC staining in germ cells was graded as 1, weak, 2, moderate, or 3, intense. Bar = 50µm.

2.7.13.2 5mC and 5hmC in Baseline Studies

During manuscript revision, semi-quantification of 5mC and 5hmC intensity throughout the seminiferous tubule was conducted using Image J software (National Institute of Health, USA). Only complete tubules were analysed, and the region of interest was identified as being inside the seminiferous tubule, within the ring of Sertoli cell nuclei. Intensity values were expressed as the mean pixel intensity for the region of interest, normalised to the mean pixel intensity for the somatic cells within the same image.

2.7.14 Negative Controls

Negative controls were conducted to confirm that staining was specific for the sites of primary antibody binding, and not simply the result of background from the detection system. Example controls from the methylation Alexa Fluor detection protocols, and the tyramide detection protocols are shown in Figures 2.10 and 2.11 respectively. Tissues were taken through the immunofluorescence protocols outlined above to give staining for the corresponding antigen (termed Positive). A section from the same testis was taken through the same protocol, substituting primary antibody for overnight incubation with blocking solution. Antibody detection was then completed as usual (termed Negative). Negative slides were then imaged using exactly the same laser settings as for the corresponding positive slide. Although a clear antibody detection is seen for the positive slides, the corresponding negatives have little or no staining.

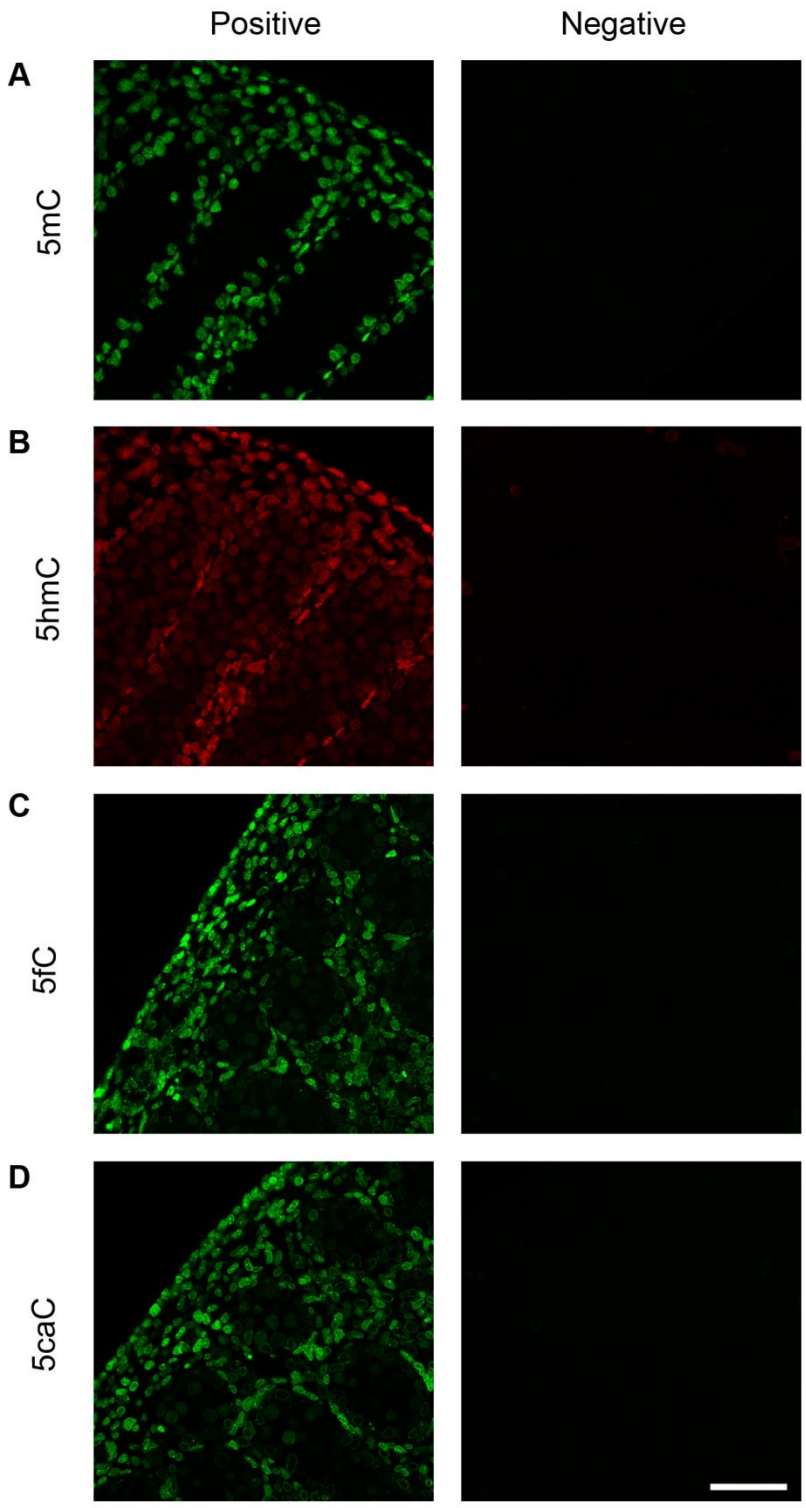

Figure 2.10. Negative controls for methylation Alexa Fluor detection protocols. e16.5 tissues were taken through immunofluorescence protocols with (positive) or without (negative) incubation with the corresponding primary 5mC, 5hmC, 5fC and 5caC antibody (A-D). Using the same confocal microscope settings, clear staining is seen in positive slides, whilst no staining is visualised in negative slides. Bar = 50µm.

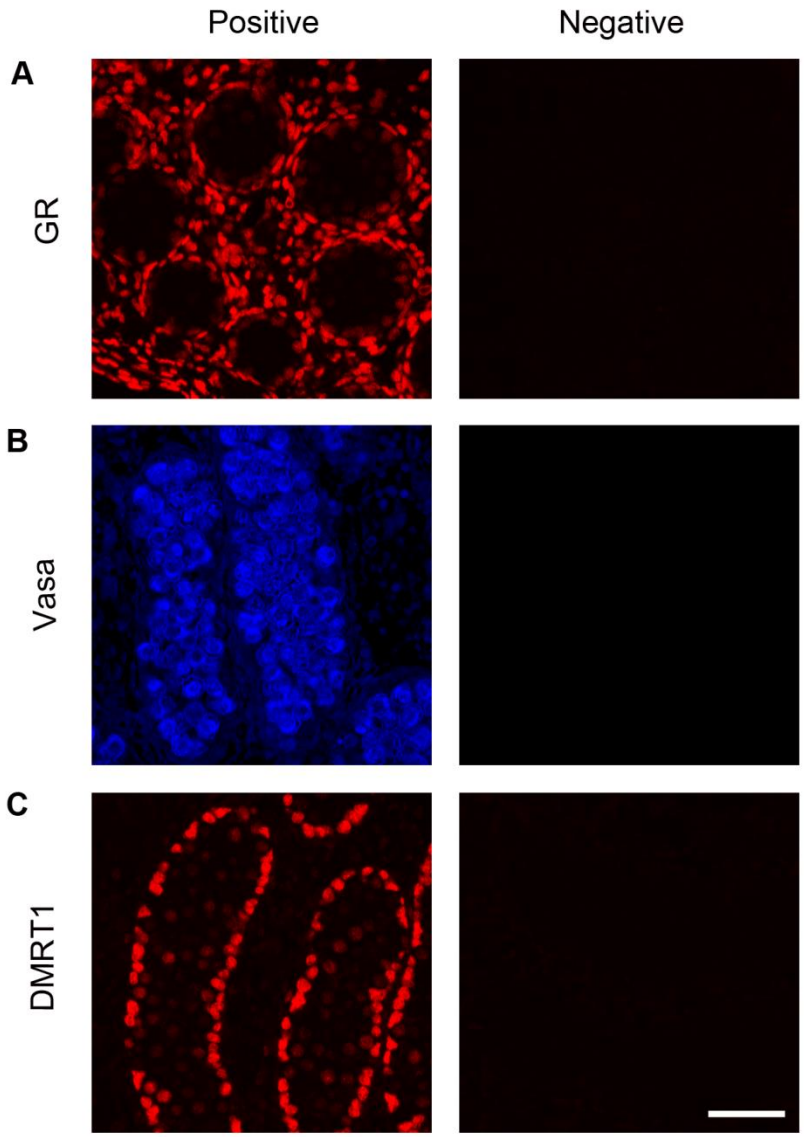

Figure 2.11. Negative controls for Tyramide detection protocols. Examples are shown of e18.5 tissues which were taken through immunofluorescence protocols with (positive) or without (negative) incubation with the corresponding primary antibody (A-C). Using the same confocal microscope settings, clear staining is seen in positive slides, whilst no staining is visualised in negative slides. Bar = 50µm.

2.7.15 Image Capture and Processing

DAB immunohistochemistry was imaged using a Provis AX70 microscope (Olympus Optical, UK) and AxioCam HRc (Carl Zeiss Ltd). An LSM 710 Meta confocal microscope (Carl Zeiss Ltd.) was used to image immunofluorescence, and all figures were produced using Photoshop CS5.1 (Adobe, USA).

2.8 Glucose Tolerance Tests

Rats were fasted for 19 hours before glucose tolerance testing at 9am. A scalpel was used to nick the tail, and a basal blood sample was drawn into a heparin-coated blood tube (Sarstedt, Germany). Following administration of glucose solution (2g glucose/kg rat) by oral gavage rats were returned to their cages. Further blood samples were drawn at 30 and 120 minutes after glucose administration. Tubes were centrifuged at 6000 rpm for 10 minutes before plasma was separated by pipette, and frozen at -20°C.

2.9 Measurement of Plasma Glucose Concentration

Glucose level in plasma from the glucose tolerance tests was assessed using an assay based on the glucose hexokinase reaction. This involves the phosphorylation of D-glucose to glucose-6-phosphate by a hexokinase reaction, and subsequent conversion to gluconate-6-phosphate by a dehydrogenase enzyme (Figure 2.12). This ultimately yields Nicotinamide Adenine Dinucleotide (reduced) (NADH) as a by-product, the concentration of which can be determined spectrophotometrically [245].

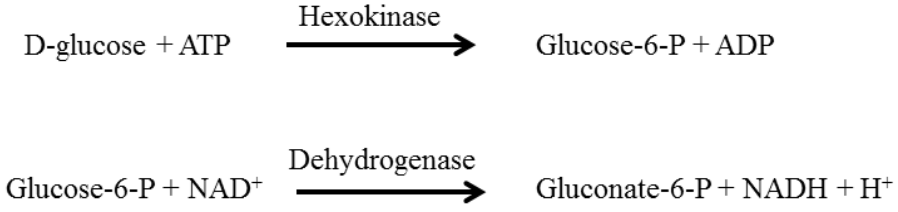

Figure 2.12. Glucose hexokinase reaction. D-glucose within the plasma sample is converted to glucose-6-phosphate (glucose-6-P), and then gluconate-6-phosphate (gluconate-6-P) by hexokinase and dehydrogenase enzymes respectively. This ultimately yields NADH which can be quantified by spectrophotometry. ADP denotes Adenosine Diphosphate; ATP, Adenosine Triphosphate, NAD, Nicotinamide Adenine Dinucleotide (oxidised).

Samples from glucose tolerance tests (2 µl) were placed in duplicate into a 96 well plate. A standard curve was also added in duplicate, ranging from 0-27.75 mmol/l glucose, constructed using the Data Cal Multi Constituent Calibrator (Thermo Fisher Scientific). Infinity Glucose Reagent (200 ul, Thermo Fischer Scientific) was added to each well before incubation for 5-60 minutes at room temperature. The amount of NADH produced was proportional to the glucose concentration (see Figure 2.12), and was quantified by measuring alteration of UV absorbance of the solution at 340nm, using an OPTImax Plate Reader (Molecular Devices, UK). Sample glucose concentrations were calculated from a standard curve of glucose concentration against UV absorbance.

2.10 Measurement of Plasma Insulin Concentration

Insulin concentrations in plasma from glucose tolerance tests was measured using the Mercodia Rat Insulin Enzyme-linked Immunosorbent Assay (ELISA) (Mercodia, Sweden), following manufacturer's instructions. The UV absorbance of the resulting solutions was read at 450nm using an OPTImax Plate Reader.

2.11 Extraction of Total RNA

2.11.1 Extraction of RNA from Fetal Testis

RNA was extracted from fetal testes using the RNeasy Micro Kit (QIAGEN) and Kontes Pellet Pestle Motor tissue ruptor (Sigma), following manufacturers' instructions. During the extraction procedure, the optional on-column DNase treatment step was performed using the RNase-free DNase 1 set (QIAGEN), following the manufacturer's protocol.

2.11.2 Extraction of RNA from FACS-Sorted Fetal Testis Cells

RNA was extracted from FACS-Sorted fetal testis cells using the RNeasy Micro Kit, as above, but homogenising by vortexing, following manufacturers' instructions.

2.11.3 Extraction of RNA from Liver

RNA was extracted from liver using an extraction method previously optimised in our laboratory (Khulan *et al.*, Unpublished). 30-40mg of tissue was homogenised in 800 µl chaos buffer (4.5M Guanidinium thiocyanate, 2% N-lauroylsarcosine, 50mM EDTA, pH8.0, 0.1M β-Mercaptoethanol, 0.2% Antifoam A) using a PRO 200 homogeniser (PRO Scientific, USA). 400 µl of the resulting homogenate was kept for DNA extraction (as outlined in section 2.14.1), whilst RNA was extracted from the remaining 400 µl. 40 µl of 2M Sodium Acetate, 400 µl of acidic phenol and 200 µl chloroform:isoamyl (all Sigma) were added in turn, with vortexing in between each addition. Samples were then left on ice for 10 minutes before centrifuging at maximum speed for 20 min at 4°C. The resulting supernatant was placed in a new 1.5ml eppendorf, before adding an equal volume of 70% isopropanol, and inverting 5 times to combine the solutions. The sample was immediately added to an RNeasy Mini column (QIAGEN), and taken through the subsequent steps in the standard RNeasy Mini Kit protocol (QIAGEN), with DNase treatment, as outlined above.

2.11.4 Assessing Quantity and Quality of RNA

RNA was quantified using a Qubit 2.0 Fluorimeter, and Qubit RNA Broad Range Assay Kit (both Life Technologies), following manufacturer's instructions. RNA purity was assessed using Nanodrop ND-1000 Spectrophotometer (Thermo Fisher Scientific, USA). Ultraviolet at 260/280nm and 260/230nm was examined, with a value of 1.8-2.1 AU deemed to indicate a satisfactory degree of RNA integrity. Quality was also assessed using the Agilent 2100 Bioanalyzer System with Agilent RNA 6000 Nano Kit (Agilent, USA) following manufacturer's instructions. This gave an RNA Integrity Number, with an optimum value of 8-10, and acceptable values from 5-8 [246]. This number was calculated based on the ratios of 28S to 18S RNA bands. These bands were also examined visually, and an approximate 28S/18S ratio of 2 considered to correspond to high quality RNA [246] (see Figure 2.13).

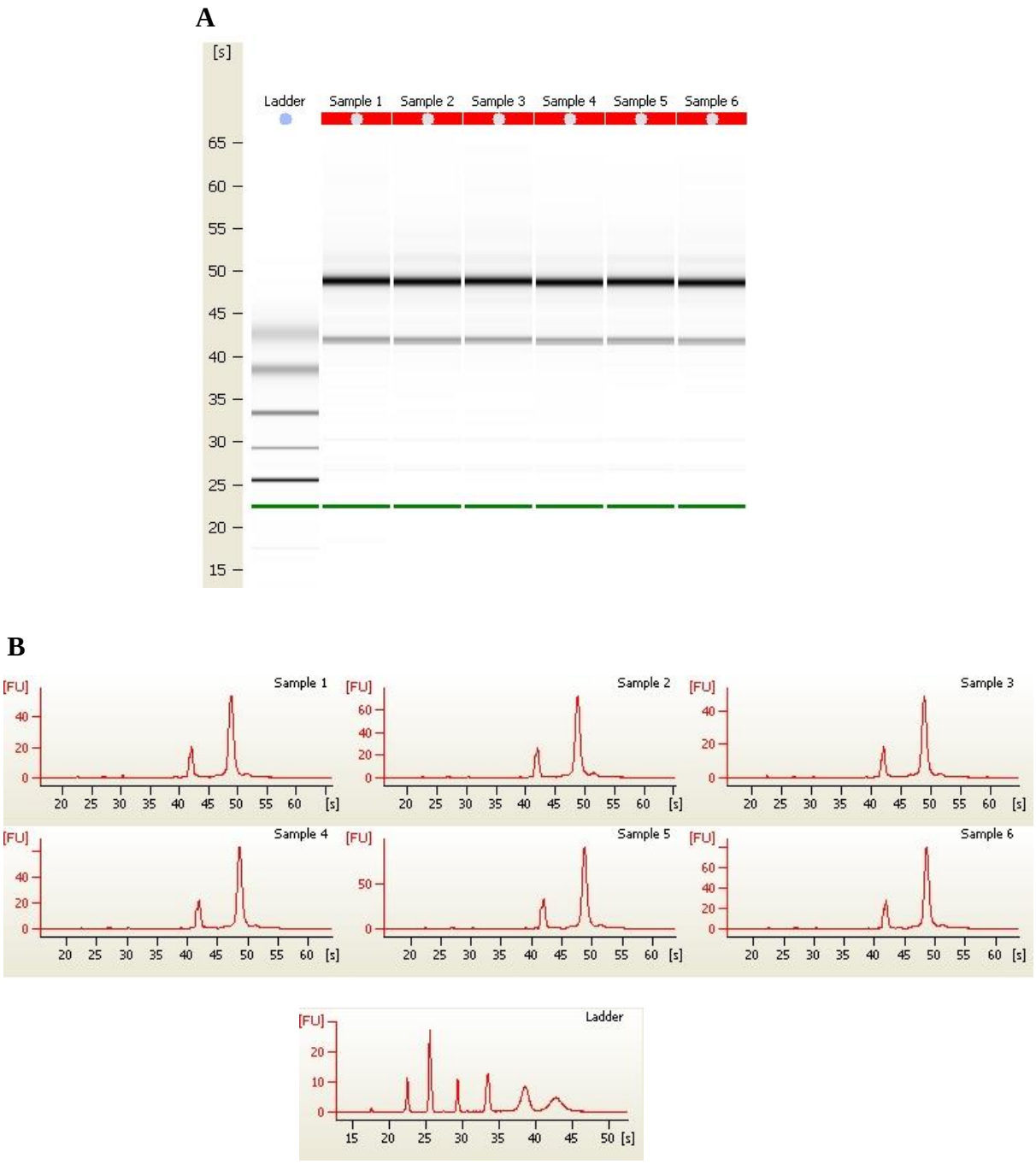

Figure 2.13. Example Agilent gel and electropherogram. RNA was run on a Bioanalyzer chip, giving a gel, with bands seen for 28S and 18S (A). The ratio of 28S/18S is approximately 2, confirming RNA integrity. Samples are also visualised on an electropherogram trace (B), and peaks are seen for 28S and 18S RNA.

2.11.5 Reverse Transcription

RNA was reverse transcribed to complementary DNA (cDNA) using the High Capacity cDNA Reverse Transcription Kit (Applied Biosystems, USA), and G-Storm thermocycler, following manufacturers' instructions.

2.12 Quantitative Polymerase Chain Reaction (qPCR) Analysis of Gene Expression

cDNA was then amplified and quantified using qPCR. cDNA (corresponding to 1ng RNA) was added to the correct primer/master mix combination. Primers for SYBR Green Assays were combined with SYBR Green Master Mix (Roche Diagnostics Ltd, USA), TaqMan Gene Expression Assays with LightCycler 480 Probes Mastermix (Roche Diagnostics Ltd), and Universal Probe Library (UPL) primers with both the correct corresponding probe (Roche Diagnostics Ltd) (see Table 2.1) and LightCycler 480 Probes Mastermix. A standard curve for each sample set was established using a serial dilution of pooled cDNA. Thermocycling and fluorescent signal detection was conducted using the Roche LightCycler 480 (Roche Diagnostics Ltd.) as in Drake *et al.* (2010) [64], and results normalised to those of housekeeping genes, chosen based on consistency of expression throughout groups.

2.13 Primer Sequences

Primers for UPL based assays were designed using the UPL Assay Design Centre (http://lifescience.roche.com/shop/CategoryDisplay?catalogId=10001&tab=&identifier=Universal+Probe+Library). Sequences and target regions for SYBR Green and basic PCR assays were identified using UCSC Genome Browser Gateway (http://genome.ucsc.edu/cgi-bin/hgGateway), and suitable primers designed with Primer 3 (http://frodo.wi.mit.edu/primer3). All primers were synthesised by Invitrogen (Table 2.1). TaqMan Gene Expression Assays (Life Technologies) were also used, for which sequences did not need to be designed.

Gene	Forward Primer (5'-3')	Reverse Primer (5'-3')	UPL Probe	TaqMan Assay ID
Alcohol Dehydrogenase 1 (*Adh1*)	GAG GAT CCA TCC ATT TCC TG	GCC GCT TTG CAT TTG ATT AC	56	
Cyclin-dependent Kinase Inhibitor 1C (*Cdkn1c*)				Rn00711097_m1
Deleted in Azoospermia-like (*Dazl*)	GCT CAG TTC ATG ATG CTG CT	ATG CTT CGG TCC ACA GAT TT	110	
Enhanced Green Fluorescent Protein (EGFP)	AGA ACG GCA TCA AGG TGA AC	TGC TCA GGT AGT GGT TGT CG	Basic PCR	
Gelsolin	CTG GCC AAG CTC TAC AAG GT	AGC CAC GAG GGA GAC TGA C	16	
Glucocorticoid Receptor (*Gr*)				Rn01405584_m1
Growth Factor Receptor-Binding Protein 10 (*Grb10*)	CAA CCA AGA AGC CAA CCA G	TCC ACG GAT GAG TTA ATA TCG TT	117	
H19, imprinted maternally expressed transcript (non-protein coding) (*H19*)	GAT GAC AGG TGT GGT CAA CG	GGC AAA GGA AAG AAC AGA CG	SYBR Green	
Heat Shock 70kDa Protein 5 (*Hspa5*)	ATC GGA CGC ACT TGG AAT	TAT GGT TTA GTT TTC TTT TCA ACC AC	18	
High Mobility Group Box 2 (*Hmgb2*)				Rn01535167_g1
11β Hydroxysteroid Dehydrogenase Type 1 (*11β-Hsd1*)	TCT ACA AAT GAA GAG TTC AGA CCA G	GCC CCA GTG ACA ATC ACT TT	1	
Hypoxanthine-guanine Phosphoribosyltransferase (*Hprt*)	TCA ACG GGG GAC ATA AAA GT	TCA ATT ATA TCT TCA ACA ATC AAG ACG	22	
Insulin-like Growth Factor 2 (*Igf2*)				Rn01454518_m1
Insulin-like Growth Factor Binding Protein 1 (*Igfbp1*)	AAT GGA TTT TAT CAC AGC AAA CAG	CAT GGG TAG ACA CAC CAG CA	58	
Peptidylprolyl Isomerase A (*Ppia*)				Rn00690933_m1

Ribosomal Protein Serine 6 (*Rps6*)	TGC TCT TGG TGA AGA GTG GA	CAA GAA TGC CCC TTA CTC AAA	53	
Ribosomal Protein Serine 6 Kinase 1 (*Rps6k1*)	GAA GCT CGA GAT CTG CTT AAA AA	GAT GCG CTT GGA CTT CTC C	81	
Ribosomal Protein Serine 6 Kinase 2 (*Rps6k2*)	TGG AGT GCC TCA GTG GTG	ATG GCC CAG GGC TAG TGT	53	
Sex-determining Region Y (*Sry*)	ACT GTT CAA GCA GTC AGC CG	CTC CAT GAA CTT GGG GTC	Basic PCR	
SRY (Sex-determining Region Y)-Box 9 (*Sox9*)	ATC TTC AAG GCG CTG CAA	CGG TGG ACC CTG AGA TTG	63	
TATA-Box Binding Protein (*Tbp*)	CCC ACC AGC AGT TCA GTA GC	CAA TTC TGG GTT TGA TCA TTC TG	129	
Tumour Protein, Translationally Controlled 1 (*Tpt1*)	TGG ACT ACC GTG AAG ATG GTG	TCC TGG TGT TGT ATG GAT GG	66	

Table 2.1. Primer sequences for basic PCR and qPCR. qPCR was conducted using TaqMan assays (where a TaqMan assay code is given), UPL assays (where probe number is supplied), or SYBR Green. Primer sequences for normal PCR are also given. All sequences are written 5'-3'.

2.14 Extraction of DNA

2.14.1 Extraction of DNA from Liver

Liver homogenate was prepared following the Chaos buffer extraction protocol outlined above. 400 µl of homogenate was then added to 300 µl of buffer AL from the DNeasy Mini Kit (QIAGEN), before thorough mixing by vortexing. 300 µl of 100% ethanol was then added, before further mixing. The resulting solution was then added to a DNeasy Mini column, and subsequent steps performed according to the DNeasy Mini Kit protocol. The optional RNase A treatment, and AE elution buffer incubation (70°C) steps were performed.

2.14.2 Extraction of DNA from Sperm

As sperm are particularly resistant to the cell lysis required for DNA extraction, optimisation of isolation protocols had to be conducted. A method with maximum DNA yield was also sought, due to limited cell numbers after FACS sorting, and the fact that sperm have a lower DNA content than other cells due to their haploid status. Candidate methods 1-3 are described below:

2.14.2.1 Method 1

Extraction was based on a protocol from Griffin *et al.* (2013), adapted for a reduced starting cell number [247]. Sperm pellet was washed by re-suspension in 1ml sperm wash buffer (150mM Sodium Chloride (NaCl), 10mM EDTA pH8), before pelleting by centrifugation at 750 xg for 10 min, and removing the supernatant. This step was repeated before loosening the pellet by vortexing for 5 seconds and resuspension in 600µl of lysis buffer (4.24M guanidine thiocyanate, 100mM NaCl, 1% sarkosyl, 150mM Dithiothreitol (DTT), 200µg/ml proteinase K) (all Sigma). Samples were incubated at 56°C for 1 hour before inverting 3 times, and incubating for a further hour.

After cooling to room temperature, 1µl of glycogen (QIAGEN) was added to bind the DNA, and make it easier to visualise in subsequent steps. 480 µl of isopropanol was then added, and each sample inverted, allowing the DNA to precipitate. DNA was then pelleted by centrifugation at 5000 xg for 3 min, and supernatant removed. 1ml of 0.1M Sodium Citrate (Sigma) in 10% ethanol was then added, and left to wash the pellet for 30 min. DNA was pelleted at 5000 xg before removing supernatant. This wash step was repeated. The pellet was then washed twice without incubation, using 1ml of 70% ethanol, and mixing each time by inversion. All ethanol was removed by pipetting, taking care not to disturb the DNA pellet. Residual ethanol was evaporated using the DNA Speed Vac DNA 110 (Savant Instruments Inc., USA). DNA was then rehydrated in 100µl of TE overnight at 4°C.

2.14.2.2 Method 2

Extraction was based on a protocol from Weyrich *et al.* (2012), without the prewash step that they suggest for semen [248]. This was omitted as only sperm remained in our samples, after FACS sorting, and in an attempt to minimise cell loss during sample processing. Concentrations of lysis buffer reagents were also reduced, as those reported were around 100 times stronger than that for other protocols, and attempted stock solutions reached saturation point before compounds were in solution. Concentrations were therefore altered to be a greater reflection of those suggested by other protocols.

500 µl of lysis buffer (10mM Tris-Chloride, pH8, 50mM NaCl, 10mM EDTA, 1% Sodium Dodecyl Sulfate (SDS)) was added to sperm pellet. 2.5 µl of 0.5% Triton-X100, 17.4 µl of 23mg/ml proteinase K and 21 µl of 1M DTT was then added to the sample before mixing, and overnight incubation on a thermomixer at 50°C and 650 rpm.

Cell debris was pelleted by centrifugation at 15,500 xg, before the supernatant, containing DNA, was transferred to a new 1.5ml eppendorf. 1 µl glycogen solution and 50 µl of 3M sodium acetate was combined with this supernatant, promoting subsequent DNA visualisation and precipitation, respectively. 1ml of ice-cold 100% ethanol was added to the solution, before inversion 3 times and leaving at -80°C for 1-2 hours to promote precipitation.

Samples were centrifuged at 15,500 xg for 20 min to pellet the DNA, before removing the supernatant. DNA was washed by the addition of 500 µl of 75% ethanol with subsequent centrifugation at 15,500 xg for 10 min. Care was taken to remove as much supernatant as possible, without disturbing the DNA pellet, with residual ethanol evaporated using the Speed Vac. The pellet was then dissolved in 50µl TE overnight at 4°C.

2.14.2.3 Method 3

Lysis buffer (50mM EDTA pH8, 1% SDS, 500 µg/ml proteinase K) was added to the sperm pellet, before incubation at room temperature overnight. 25 µl of 1M DTT was

added to the solution before mixing, and incubation on the thermomixer at 50°C and 650 rpm overnight. Cell debris was then removed and DNA precipitated following method 2 above.

2.14.2.4 Method 4

Extraction was carried out in accordance with the QIAGEN Gentra Puregene Handbook (2011). Clumps of cells were visible in the cell lysate, suggesting the lysis had been incomplete for our samples. Therefore the protocol was adapted following online advice from QIAGEN.

600 µl of Cell Lysis Solution (QIAGEN) was added to the sperm pellet, before mixing by pipetting. As cell clumps indicated that lysis was incomplete, samples were incubated at 37 °C for 1 hour before the addition of 3.9 µl of 23mg/ml proteinase K, and an additional 300 µl of Cell Lysis Solution. Samples were incubated on the thermomixer at 55°C and 650 rpm overnight.

0.9 µl of 50mg/ml RNase A solution (QIAGEN) was added to the lysate, followed by mixing by inversion and incubation at 37 °C for 30 min. Samples were cooled on ice for 20 min before addition of 300 µl Protein Precipitation Solution. The resulting solution was mixed by vortexing for 20 seconds, and protein and cell debris was pelleted by centrifugation at 16,000 xg for 3 min. The supernatant was transferred to a new 2ml eppendorf, taking care not to move the white pellet. 900 µl of 100% isopropanol was added to this supernatant before inverting 30 times to precipitate the DNA. Samples were centrifuged at 16,000 xg for 3 min to pellet the DNA, before removing the supernatant. The pellet was then washed by adding 600 µl of 70% ethanol, with inversion, before further centrifugation at 13,000 xg for 2 min. Supernatant was carefully removed by pipetting, and residual ethanol removed using the Speed Vac. DNA was rehydrated in 100 µl TE at 4°C overnight.

2.14.3 Analysis of DNA Quantity and Quality

DNA concentration was then quantified by spectrophotometry using the Qubit, following manufacturer's High Sensitivity protocol. DNA quality and purity was then assessed using the Nanodrop, examining the 260/280 ratio for protein and RNA contamination, and 260/230 for chemical contamination (see Table 2.2). DNA was also analysed by gel electrophoresis, giving a visual indication of DNA integrity, and RNA contamination. Each sample was combined with 5 µl of Orange G loading buffer, before loading into a 2 % agarose gel, and electrophoresing as previously. DNA ladder (100bp) was run in parallel, as a marker for band size. Gels were imaged using a BXT-20.M Transilluminator (see Figure 2.14). Method number 2 was found to give the greatest DNA yield, and purity ratios closest to the optimal (2), therefore this method was used for the processing of DNA samples.

Method Number	**DNA Yield/ 2 million cells (ng)**	**260/280 Ratio**	**260/230 Ratio**
1	91.8	11.63	0.01
2	585	1.96/1.79	1.32/1.58
3	540	1.44	0.65
4	8.3	1.18	2.77

Table 2.2. Concentration and purity of sperm DNA. DNA quantity was analysed by Qubit and purity by 260/280 and 260/230 ratios obtained from the Nanodrop. Protocol number 2 gave the greatest DNA yield, and purity ratios closest to the optimal (2).

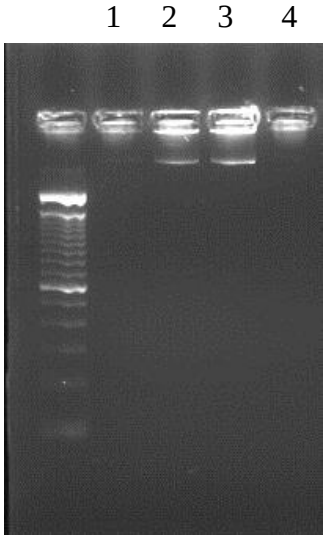

Figure 2.14. Quality of sperm DNA examined by gel electrophoresis. DNA was extracted using trial methods 1-4 and electrophoresed on an agarose gel. Distinct bands of genomic DNA were seen for methods 2 and 3, with no visible DNA shearing or RNA contamination.

2.14.4 Extraction of DNA from Germ Cells

2.14.4.1 Extraction from Cell Culture Cells

A protocol for extracting DNA from germ cells had to be optimised to allow for isolation from cell pellets, and very limited sample sizes. In order to preserve the limited quantities of FACS sorted germ cell samples it was decided to perform an initial optimisation of DNA extraction using an equivalent number of cell culture cells. Candidate methods 1-5 were tested on aliquots of 30,000 AS4.1 cells, as described below:

2.14.4.2 Method 1

Extraction was based on a method from Mortensen *et al.* (2008) which involved DNA isolation as part of a homologous recombinant screen. This was adapted to try and give greater purity. Cell pellets were incubated with 300 µl digestion buffer (20mM Tris-Chloride, pH 8.0, 10mM NaCl, 10mM EDTA, 0.5% SDS, 1mg/ml

proteinase K) at 55°C overnight. Samples were then centrifuged at 15,500 xg for 10 min to pellet protein, before transferring the supernatant to a new eppendorf. 150 µl 5M NaCl was then added to the solution before vortexing for 15 seconds. 1 µl of glycogen was then added, before DNA precipitation using 2 volumes of 95% ethanol. DNA was then pelleted by centrifugation for 10 min at 15,500 xg, and washed with 500µl of 75% ethanol. Centrifugation was repeated before supernatant was removed and residual ethanol evaporated using the SpeedVac. DNA was then resuspended in TE.

2.14.4.3 Method 2

A second method was tried, adapted from the QIAGEN Gentra Puregene Handbook (2011). Thawed AS4.1 aliquots were vortexed to loosen cell pellets before adding 300 µl of Cell Lysis Solution (QIAGEN). Samples were vortexed for 10 seconds to promote cell lysis, before incubation at 37°C for 45 min. Solutions were then cooled on ice for 5 min. 100µl of Protein Precipitation Solution (QIAGEN) was added to the sample before vortexing vigorously for 20 seconds. Precipitated protein was pelleted by centrifugation for 1 min at 16,000 xg, and supernatant placed in a new eppendorf. Glycogen was added as previously, and DNA precipitated by addition of 300 µl of isopropanol, and mixing by inverting 50 times. DNA was pelleted by centrifugation for 10 min at 16,000 xg, and supernatant removed. The pellet was then washed by adding 300µl of 70% ethanol. Following further centrifugation, all ethanol was removed from the pellet, first by pipette, then by using the SpeedVac. DNA was then dissolved in TE overnight at 4°C.

2.14.4.4 Methods 3-5

Extraction was also carried out using the Promega Wizard SU Genomic DNA Purification System (Promega, USA), following manufacturer's instructions for tissue culture cell lysates (Method 3). The DNeasy Blood and Tissue, and AllPrep DNA/RNA Micro kits (both QIAGEN, Methods 4 and 5 respectively), were also used. It was hoped that the latter would be particularly effective as it is specifically

designed for small samples, and as RNA is purified from the same sample, that this would avoid the use of RNase A, which might compromise DNA integrity.

2.14.5 Analysis of DNA Quantity and Quality

DNA quantity and quality was then analysed by Qubit, Nanodrop and gel electrophoresis as previously (see Table 2.3 and Figure 2.15). Protocol number 2 was found to give the greatest DNA yield, with a reasonable 260/280 ratio. DNA also appeared intact, with analysed by electrophoresis, with some evidence of RNA contamination.

Method Number	Cell Type	DNA Yield/30,000 Cells	260/280	260/230
1	AS4.1	79	1.74	0.51
2	AS4.1	725	2.11	0.44
3	AS4.1	89.7	2.09	0.77
4	AS4.1	43.2	1.58	0.16
5	AS4.1	36.45	6.31	0.01

Table 2.3. Concentration and purity of DNA extracted from 30,000 AS4.1 cells. DNA quantity was analysed by Qubit and purity by 260/280 and 260/230 ratios obtained from the Nanodrop. Method number 2 gave the greatest DNA yield, and 260/280 purity ratios closest to the optimal (2).

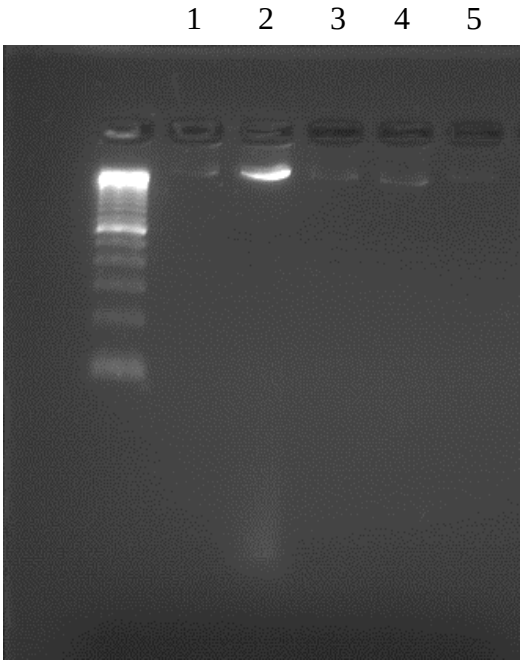

Figure 2.15. Quality of AS4.1 cell DNA examined by electrophoresis. DNA was extracted using trial Methods 1-5 and electrophoresed on an agarose gel. Distinct bands of genomic DNA were seen for all methods, with varying intensity. Some nucleotide contamination is seen for the sample extracted using Method 2.

2.14.6 Optimising RNase A Treatment Conditions

As gel electrophoresis indicated some RNA contamination, but there was concern that RNase treatment could decrease the DNA yield of precious samples, it was decided to explore the effect of RNase on DNA concentrations. Three pellets of AS4.1 (30,000 cells) were taken through extraction using Method 2 (Puregene Protocol). Following cell lysis, either 1.5 µl or 0.75 µl of RNase A (diluted to 4mg/ml in dH_2O, QIAGEN) was added to each of 2 samples, with a third given no treatment. All samples were then incubated at 37°C for 5 min before continuing the protocol as previously. DNA was analysed using the Qubit and Nanodrop as previously (see Table 2.4). Concentration was not found to differ between the sample treated with 0.75µl and that without RNase A (both 31 ng/µl). However with 1.5 µl RNase A, DNA concentration was found to decrease to 12.9 ng/µl. This was confirmed visually by electrophoresis (Figure 2.16).

To assess the effectiveness of each RNase A concentration, resulting RNA yield was analysed by Qubit using the RNA Broad Range quantification kit, and following manufacturer's instructions. RNA concentration was found to be greatest without RNase treatment, reduced to 8.7% of that value with 0.75 µl, and unquantifiable with 1.5 µl RNase A (see Table 2.5). It was decided therefore that the optimum balance between RNA contamination and DNA integrity was to use 0.75 µl enzyme.

Sample	**Qubit DNA Conc. (ng/µl)**	**260/280**	**260/230**
No RNase A	31	2.08	1.29
0.75 µl RNase A	31	1.96	0.66
1.5 µl RNase A	12.9	2.29	0.35

Table 2.4. DNA quantity and quality following RNase A treatment. The highest volume of RNase A was found to decrease DNA concentration and move the 260/280 ratio out with the recommended range (1.8-2.1 AU).

Sample	**Qubit RNA Conc. (ng/µl)**	**260/280**	**260/230**
No RNase A	22.9	2.00	1.38
0.75 µl RNase A	2.64	1.96	0.7
1.5 µl RNase A	Unquantifiable	1.99	0.4

Table 2.5. Contaminant RNA quantity and quality following RNase A treatment. Treatment with 0.75 µl of RNase A reduced RNA contamination to around 10% of that in untreated sample. 1.5 µl of RNase A reduced contaminant to an unquantifiable level.

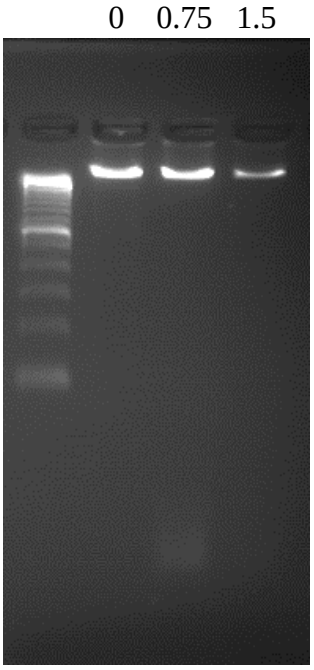

Figure 2.16. DNA quality following RNase A treatment. Quality was assessed visually by gel electrophoresis. A clear DNA band is seen without treatment, and with 0.75 µl RNase A. A smaller band is seen following 1.5 µl RNase A.

2.14.7 Confirming DNA Extraction Procedure on Fetal Germ Cells

It was necessary to ensure that the final extraction procedure, using Method 2 and 0.75 µl RNase A would work well on the final samples. Therefore 2 test litters were bred without treatment, and germ cells FACS-sorted at e19.5 as previously. DNA was then isolated from 2 test FACS-sorted fetal germ cell pellets (see Table 2.6). The optimisation litter 1 sample was extracted without RNase A treatment, whilst that for litter 2 was exposed to 0.75 µl of the enzyme.

DNA concentration was seen to be decreased (to around 10%) in both litters relative to those for AS4.1 cells. It is thought that the number of cells counted by the FACS machine is very inaccurate (Buckley *et al.*, unpublished observation), and that this could account for the difference in concentration. There may also be some variation in DNA content between fetal germ cells and AS4.1 cells in culture. However, RNase A treatment was not found to decrease DNA content, whilst effectively

removing RNA contamination, as confirmed by Qubit quantification (Table 2.6), and visualisation on an agarose gel (Figure 2.17).

Sample	Number of cells	Qubit DNA Conc (ng/µl)	260/280	260/230	Qubit RNA Conc (ng/µl)
Litter 1 (No RNase A)	45,657	2.19	2.56	0.45	4.39
Litter 2 (0.75 µl RNase A)	44,835	2.42	1.94	0.15	Unquantifiable

Table 2.6. DNA quantity and quality and RNA contamination in fetal germ cells. DNA was extracted from fetal germ cells of optimisation litters to ensure that the protocol optimised on cell culture cells was suitable for use in the fetal germ cell study. DNA quantity was reduced to approximately 10% of the equivalent number of fetal germ cells. RNase A treatment (0.75 µl) reduced RNA contamination to an unquantifiable level.

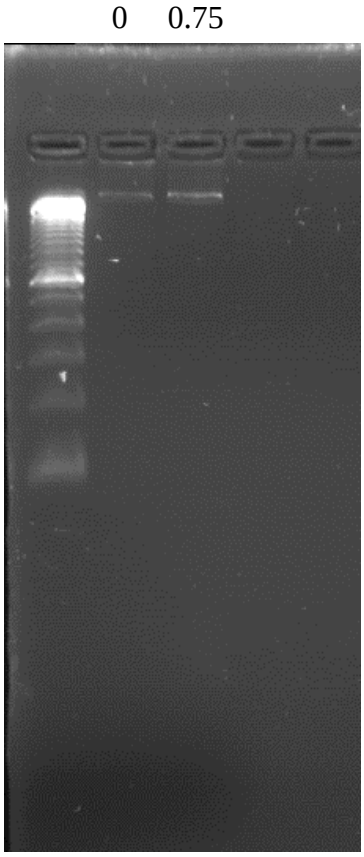

Figure 2.17. Quality of fetal germ cell DNA examined by electrophoresis. DNA was extracted using trial Method 2 with (0.75 (µl)) or without (0) RNase A treatment, before electrophoresis on an agarose gel. Bands of genomic DNA are seen for both samples, with no visible RNA contamination.

2.14.8 Investigating Problems with Nanodrop Readings

I noted that 260/280 and 260/230 ratios were quite low in my samples, and that when read multiple times on the Nanodrop, variation was found between the readings for the same sample. I therefore explored the variability of Nanodrop readings at different sample concentrations. A trial liver DNA sample was quantified, and an aliquot diluted 1:100 in QIAGEN AE buffer, giving a concentration of ~10 ng/µl, in a similar range to sperm and germ cell DNA extracts. Both the neat and the diluted versions of the sample were quantified three times, with the computer turned off, and Nanodrop blanked in between each reading. Samples were first quantified using a Nanodrop within the Centre for Cardiovascular Science (CVS) (Table 2.7), and then

one from the Centre for Reproductive Health (CRH), The University of Edinburgh (Table 2.8). Great variation was seen in the DNA concentrations given in each replicate, particularly on the CVS Nanodrop, which varied from 676.7ng/µl – 1241.4ng/µl.

Variation was also found in the 260/280 ratios between quantification replicates. The range of values in the neat sample replicates was lower (0.03 for both Nanodrops), than for the diluted sample replicates (0.52 and 0.12 for CVS and CRH Nanodrops respectively). Indeed when using the CRH Nanodrop, the mean 260/280 ratio was 1.68 in the diluted, compared to 1.89 in the undiluted versions of the sample. This takes the diluted version further from the optimum value of 2, and below the standard threshold for acceptable purity (1.8).

Similarly, variation was also found in the 260/230 ratios. The range of values in the neat replicates was lower (0.18 for CVS and 0.03 for CRH Nanodrops) than for diluted sample replicates (1.41 and 0.38 respectively). Diluting was therefore seen to take the neat sample below the standard threshold. This indicates that very small or dilute DNA samples (as for sperm and germ cell extractions) may not be able to be accurately assessed on the Nanodrop, and if samples have ratios below the expected threshold, they may still contain high quality DNA.

Sample	Nanodrop Concentration (ng/µl)	260/280	260/230
Neat x1	676.7	1.93	2.05
Neat x2	1011.7	1.90	1.87
Neat x2	1241.4	1.92	1.89
Mean Neat	976.6	1.92	1.94
Range Neat	564.7	0.03	0.18
Diluted x1	-113.1	1.90	1.21
Diluted x2	96.4	1.83	1.25
Diluted x3	11.7	2.35	2.62
Mean Diluted	-1.67	2.03	1.69
Range Diluted	209.5	0.52	1.41

Table 2.7. Assessing quantity and quality of trial DNA using CVS Nanodrop. A Trial liver DNA sample was read 3 times on the CVS Nanodrop, before and after dilution 1:100 in AE. 260/280 and 260/230 ratios were less variable between replicates in the neat, compared to diluted sample. Quantity reading varied in both neat and diluted states.

Sample	Nanodrop Concentration (ng/µl)	260/280	260/230
Neat x1	794.1	1.91	1.93
Neat x2	886	1.88	1.92
Neat x2	933.7	1.89	1.90
Mean Neat	871.3	1.89	1.92
Range Neat	139.6	0.03	0.03
Diluted x1	12.9	1.68	1.62
Diluted x2	14.2	1.62	1.4
Diluted x3	15.2	1.74	1.24
Mean Diluted	14.1	1.68	1.42
Range Diluted	2.3	0.12	0.38

Table 2.8. Assessing quantity and quality of trial DNA using CRH Nanodrop. A Trial liver DNA sample was read 3 times on the CRH Nanodrop, before and after dilution 1:100 in AE. 260/280 and 260/230 ratios were higher and less variable between replicates in the neat, compared to diluted sample. Quantity readings were less variable in the diluted sample.

2.14.9 Extraction of DNA for Genotyping

DNA for *Sry* and EGFP genotyping was extracted using the DNeasy Blood and Tissue Kit (QIAGEN), following manufacturer's instructions. DNA was quantified to confirm that the extraction process had been successful. This was done using the Nanodrop as large yields were expected, and the exact DNA concentration was not required.

2.15 Enhanced Reduced Representation Bisulfite Sequencing

Enhanced Reduced Representation Bisulfite Sequencing (ERRBS) was performed at Weill Cornell University Epigenetics Core, New York, USA. Bioinformatic analysis was then conducted by Dr Thomas Smith (Computational Genomics Analysis and Training Programme (CGAT)), University of Oxford, UK).

2.16 FACS

Single cell suspensions, prepared as outlined in Chapter 2.5.2.1 and 2.5.2.2 were FACS sorted using a FACSAria II Special Order System sorter (Becton Dickinson Falcon). Sorting was conducted by Fiona Rossi and William Ramsay in the Centre for Inflammation Research Flow Cytometry Facility, The University of Edinburgh. EGFP-positive cells were separated from EGFP-negative cells based on their emission wavelength (525±50nm for EGFP). This was compared to a negative wild-type control, so that consistent gates for EGFP-positive fluorescence could be set. For fetal germ cell sorting, DAPI was added (1µl DAPI/250µl sample) to the suspension, to act as a marker for dead cells, the membranes of which would be sufficiently disrupted to allow DAPI to enter, and bind DNA. DAPI-positive cells were identified as having a fluorescent emission of 450±50nm. Only live, DAPI-negative cells were gated into the sample. Furthermore, only cells in single-cell suspension were selected, to prevent for example, a EGFP-negative cell being pulled into the EGFP-positive sample whilst attached to a EGFP-positive cell. Therefore the fetal germ cell sample was gated to include only cells which were DAPI-negative (live cells), singlets, and EGFP-positive. Distinct populations were seen for the

EGFP fetal germ cell sort. Their identity was confirmed by extraction of RNA and RT PCR as outlined in sections 2.11.2 and 2.11.5 respectively, followed by qPCR for *Dazl*, a germ cell-specific and *Sox9* a Sertoli cell-specific marker, using the primers detailed in section 2.13 (data shown in Chapter 5.3.1.1).

Due to the non-spherical morphology of sperm cells, doublets were not gated out of these samples. Indeed cells with a traditional forward-scatter for singlets were deemed to represent somatic cell contamination. DAPI was not used as a live/dead marker, due to its observed adherence to sperm which were seen to be moving under the microscope. We hypothesize that the marker might adhere to the sperm tails, seen in immunofluorescence studies to be particularly susceptible to non-specific staining (Chambers *et al*., unpublished observation). Therefore sperm were sorted based on EGFP fluorescence, relative to a wild-type control.

Positive and negative fractions were collected into eppendorfs coated with 2% FCS/PBS, to reduce the risk of cells adhering to the plastic. After FACS sorting, all samples were centrifuged at 1200 xg for 5 min to give a cell pellet. The supernatant was then removed before cells were snap frozen on dry ice and stored at -80°C.

2.17 Statistical Analyses

Numerical data were tested for normality of distribution using the Lilliefors test. Normally distributed data were then analysed by Student's t-tests or Analysis of Variance (ANOVA), with subsequent post-hoc Fisher's Least Significant Difference (LSD) analysis. Nonparametric data were analysed by Mann Whitney U test, or log transformed before performing an ANOVA. The influence of intra-litter association of pups on weight data was analysed using Multivariate Linear Regression. Statistical analyses were performed using Statistica (StatSoft, UK) or SPSS (IBM, USA). Figures were created in Excel (Microsoft, USA), and data expressed as mean value ± standard error.

Chapter 3 Characterising Epigenetic Reprogramming in the Rat

3.1 Introduction

As discussed in Chapter 1, disease risk might be transmitted across generations through influences on developing fetal germ cells. In the Dex model of programming, the phenotype of low birth weight and altered cardiometabolic parameters is transmitted through both the maternal and the paternal line [12]. Offspring exposed to an insult *in utero* might have alterations in their germ cells which could allow a transmission of phenotype to the second generation.

I hypothesise that one effect of Dex exposure may be to influence the period of epigenetic reprogramming in the developing germ cell. This process has been previously characterised in the mouse, and shown to involve an erasure and subsequent re-establishment of DNA methylation across the majority of the genome [14]. Germline epigenetic reprogramming has not however, been previously reported in the rat, which is used in many models of intergenerational disease transmission.

I therefore sought to investigate whether epigenetic reprogramming occurs in the rat, as for the mouse. I also aimed to characterise the time-frame of remethylation in this species, in order to identify key time-points for exploring the influence of Dex exposure. I also investigated the presence of 5hmC, 5fC and 5caC, as they have not been previously studied in germ cell epigenetic reprogramming in any species, and it has been suggested that they may have a role in early stage development [157]. A broader understanding of germ cell methylation was obtained by studying postnatal tissues, and the TDG enzyme, which has been implicated in the excision of 5fC and 5caC during active demethylation [150,151].

By gaining a global insight into the changes in DNA methylation across mid-late gestation and postnatal development, key time-points and forms of methylation were identified allowing more focused studies into the effects of Dex exposure on germ cell methylation.

3.2 Materials and Methods

Tissues for this study were a kind gift from Richard Sharpe's group.

Virgin female Wistar rats had been timed-mated with stock Wistar males before sacrifice at e14.5-e21.5 (n=3-4 at each time-point) and all pups removed. Testes had been extracted from male pups and fixed in Bouins, before embedding in paraffin wax. Tissue blocks were then microtomed to give 5 μm sections, which were then mounted on microscope slides.

For postnatal studies, rats were mated as previously, and pregnant dams allowed to deliver their pups naturally. Males were then sacrificed at PND4, PND8, PND10, PND15, PND25 and adulthood (≥90 days) (n=2-3 at each time-point). Tissues were fixed, embedded and sectioned as previously.

I then used immunofluorescence to explore the localisation of 5mC, 5hmC, 5fC, 5caC and TDG in the developing testis, following the protocols in Chapter 2.7. DAZL was used to confirm the location of germ cells within the testis throughout development, and Propidium Iodide was used as a nuclear counterstain. Image J was used to explore whether methylation patterns observed visually could be confirmed by pixel intensity analysis, as outlined in Chapter 2.7.13.2.

3.3 Results

3.3.1 Localisation of 5mC and 5hmC in Fetal Rat Testis

Immunohistochemistry with DAB detection was used to identify the localisation of 5mC (Figure 3.1) and 5hmC (Figure 3.2) in the developing fetal testis between e14.5 and e21.5. 5mC was largely undetectable in germ cells between e14.5 and e18.5 (Figure 3.1A-E). At e19.5, 5mC was detected in some germ cells (Figure 3.1F), with staining becoming augmented by e21.5 (Figure 3.1G). Conversely, 5hmC was detectable in germ cells between e14.5 and e16.5 (Figure 3.2A-C), but not from e17.5-e21.5 (Figure 3.2D-G). Both forms of methylation were found in somatic cells throughout the time-course.

In order to further explore the localisation, or potential co-localisation of 5mC and 5hmC, protocols were optimised for double immunofluorescence. Consistent with the immunohistochemistry results, little 5mC was detectable in germ cells between e14.5-e16.5 relative to the somatic component (Figure 3.3A-C) and was undetectable between e17.5 and e18.5 (Figure 3.3D and Figure 3.4A respectively). At e19.5 some 5mC was detectable in germ cells (Figure 3.4B), becoming augmented by e21.5 (Figure 3.4D). Some 5hmC was detectable in germ cells between e14.5 and e16.5 (Figure 3.3A-C), but was thereafter undetectable. Both 5mC and 5hmC co-localised in the somatic component between e14.5-e21.5 (Figures 3.3A-D and 3.4A-D).

In order to explore whether all germ cells become re-methylated at e19.5, I sought a nuclear counterstain that would be compatible with the HCl antigen retrieval required for methylation immunofluorescence. Propidium Iodide retained nuclear specificity after acid treatment (see Chapter 2.7.4). Tissues were therefore stained for 5mC and Propidium Iodide during the observed period of remethylation (Figure 3.5). Although germ cells were clearly present at e18.5 (Figure 3.5A), as identified by the position and morphology of their nuclei, 5mC was undetectable in the germ cells at this time-point. At e19.5 5mC was weakly detectable in some germ cells but stronger in others (Figure 3.5B). At e21.5 all germ cells identified by Propidium Iodide had a corresponding stain for 5mC (Figure 3.5C).

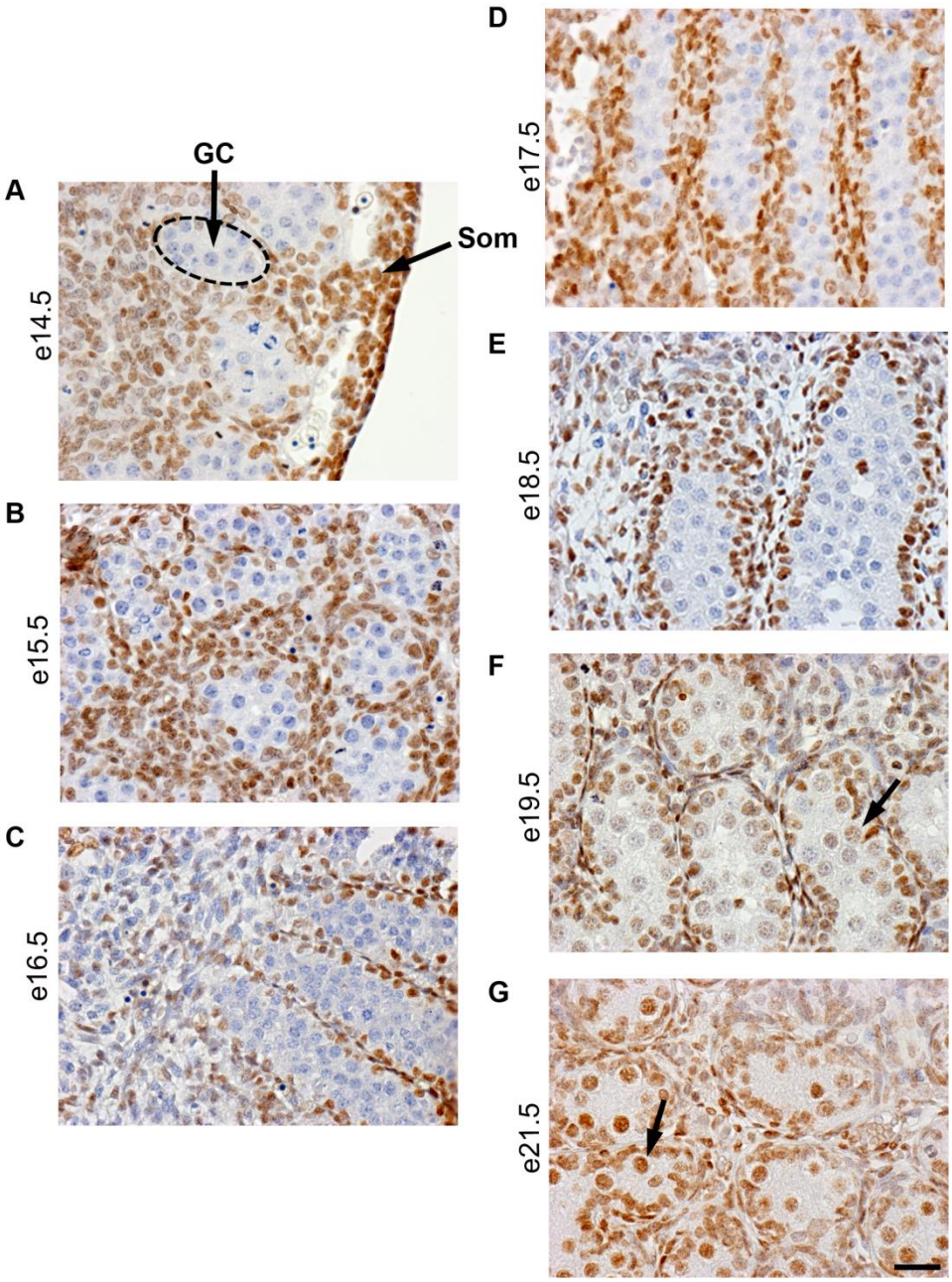

Figure 3.1. Localisation of 5mC during mid to late gestation. Images of immunostained testis show that 5mC (brown, arrows) is undetectable between e14.5 and e18.5 (A-E), appears at e19.5 (F) and becomes marked in germ cells at e21.5 (G). 5mC is found in somatic cells throughout the time course. Dotted line indicates a representative tubule within which germ cells (GC) exist, surrounding which are somatic cells (Som). Haematoxylin nuclear counterstain is shown in blue. Bar = 20µm.

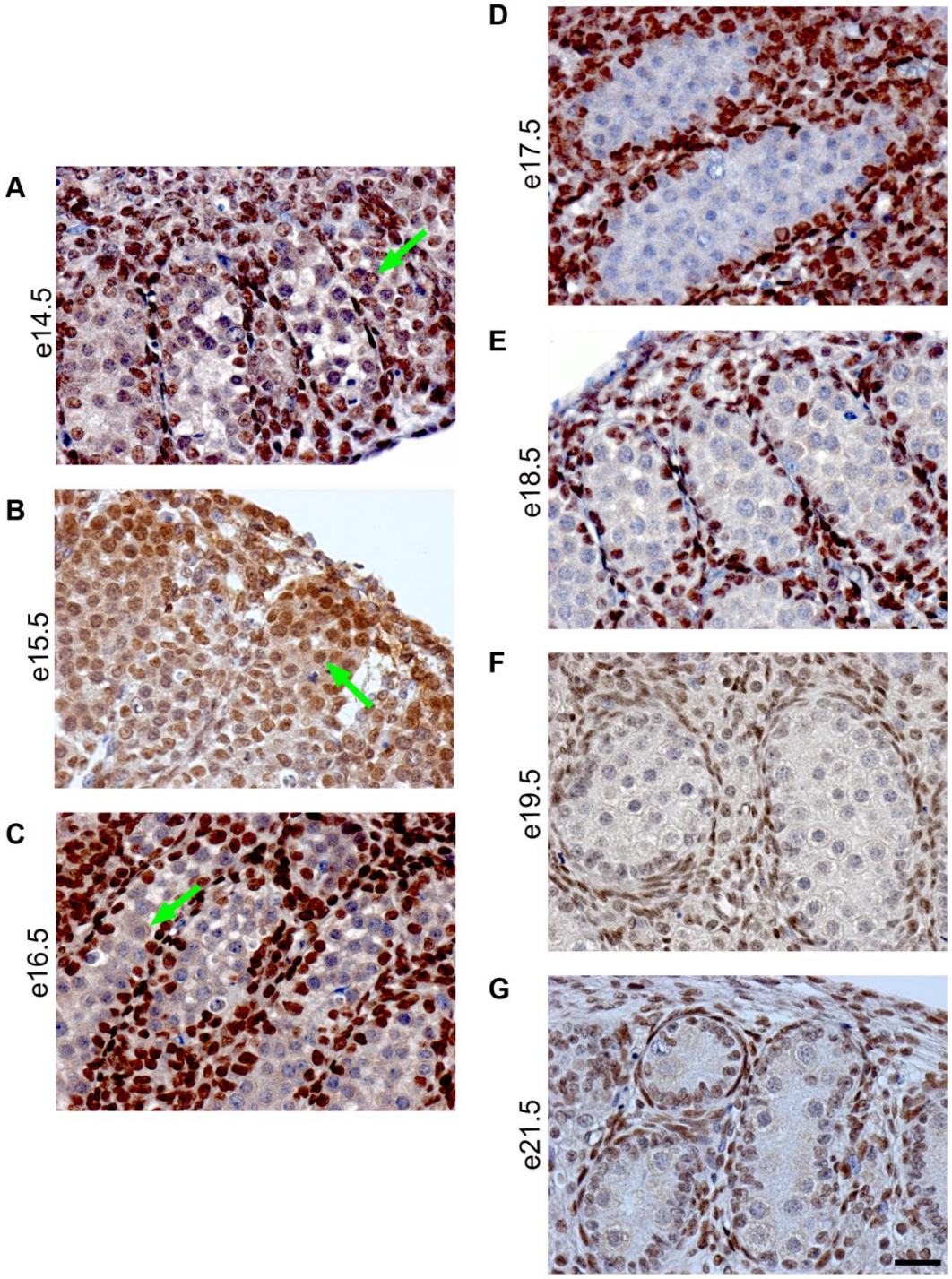

Figure 3.2. Localisation of 5hmC during mid to late gestation. Images of immunostained testis show some detection of 5hmC (brown, green arrows) in germ cells between e14.5 and e16.5 (A-C), not found from e17.5 to e21.5 (D-G). Haematoxylin nuclear counterstain is shown in blue. 5hmC (brown) is detected in somatic cells throughout the time course. Bar = 20µm.

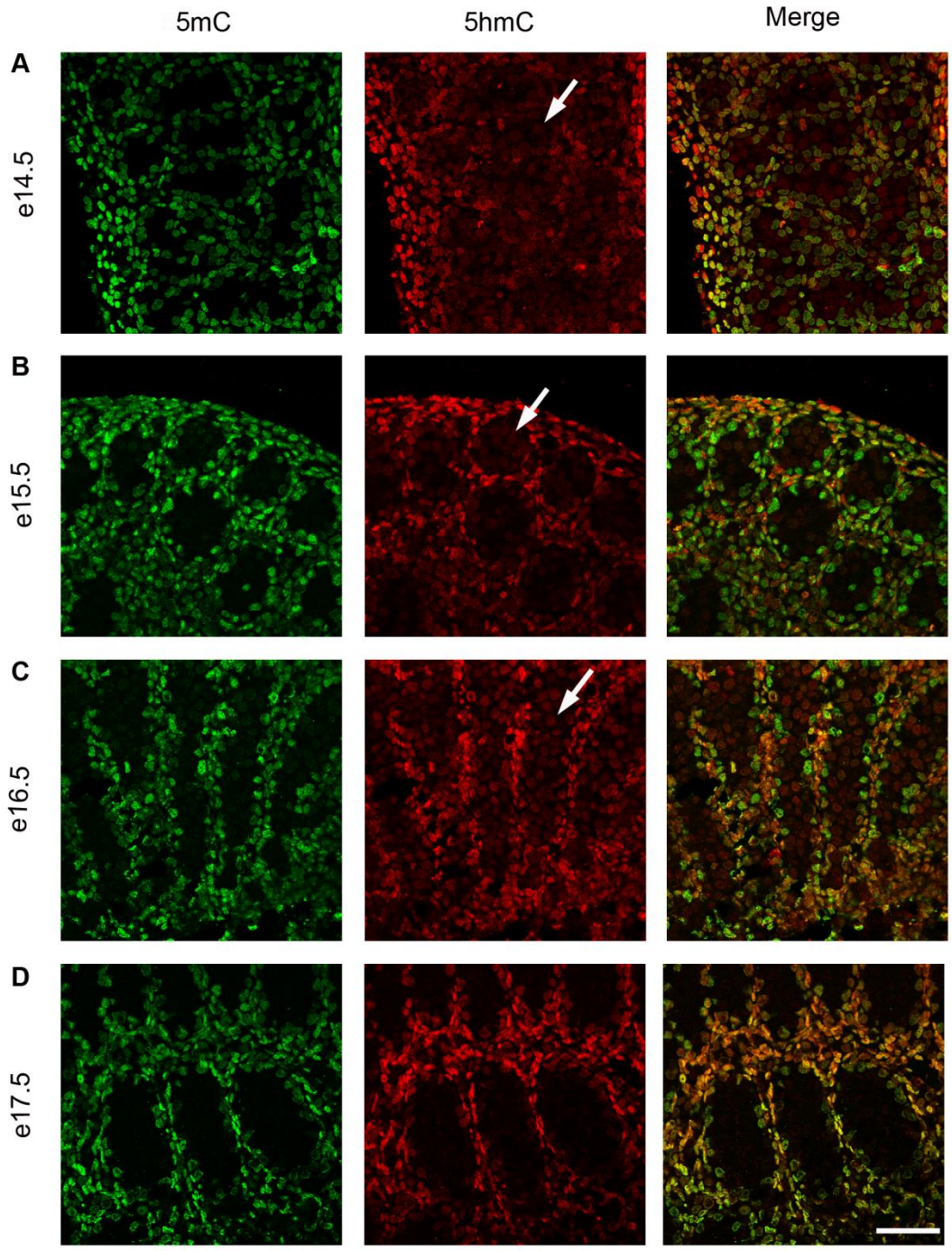

Figure 3.3. Localisation of 5mC and 5hmC during mid gestation. Images of immunostained testis show 5hmC localisation in germ cells between e14.5-e16.5 (A-C) (red, arrows). Some 5mC is also weakly detectable. Neither forms of methylation are detectable in germ cells at e17.5 (D). Both 5mC and 5hmC are detectable in somatic cells throughout the time course. Bar = 50µm. An enlarged version of this figure is presented in appendix Figures A1 and A2.

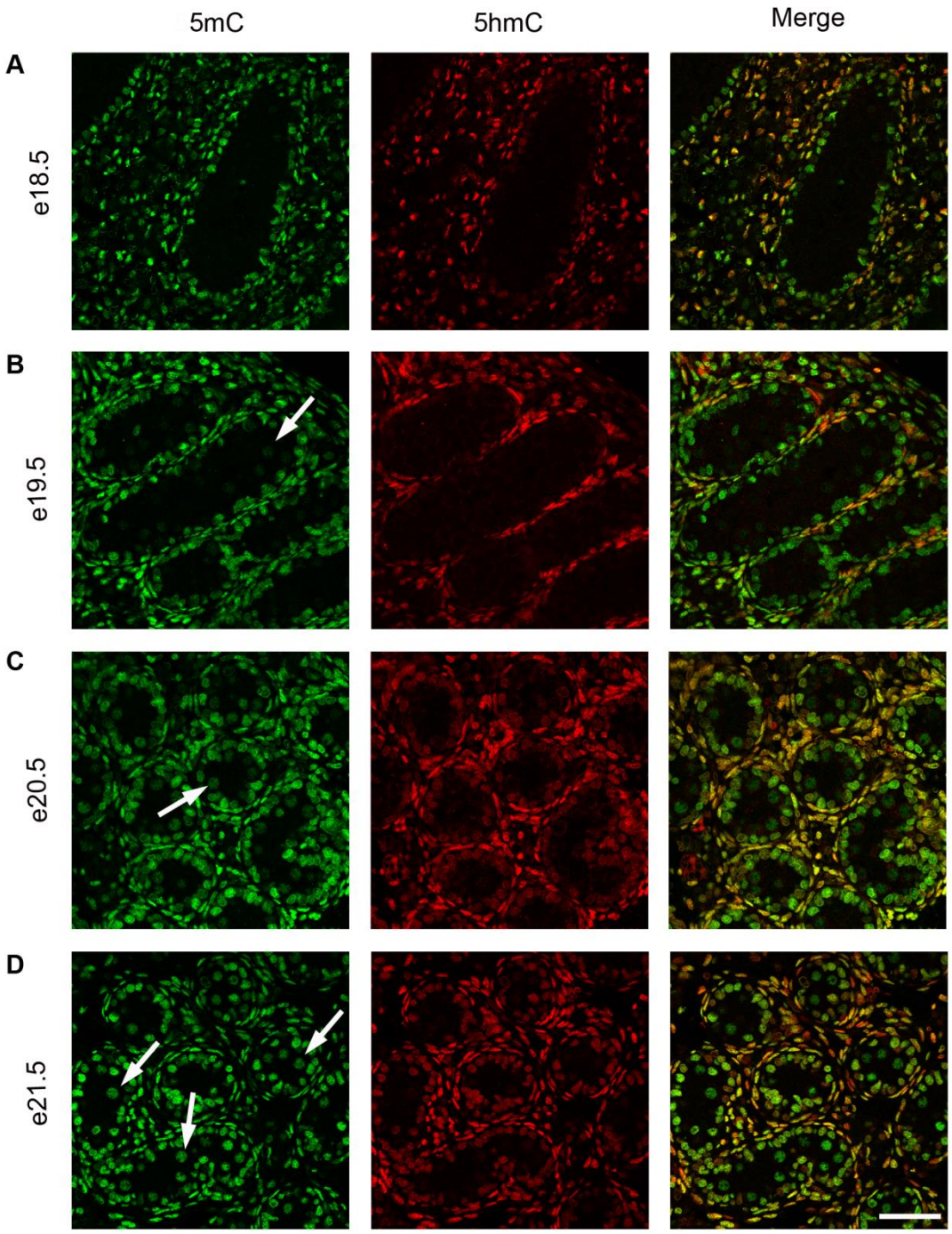

Figure 3.4. Localisation of 5mC and 5hmC during late gestation. Images of immunostained testis show that 5mC (green, arrows) is undetectable at e18.5 (A), appears at e19.5 (B) and becomes marked in germ cells between e20.5-e21.5 (C-D). 5hmC (red) is not detectable in germ cells. Both forms of methylation are found in somatic cells throughout the time course. Scale bar = 50µm.

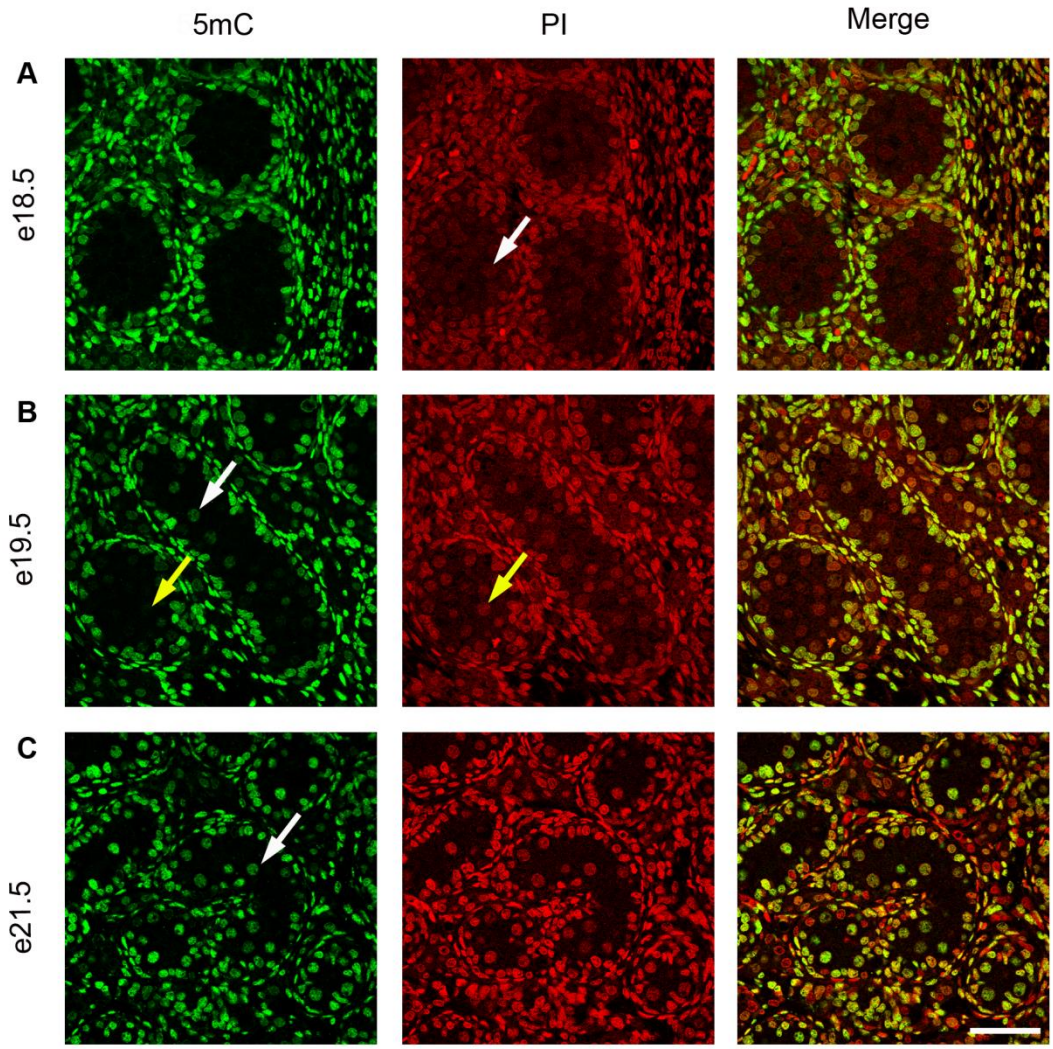

Figure 3.5. Details of germ cell remethylation. As previously shown, 5mC is not detectable in germ cells at e18.5 (A), appears at e19.5 (B) and becomes marked at e21.5 (C, green, white arrows). At e19.5, some germ cells identified by Propidium Iodide (PI) nuclear counterstain (red) have very little corresponding methylation (yellow arrows). Others have strongly detectable 5mC (white arrow). At e21.5 all germ cells visualised with Propidium Iodide have corresponding 5mC staining. Bar = 50µm.

3.3.2 Exploring the Localisation of 5fC and 5caC in Fetal Rat Testis

I also explored the localisation of the two additional forms of cytosine methylation, 5fC and 5caC, particularly as it has been suggested that they form part of the putative DNA demethylation pathway, or potentially have a role in development [149,150,157]. Immunofluorescence indicates that 5fC and 5caC are present in germ cells from e14.5-16.5 (Figures 3.6A-C and 3.8A-C), but are undetectable from e17.5 (Figures 3.6D and 3.8D), and that this is maintained through to e21.5 in the germ cells (Figures 3.7A-D and 3.9A-D). Both 5fC and 5caC were identified in somatic cells throughout the time-course.

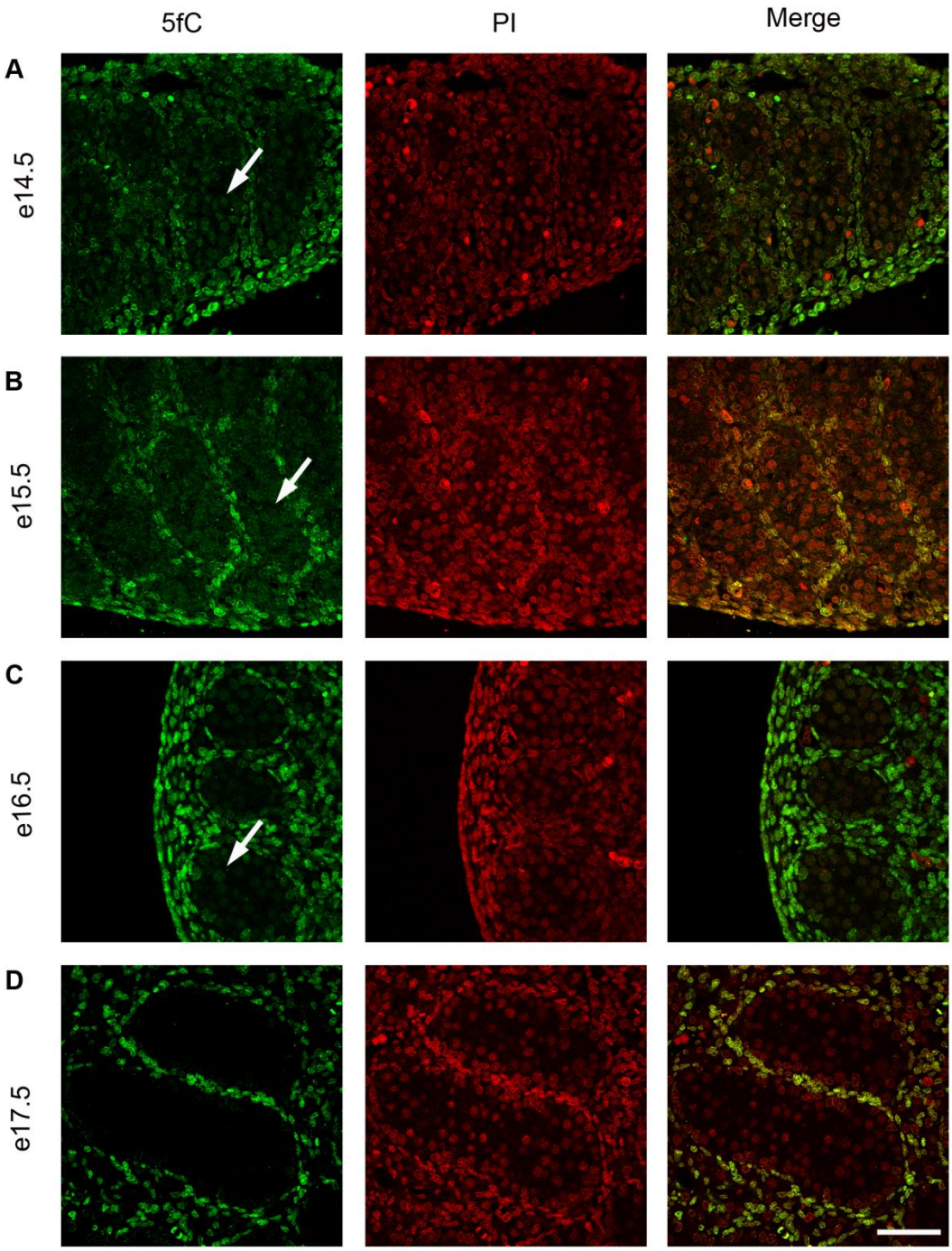

Figure 3.6. Localisation of 5fC during mid gestation. Images of immunostained testis show 5fC localisation in germ cells between e14.5-e16.5 (A-C) (green, arrows), which is undetectable at e17.5 (D). Propidium Iodide (PI) acts as a nuclear counterstain (red). 5fC is detected in somatic cells throughout the time course. Bar = 50µm.

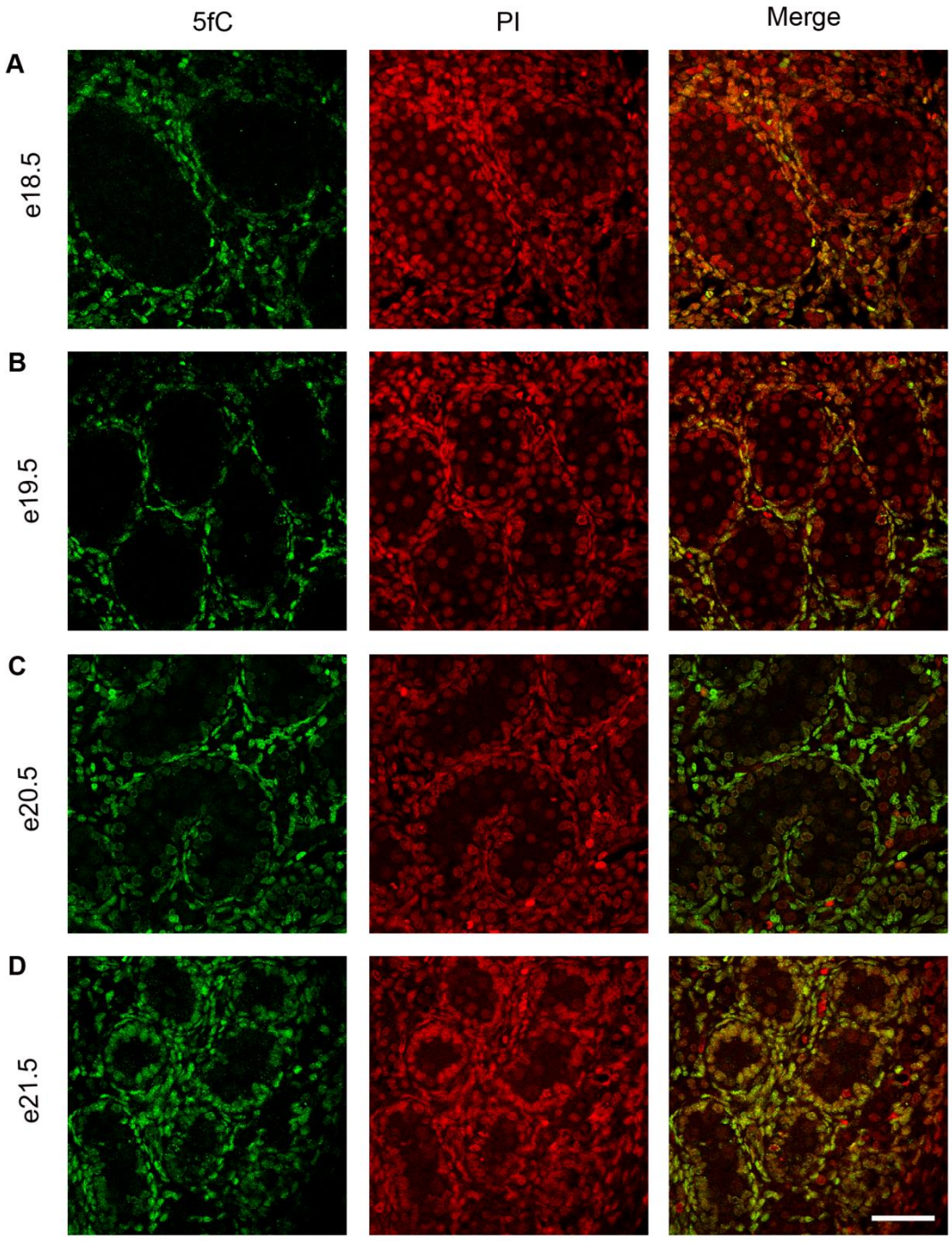

Figure 3.7. Localisation of 5fC during late gestation. Images of immunostained testis show that 5fC (green) is not detectable in germ cells between e18.5 and e21.5 (A-D). Propidium Iodide (PI) acts as a nuclear counterstain (red). 5fC is found in somatic cells throughout the time course. Bar = 50µm.

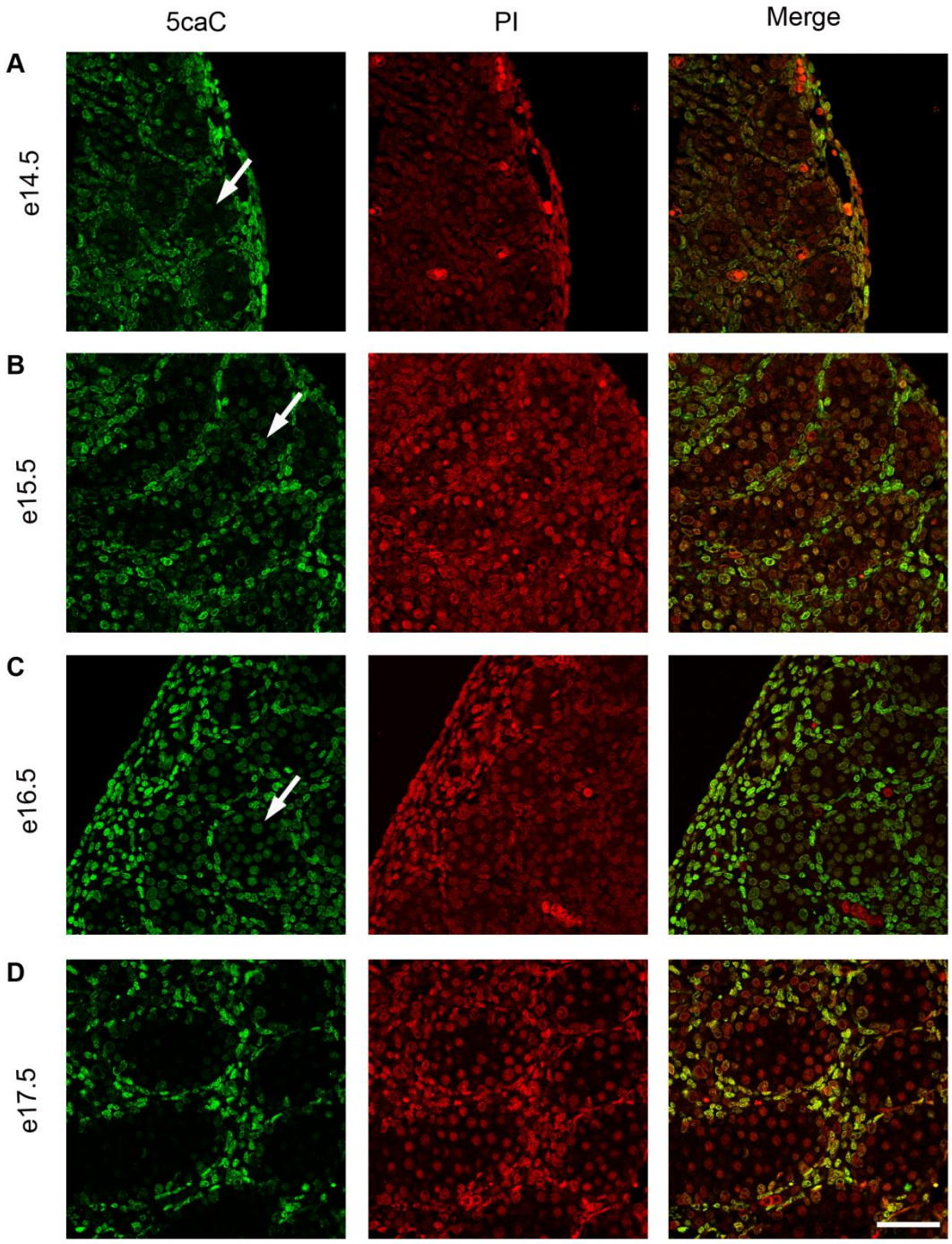

Figure 3.8. Localisation of 5caC during mid gestation. Images of immunostained testis show 5caC localisation in germ cells between e14.5-e16.5 (A-C) (green, arrows). Propidium Iodide acts as a nuclear counterstain (red). 5caC is found in somatic cells throughout the time course. Bar = 50µm.

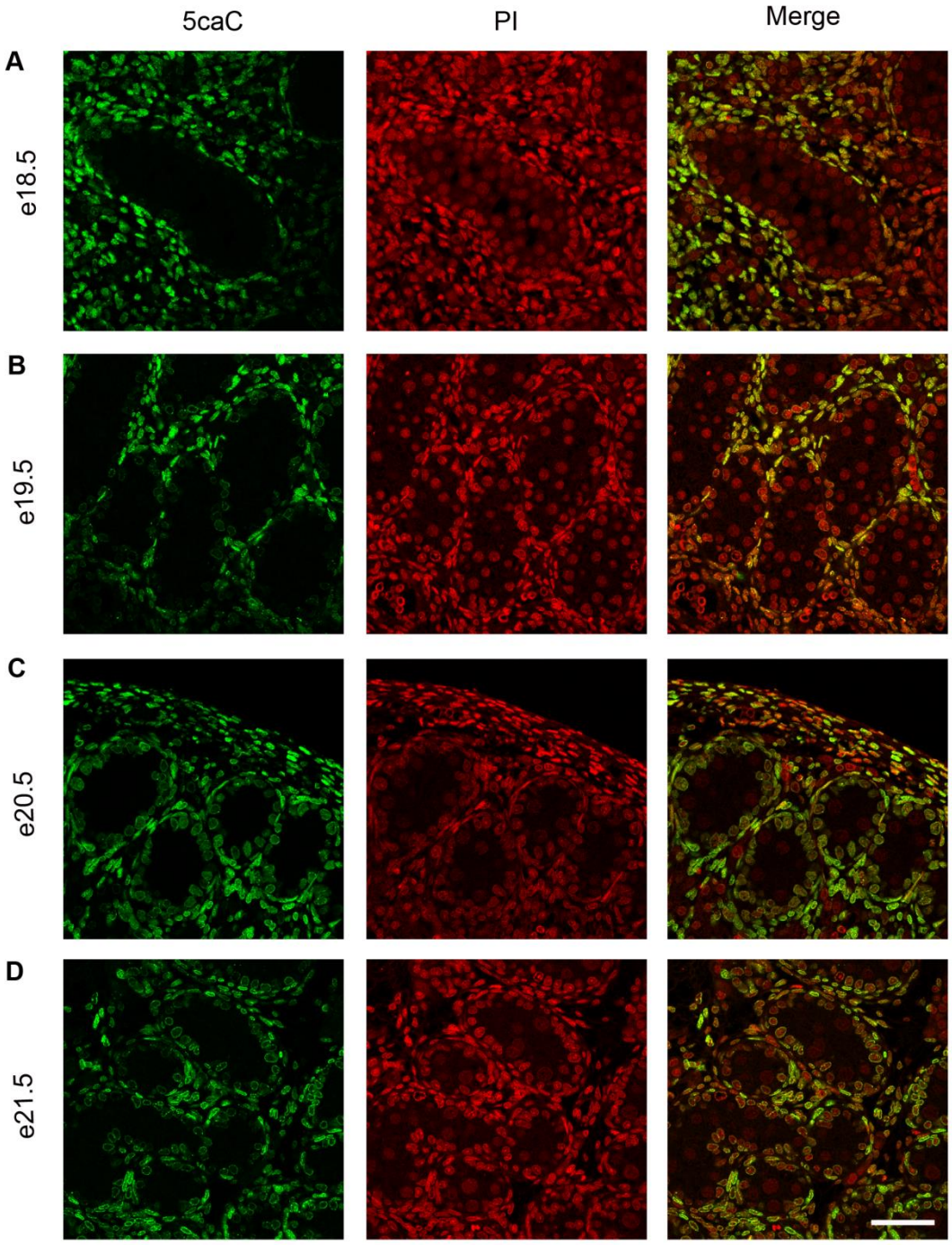

Figure 3.9. Localisation of 5caC during late gestation. Images of immunostained testis show that 5caC (green) is not detectable in germ cells between e18.5 and e21.5 (A-D). Propidium iodide acts as a nuclear counterstain (red). 5caC is found in somatic cells throughout the time course. Bar = 50µm.

3.3.3 A Potential Peak of 5hmC, 5fC and 5caC

During the studies of global fetal germ cell methylation I noted that there was variability in the intensity of detection of 5hmC, 5fC and 5caC at e16.5. Although immunofluorescence is only semi-quantitative, one particular sample had a strikingly intense antibody detection in germ cells. This was seen in multiple sections from different runs of staining. Immunofluorescence in this tissue is compared to that of a pup from another litter at the same time-point for 5hmC (Figure 3.10), 5fC (Figure 3.11) and 5caC (Figure 3.12).

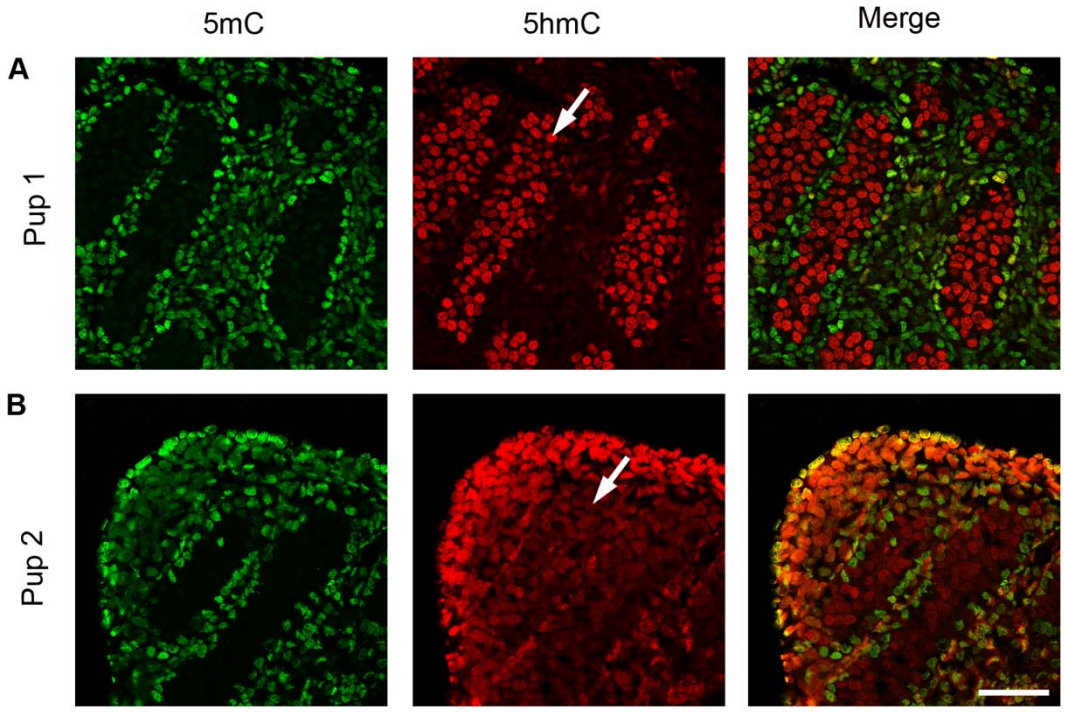

Figure 3.10. Exploring the homogeneity of 5hmC at e16.5. An example of variation in germ cell 5hmC staining (red, arrows) between litters. 5hmC is present in both samples, but staining is more intense, relative to somatic cells, in Pup 1 (A) compared to Pup 2 (B). Bar = 50µm.

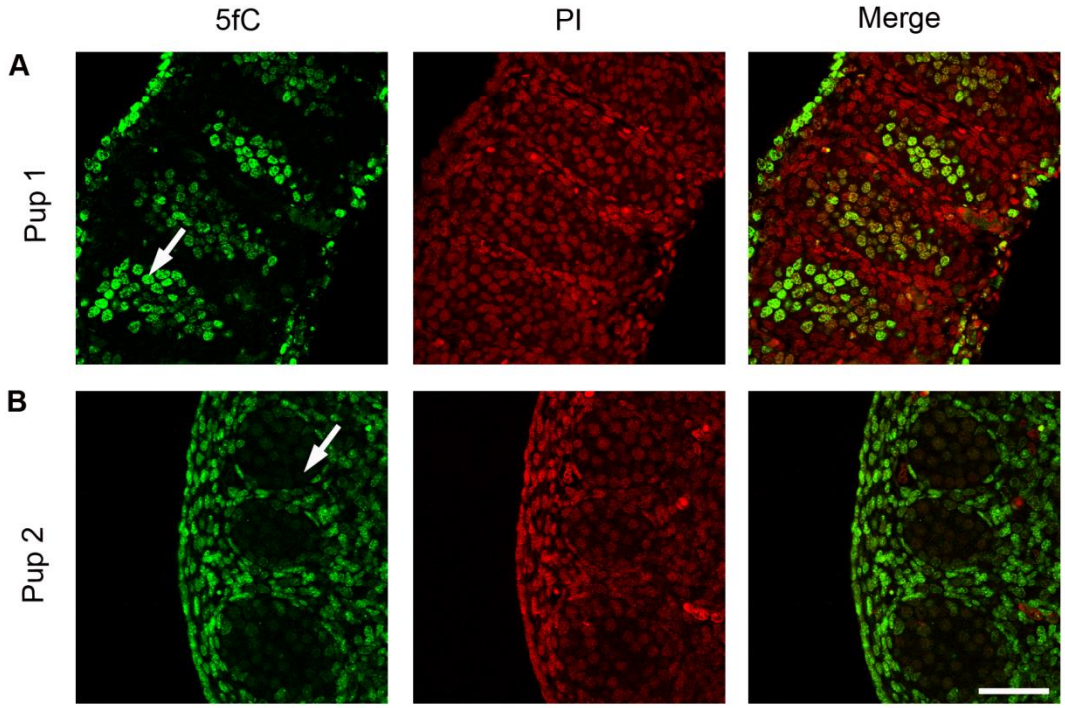

Figure 3.11. Exploring the homogeneity of 5fC at e16.5. An example of variation in germ cell 5fC staining (green, arrows) between litters. Propidium Iodide (PI) acts as a nuclear counterstain. 5fC is present in both samples, but staining is more intense, relative to somatic cells, in Pup 1 (A) compared to Pup 2 (B). Bar = 50µm.

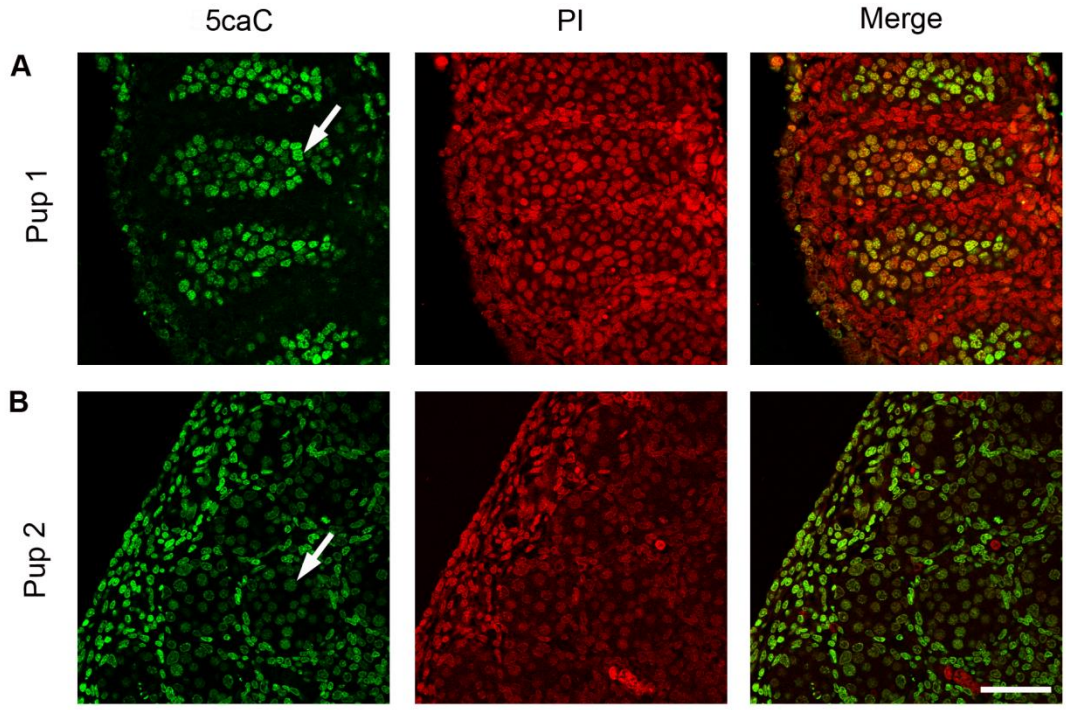

Figure 3.12. Exploring the homogeneity of 5caC at e16.5. An example of variation in germ cell 5caC staining (green, arrows) between litters. Propidium Iodide (PI) acts as a nuclear counterstain. 5caC is present in both samples, but staining is more intense, relative to somatic cells, in Pup 1 (A) compared to Pup 2 (B). Bar = 50µm.

3.3.4 Further Definition of the Localisation of Cytosine Methylation in Fetal Testis

As discussed previously, the HCl antigen retrieval required for the methylation immunodetection protocol meant that traditional counterstains, such as DAPI were no longer nuclei-specific. I had also tried to detect Vasa, a germ cell specific marker, but found that it was unable to bind after HCl treatment. This, however, did not inhibit the study of reprogramming as the germ cell nuclei have a well characterised morphology and location within the developing testis. Following reviewers comments on the manuscript which subsequently became Rose *et al*. (2014) [249], I sought to optimise a protocol for germ cell identification along with 5mC immunohistochemistry, to provide an extra confirmation of germ cell location.

A protocol was optimised for 5mC and the germ cell marker DAZL (see Chapter 2.7.6), altering the pH of antigen retrieval. Immunohistochemistry indicates the location of germ cells across the prenatal time-course (Figure 3.13), and confirms that the 5mC remethylation identified is occurring in this cell type.

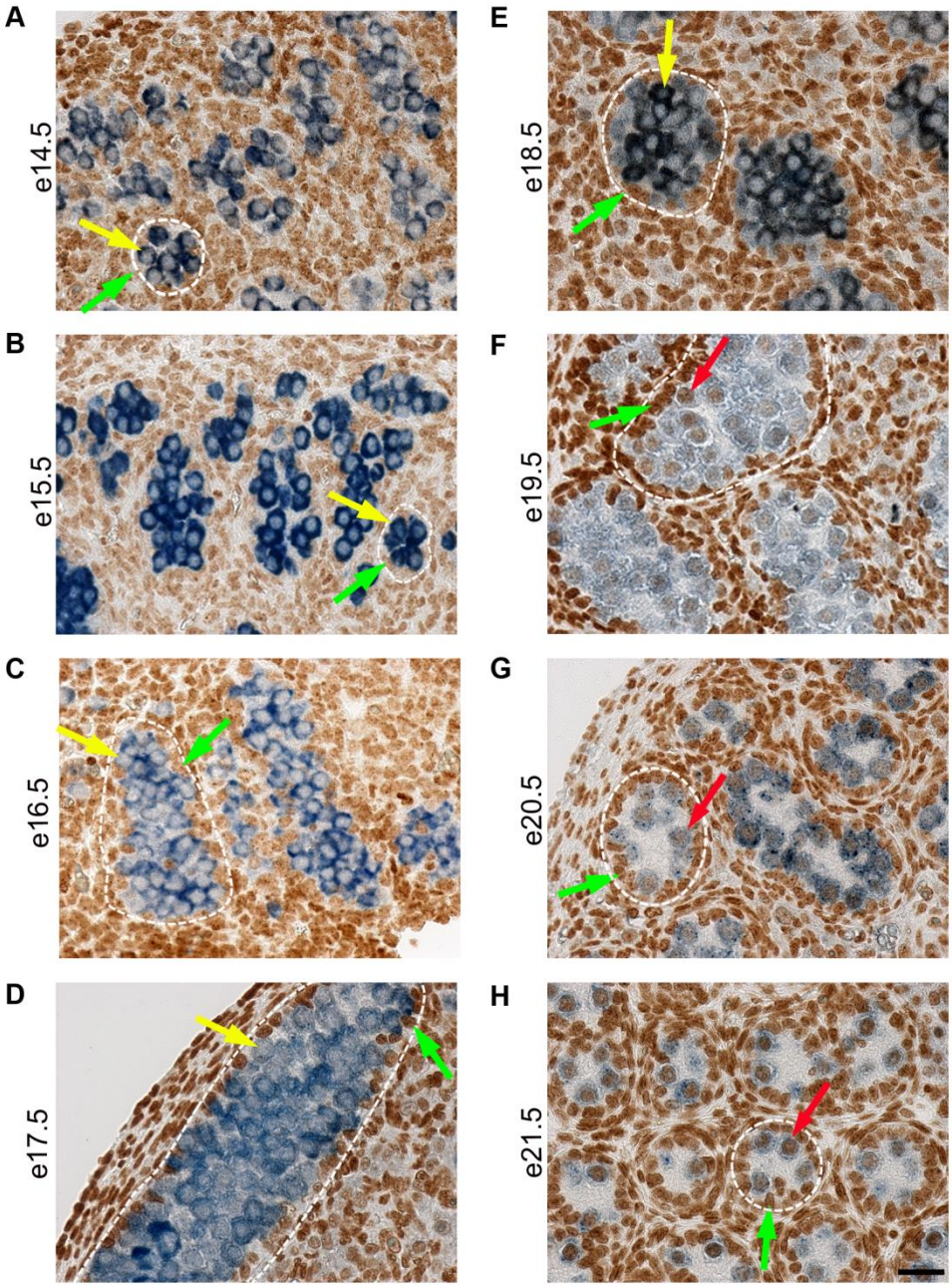

Figure 3.13. Localisation of 5mC with DAZL germ cell marker. Images of immunostained testis show the localisation of 5mC (brown) and DAZL (blue, yellow arrows) from e14.5-e21.5 (A-H). Somatic cells (representative green arrows) line the seminiferous cords (dotted line), within which the germ cells exist (yellow arrows). Images show that 5mC is undetectable between e14.5 and e18.5 (A-E) in germ cells. 5mC is detectable in germ cells at e19.5 (F) (red arrows) becoming augmented at e20.5-e21.5 (G-H). 5mC is present in somatic cells throughout the time course. Bar = 20µm.

3.3.5 Semi-Quantitative Confirmation of Methylation Patterns Visualised by Immunofluorescence

In order to explore whether methylation patterns observed visually could be confirmed by pixel intensity analysis of immunofluorescence, Image J software was used. An estimate of germ cell pixel intensity was obtained by setting the region of interest to be within the seminiferous tubule, just inside the ring of Sertoli cell nuclei. The mean pixel intensity within each tubule was then normalised to that for somatic cells within the same image. Across 4 pups from 4 separate litters, the normalised pixel intensity was significantly increased ($p<0.01$, Figure 3.14A) for 5mC and decreased ($p<0.05$, Figure 3.14B) for 5hmC at e21.5, compared to e16.5.

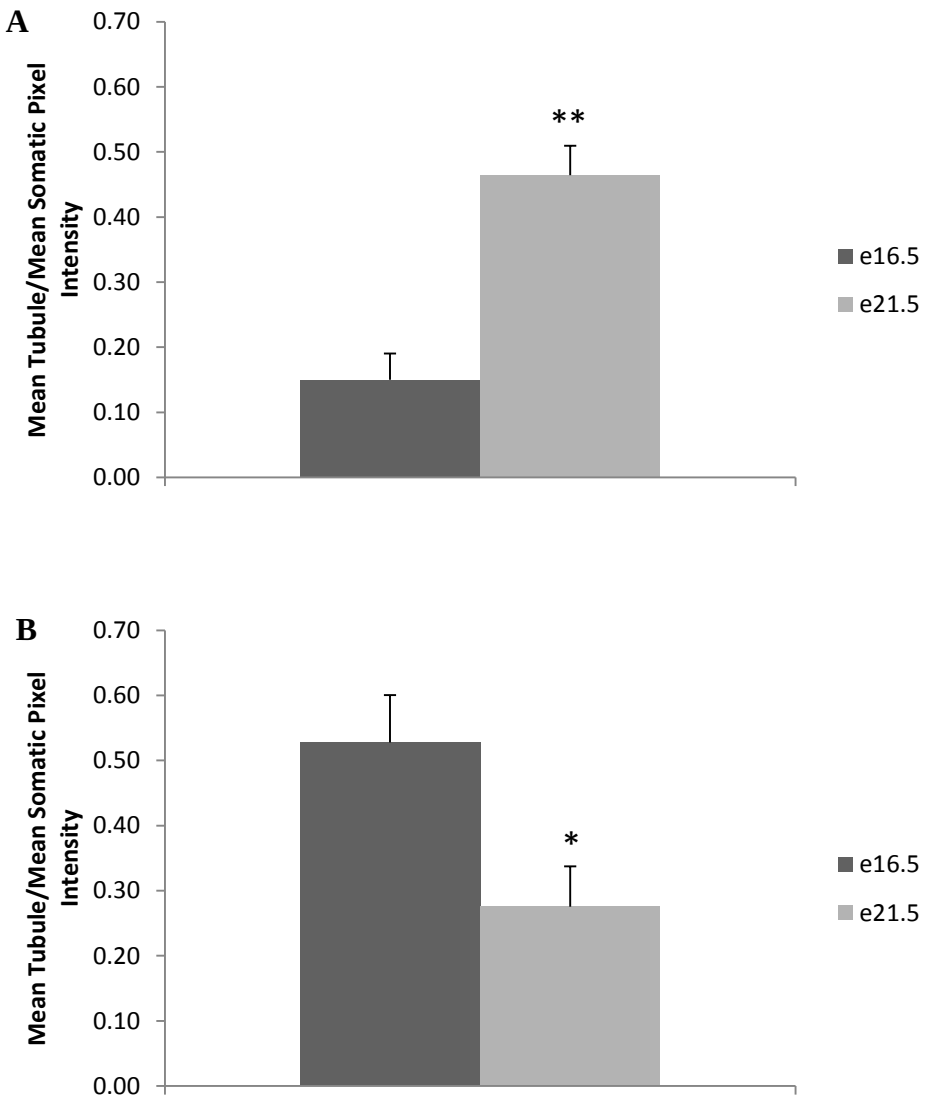

Figure 3.14. Semi quantification of 5mC and 5hmC immunofluorescence. Mean tubule pixel intensity is normalised to the mean for somatic cells within the same image. Mean normalised tubule intensity was significantly increased ($p<0.01$) for 5mC (A) and decreased ($p<0.05$) for 5hmC (B) staining at e21.5, compared to e16.5. All data were analysed by t-test. Bars represent mean ± standard error. *$p<0.05$, **$p<0.01$

3.3.6 The Localisation of Cytosine Methylation in Postnatal Testis Development

In order to gain a broader understanding of germ cell epigenetics in early development, immunofluorescence was performed on postnatal tissues. Testes were studied at PND4-25, covering early life and puberty, and in the adult rat (>90 days). 5mC was detectable in germ cells and somatic cells from PND4-15 (Figure 3.15A-C and Figure 3.16A-B), and in spermatogonia from PND25 (Figures 3.16C-D). 5hmC was largely undetectable in germ cells from PND4-8 (Figure 3.15A-C), with some detection from PND10 (Figure 3.16A-B). Intriguingly, strong 5hmC staining was seen in the spermatogonia of some tubules at PND25 (Figure 3.16C), which was largely absent in adult testis (Figure 3.16D). 5hmC was detectable in Sertoli cells from PND4-PND15, and staining was particularly intense at PND10 and PND15 (Figure 3.16A-B).

I performed a subsequent study examining the localisation of 5caC at key points in the previous time-course. Intriguingly, there was little detectable 5caC staining in any cell type at PND4 (Figure 3.17A), but staining was strikingly intense at PND10 (Figure 3.17B) in Sertoli cell nuclei, with some also detectable in germ cells. At PND15 (Figure 3.17C), some 5caC was detectable in germ and Sertoli cell nuclei. At PND25 (Figure 3.17D), 5caC was undetectable in the germ cells lying within many tubules, whilst it was very intense in others. In adult testis, 5caC was detectable in spermatogonia within some tubules (Figure 3.17E).

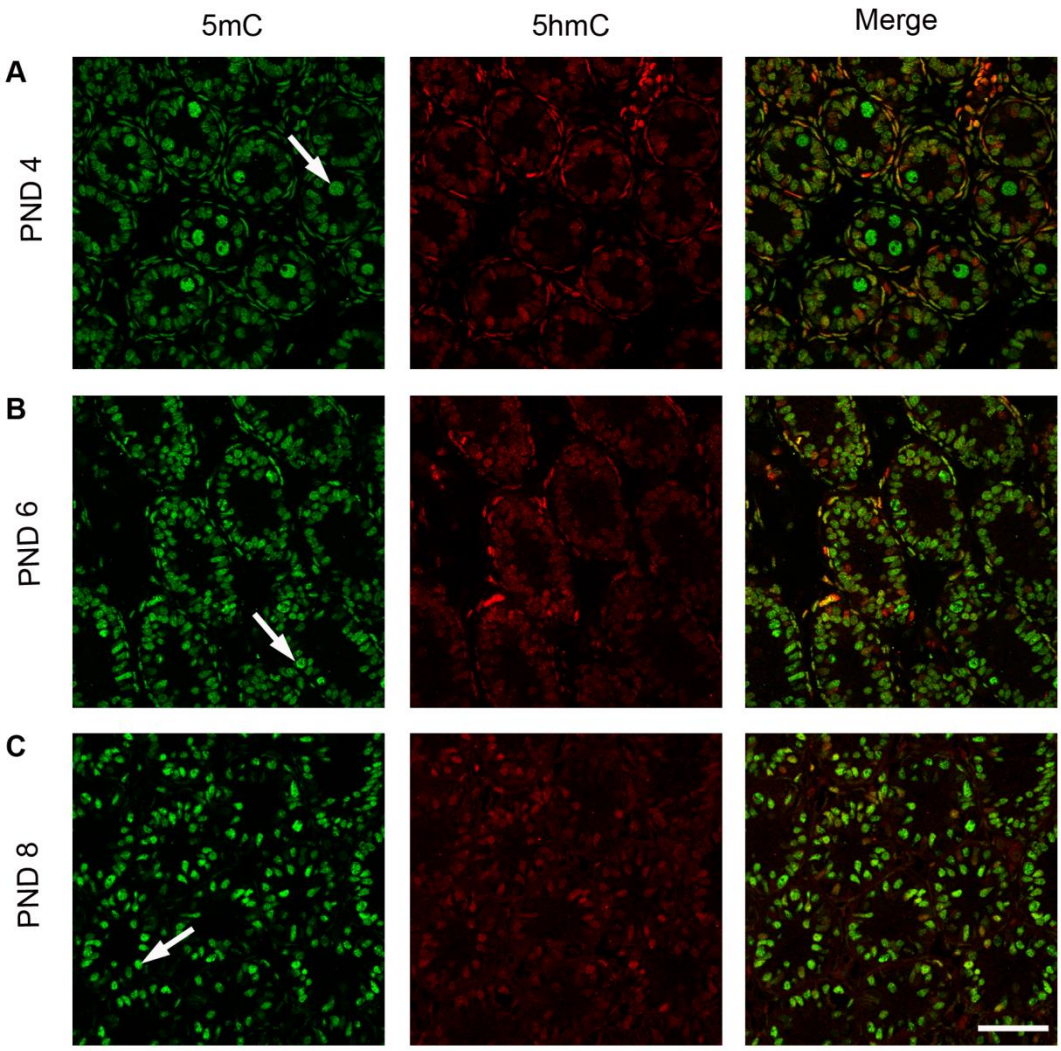

Figure 3.15. Localisation of 5mC and 5hmC during early postnatal period. Images of immunostained testis show 5mC localisation in germ cells between PND4 and 8 (A-C) (green, arrows). 5hmC is not detectable within the germ cells. Both forms of methylation are detectable in somatic cells throughout the time course. Bar = 50µm.

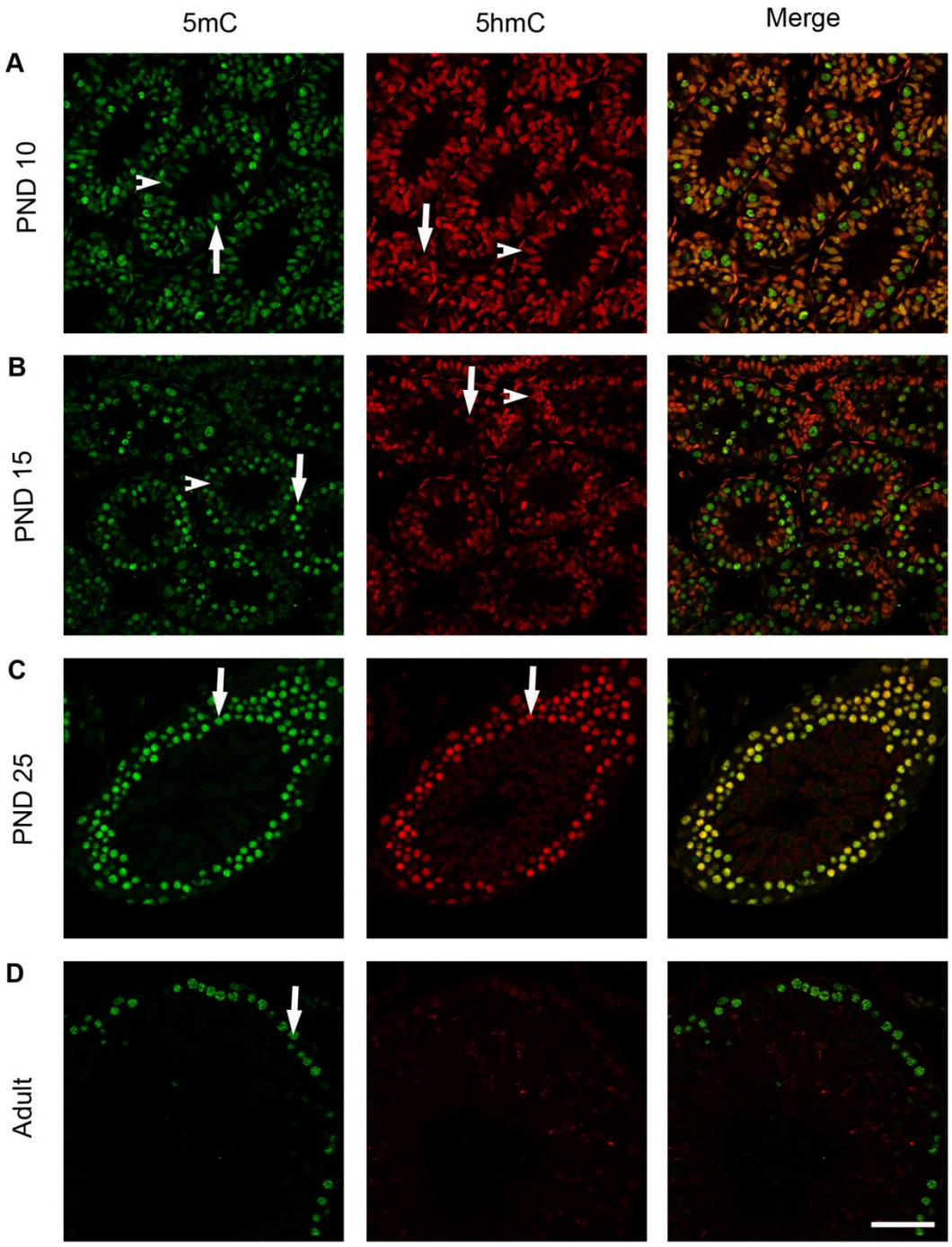

Figure 3.16. Localisation of 5mC and 5hmC during late postnatal period. Images of immunostained testis show 5mC localisation in germ cells (green, arrows) and somatic cells (green, arrowheads) at PND10-PND15 (A-B). 5mC is detectable in spermatogonia in PND25 and adult testis. 5hmC was detectable in germ cells (red, arrows) from PND10-PND15, with an intense stain at PND25. 5hmC was strongly detectable in Sertoli cell nuclei at PND10-PND15 (A-B) (red, arrowheads). Bar = 50µm.

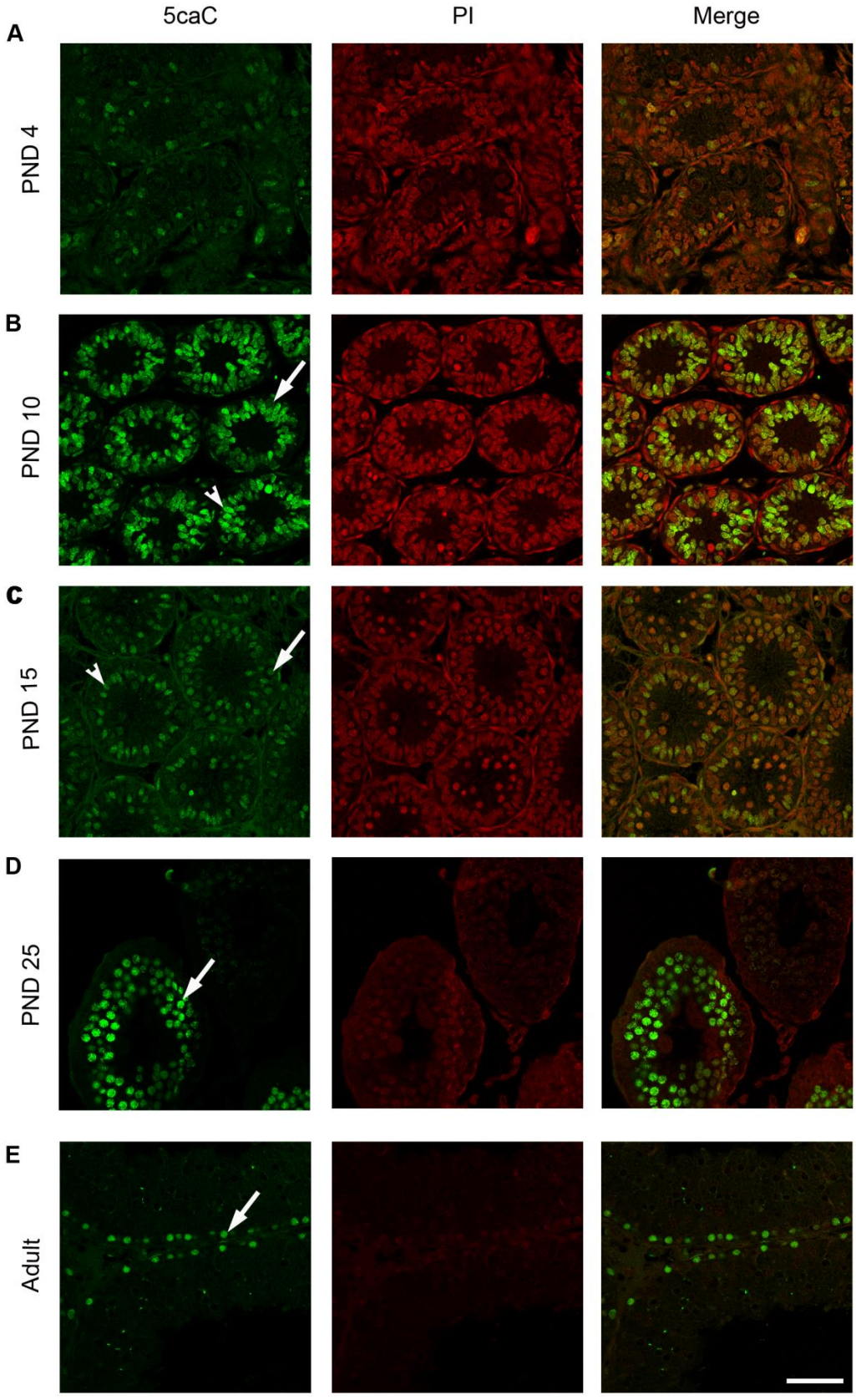

Figure 3.17. Localisation of 5caC during postnatal period. Images of immunostained testis show some 5caC localisation in germ cells (green, arrows) at PND10-PND15, with strong staining in the germ cells within some tubules at PND25. 5caC was also detectable in the spermatogonia of some tubules in adult tissue (green, arrow). Strong staining for 5caC was seen in Sertoli cell nuclei at PND10, with some staining remaining at PND15 (green, arrowheads). Little 5caC was detectable in any cell at PND4. Propidium Iodide (PI) acts as a nuclear counterstain. Bar = 50µm.

3.3.7 The Localisation of TDG

I studied the localisation of TDG throughout the pre- and post-natal time-course as it has been suggested that this enzyme excises 5fC and 5caC, completing a chain of demethylation [150,151]. It has not, however, been previously characterised in the developing testis. TDG was identified in germ cells between e14.5 and e16.5 (Figure 3.18A-C), but was not detectable from e17.5-e21.5 (Figure 3.18D and Figure 3.19A-D). TDG was detectable in the somatic component at all time-points, and staining was particularly striking in Sertoli cells from e17.5-e21.5.

Between PND4 and PND15, TDG was detectable in Sertoli cell nuclei, with the greatest intensity of staining from PND10-PND15 (Figure 3.20B-C). There was little detectable TDG in germ cells. Intriguingly, although this enzyme was not detectable in adult germ or Sertoli cell nuclei, it did appear to localise to unknown punctate structures beside the germ cell nuclei (Figure 3.20E).

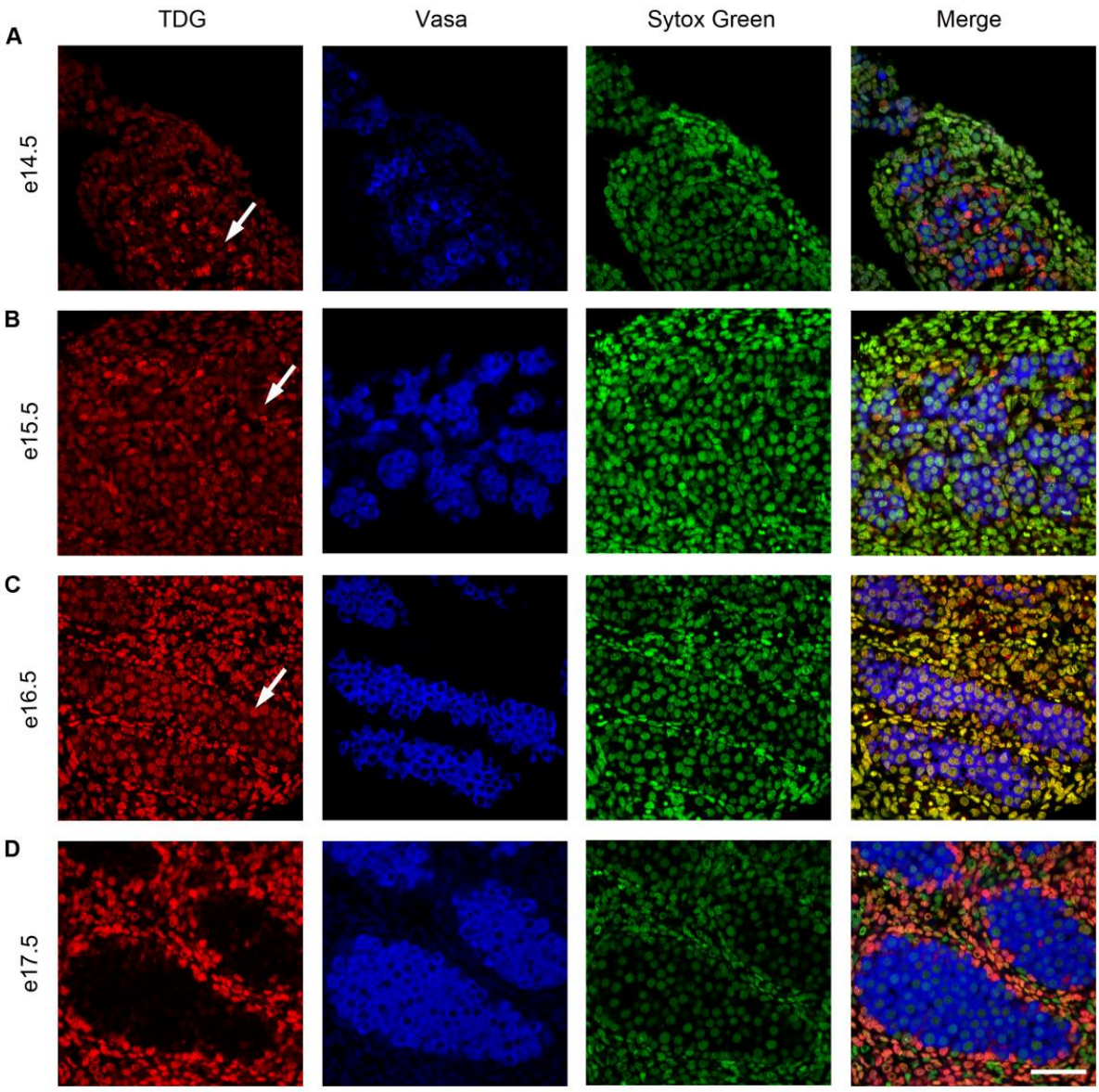

Figure 3.18. Localisation of TDG during mid gestation. Images of immunostained testis show TDG localisation in germ cells between e14.5-e16.5 (A-C) (red, arrows), which is largely undetectable by e17.5 (D). TDG is found in somatic cells throughout the time course. Vasa and Sytox Green act as germ cell and nuclear markers respectively. Bar = 50µm.

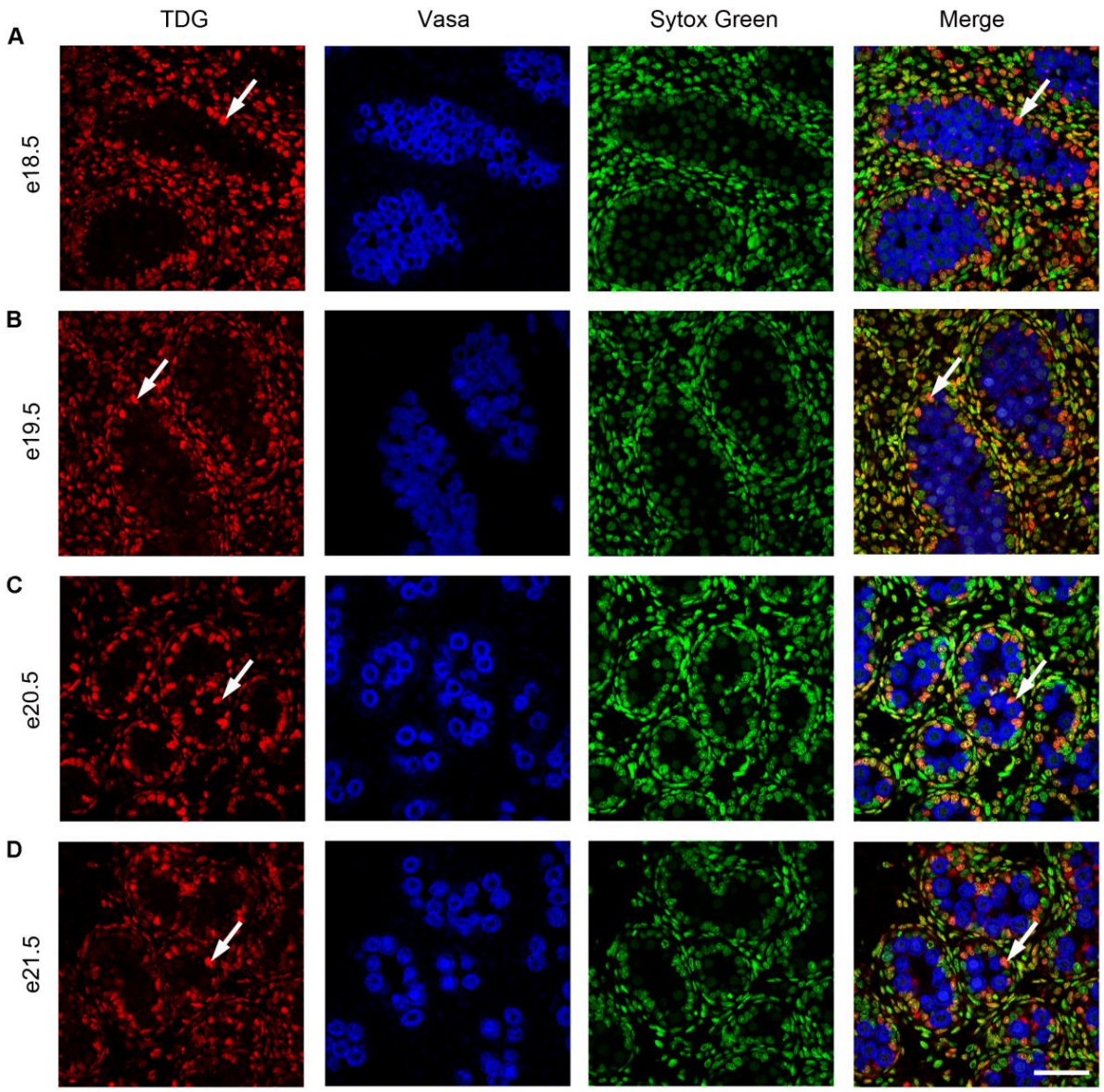

Figure 3.19. Localisation of TDG during late gestation. Images of immunostained testis show TDG is largely undetectable in germ cells between e18.5-e21.5 (A-D). TDG is detectable in somatic cells throughout the time course, with notable intensity in Sertoli cell nuclei (red, arrows). Vasa and Sytox Green act as germ cell and nuclear markers respectively. Bar = 50μm.

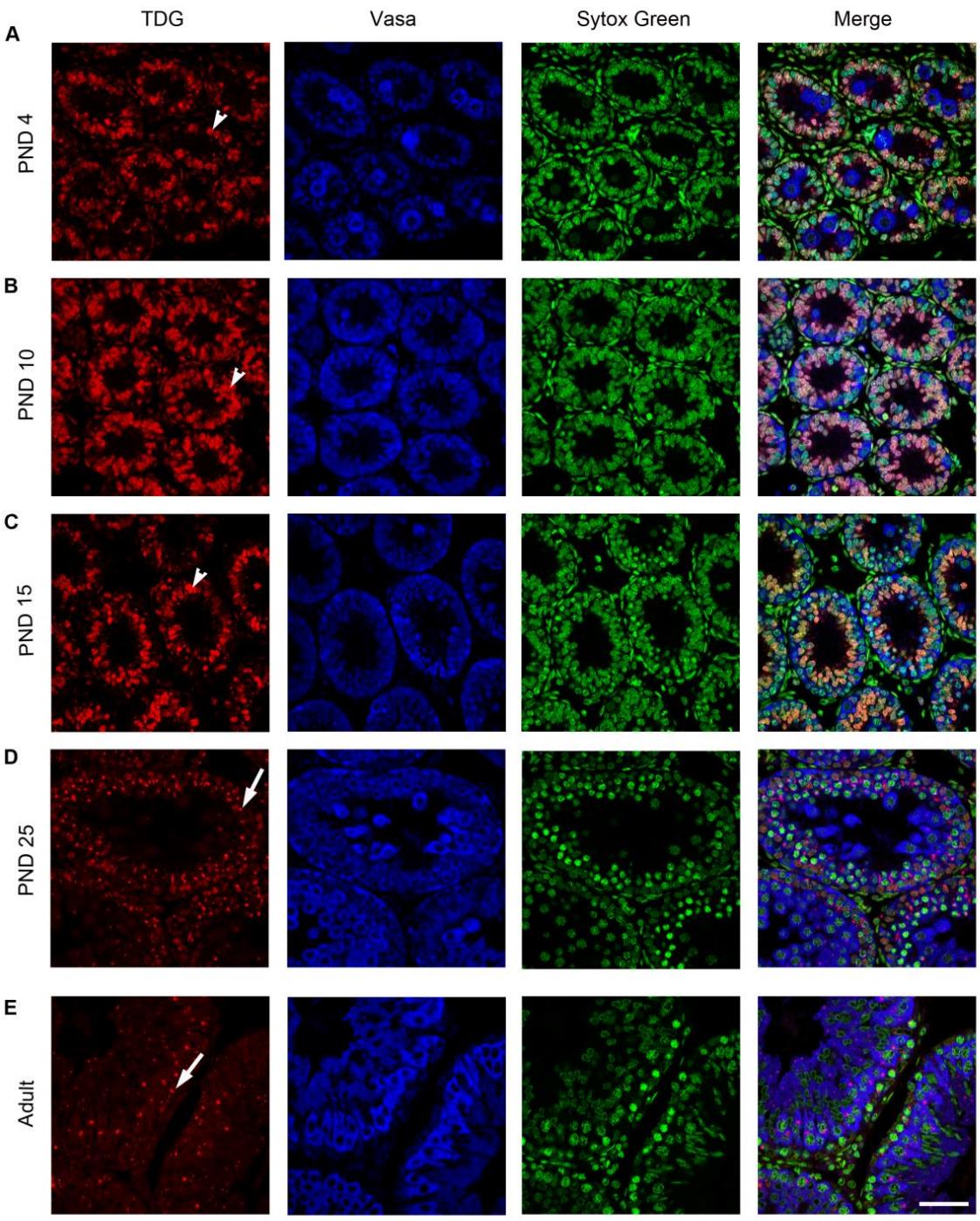

Figure 3.20. Localisation of TDG during the postnatal period. Images of immunostained testis show little detectable TDG in germ cells. Strong staining for TDG was seen in Sertoli cell nuclei at PND4-PND15 (A-C) (red, arrowheads), which was thereafter absent. TDG also gave a punctate staining pattern in PND25 (D) and adult tissues (E) (red, arrows). Vasa and Sytox Green act as germ cell and nuclear markers respectively. Bar = 50µm.

3.4 Discussion

These data indicate for the first time that epigenetic reprogramming occurs in the rat, and that global cytosine methylation is re-established between e18.5 and e20.5. Dynamic changes were also seen in the localisation of 5hmC, 5fC and 5caC in both prenatal and postnatal development (Figure 3.21). The localisation of TDG during rat fetal development was also characterised for the first time, and immunofluorescence suggests that its pattern of expression largely follows that of 5caC.

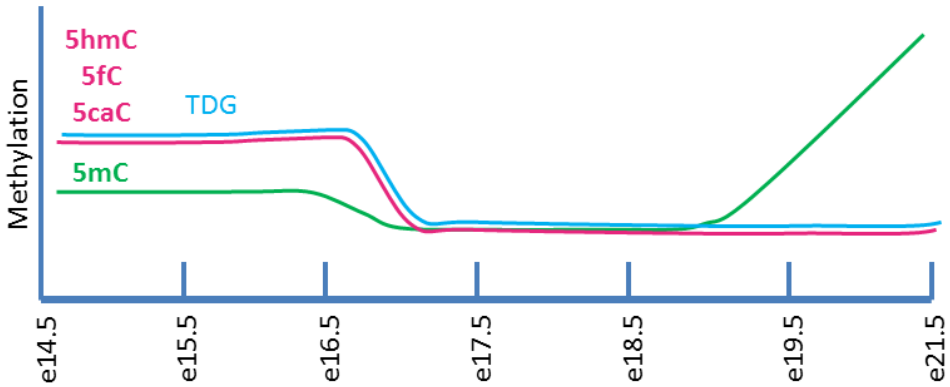

Figure 3.21. Proposed epigenetic reprogramming time-line in the rat. Germ cells showed asynchronous 5mC remethylation between e18.5 and e21.5. 5hmC, 5fC and 5caC were moderately detectable in germ cells from e14.5-16.5 but were thereafter undetectable.

There was little detectable 5mC in the germ cells from e14.5-e16.5, suggesting that the phase of bulk global demethylation may have been completed by this time. This is in keeping with mouse studies which indicate that a phase of demethylation occurs across the majority of the genome between e11.5-e12.5 [14]. Although this appears to be completed slightly later in the rat, it should be considered that they have a longer gestation (22 days in Wistar rats, compared to approximately 19 days in the mouse [250]).

At e17.5 and e18.5, 5mC was not detectable in germ cells. Studies in the mouse suggest that although demethylation occurs across most of the genome there are some exceptions, for example IAP retrotransposons. These remain highly methylated

[166,180,187] which may act to prevent IAP retrotransposition, potentially protecting against epimutations [172]. Furthermore, recent data indicates that a number of non-IAP associated CpG islands may also escape epigenetic reprogramming in the male germline and could represent candidates for transgenerational epigenetic inheritance [187]. I would therefore hypothesise that at e17.5 in our model, 5mC levels have decreased below the threshold of detection for the antibody, and therefore cannot be imaged in the germ cells.

At e19.5 5mC was detectable in some germ cells, and this became augmented at e20.5-e21.5. Staining with Propidium Iodide further indicates that there are germ cells present within the tubule which have no detectable 5mC at e19.5, whilst staining in others is comparatively strong. This suggests that the phase of remethylation occurs asynchronously from e18.5-e21.5. The remethylation phase has been less extensively characterised in mouse germ cells, although gene-targeted studies suggest that in male germ cells, the onset of DNA remethylation occurs at some imprinted loci and at repetitive elements from e15.5, with global remethylation re-established by e18.5 which may be further augmented perinatally [178,184,196,251].

Asynchronous remethylation between germ cells has not been reported in the literature and might only be detectable using immunofluorescence, or single-cell studies. There is however evidence that remethylation occurs at different genes at different time-points [178]. This is consistent with studies showing that different genes are demethylated at different time-points [177,206].

Intriguingly, 5hmC, 5fC and 5caC were identified in germ cells at e14.5-e16.5, but not from e17.5-e21.5. The presence of 5fC and 5caC in germ cells has not previously been reported, although 5hmC has been identified in the developing mouse germ cell [252]. It has also been shown that 5hmC, 5fC and 5caC are produced from 5mC, and that they may form part of a putative demethylation pathway, concluding with 5fC or 5caC removal via the action of TDG and the BER pathway [149-151]. Support for this comes from recent work suggesting that 5fC is detectably enriched over the bodies of actively transcribing genes as well as over CpG islands and promoters in ES cells and these levels increase in the absence of TDG activity [171]. It would

therefore fit that 5hmC, 5fC and 5caC would be formed during the demethylation phase of epigenetic reprogramming.

It is interesting that 5fC and 5caC are present for at least a 3 day period, rather than being rapidly removed. An *in vitro* study indicated that within a 10 minute incubation, TET2 was capable of converting over 95% of total 5mC, giving 60% progression to 5hmC, 30% to 5fC and 5% to 5caC by the end of the time period [149]. Intriguingly, the reaction rate of TET2 was found to be 4.9-fold or 7.6-fold lower when the starting substrate was 5hmC or 5fC respectively [149]. Even if the conversion of these forms takes longer than for 5mC, this does suggest that the action of TET2 enzymes and conversion through methyl forms could potentially be complete within a matter of hours. The more stable presence of 5fC and 5caC exhibited in our model suggests a number of potential hypothesises. The continuing presence of 5fC and 5caC could result from a gradual and constant removal of 5mC during e14.5-e16.5 which results in a steady production of methylation in its various forms. In this case the 5fC or 5caC at any particular base may be rapidly removed, but the constant turnover might give the appearance of a more stable expression of 5fC and 5caC when assessed globally. This is supported by the identification of TDG throughout e14.5-e16.5, which indicates there is the potential for continual removal of 5fC and 5caC throughout the time period. Indeed, in pigs the phase of demethylation was shown to be complete at e22 for DMR2 of the IGF2 receptor (*Igf2r*), but found to occur gradually between e22-e42 in the *Igf2-H19* regulatory region, suggesting that it is not always a rapid process, and that there is variation between genes, and indeed species [206].

A second hypothesis is that the presence of 5fC and 5caC in fetal germ cells reflects an accumulation of unconverted intermediates during global demethylation. Indeed, a study of mouse zygotes indicates that 5hmC, 5fC and 5caC levels gradually decrease with increasing numbers of cell division, rather than exhibiting rapid removal [157,167]. These hypotheses could be tested by conducting genome-wide single base resolution studies of 5fC and 5caC, as in Wang *et al.* (2014) [169]. A number of precise time-points could be studied, giving an indication as to whether these modifications are rapidly or gradually removed. For example, 5fC and 5caC levels at

several loci could be examined at e14.5, e15.0, e15.5, e16.0 and e16.5. This would determine how rapidly demethylation occurs at a loci-specific level.

In both cases it could be hypothesised that these forms of methylation have some functionality during mid-gestation, necessitating either their constant production from 5mC, or their lack of conversion and removal. Much has still be discovered about 5fC and 5caC, but Inoue *et al.* (2011) conclude from their observations of replication dependent dilution of these modifications in mouse zygotes that 5fC and 5caC could have functionality in early development [157]. Indeed, a recent paper identifies transcriptional and chromatin regulators which are able to interact with 5fC, and have a strong preference for this modification, compared to others. The authors conclude that although 5fC is part of a demethylation pathway, it may also have signalling properties [253].

Although the presence of 5fC and 5caC at e14.5-e16.5 might be expected as part of demethylation, the unexpected dynamics of these forms in both prenatal and postnatal development gives an additional suggestion of functionality. For example, it is intriguing that variability was identified in the germ cell staining at e16.5, with one particular pup having a very intense detection of 5hmC, 5fC and 5caC, relative to the somatic component. This could reflect a peak in these forms of methylation around e16.5. The fact that this was not replicated in the other litters could indicate that the peak was very brief, and that the exact time of fertilisation was slightly different between matings. A study using *In Vitro* Fertilisation (IVF) and looking at additional time-points around this time period, for example e16.3 and e16.7 might give greater indication as to whether this is a true phenomenon, or an experimental artefact.

It is also intriguing that there were dynamic changes in the localisation of 5hmC and 5caC postnatally, long after the period of demethylation in epigenetic reprogramming appears complete. Both forms of cytosine methylation were identified in Sertoli cells at PND10 and PND15, and a very intense stain was seen in the germ cells of some tubules at PND25. This could indicate that further demethylation is occurring in postnatal development, or indeed that 5hmC and 5caC have functionality at these time-points. It is interesting to note that although 5hmC and 5caC are being formed,

global 5mC is evident. For example, although 5hmC and 5caC are seen at PND25, they are co-localised with 5mC. It could be suggested that this may be followed by a decrease in 5mC, for example at PND26, but this is not evident in the adult tissues, where the spermatogonia appear 5mC positive. It is also notable that although 5caC is present, TDG was not detectable in germ cells at the corresponding time-point. Interestingly, although an intense stain for 5hmC was seen in many tubules at PND25, fewer tubules were 5caC positive. It is possible that this time-point might represent the beginning of 5caC formation, and that if for example PND26-PND28 was studied, 5caC might be found in the majority of tubules, subsequently followed by a positive stain for TDG. Conversely, it could be suggested that 5caC is not being removed by TDG, as this time-point does not reflect demethylation, but that 5caC is being regulated by other, as yet undetermined means.

It is unknown why 5hmC, 5fC and 5caC should be formed at this stage, whether as part of some 5mC removal, or by other undefined processes. PND25 is a key time-point in functional maturation just prior to the start of puberty, where plasma testosterone levels begin to increase, and Sertoli cell numbers are fixed and are more similar to that of the adult rat, than in pre-natal development [254,255]. It is possible that during this time of change 5hmC, 5fC and 5caC have a role in germ cell development. It could also be suggested that there is some change in chromatin compaction as the chromatin remodelling of spermatogenesis begins [256], and therefore differences in the intensity of 5hmC and 5caC staining at PND25 could reflect a change in the accessibility of these antigens for antibody binding.

Although little TDG was detectable in germ cells at PND25, its dynamics were largely seen to correspond to that of 5caC, one of its proposed substrates. The global dynamics of TDG localisation in the germ cell throughout development has not been characterised previously. However, data mining of RNA-seq data from Seisenberger *et al*. (2012) indicates that TDG expression is low in late-stage mouse germ cells (after e13.5). Data mining also indicates that TDG expression is relatively high in the early postnatal whole testis, with expression decreasing progressively from PND10 (R Meehan, unpublished data).

Immunofluorescence studies are not predominantly quantitative, but can provide key information about the location of the antigen within tissue, at a cellular level. In this study immunofluorescence was used to provide a broad picture of the localisation of global methylation in the testis throughout mid to late gestation, so that gene-specific, quantitative analysis could then be performed at key time-points. Furthermore, Image J studies gave a second, semi-quantitative analysis of immunofluorescence, and supported the conclusions drawn visually from the images.

This study indicates that germ cell epigenetic reprogramming does occur in the rat, and that remethylation occurs between e18.5 and e20.5. As this time-period shows dynamic changes in 5mC, and is within the window of Dex exposure (e15.5-e22.5), it was decided that this is a critical timeframe for study in the Dex programming model. The dynamics of all known forms of methylation, and the regulatory enzyme TDG were also explored in both pre and postnatal life, giving a more global understanding of the dynamics of germ cell methylation in the rat. The presence of 5hmC, 5fC and 5caC and TDG from e14.5-e16.5 supports the theory that they may form a pathway for demethylation, but their continuing presence during this time-period, and unexpected dynamics postnatally suggest that they could also have functionality. This indicates that there is still much to be discovered about DNA methylation in the germ cell.

Chapter 4 Effects of Glucocorticoid Exposure on Fetal Germ Cell Development

4.1 Introduction

As discussed in the Chapter 1, fetal programming of disease risk has been shown to be transmissible through both maternal and paternal lines. In the Dex model of programming, the phenotype of low birth weight and altered cardiometabolic parameters is also transmitted through the paternal line [12]. In this animal model, one of the few methods of influence of the father on his offspring is the contribution of his sperm, as he is absent shortly after the point of fertilisation.

One hypothesis is that first generation male offspring exposed to an insult *in utero* might have alterations in their sperm which allow a transmission of the phenotype to the second generation. One mechanism by which such an alteration might occur is by the direct influence of Dex treatment on their spermatogonial progenitor cells whilst they themselves are *in utero*.

An initial exploration of the effects of Dex exposure on the epigenetic reprogramming time-line established in Chapter 3 was therefore conducted. A number of time-points were studied to give a broad investigation of any influence of Dex exposure on global methylation, so that a key time-window could be identified for a more in-depth gene-specific study.

The DNA methyl transferase enzymes DNMT3a and DNMT3b have been shown to be key in the remethylation phase of epigenetic reprogramming in the mouse [200,257]. Their action is dependent on the co-factor DNMT3L [201,258]. The presence of these enzymes in the rat, and any influence of Dex on their localisation during remethylation was also investigated, giving an additional analysis of the effects of treatment on epigenetic reprogramming.

An indication of the effect of Dex treatment on general testis development was also given by examining the localisation of Doublesex and Mab-3 Related Transcription Factor 1 (DMRT1). Previous research has indicated that this transcription factor is switched off in germ cells at around e19.5, but is present in somatic cell nuclei

throughout late gestation [259]. Therefore DMRT1 was used to give a marker of general testis development, apart from effects on epigenetic reprogramming.

4.2 Methods

Virgin female Wistar rats were timed-mated with stock Wistar males, and injected daily with either Dex (100µg/kg body mass) suspended in 0.9% Saline, or an equivalent volume of Saline from e15.5 until termination. Pregnant dams were sacrificed at e18.5-e21.5 (n=3-4 at each time-point), and all pups and placentas removed. Pup and placental mass was recorded for all litters at each time-point. Normality of data distribution was confirmed using the Lilliefors test. Normally distributed data ($p>0.05$) was analysed by Student's t-test, and nonparametric data by Mann Whitney U test.

Testes were extracted from male pups with the instruction and assistance of Dr Sander van den Driesche (Centre for Reproductive Health, The University of Edinburgh) and fixed in Bouins, before testes were embedded in paraffin wax by SURF staff. Tissue blocks were then microtomed to give 5µm sections, which were then mounted on microscope slides. Immunofluorescence was used to explore the localisation of GR within the testis, and to indicate any global changes in the established epigenetic reprogramming time-line with glucocorticoid exposure. Slides were immunostained for GR, 5mC, 5hmC, 5fC and 5caC, following the protocols outlined in Chapter 2.

In order to give semi-quantification of 5mC staining, 2 sections were taken from a testis in every e19.5 and e20.5 litter, spaced 50 µm apart, and immunostaining for 5mC and Propidium Iodide was conducted. Tile scans were used to capture an image of the entire cross-section. Images were put into random order, and titles changed to show only the time-point, colour channel, and a letter. Images were then assessed blindly by Ashley Boyle, MSc student, Centre for Reproductive Health, The University of Edinburgh. Germ cells were counted using Propidium Iodide, and counted and graded using 5mC staining, with 1 corresponding to a weak, 2 a moderate, and 3 an intense 5mC stain. 5mC intensity scores were normalised to the

total number of germ cells identified by Propidium Iodide in each tubule and a mean calculated by combining the data from both sections in every testis. The resulting data was then analysed by 1-way Analysis of Variance (ANOVA), with Fisher's Least Significant Difference (LSD) post-hoc analysis. Data are expressed as mean percentage of germ cells expressing 5mC ± the standard error of the mean.

To investigate any corresponding changes in the machinery of remethylation, the DNMT3 family was studied. Immunofluorescence was conducted for DNMT3a and DNMT3b by Ashley Boyle, under my instruction and supervision. I also conducted immunofluorescence for their co-factor DNMT3L. As an indicator of the general developmental stage of the Dex and Saline testes, I also investigated DMRT1 localisation by immunofluorescence.

4.3 Results

4.3.1 Confirming the Effectiveness of Dex Treatment

Pup and placental weights were analysed in order to confirm that Dex exposure had given the expected phenotype. Pup weight was significantly decreased at e21.5 in litters exposed to Dex *in utero*, relative to Saline controls (Figure 4.1). However no significant difference was found at e18.5-e20.5.

Placental weight was decreased at e19.5-e21.5, but not at e18.5, in litters exposed to Dex relative to controls (Figure 4.2).

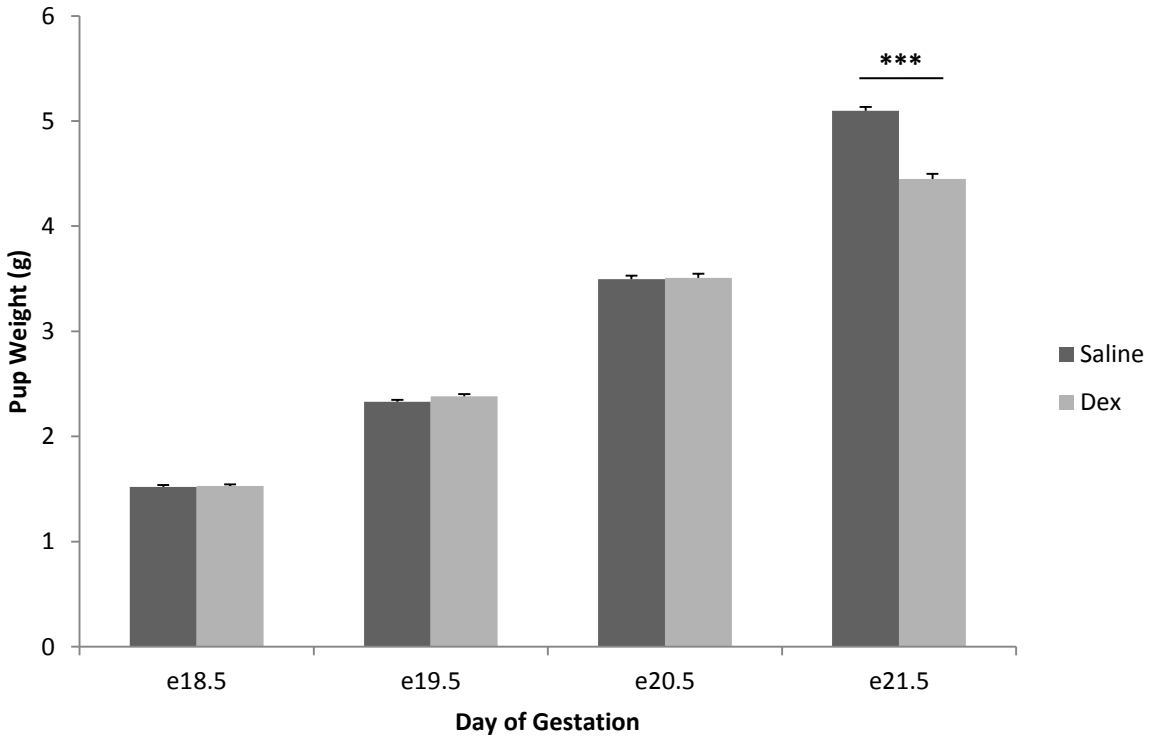

Figure 4.1. Pup weight at experimental time-points. All pups of both sexes were weighed prior to dissection. Pups exposed to Dex *in utero* were found to have a significantly decreased ($p<0.001$) weight at e21.5 relative to Saline controls. Weight at e18.5-e20.5 did not differ between groups. Data were analysed by Student's t-test for all time-points, except for e18.5 and e21.5, which were not normally distributed (Lilliefors $p<0.05$), and for which a Mann-Whitney U test was therefore performed. Bars represent mean ± standard error. ***$p<0.001$

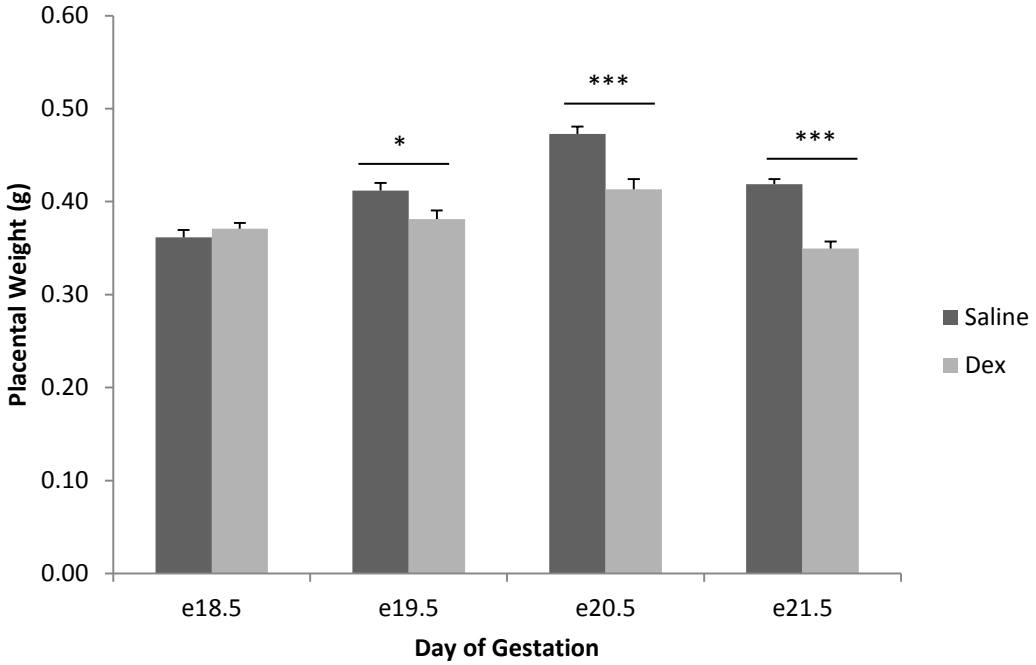

Figure 4.2. Placental weight at experimental time-points. All placentas were weighed during dissection. Placentas of litters exposed to Dex *in utero* were found to have a significantly decreased weight at e19.5 ($p<0.05$), e20.5 ($p<0.001$) and e21.5 ($p<0.001$), relative to Saline controls. Weight at e18.5 did not differ significantly between groups. Data were analysed by Student's t-test for all time-points, except for e18.5 and e21.5, which were not normally distributed (Lilliefors $p<0.05$), and for which a Mann-Whitney U test was therefore performed. Bars represent mean ± standard error. *$p<0.05$, ***$p<0.001$

4.3.2 Exploring the Localisation of GR

The localisation of GR was investigated, in order to explore whether any influence of Dex on the testis was likely to be direct, through GR in germ cells, or indirect, through somatic cells. GR was detected in somatic cells from e18.5-e21.5 in both Saline and Dex groups (Figure 4.3 and Figure 4.4 respectively). Notably weaker staining was seen for GR in germ cells in both groups. Arguably slightly weaker detection was found in Dex germ cells, compared to controls. However, all germ cells indicated by Sytox Green staining had some corresponding detection for GR.

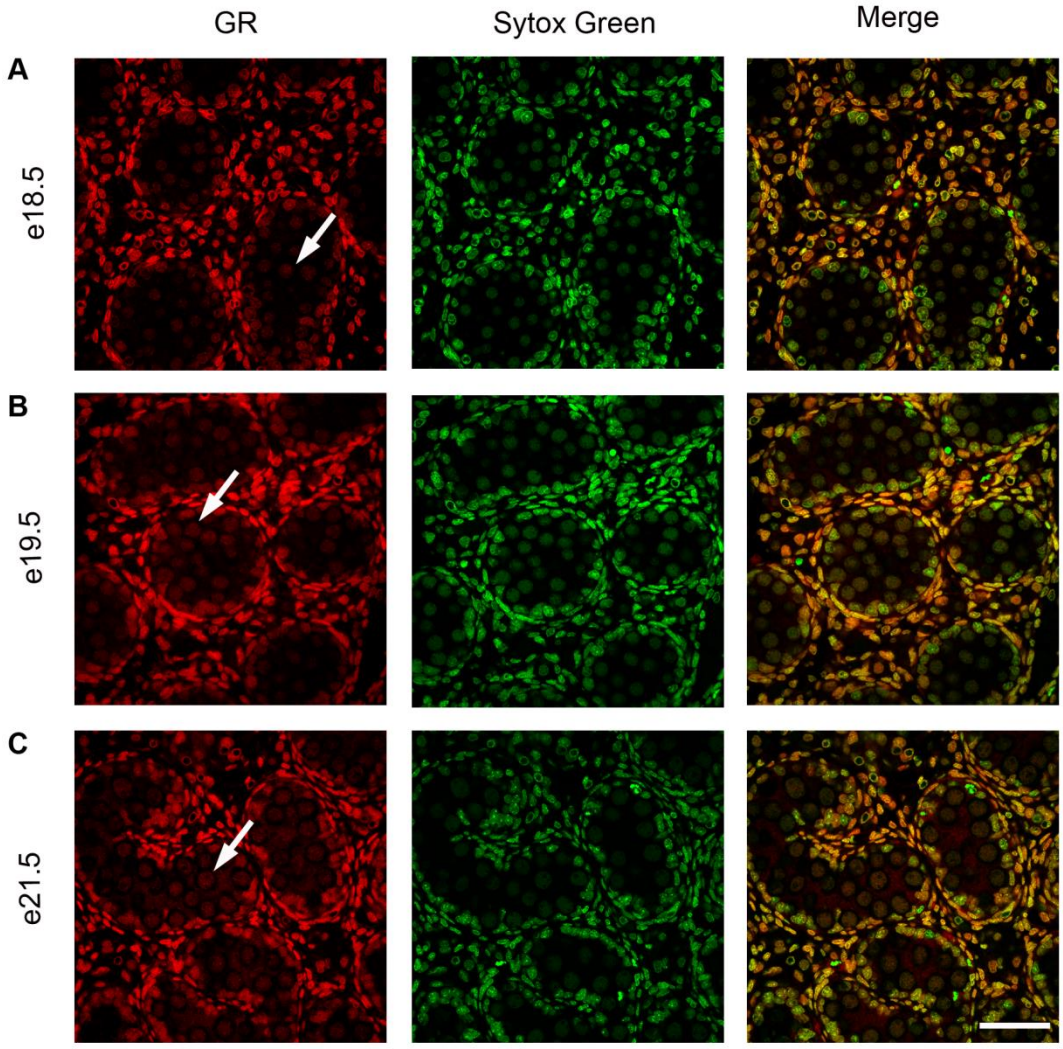

Figure 4.3. Location of GR within the testis – Saline pups. Images of immunostained testes from Saline pups show detection of GR in somatic and germ cells (red, arrows) at e18.5-e21.5 (A-C). All germ cells indicated by Sytox Green have a corresponding stain for GR. Bar = 50µm.

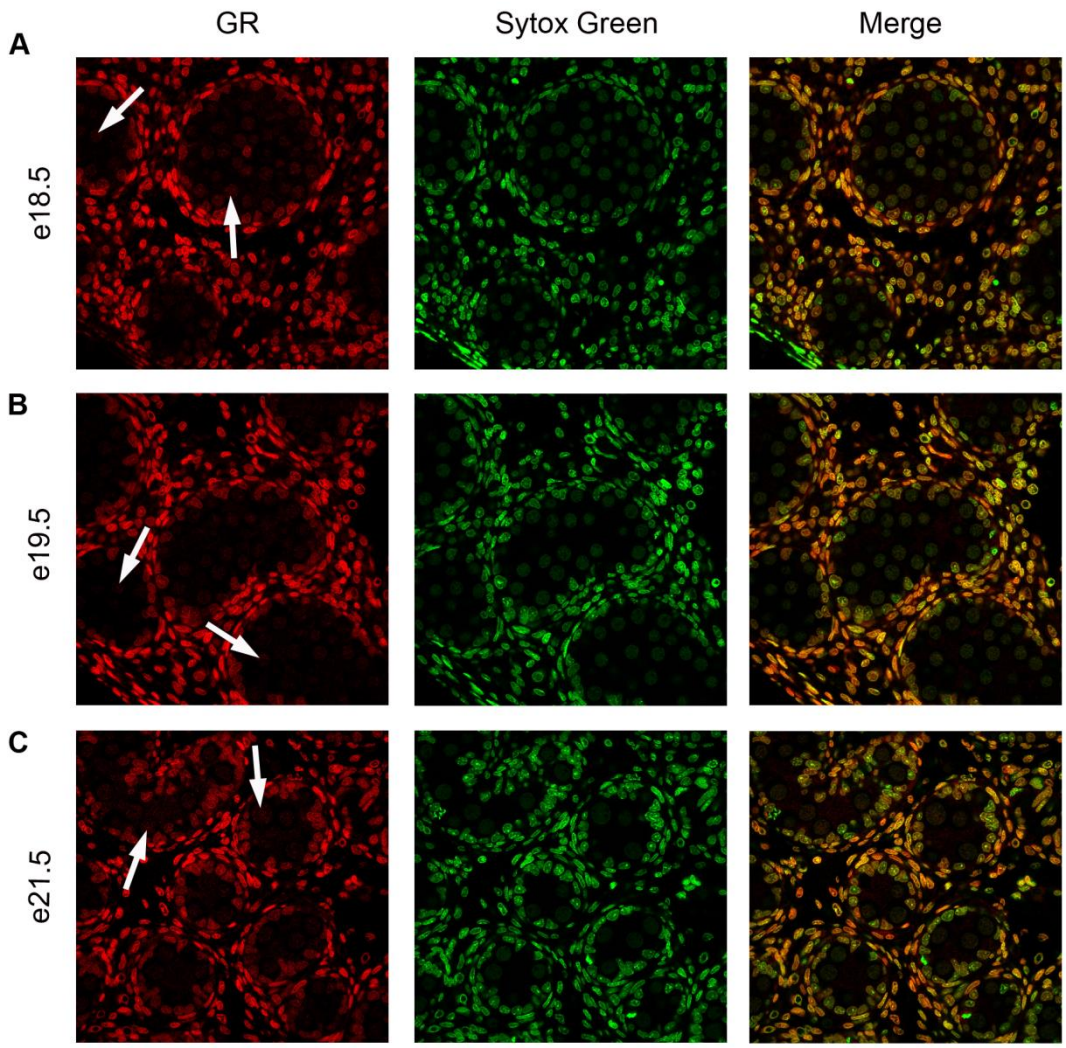

Figure 4.4. Location of GR within the testis – Dex Pups. Images of immunostained testes from Dex pups show marked detection of GR in somatic cells (red, arrows) at e18.5-e21.5 (A-C). Weak staining is seen within germ cells at all time-points. Sytox Green acts as a nuclear counterstain. Bar = 50μm.

4.3.3 Exploring Effects of Glucocorticoid Exposure on Global Germ Cell Methylation

In order to explore any global effects of glucocorticoid exposure on the epigenetic reprogramming time-line, Dex and Saline slides were immunostained. In Saline tissues, 5mC was not detected in germ cells at e18.5 or e19.5 (Figure 4.5A-B), but staining became marked by e21.5 (Figure 4.5D). Conversely, whilst 5mC was not detected at e18.5 in Dex tissues (Figure 4.6A), some germ cells had a positive stain for 5mC at e19.5 (Figure 4.6B), intensifying by e21.5 (Figure 4.6D). Germ cell 5hmC was not detected in either treatment group across the time-course (Figure 4.5 and Figure 4.6).

To gain a greater insight into methylation within these tissues, testes were also stained for 5fC (Figure 4.7 and Figure 4.8) and 5caC (Figure 4.9 and Figure 4.10). In keeping with previous results, 5fC and 5caC were localised to somatic cells throughout the time course for both treatment groups, but largely undetected in germ cells. However, a weak detection for 5fC was found in the germ cells of some tubules at e20.5 and e21.5 in Saline (Figure 4.7C-D) and e19.5 in Dex (Figure 4.8B) tissues.

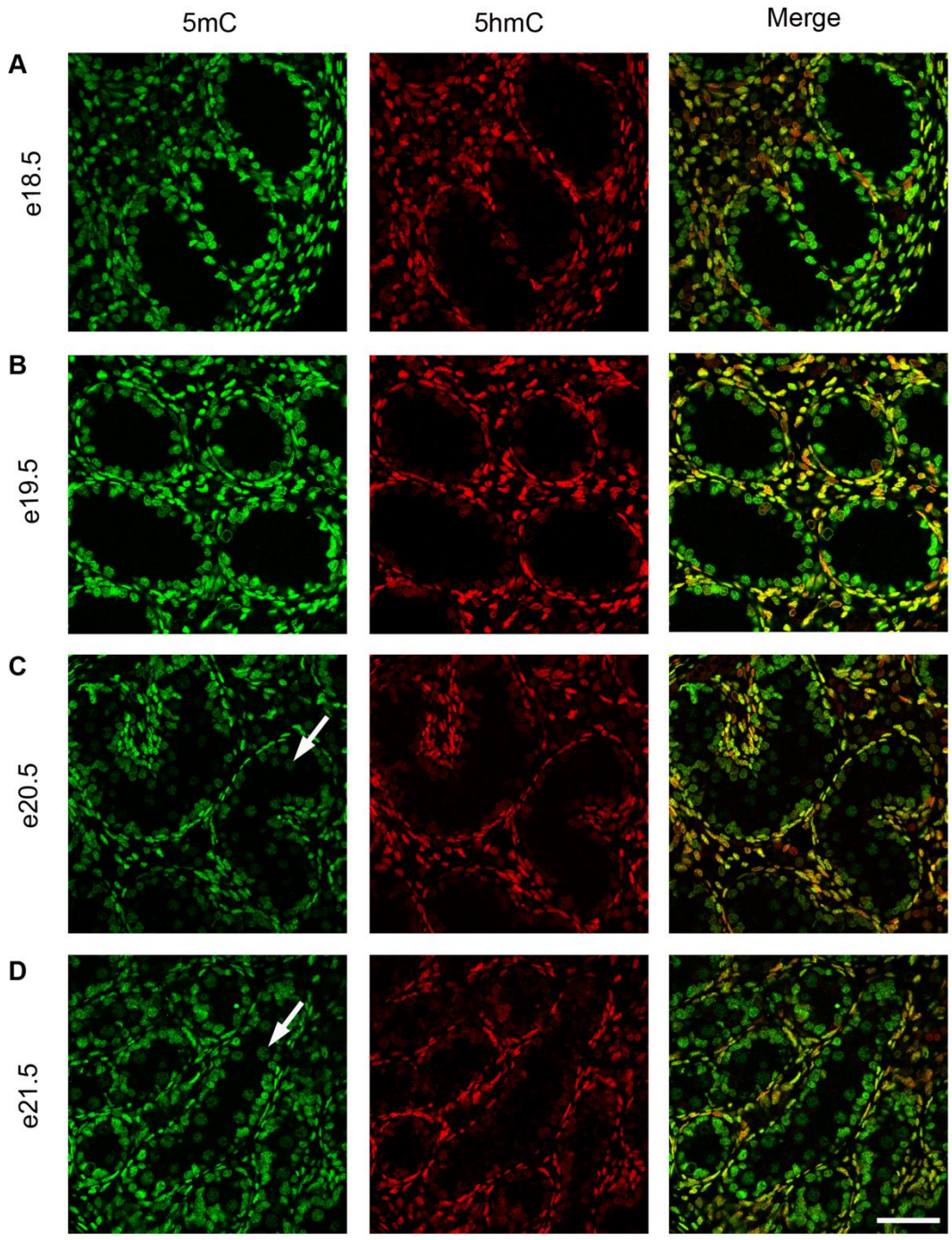

Figure 4.5. Localisation of 5mC and 5hmC in Saline testis. Images of immunostained testis show that 5mC (green, arrows) is not detected at e18.5 and e19.5 (A, B), and has some detection in germ cells at e20.5 (C), becoming marked by e21.5 (D). 5hmC (red) is not visualised in germ cells. Both forms of methylation are found in somatic cells throughout the time course. Bar = 50μm.

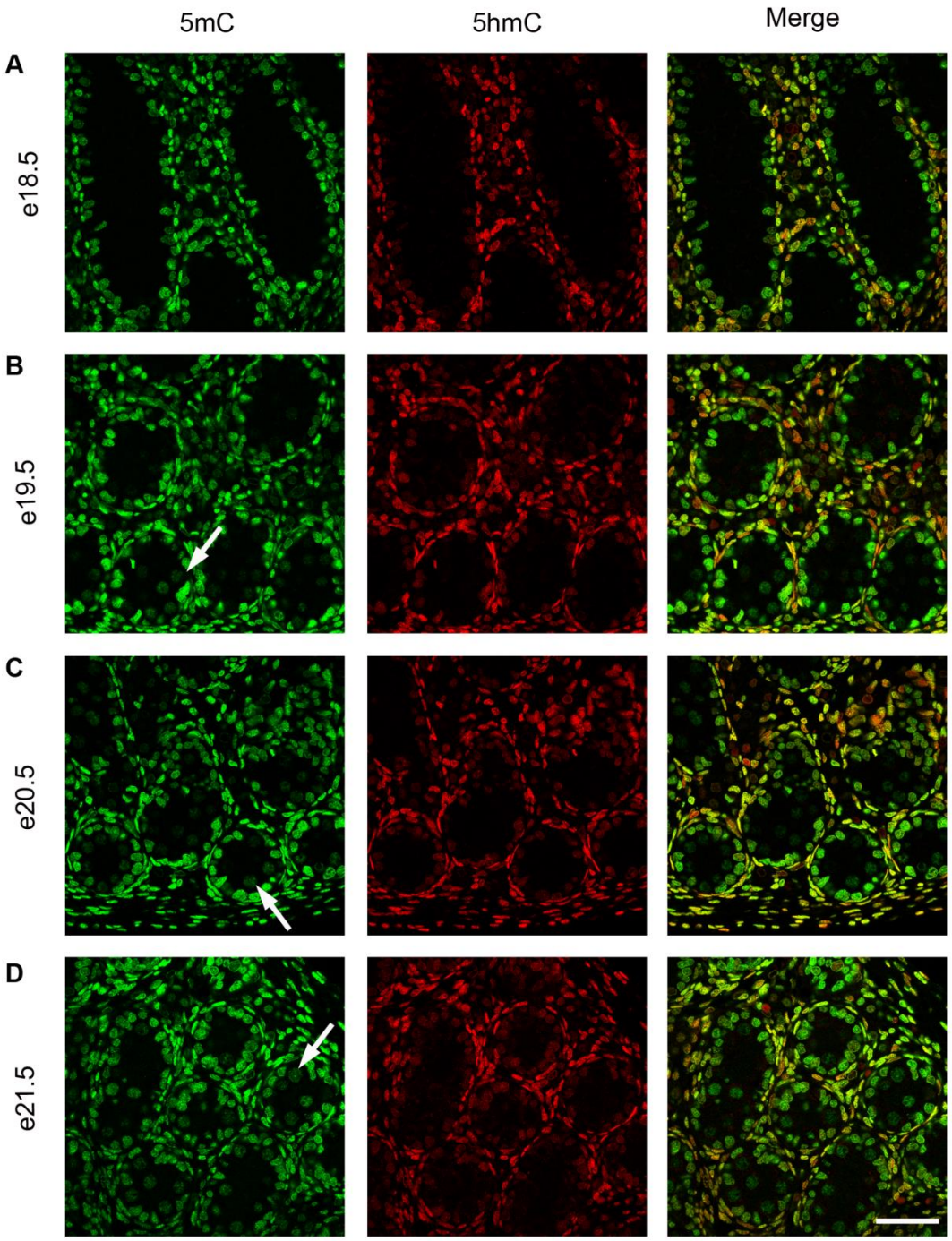

Figure 4.6. Localisation of 5mC and 5hmC in Dex testis. Images of immunostained testis show that 5mC (green, arrows) is undetected at e18.5 (A), and is detected in some germ cells by e19.5 (B). At e21.5 there is a marked 5mC detection in germ cells (D) 5hmC (red) is not visualised in germ cells. Both forms of methylation are found in somatic cells throughout the time course. Bar = 50μm.

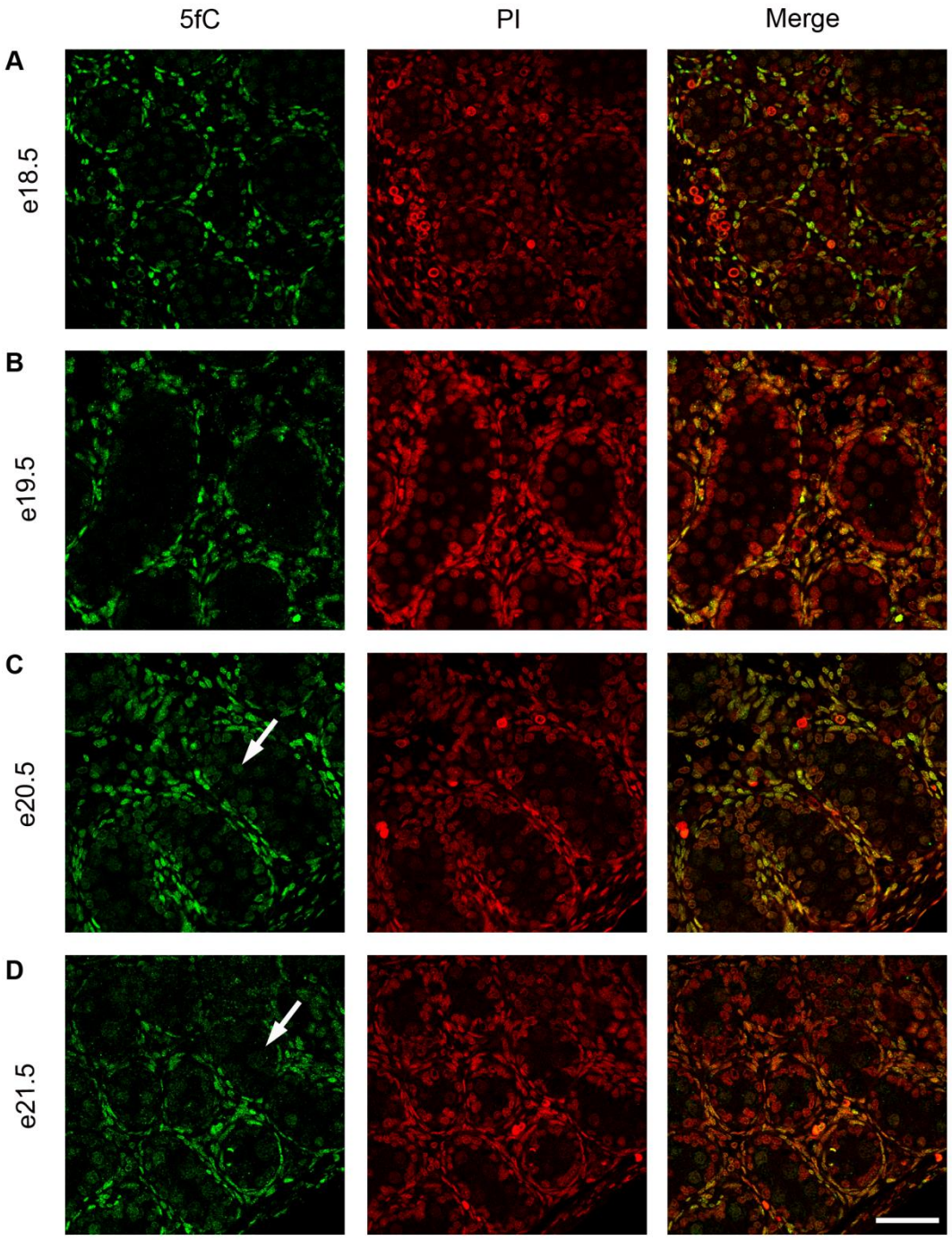

Figure 4.7. Localisation of 5fC in Saline testis. Images of immunostained testis show that 5fC (green, arrows) is largely undetectable at e18.5 and e19.5 (A, B), and has some detection in germ cells at e20.5 (C) and e21.5 (D). 5fC was found in somatic cells throughout the time course. Propidium Iodide (PI) acts as a nuclear counterstain. Bar = 50μm.

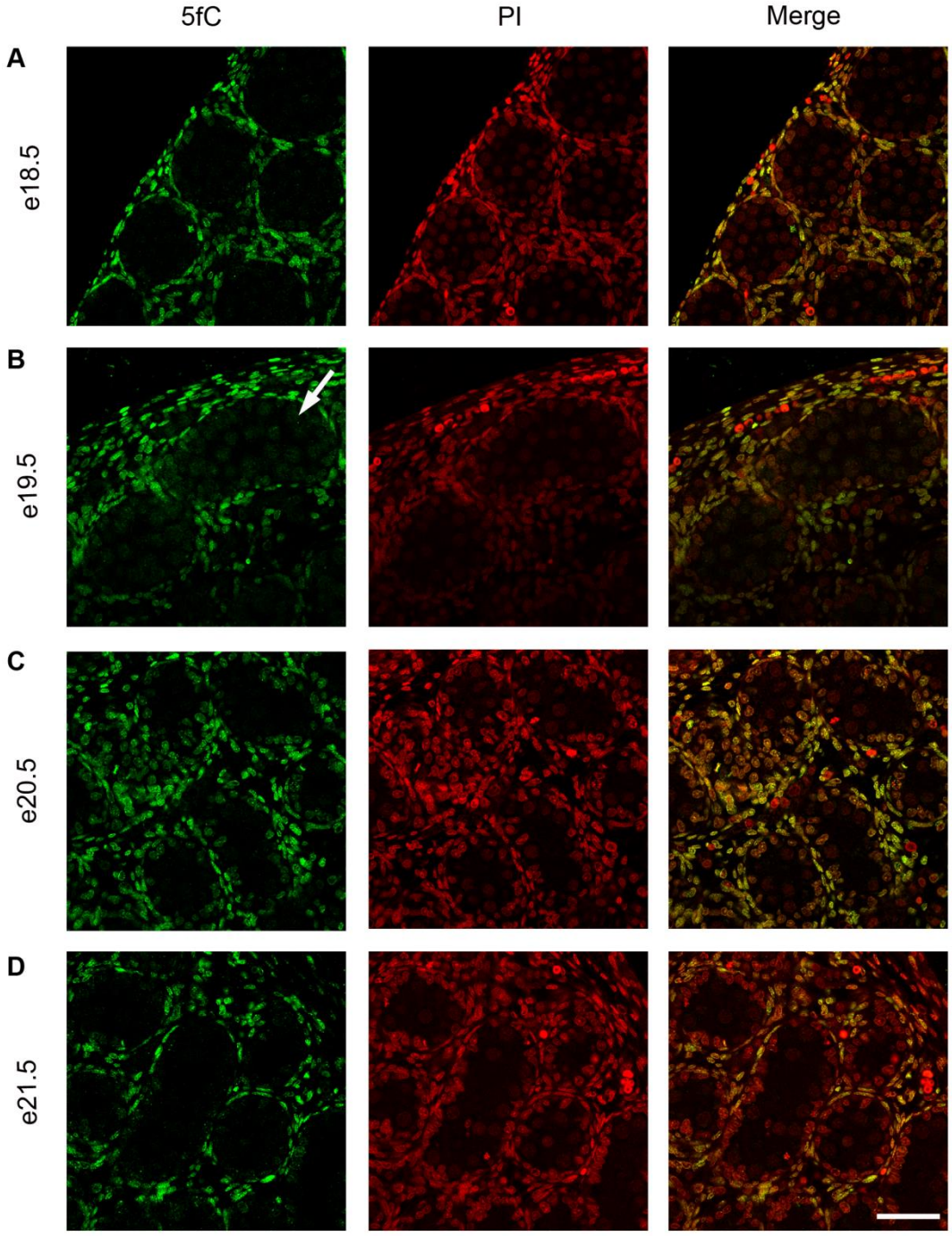

Figure 4.8. Localisation of 5fC in Dex testis. Images of immunostained testis show that 5fC (green, arrows) is largely undetectable at e18.5 (A), e20.5 (C) and e21.5 (D), but there is some positive staining in germ cells at e19.5 (B). 5fC was found in somatic cells throughout the time-course. Propidium Iodide (PI) acts as a nuclear counterstain. Bar = 50µm.

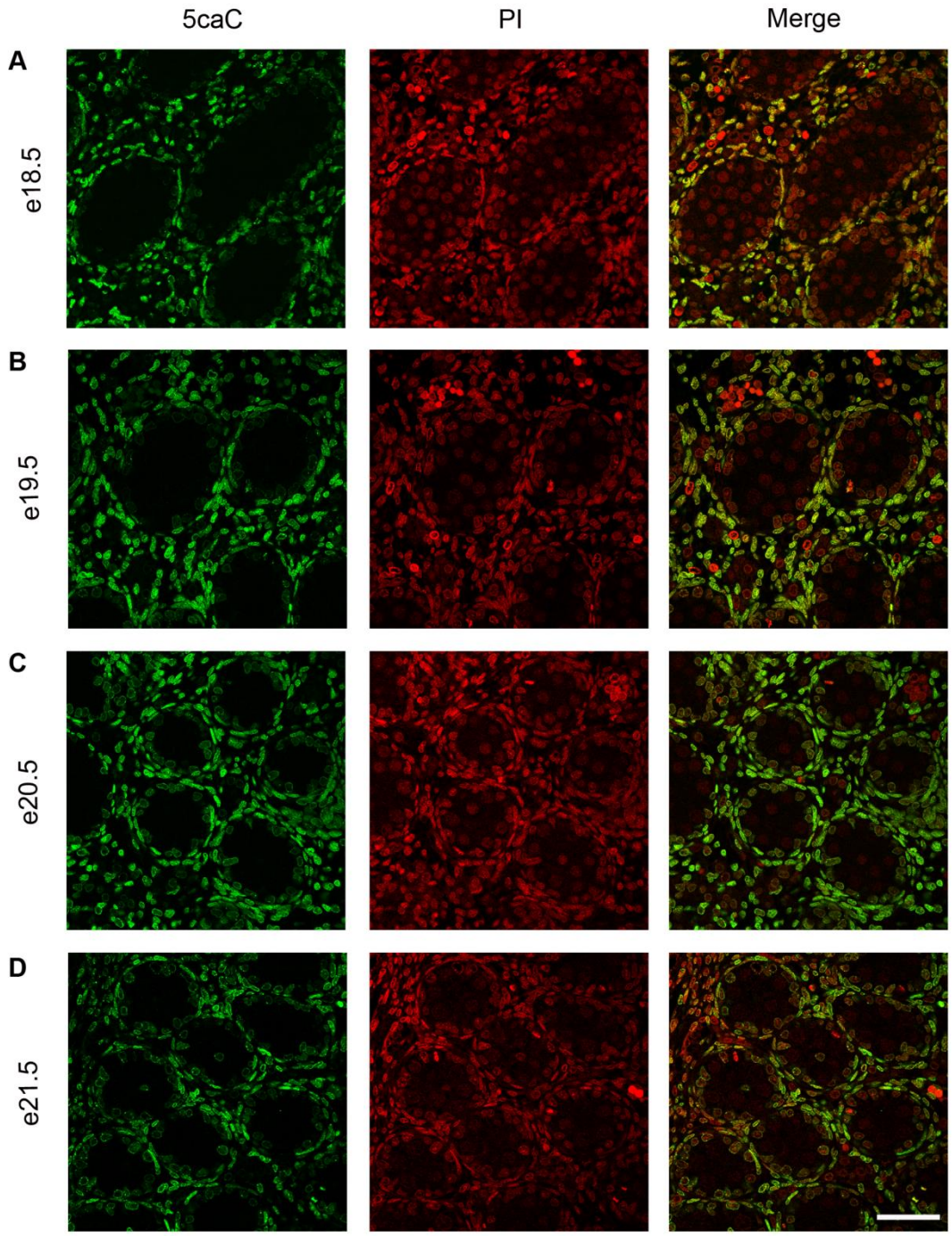

Figure 4.9. Localisation of 5caC in Saline testis. Images of immunostained testis show that 5caC (green) is undetectable in germ cells from e18.5-e21.5 (A-D), but found in somatic cells throughout the time course. Propidium Iodide (PI) acts as a nuclear counterstain. Bar = 50μm.

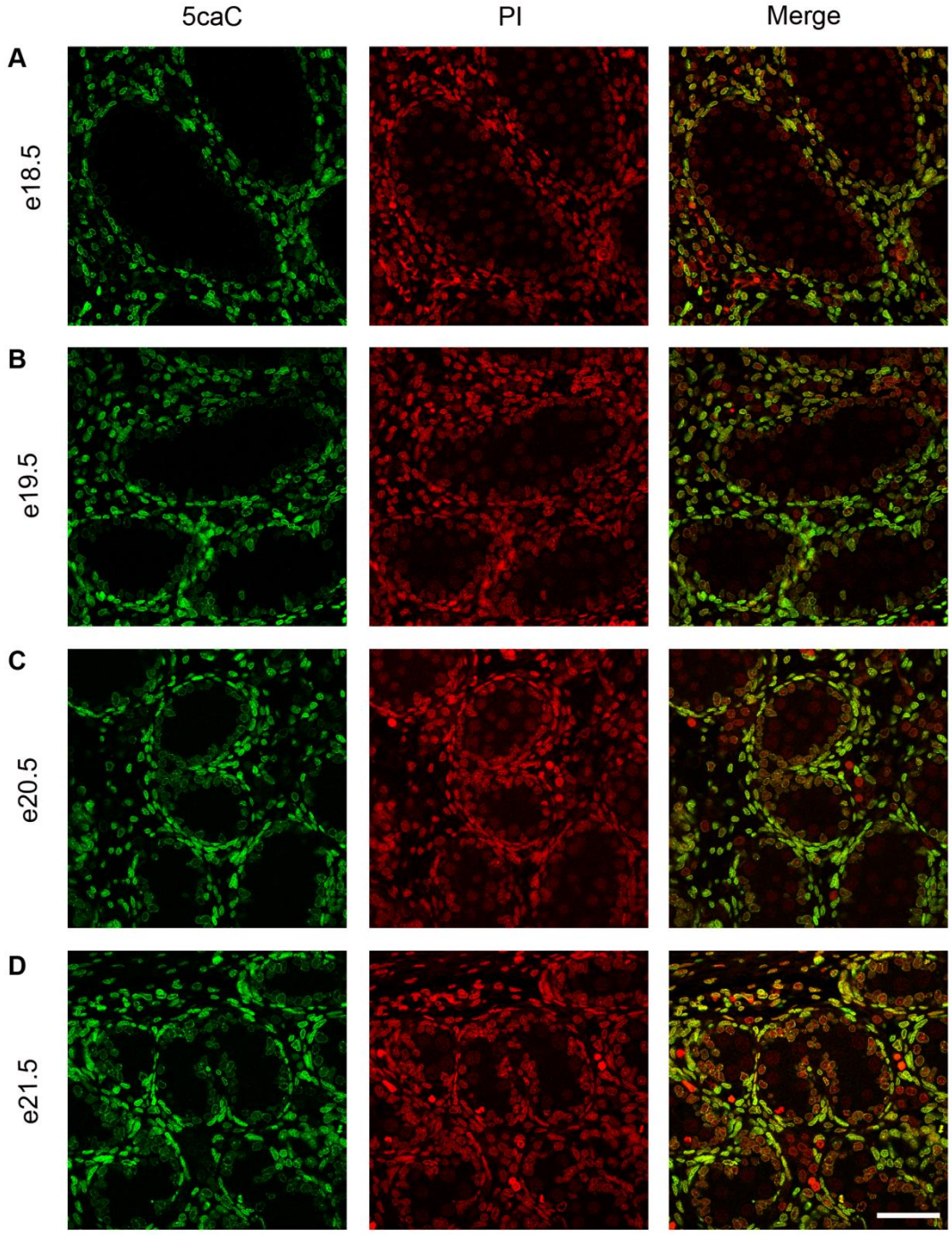

Figure 4.10. Localisation of 5caC in Dex testis. Images of immunostained testis show that 5caC (green) is undetectable in germ cells from e18.5-e21.5 (A-D), but is found in somatic cells throughout the time course. Propidium Iodide (PI) acts as a nuclear counterstain. Bar = 50μm.

4.3.4 Semi-Quantification of 5mC Immunofluorescence

The potential difference in 5mC germ cell staining between Dex and Saline groups at e19.5 was further explored. 5mC staining in germ cells was scored as outlined in Chapter 2 and expressed as a percentage of the total number of germ cells, counted using Propidium Iodide. The total percentage of germ cells with a positive stain was greater in Dex tissues at e19.5, relative to Saline controls (Figure 4.11). These positive counts were predominantly split over intensity scores 1 and 2, indicating weak to moderate detection (Figure 4.12).

In order to explore whether this difference was persistent, e20.5 tissues were examined in the same way. No difference was identified in the percentage of germ cells positive for 5mC between Dex and Saline groups. This was found when analysing both the total number of germ cells positive for 5mC (Figure 4.13) and each intensity scoring individually (Figure 4.14).

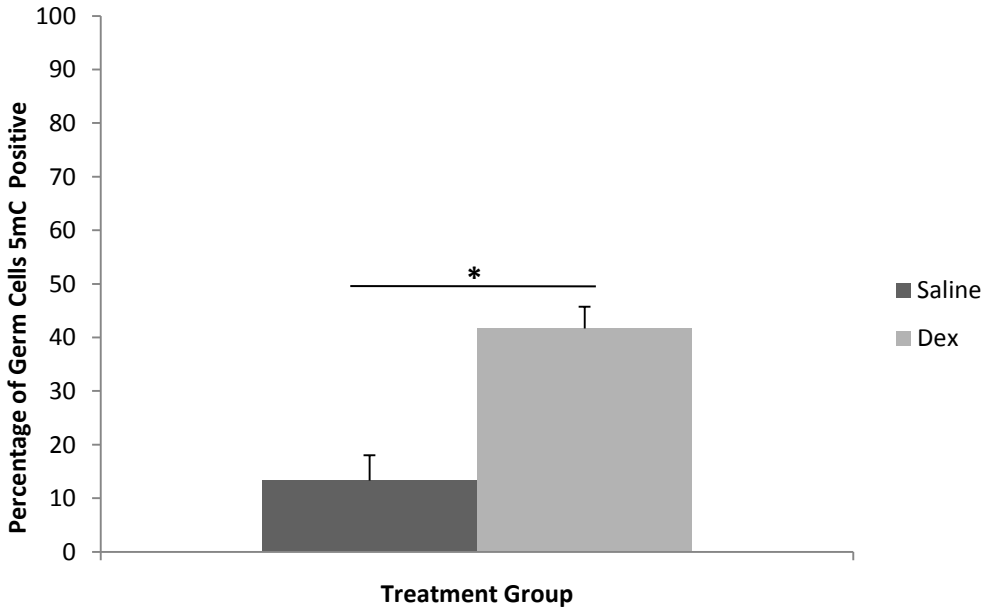

Figure 4.11. Percentage of germ cells 5mC positive at e19.5. Number of germ cells detected with 5mC antibody is expressed as a percentage of the total number of germ cells identified by Propidium Iodide stain. This percentage was greater ($p<0.05$) in Dex samples relative to Saline controls. Bars represent mean ± standard error. *$p<0.05$

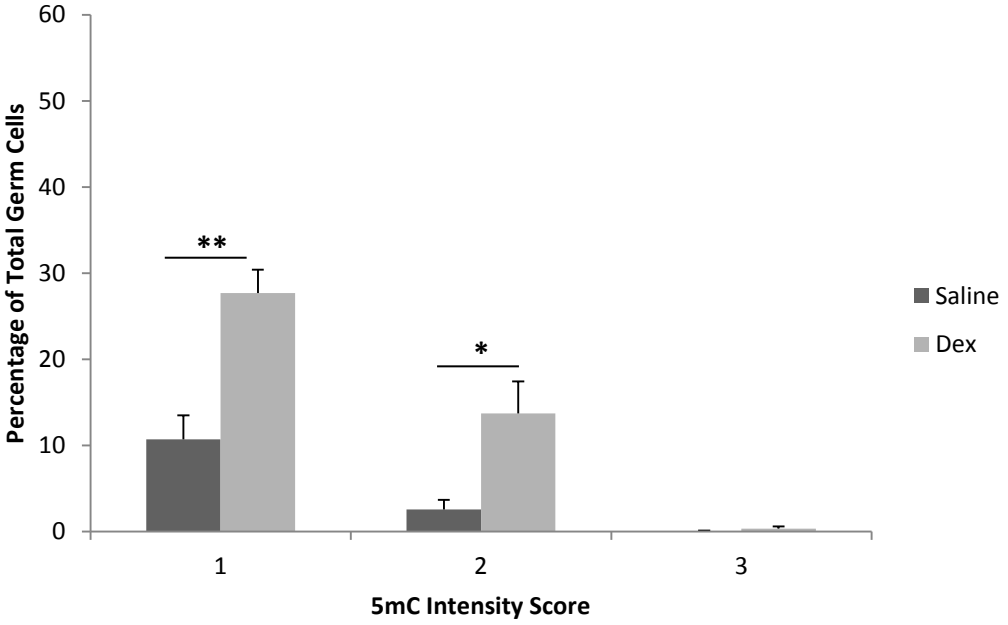

Figure 4.12. Intensity scoring of 5mC positive germ cells at e19.5. Number of germ cells graded to be at each intensity score is expressed as a percentage of the total number of germ cells identified by Propidium Iodide stain. This percentage was greater ($p<0.05$) in Dex samples relative to Saline controls, split over intensity scores 1 ($p<0.01$) and 2 ($p<0.05$). Bars represent mean ± standard error. *$p<0.05$, **$p<0.01$

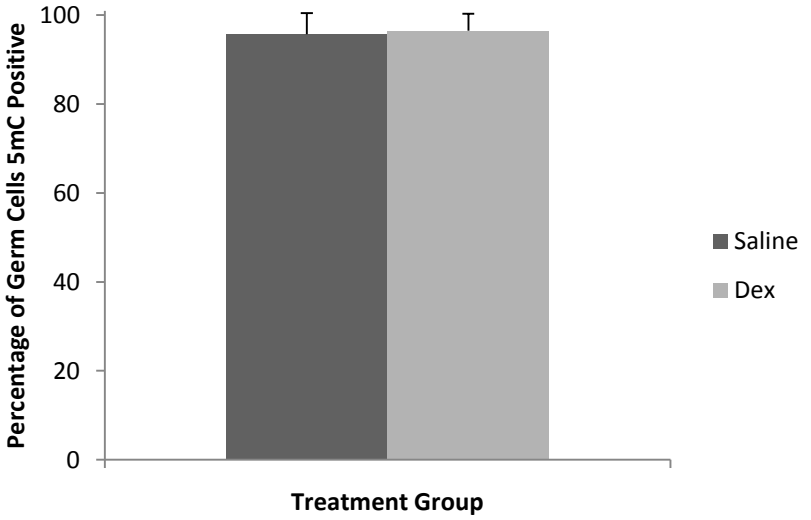

Figure 4.13. Percentage of germ cells 5mC positive at e20.5. Number of germ cells detected with 5mC antibody is expressed as a percentage of the total number of germ cells identified by Propidium Iodide stain. This percentage was not significantly different between Dex and Saline samples. Bars represent mean ± standard error.

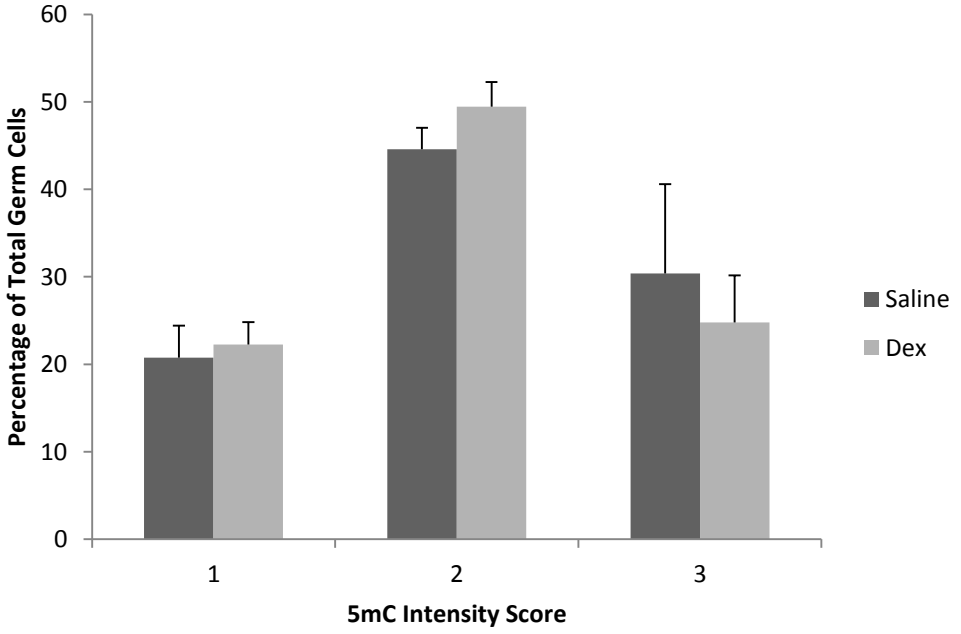

Figure 4.14. Intensity scoring of 5mC positive germ cells at e20.5. Number of germ cells graded to be at each intensity score is expressed as a percentage of the total number of germ cells identified by Propidium Iodide stain. This percentage was not significantly different between Dex and Saline groups at any intensity score. Bars represent mean ± standard error.

4.3.5 Exploring Mechanisms of Potential Time-line Shift

4.3.5.1 DNMT3a and 3b

The potential mechanisms of a change in the epigenetic timeframe with Dex treatment were explored. The DNMT3 family were investigated as an indication of impact upon other epigenetic mechanisms, and because of their known role in mouse remethylation [200,201,260]. DNMT3a and DNMT3b were detected in germ and somatic cells in both Dex and Saline groups (Figures 4.15-4.18). No notable difference in DNMT3a/3b localisation was seen between treatment groups. Comparison with Vasa suggests that all germ cells present have a corresponding DNMT3a or 3b stain.

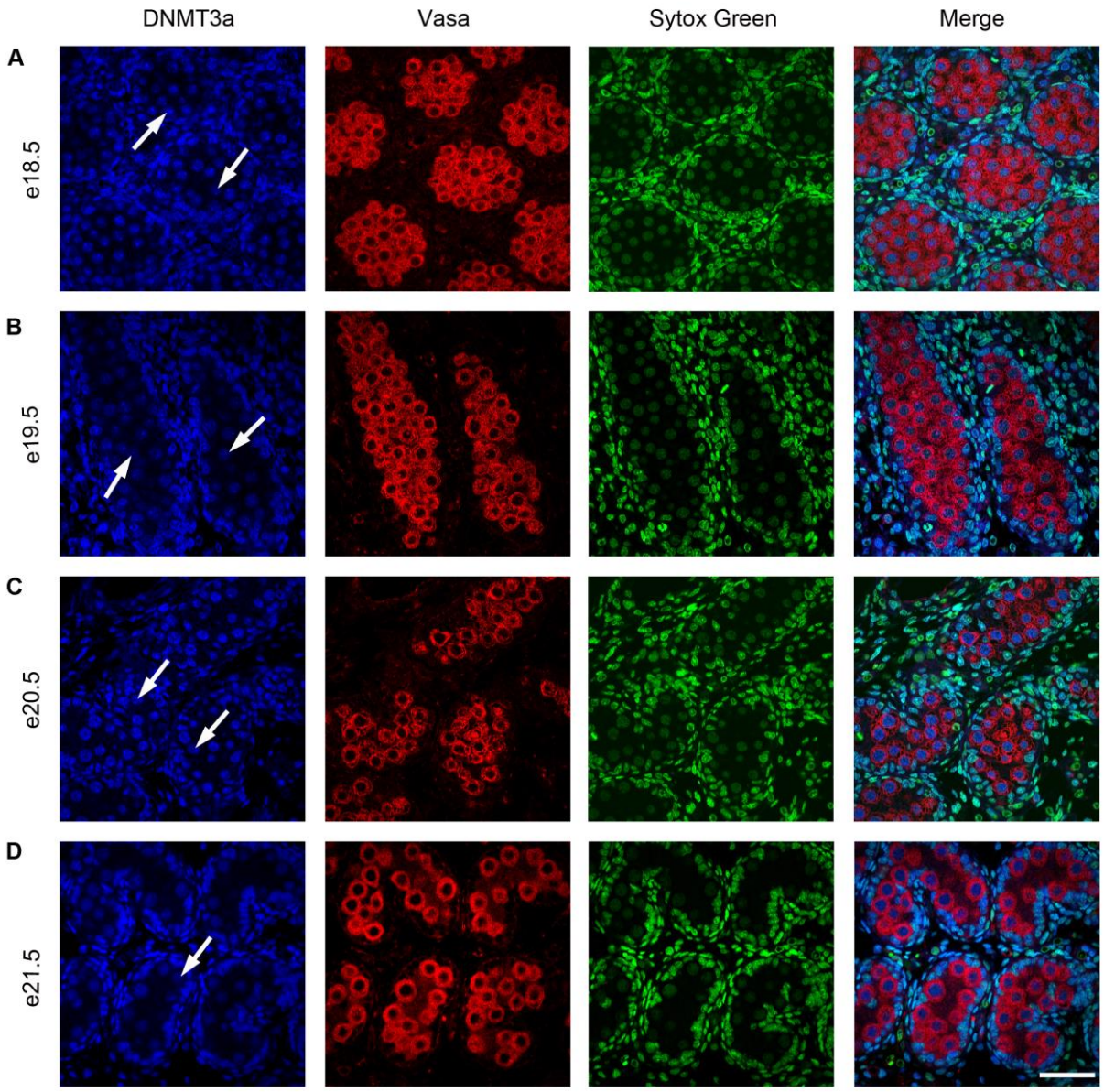

Figure 4.15. DNMT3a immunofluorescence in Saline tissues. Images of immunostained testis show that DNMT3a was detected in germ cells (blue, arrows) at e18.5-e21.5. Staining was detected in the somatic component throughout the time-course. Vasa staining (red), compatible with this protocol, was used to identify germ cells. Sytox Green acted as a nuclear counterstain. Bar = 50μm.

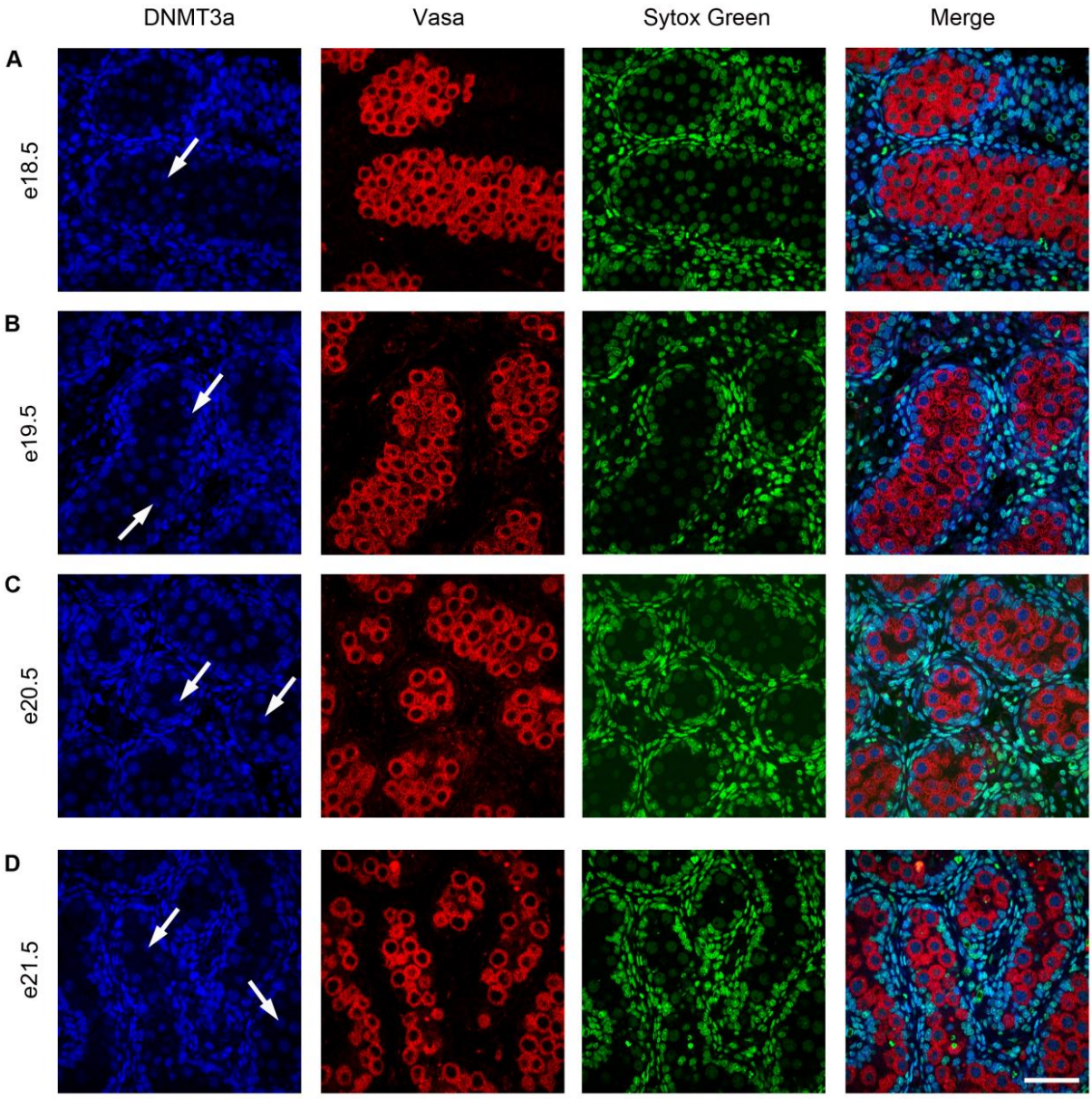

Figure 4.16. DNMT3a immunofluorescence in Dex tissues. Images of immunostained testis show that DNMT3a was detected in germ cells (blue, arrows) at e18.5-e21.5. Staining was detected in the somatic component throughout the time-course. Vasa staining (red), compatible with this protocol, was used to identify germ cells. Sytox Green acted as a nuclear counterstain. Bar = 50μm.

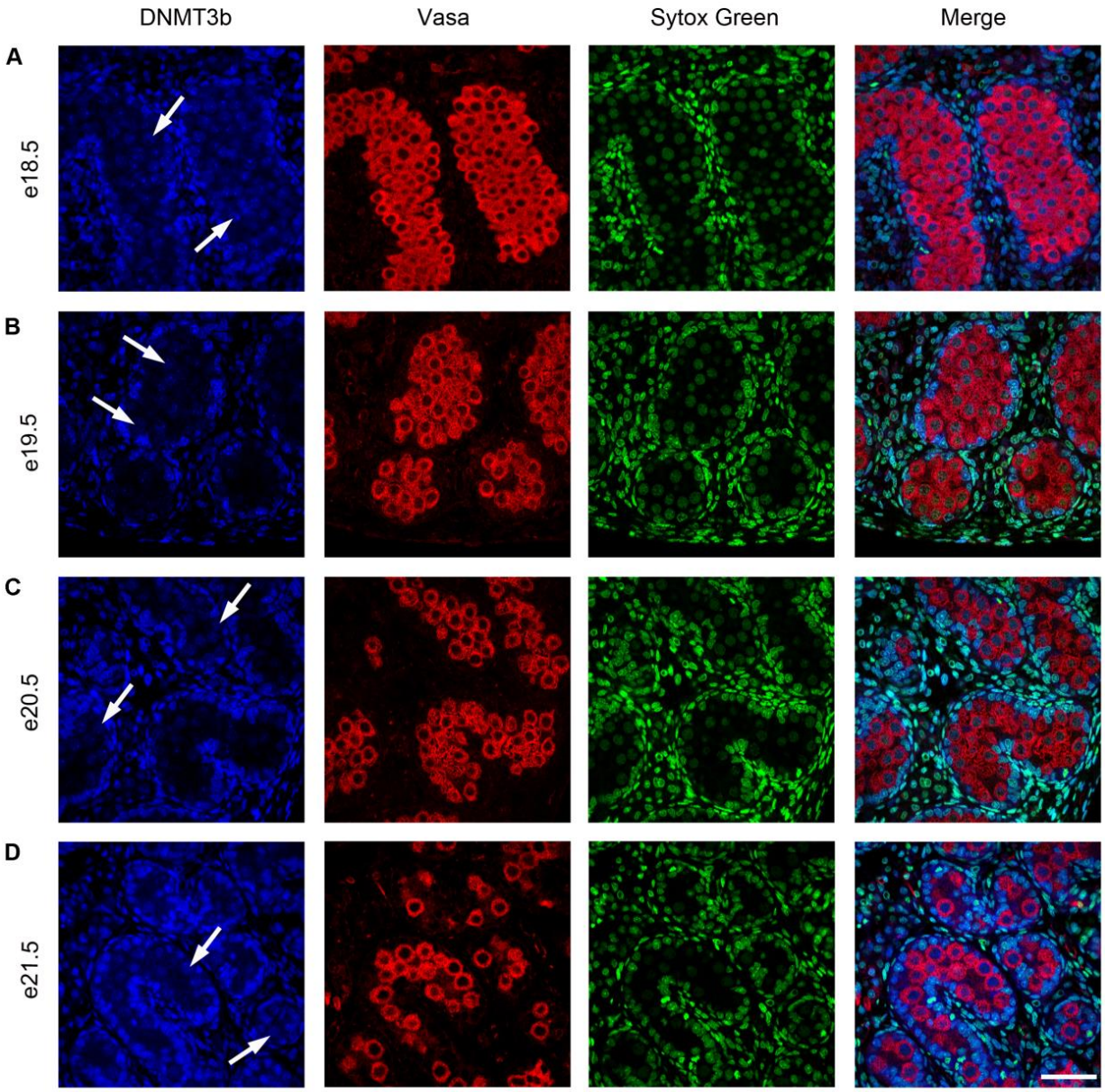

Figure 4.17. DNMT3b immunofluorescence in Saline tissues. Images of immunostained testis show that DNMT3b was detected in germ cells (blue, arrows) at e18.5-e21.5. Staining was detected in the somatic component throughout the time-course. Vasa staining, compatible with this protocol, was used to identify germ cells. Sytox Green acted as a nuclear counterstain. Bar = 50μm.

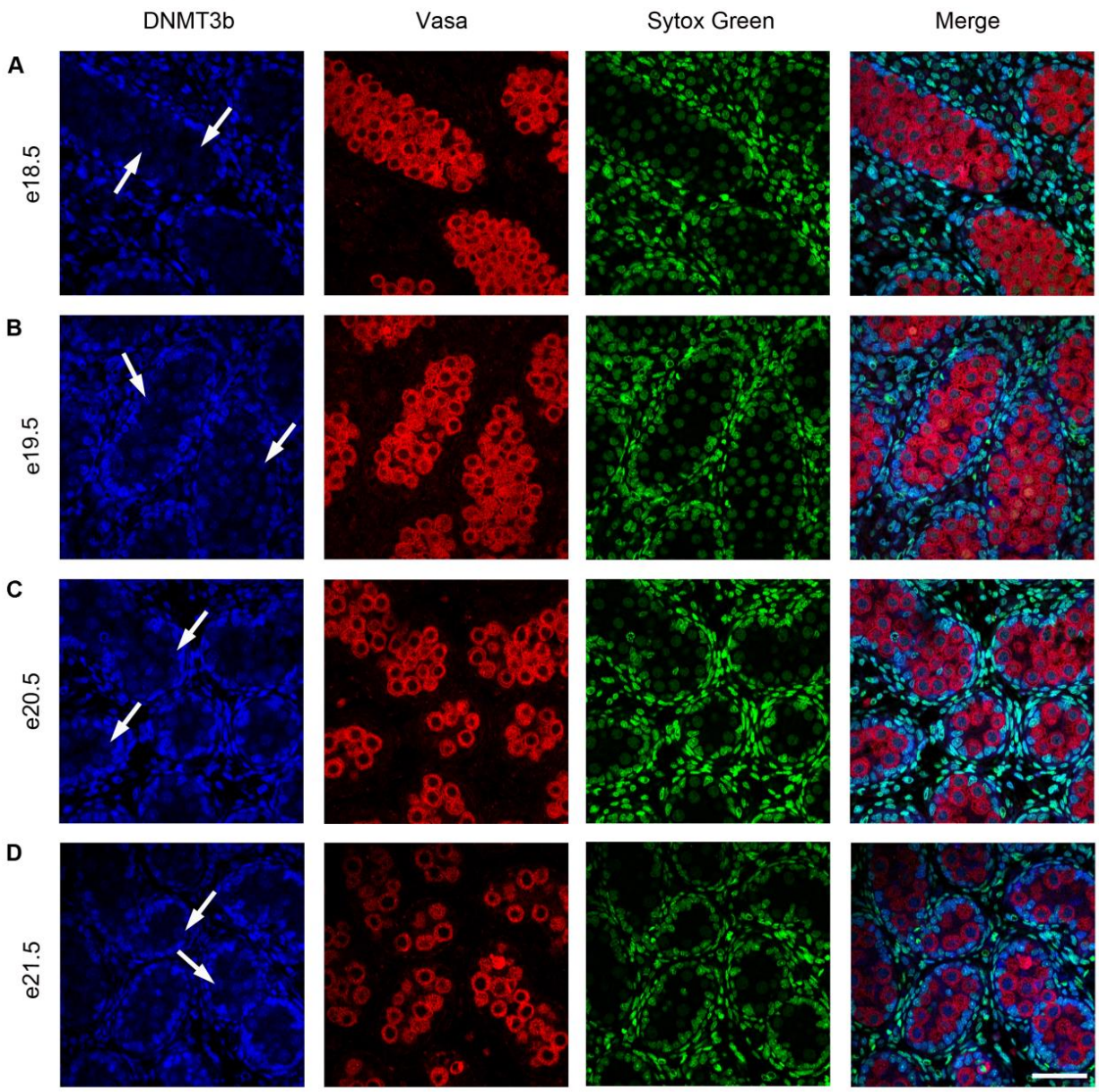

Figure 4.18. DNMT3b immunofluorescence in Dex tissues. Images of immunostained testis show that DNMT3b was detected in germ cells (blue, arrows) at e18.5-e21.5. Staining was detected in the somatic component throughout the time-course. Vasa staining (red), compatible with this protocol, was used to identify germ cells. Sytox Green acted as a nuclear counterstain. Bar = 50μm.

4.3.5.2 DNMT3L

As no visible change in DNMT3a or 3b staining was seen to account for an alteration in the timeframe of remethylation, expression of DNMT3L was explored. Since this methyl transferase acts as a co-factor for DNMT3a and 3b action [201], my hypothesis was that the expression or localisation of DNMT3L could be altered by Dex treatment, thus changing the remethylation activity of the other methyl transferases. Surprisingly, the DNMT3L antibody gave a diffuse cytoplasmic stain at e18.5-e21.5 in both Dex and Saline tissues (Figures 4.19 and 4.20). A previous study indicated germ cell staining was seen at PND25, but not at PND4 (Sharpe *et al*., unpublished data). I therefore studied these postnatal time-points to give an indication as to whether the current immunofluorescence protocol was working as previously. Whilst a weak diffuse cytoplasmic stain was seen for DNMT3L at PND4 (Figure 4.21A), an intense detection was found in germ cell nuclei at PND25 (Figure 4.21B). Interestingly, whilst this staining pattern was seen in some tubules, it was largely absent from others within the same testis section.

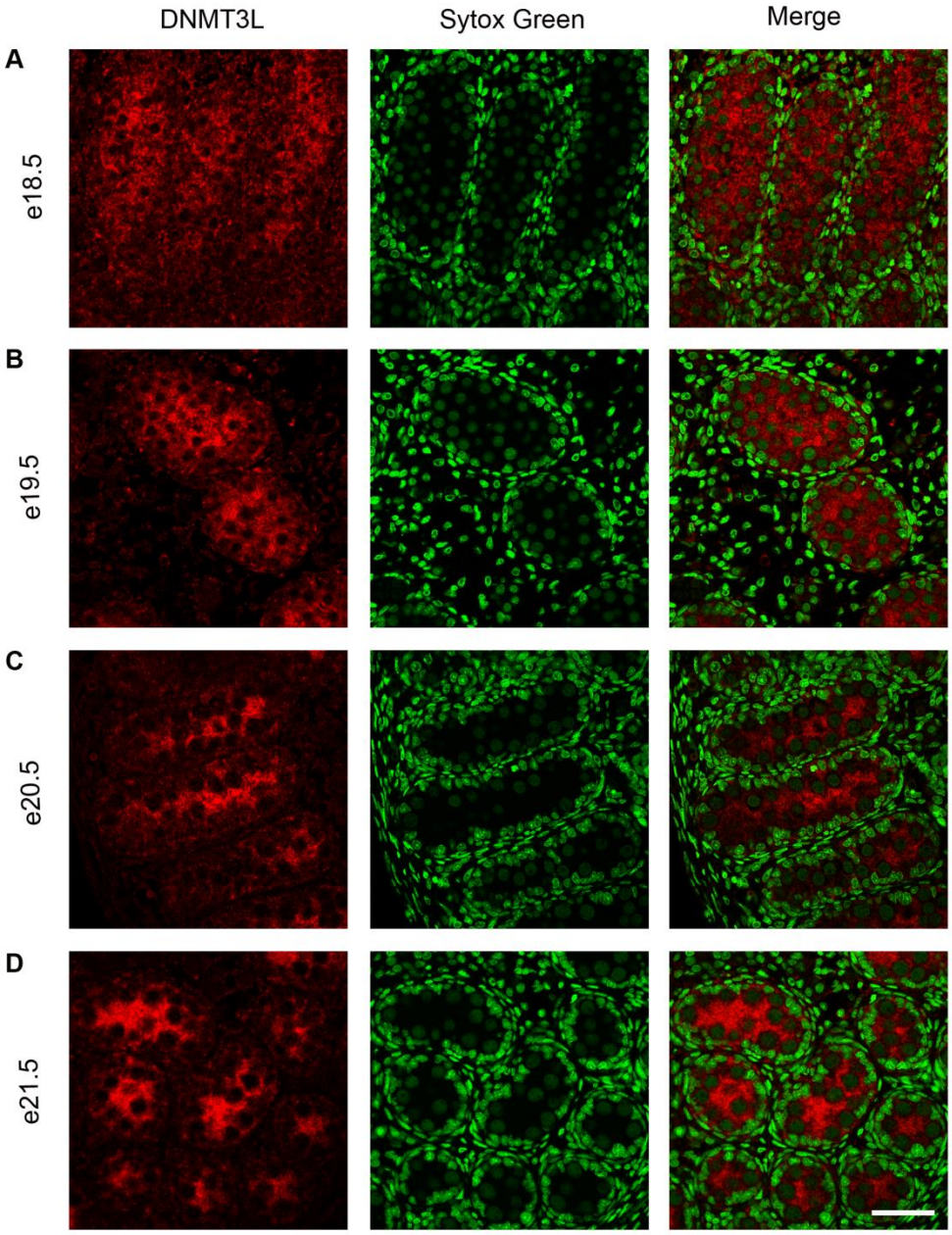

Figure 4.19. DNMT3L immunofluorescence in Saline tissues. Images of immunostained testis show a diffuse cytoplasmic detection of DNMT3L (red) at e18.5-e21.5, which is absent from germ cell nuclei. Sytox Green acted as a nuclear counterstain. Bar = 50μm.

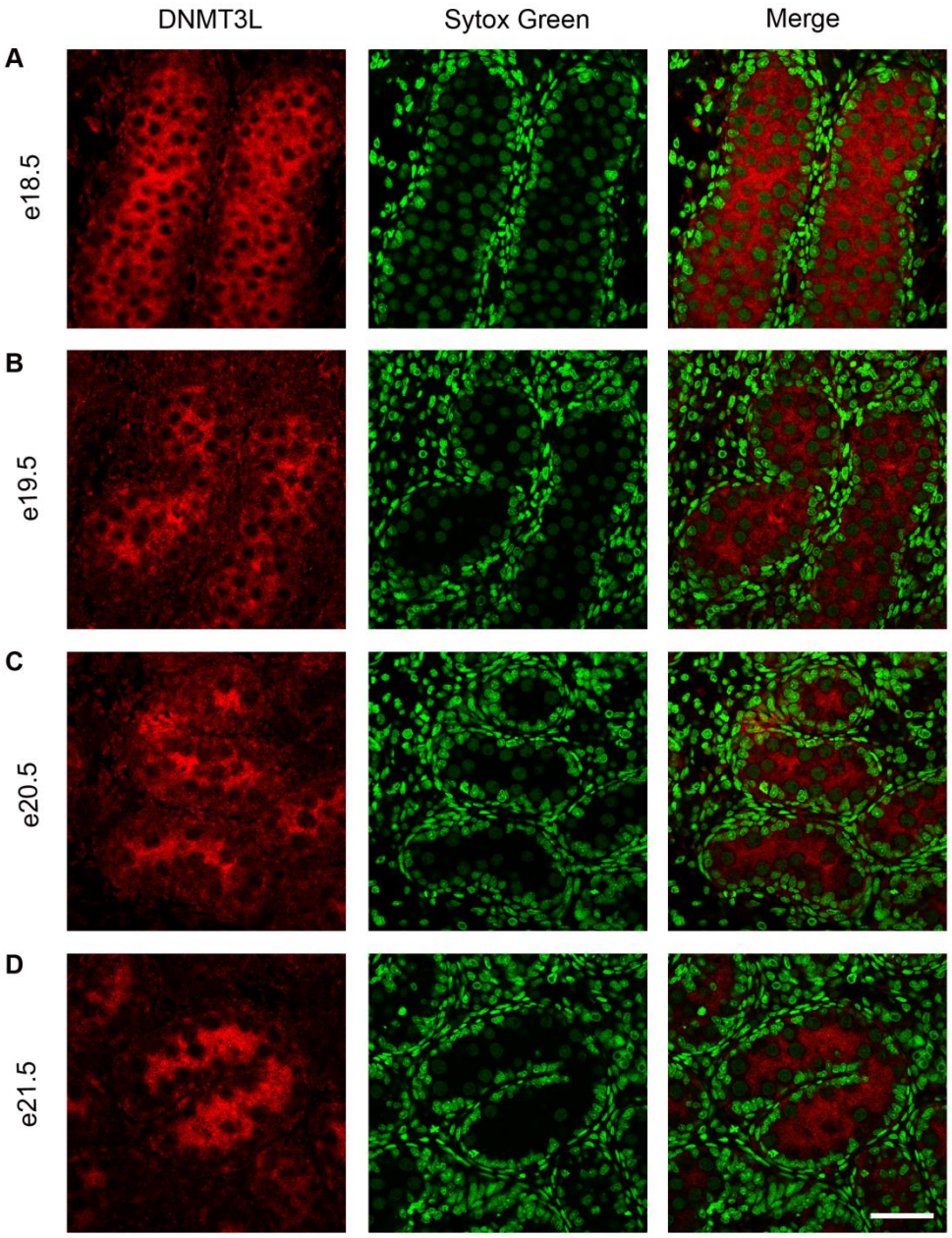

Figure 4.20. DNMT3L immunofluorescence in Dex tissues. Images of immunostained testis show a diffuse cytoplasmic detection of DNMT3L (red) at e18.5-e21.5, which is absent from germ cell nuclei. Sytox Green acted as a nuclear counterstain. Bar = 50μm.

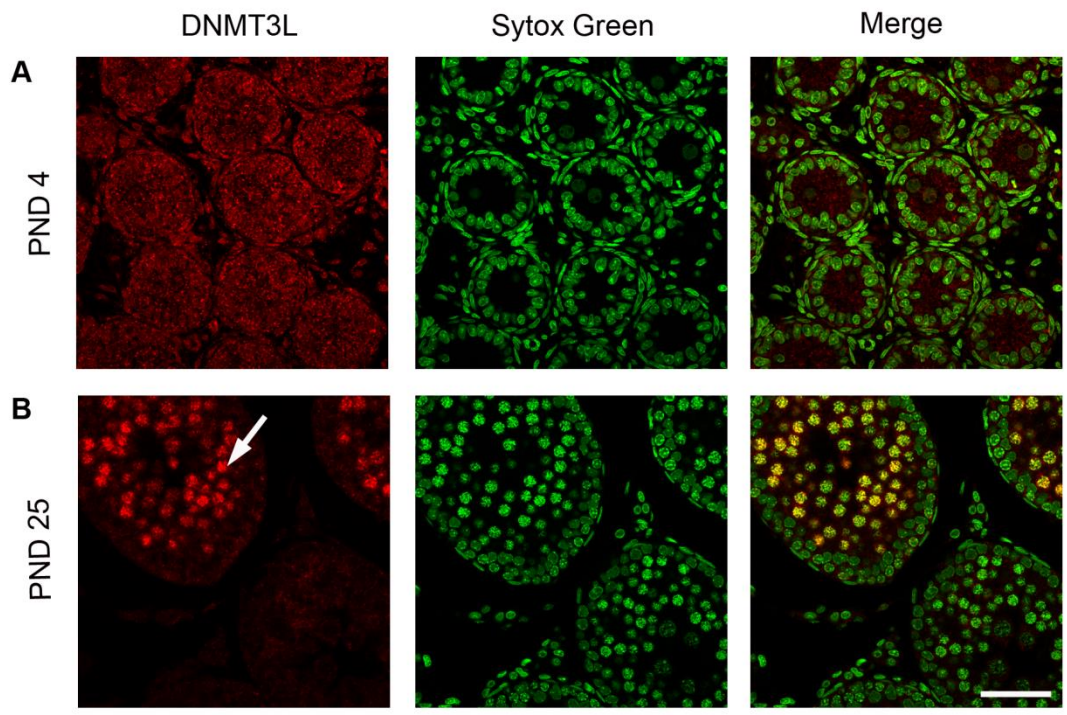

Figure 4.21. DNMT3L immunofluorescence in Dex tissues. Images of immunostained testis show a diffuse cytoplasmic detection of DNMT3L (red) at PND4 (A). However at PND25 (B), an intense nuclear stain is found in the germ cells of some tubules (arrow), but not others. Sytox Green acted as a nuclear counterstain. Bar = 50μm.

4.3.5.3 DMRT1

In an attempt to gauge the development of the testis as a whole, beyond changes in DNA methylation, DMRT1 was studied. This transcription factor was chosen as it is not directly linked to epigenetic mechanisms, it is present within the germ cells during mid-late gestation, when many traditional markers are absent, and immunodetectable protein expression is lost at e19.5-e20.5, a key time-point for change in our studies [259]. DMRT1 was detected in germ cells at e18.5 and e19.5, but not at e20.5-e21.5 in both Saline (Figure 4.22) and Dex (Figure 4.23) tissues.

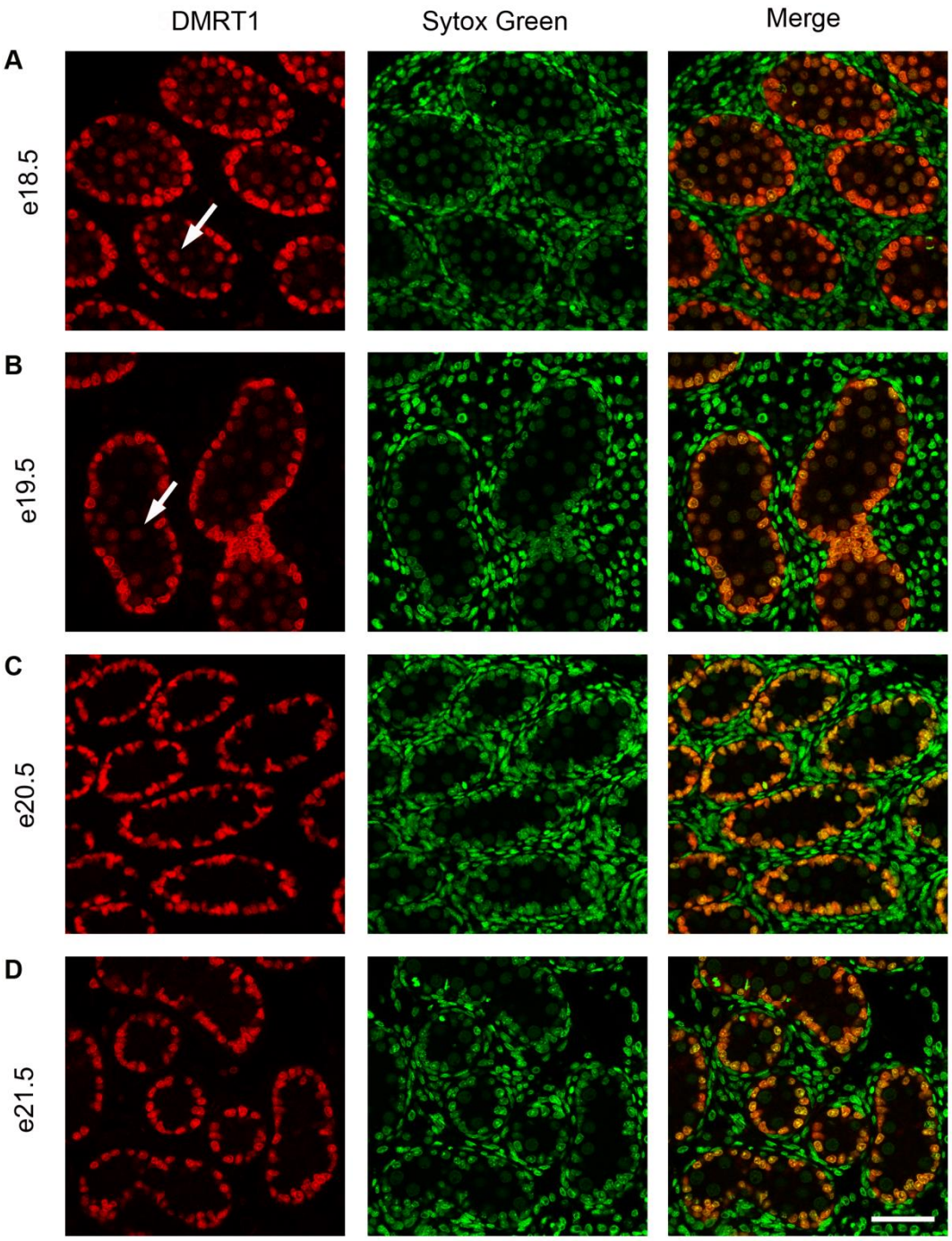

Figure 4.22. Localisation of DMRT1 in Saline testis. Images of immunostained testis show that DMRT1 (red, arrows) is present in germ cells at e18.5 and e19.5, and is undetected by e20.5. DMRT1 is seen in Sertoli cell nuclei throughout the time course. Sytox Green acts as a nuclear counterstain. Bar = 50μm.

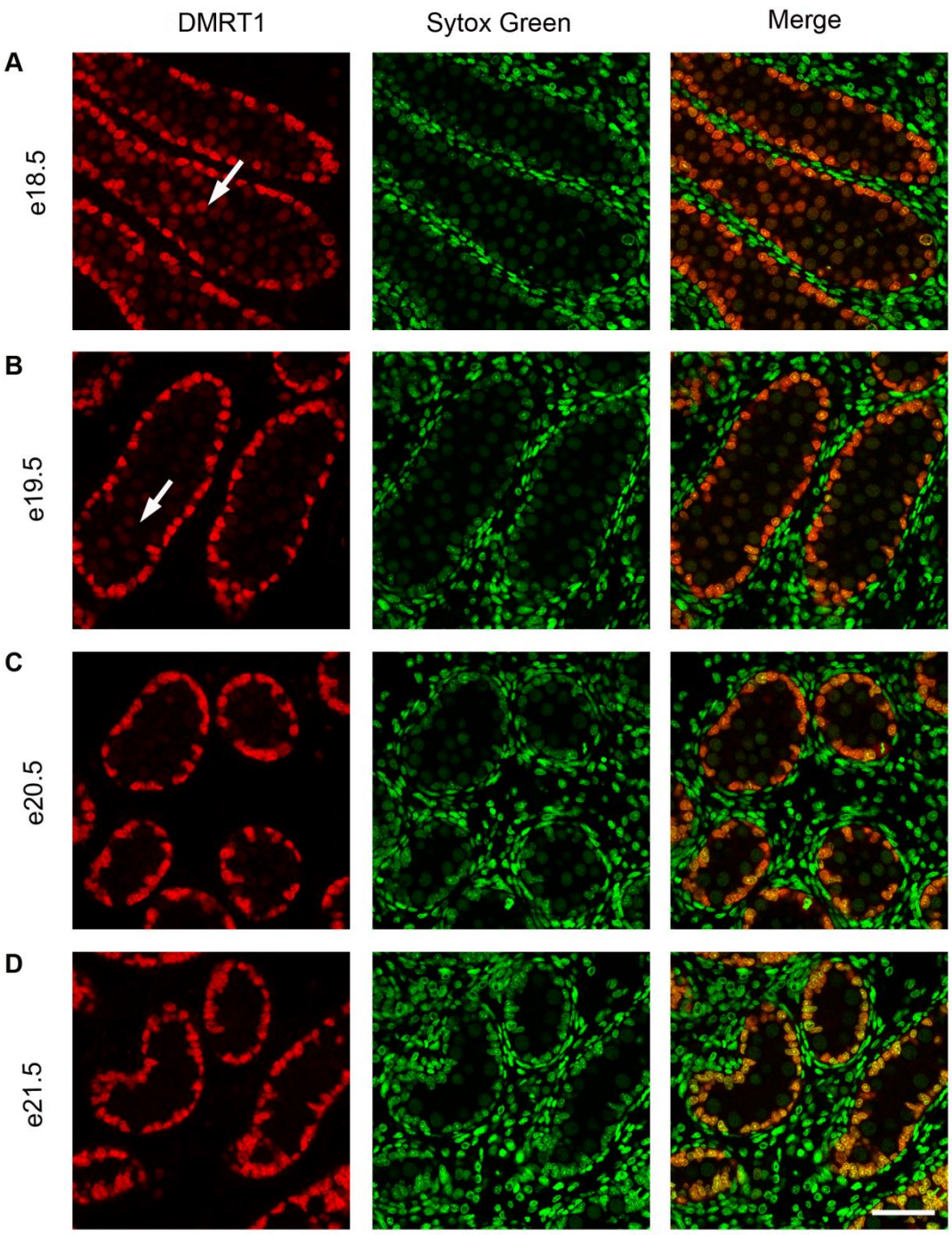

Figure 4.23. Localisation of DMRT1 in Dex testis. Images of immunostained testis show that DMRT1 (red, arrows) is present in germ cells at e18.5 and e19.5, and is undetected by e20.5. DMRT1 is seen in Sertoli cell nuclei throughout the time course. Sytox Green acts as a nuclear counterstain. Bar = 50μm.

4.4 Discussion

These data indicate that Dex exposure *in utero* may alter the epigenetic reprogramming time-line of developing fetal germ cells. I explored the localisation of GR within the testis, and therefore its susceptibility to glucocorticoid exposure, and then demonstrated for the first time that Dex treatment may correspond to a premature re-establishment of global germ cell 5mC. This however does not correspond to changes in localisation of DNMTs, as assessed by immunofluorescence.

As in previous studies, *in utero* Dex exposure decreased placental and fetal weight. The former was demonstrated between e19.5-e21.5, which is in keeping with studies reporting this decrease at e20.5 [12]. A reduction in fetal weight was only demonstrated at e21.5, although previous work indicates that this would be expected to occur by e20.5 [12]. This discrepancy could reflect the smaller replicate number used in this study. The effect of Dex exposure on placental weight, however, gives an assurance that our treatment had some effect on the e18.5-e20.5 litters, even before this was evident in pup weight.

The detection of GR in the somatic component of the fetal testis confirms that Dex may be able to act upon this tissue. As these cells promote the development of the germ cell, glucocorticoid exposure could have an indirect effect upon the germline in this way. Low levels of GR detection were also seen within the germ cells themselves suggesting that Dex could also have a direct action upon these cells. The location of GR within the fetal testis has not previously been reported, however my results are in keeping with studies examining expression within the testis of adult rats. GR has been shown to be located within Sertoli cells and interstitial components, such as Leydig cells and blood vessel endothelium during postnatal development [261,262]. Indeed, the Sertoli cell-specific GR knockout mouse has decreased Sertoli cell numbers, and intriguingly, a reduction in the circulating levels of Luteinizing Hormone (LH) and Follicle-stimulating Hormone (FSH) [263]. The authors propose that decreased Sertoli-cell GR may therefore inhibit the pituitary secretion of these gonadotrophins. In this study, the numbers of meiotic spermatocytes and postmeiotic spermatids were also reduced, and atypical germ cell

morphology was reported in the adult testis [263]. GR is also expressed within the nuclei of postnatal rat germ cells, with an increase in immunoreactivity reported from PND14 [261]. In the current study, Dex exposure did not visibly alter the localisation of GR. However, slightly weaker staining was observed in Dex-exposed germ cells, relative to Saline controls. Although immunofluorescence is only semi-quantitative, this may indicate a decrease in germ cell GR expression with Dex treatment, which would need further validation. Previous studies have shown that Dex, acting through GR, can alter the expression of the androgen binding protein and the glycoprotein hormone stanniocalcin-1 in cultured Sertoli cells [264,265] and reduces the proliferation of cultured peritubular cells [261]. Thus, even if Dex exposure does not confer changes in germ cell GR expression, it may alter gene regulation within somatic cells, which could ultimately impact upon germ cells.

My data indicate that Dex exposure may influence remethylation during germ cell reprogramming. Visually, more germ cells appeared to be 5mC-positive at e19.5 following Dex exposure, relative to Saline controls. This was supported by semi-quantification, indicating this was a statistically significant difference. As 5mC staining between groups was not significantly different by e20.5, I hypothesise that Dex is promoting a pre-mature remethylation phase during germ cell epigenetic reprogramming (Figure 4.24).

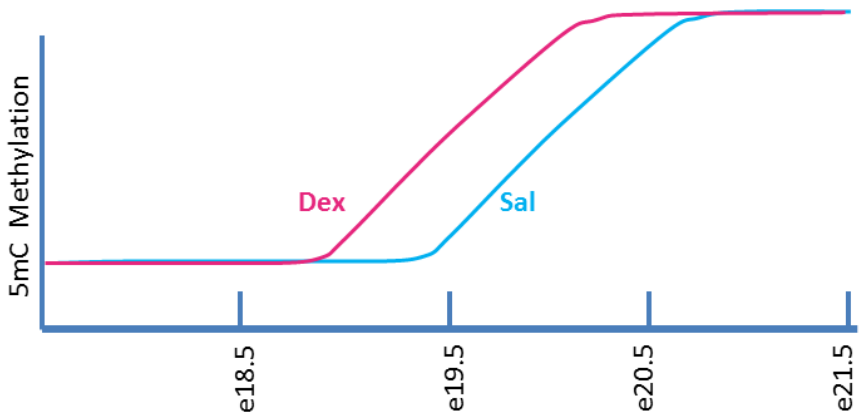

Figure 4.24. Hypothesised effect of Dex treatment upon reprogramming time-line. Exposure to Dex may promote premature re-establishment of 5mC in germ cells.

An effect of Dex exposure on epigenetic reprogramming has not previously been reported. It is, however, in keeping with the hypothesis that an altered intra-uterine environment can influence DNA methylation in the offspring [266]. Dex exposure in cultured rat hepatocytes has also been shown to promote a stable state of demethylation of the promoter region of the tyrosine aminotransferase gene in liver, which *in vivo* may prepare the genome to respond to postnatal hypoglycaemia [267]. Maternal Dex treatment has been shown to reduce levels of 5mC at *Igf2* [12] and *Tex.19* (Drake, unpublished) in fetal liver. As the latter is predominantly expressed in germ and pluripotent cells, and is involved in the regulation of spermatogenesis [268] this indicates that an influence on methylation within the fetal germline itself might be anticipated.

The mechanisms by which a Dex-induced change in epigenetic reprogramming could be mediated are yet to be deduced. DNMT3a and DNMT3b are implicated in germ cell remethylation in mice [269]. It was therefore hypothesised that their localisation might be altered following Dex exposure, influencing the timing of remethylation. The localisation of DNMT3a and DNMT3b in the rat has not previously been reported in the literature, although laboratory data suggests that it is present in the fetal testis. Immunofluorescence indicated that both DNMT3a and DNMT3b were present in germ and somatic cells from e18.5-e21.5 in the rat. No noticeable variation in staining was recorded between testes of Dex and Saline-exposed fetuses. The localisation of DNMT3L, known to act as a co-factor for DNMT3a and DNMT3b [200,201] was therefore studied however an unexpected staining pattern was seen for DNMT3L in fetal tissues. A very intense nuclear stain within some seminiferous tubules at PND25 suggested that the antibody staining conditions were correct, at least for some time-points. It is therefore unclear if this represents a true cytoplasmic localisation in the fetal rat seminiferous tubule, or an experimental artefact. Certainly, no observable difference in localisation between Dex and Saline groups was noted. Thus, if Dex mediates its actions on fetal programming through an alteration in the expression of the DNMT3 enzymes, it is not detectable by these methods.

It has recently been suggested that Dex may influence gene expression through DNMT3b. Data indicates that Dex may promote the formation of a repressor complex, comprising of GR, HDAC1 and MeCP2, which recruits DNMT3b to gene promoter regions, and subsequently increases methylation [270]. GR has been shown to be capable of interacting with DNMT3b, but intriguingly, not DNMT3a [270]. This study, however, was conducted in rat hypothalamic cells. The response may be different depending on tissue type and stage in development. Thus the mechanism by which a shift in the epigenetic timeframe could be mediated has yet to be elucidated.

Further research is also required to determine if any shift in epigenetic reprogramming is a specific action upon the germ cell, or simply an extension of the accelerated maturation promoted by Dex administration, shown in other organs. An increase in fetal glucocorticoids in late gestation is key for the development of lungs, kidney, liver and the gastrointestinal tract in preparation for birth (reviewed in [271]). As such, premature babies can have problems with organ development, and therefore Dex is administered to pregnant mothers at risk of a premature delivery. For example, in a large epidemiological study, prenatal Dex exposure was found to reduce the incidence of respiratory distress syndrome in neonates, due to accelerated lung maturation [272]. In the Dex-programmed rat, liver maturation has also been shown to be accelerated [273]. It could therefore be hypothesised that Dex exposure accelerates maturation of the testis as a whole, rather than having a specific effect on epigenetic reprogramming.

In order to give an initial indication of the maturation state of the testis as a whole, tissues were stained for DMRT1. This transcription factor was found to be present in germ cells at e18.5 and to a lesser extent e19.5, becoming undetectable in the majority of germ cells by e20.5. The same progression was seen for both Dex and Saline groups, giving an initial indication that testis maturation was occurring normally. This is in keeping with the work of Jobling *et al*. (2011) who noted that DMRT1 was expressed in the majority of germ cells at e17.5, decreasing to 7% by e19.5, and to 0% by e21.5. Intriguingly, this group identified significantly more DMRT1-positive germ cells at e19.5 following fetal DBP exposure, relative to

controls, and hypothesised that this represents a delay in germ cell differentiation [259].

In conclusion, it appears that Dex exposure may alter epigenetic reprogramming, with more germ cells remethylated at e19.5 relative to controls. Genome-wide studies, capable of highlighting methylation changes at specific genes, are required to give a more quantitative analysis of this effect. This should give a greater understanding as to whether a shift in epigenetic reprogramming would be detrimental to the development of the pup, and that of future generations.

Chapter 5 Profiling DNA Methylation in Germ Cells

5.1 Introduction

I hypothesised that Dex exposure might affect DNA methylation in developing fetal germ cells which would then go on to form the next generation. Based on Chapters 3 and 4, which explored global changes in methylation, I conducted studies with base-pair resolution in the developing germ cell. Chapter 3 indicated that global remethylation during epigenetic reprogramming occurs between e18.5-e21.5, and in Chapter 4, global methylation appeared to be increased at e19.5 following Dex exposure, suggesting that the epigenetic reprogramming time-line might be shifted with treatment. The e19.5 time-point was therefore chosen for detailed gene-specific studies as 5mC appeared to be present, and the data from immunofluorescence studies suggested it was a key point of change as a consequence of Dex exposure.

In order to isolate pure populations of fetal germ cells and sperm, a transgenic rat strain was used. GCS-EGFP Sprague Dawley rats were reported to express EGFP specifically within germ cells and sperm [92]. Founder rats were a kind gift of Bob Hammer (University of Texas Southwestern Medical Centre, USA). As they were new to The University of Edinburgh, a homozygous colony had to be established, and use of their tissues optimised. I also sought to confirm that EGFP expression was germ cell-specific, and that the epigenetic reprogramming timeframe and Dex programming phenotype was similar to the Wistar rats used in previous Chapters and in published literature.

After establishing that the GCS-EGFP rats were suitable for our programming studies, I collected fetal germ cells at e19.5. DNA extraction methodology was optimised and Enhanced Reduced Representation Bisulfite Sequencing (ERRBS) used to give a genome-wide view of specific cytosines that are differentially methylated following Dex exposure. This is based on the technique RRBS, first developed in 2005, which allows genome-wide methylation to be detected at single-base resolution whilst focussing on regions that are most likely to be methylated, thus reducing the number of nucleotides to be sequenced to around 1% of the genome [274]. DNA is first cleaved by a restriction endonuclease such as

Microsomal Serine Proteinase 1 (MSP1), which cuts the DNA following a CpG. Other enzymes may be used to fragment the genome, but some have alternative cleavage sites, meaning that there is no bias towards CpG dinucleotides [275]. The majority of methylation occurs at CpGs, and therefore favouring the presence of CpG sites is advantageous for methylation sequencing studies [276]. Employing an enzyme such as MSP1 ensures that there will be at least 2 terminal CpG sites in every fragment. Crucially, MSP1 digestion is not sensitive to DNA methylation, thus there is no bias towards methylated or non-methylated CpGs [275]. The 3'-terminal ends are then repaired, and an extra adenosine base added to the ends of both strands in a process called A-tailing. This allows ligation of methylated adaptors on to the ends of the fragment. The methylation of these adapters ensures the integrity of their sequence during the bisulfite conversion step. Gel electrophoresis is used to isolate fragments of the desired length, which are then bisulfite converted [275]. This process converts unmodified cytosine to uracil, whilst methylated cytosines are protected from this conversion [277]. Bisulfite-converted DNA is then amplified by PCR, using primers specific to the adapter sequences previously added to the fragment. The amplified DNA is then sequenced, with uracil bases indicating sites of unmethylated (converted) cytosine and cytosine bases indicating those of methylated (unconverted) cytosine, in the original DNA sample [275].

ERRBS follows the same protocol, but with some modifications to facilitate the analysis of small samples, and to enhance coverage of CpGs that exist out with CpG islands [278]. The two rounds of bisulfite conversion found in RRBS are substituted for one extended conversion period, eliminating an intermediate DNA clean-up step previously conducted, and thus reducing sample loss [278]. This also yields improved bisulfite conversion rates. A wider range of fragment sizes are also selected, encompassing longer lengths, and ensuring more of the regions beyond CpG islands are captured [278]. A recent study suggests that 25% of DNA methylation may occur out with CpGs, and therefore increasing the fragment length and the capture of these regions may be of relevance [276].

The resulting ERRBS analysis gives a predicted methylation status for each CpG studied across all the given reads for that base. The percentage ratio of methylated to

unmethylated cytosines aligning to each CpG is therefore used to give a 'methylation score'. Thus theoretically, if all reads from all samples in a group indicated CpG methylation, the predicted status would be 1 or 100% [278]. A preliminary descriptive analysis of differentially methylated cytosines (DMCs) was performed by Thomas Smith, CGAT, University of Oxford. This included all DMCs which exhibited altered methylation consistently across the samples. The numbers of DMCs exhibiting hypermethylation with Dex exposure were compared to those found to be hypomethylated. DMCs were then grouped based on their corresponding methylation status in control liver samples, as determined by ERRBS in Chapter 6. The liver methylation status was used to give an imperfect indication of the baseline methylation state for that DMC, and whether Dex exposure might cause cytosines to be reprogrammed to their 'normal' methylation state more quickly. Biseq analysis was then performed. This analysis indicates which of the observed differences in cytosine methylation in a data set are statistically significant, and identifies clusters of significant DMCs, which we hypothesise could indicate particular relevance for gene expression [279]. It was hoped that this technique would give further insight into the relationship between Dex exposure and germ cell methylation.

A second cohort of rats was taken to maturity (90 days) following *in utero* Dex or Saline exposure. Pure sperm populations were isolated by FACS sorting of the epididymis and DNA extraction protocols optimised. These samples were also prepared for ERRBS, so that any changes in methylation seen in germ cells with Dex exposure might be compared to those carried in the sperm. Two main aims therefore directed the experiments in this chapter; to characterise the GCS-EGFP rat as a potential programming model, and to use it to isolate pure populations of germ cells and sperm for ERRBS studies.

5.2 Materials and Methods

We were provided with homozygous male GCS-EGFP rats from the University of Texas. In order to establish a homozygous colony of GCS-EGFP rats for our studies, one founder homozygous male was mated with a Sprague Dawley wild-type female. The resulting hemizygous offspring were mated. Genotyping was optimised to determine whether EGFP was present in the genome, as outlined in Chapter 2.6.2. EGFP-positive rats were continually mated, and if they consistently produced litters in which all pups had the EGFP insert, they were determined to be a homozygous pair.

5.2.1 Confirming Germline-Specific Expression of EGFP in GCS-EGFP Rats

In parallel, the founder males were sacrificed, and testis, heart, liver, kidney and spleen tissues were isolated. These tissues were fixed in formalin, embedded in paraffin wax, and sectioned by staff at SURF. They also used the Bond-Max immunostaining machine to give immunostaining for EGFP and the vimentin Sertoli cell marker. I then imaged slides to confirm both the tissue- and the cell-specific localisation of EGFP in the GCS-EGFP rats.

Further confirmation of the expression of EGFP in the testis was obtained by extracting fetal testes from offspring of the established homozygous colony. Before any processing, testes were imaged under the fluorescent microscope, to ensure the expression of active EGFP. A single-cell suspension was then created from these tissues, as outlined in Chapter 2.5.2.1. The sample was then FACS sorted to confirm that a distinct EGFP-positive population was present. All FACS sorting was conducted by Fiona Rossi and William Ramsay of the Centre for Inflammation Research Flow Cytometry Unit, The University of Edinburgh, following the procedures outlined in Chapter 2.16. Additional confirmation of the identity of EGFP-positive cells was obtained by exploring the expression of a germ cell-specific marker. Homozygous females (n=3) were time-mated with homozygous males, and the morning a plug was found was denoted as e0.5. Pregnant dams were culled at e19.5, and fetal testes were extracted. A single-cell suspension was created as previously, pooling testes from every pup within a litter. The sample from each litter

was then FACS sorted separately, and EGFP-positive and EGFP-negative fractions collected. Cells were pelleted by centrifugation, supernatant was removed and cells were snap frozen on dry ice, before storing at -80°C. RNA was extracted as outlined in Chapter 2.11.2 and reverse transcribed to cDNA as outlined in Chapter 2.11.5. qPCR was then performed for the germ cell-specific marker *Dazl*, the Sertoli cell marker *Sox9*, and the housekeeping gene *Tbp*. qPCR was performed in parallel using liver cDNA, as a negative control.

5.2.2 Isolation and DNA Extraction of F1 Germ Cells and Sperm

In order to confirm that the global remethylation of epigenetic reprogramming occurs at similar time-points in wild-type Wistar and GCS-EGFP Sprague Dawley rats a litter was produced for each genotype at both e19.5 and e20.5, and tissues collected and processed as in Chapters 3 and 4. Immunofluorescence was then used to explore the localisation of 5mC at each time-point, as previously.

Homozygous virgin female GCS-EGFP rats were then time-mated with homozygous males. Pregnant dams were injected with Dex or Saline solutions from e15.5 as previously, and culled by cervical dislocation at e19.5 (n=10 Saline and 9 Dex litters). All pups and placentas were then weighed, and pups sexed by identification of either testes or ovaries. Testes were collected and incubated with collagenase to create a single cell suspension, as previously. EGFP-positive and negative cells were then separated using FACS, as above. A wild-type control litter was also processed in the same way to give a negative control so that the appropriate EGFP-positive gates could be established.

Isolated EGFP-positive and negative cells were then pelleted, the supernatant removed and cells were snap-frozen on dry ice. Samples were then stored at -80°C. DNA extraction was optimised because of the very low cell numbers (around 30,000 germ cells per litter). Initial optimisation was performed on pellets of an equivalent number of AS4.1 cell culture cells, kindly supplied by Charlotte Buckley, as outlined in Chapter 2.14.4.1. This allowed initial trials to be performed without the excessive

use of animals. The optimised conditions were then used to extract DNA from the germ cells.

A second animal study was conducted to explore methylation in sperm of rats exposed to Dex *in utero*. Homozygous virgin female GCS-EGFP rats were time-mated with homozygous males, and Dex or Saline solutions given to pregnant dams as previously. Dams were allowed to deliver naturally, and pups weighed, and culled to 8 per litter. Pups were also weighed at weaning (PND22 ± 1 day) and at maturity (90 days).

At 90 days, one male per litter was sacrificed and the epididymes were removed (n=8 Saline and 9 Dex). Four incisions were made along the length of each epididymis before incubating in sperm swim buffer for 45 min on a rocking platform, allowing the motile sperm to swim out of the tissue. The epididymis was then removed and sperm pelleted by centrifugation. Sperm was re-suspended in TBS before being passed through a 70 µm cell strainer. EGFP-positive cells were removed from debris by FACS sorting, as outlined in Chapter 2.16. Sperm of a wild-type Sprague Dawley was also processed, giving a negative control, and allowing accurate EGFP FACS gates to be set. The resulting EGFP-positive sperm was pelleted by centrifugation, snap frozen, and stored at -80°C. DNA extraction from sperm was optimised, due to the ineffectiveness of standard extraction procedures on this cell type (see chapter 2.14.2). Extraction was then conducted on each experimental sample.

5.2.3 Exploring Programming Phenotype in GCS-EGFP Rats

Glucose tolerance tests were performed at 90 days to explore the metabolic phenotype of Dex programming in the GCS-EGFP rat. All rats were fasted for 16 hours and 1 male from each litter was randomly selected for experimentation. A tail bleed was conducted at 9am (time 0), and blood collected in heparin coated tubes. Glucose solution (0.5g/ml giving 2g glucose/kg rat) was administered immediately after by an oral gavage, performed by William Mungall (BRF, Little France). Subsequent tail bleeds were conducted after 30 and 120 min. Samples were centrifuged at 6000 rpm for 10 min and the plasma supernatant removed and stored

at -20°C. Glucose levels were then analysed by the glucose hexokinase assay, and insulin using an insulin ELISA kit as outlined in Chapter 2.9 and 2.10.

A second generation was also bred from these rats, to confirm that a birth weight phenotype was being transmitted across generations. In order to minimise animal numbers and cost, only 2 of the 4 potential crosses were bred. Control females were crossed with control males (Saline x Saline, SS) and also with Dex-exposed males (Saline x Dex, SD). The SD experimental cross was chosen as it explores transmission through the male line, which is most relevant to these studies. This cross had also shown the greatest effect of treatment on birth weight in Drake *et al*. (2011) [12].

Normality of weight data distribution was confirmed using the Lilliefors test. Normally distributed data ($p>0.05$) was analysed by Student's t-test, and nonparametric data by Mann Whitney U test, in keeping with previous studies [10,12]. As a second confirmation, data was analysed by multivariate linear regression, accounting for the intra-litter association of pups.

ERRBS was performed on germ cell and sperm samples at Weill Cornell University Epigenetics Core, New York, USA. Bioinformatic analysis was then conducted by Dr Thomas Smith (CGAT, University of Oxford, UK).

5.3 Results

5.3.1 Exploring GCS-EGFP rats as Programming Models

5.3.1.1 Confirming the Germ Cell-Specific Localisation of EGFP

Immunofluorescence showed no positive detection for EGFP in heart, liver, kidney and spleen tissues, as for negative controls, where no primary antibody was used (Figure 5.1 B-E). However in testis tissue, the majority of cells have a strongly positive EGFP detection (Figure 5.1A).

Within the testis, little detection of EGFP was found in the nuclei of Sertoli cells, the cytoplasm of which was identified by vimentin staining (Figure 5.2B). A strong detection of EGFP was found in nuclei of other cells within the seminiferous tubule, counterstained with DAPI (Figure 5.2 A).

EGFP was visualised in the testes of pups culled at e18.5, shown to be bright green under the fluorescent microscope, without any manipulation (Figure 5.3A). Testes were then FACS sorted, and a distinct EGFP-positive cell population visualised (Figure 5.3B). Further confirmation of the germ cell-specific expression of EGFP was obtained by reverse transcription and qPCR of RNA extracted from FACS sorted EGFP-positive and negative cells, and a liver tissue negative control. Significantly higher expression of the germ cell-specific marker *Dazl* was found in the EGFP-positive, compared to EGFP-negative samples ($p<0.001$). Higher expression of the Sertoli cell-specific marker *Sox9* was found in the EGFP-negative ($p<0.001$) compared to EGFP-positive samples. Expression of *Dazl* and *Sox9* in liver was negligible.

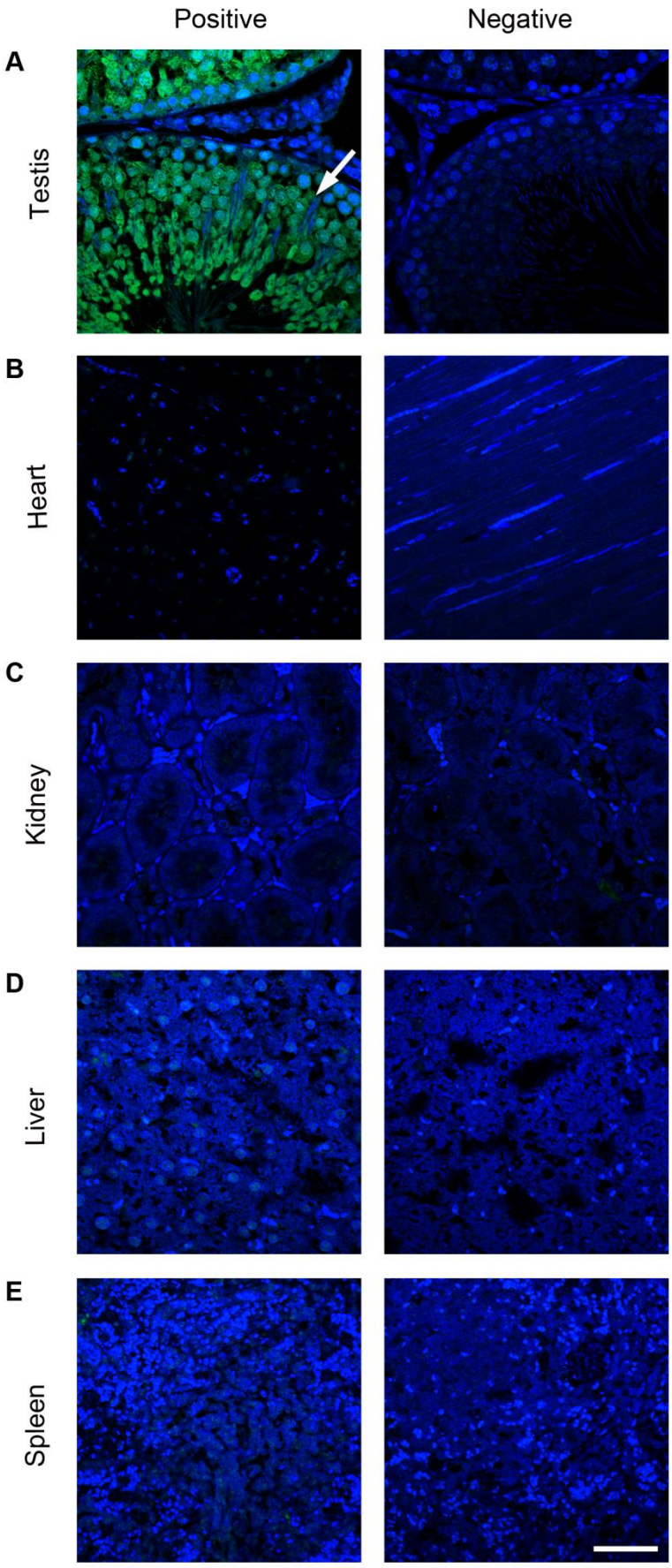

Figure 5.1. Confirming the testis-specific localisation of EGFP. Testis, heart, kidney, liver and spleen from GCS-EGFP founder males were stained for EGFP. Fluorescent secondary antibody immunostaining, without prior EGFP primary antibody incubation, was used as a negative control. Positive EGFP detection (green, arrow) was found in the testis, whilst images for other tissues resemble that of the corresponding negative controls. Bar = 50µm.

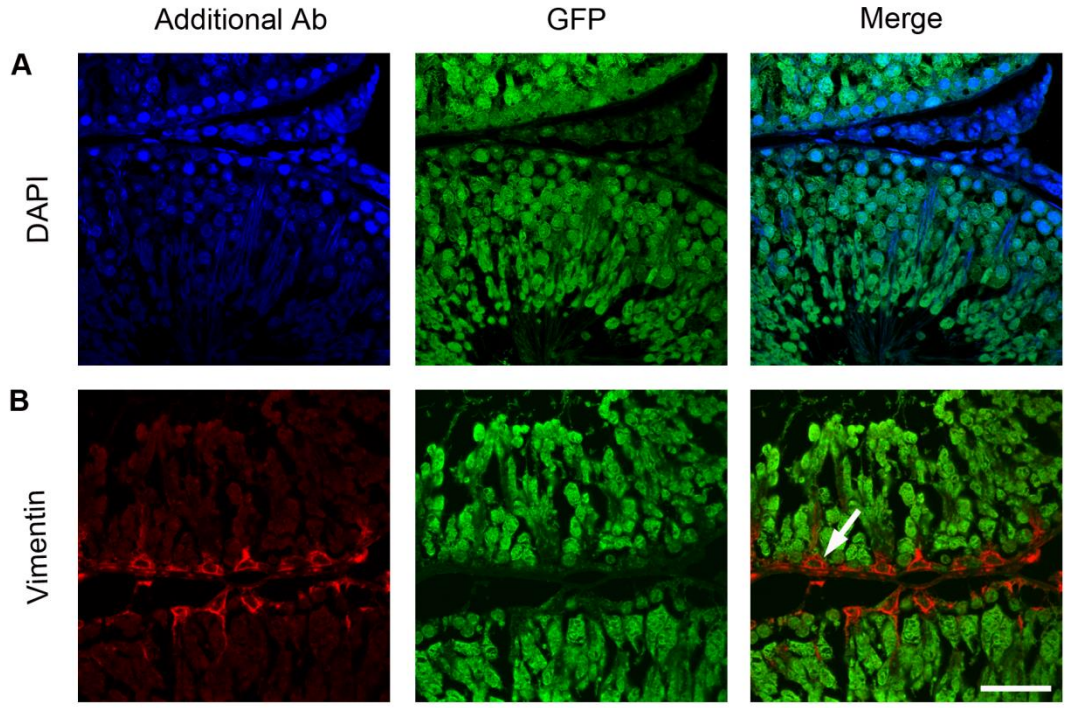

Figure 5.2. Exploring the localisation of testicular EGFP expression. Testes from GCS-EGFP rats were immunostained for EGFP and either DAPI (blue, A) or vimentin (red, B). Weak EGFP staining is identified in some extra-testicular cells identified by DAPI (blue), and cytoplasm of Sertoli somatic cells, stained by vimentin (red, arrow). Bar = 50µm.

A

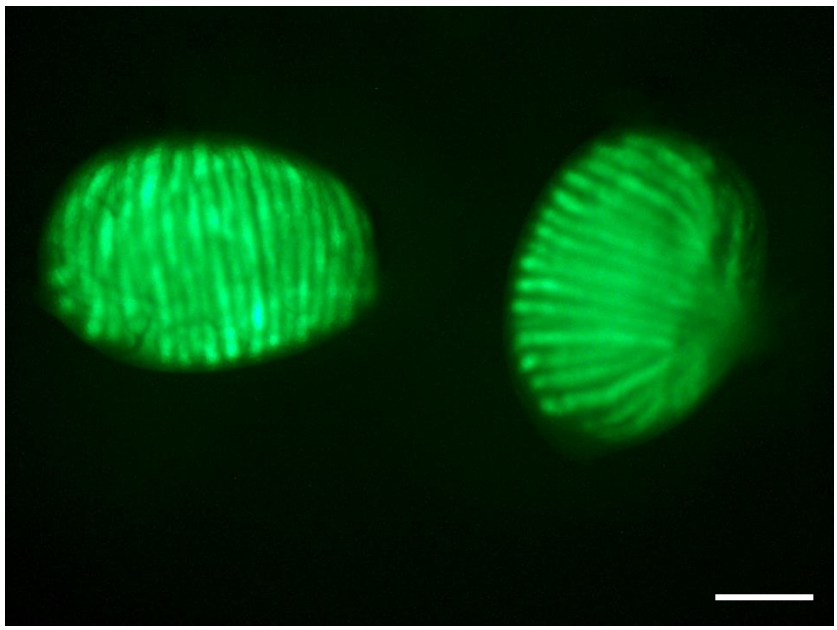

B

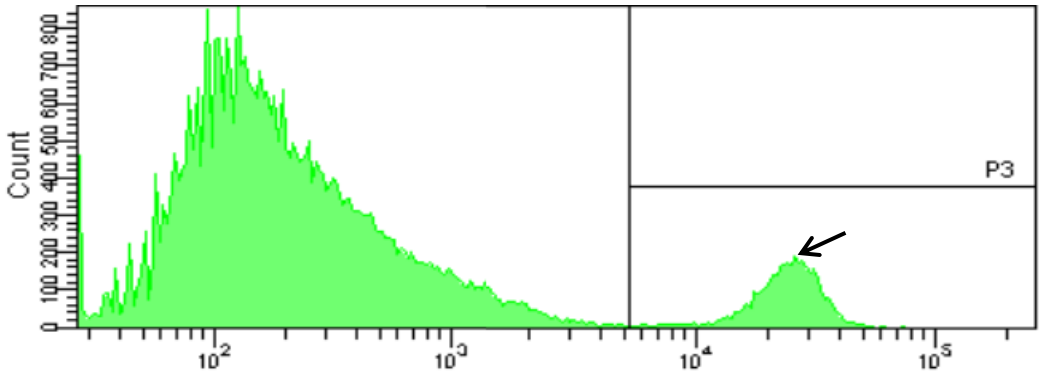

Figure 5.3. EGFP-positive cells in founder offspring at e18.5. Testes of GCS-EGFP offspring have green fluorescence (A). FACS analysis confirms that testes contain a EGFP-positive cell population (B, arrow). X-axis shows the relative fluorescence in logarithmic scale. Y-axis indicates the number of cells counted. Emission wavelength = 525±50nm. Bar = 250µm.

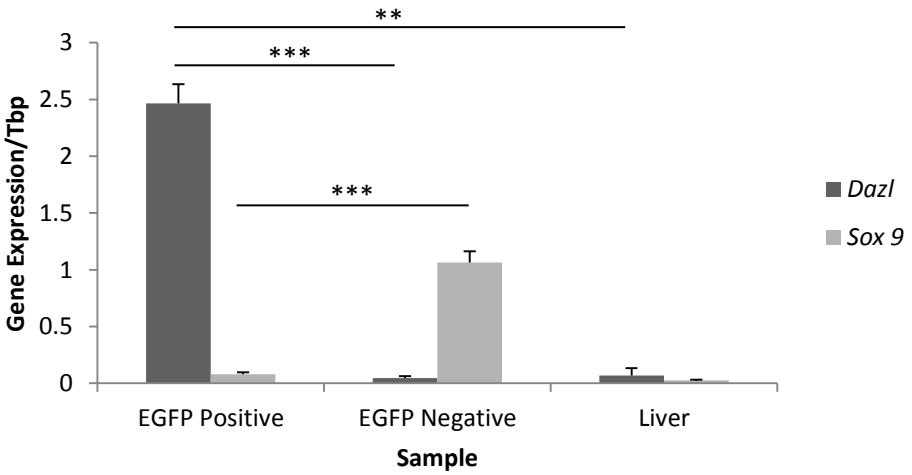

Figure 5.4. Confirming the expression of *Dazl* germ cell marker in EGFP-positive cells. Expression of *Dazl*, and *Sox9* Sertoli cell marker is expressed relative to *Tbp*. *Dazl* was significantly increased in the EGFP-positive FACS sorted fraction relative to EGFP-negative cells ($p<0.001$) and liver ($p<0.01$). Conversely *Sox9* expression was significantly reduced in the EGFP-positive, relative to negative fractions ($p<0.001$). Bars represent mean ± standard error. ** $p<0.01$, *** $p<0.001$

5.3.1.2 Exploring Global Remethylation Patterns

At e19.5, 5mC was detected in few germ cells (Figure 5.5) whilst at e20.5 (Figure 5.6) all germ cells identified with Propidium Iodide had a corresponding 5mC stain, for both Wistar and GCS-EGFP rats.

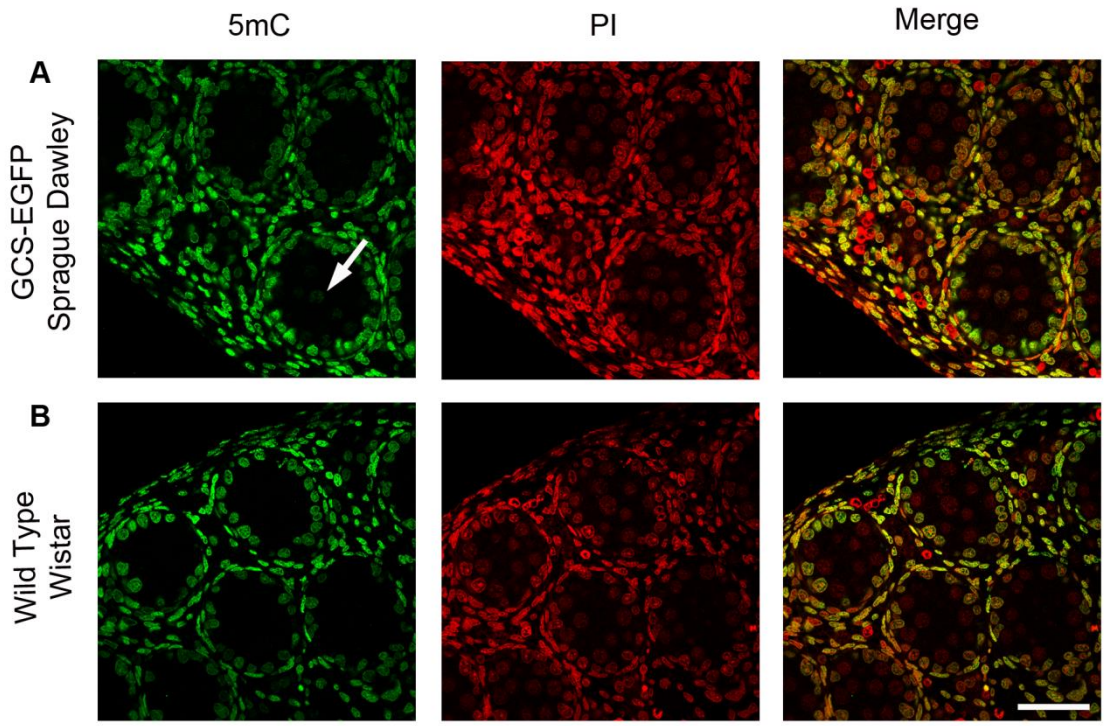

Figure 5.5. Comparing 5mC localisation in GCS-EGFP Sprague Dawley and wild-type Wistar rat testis at e19.5. 5mC was identified in the somatic cells of both strains, and some of the germ cells of GCS-EGFP rats at e19.5 (green, arrows). Propidium Iodide (PI) acts as a nuclear counterstain. Bar = 50µm.

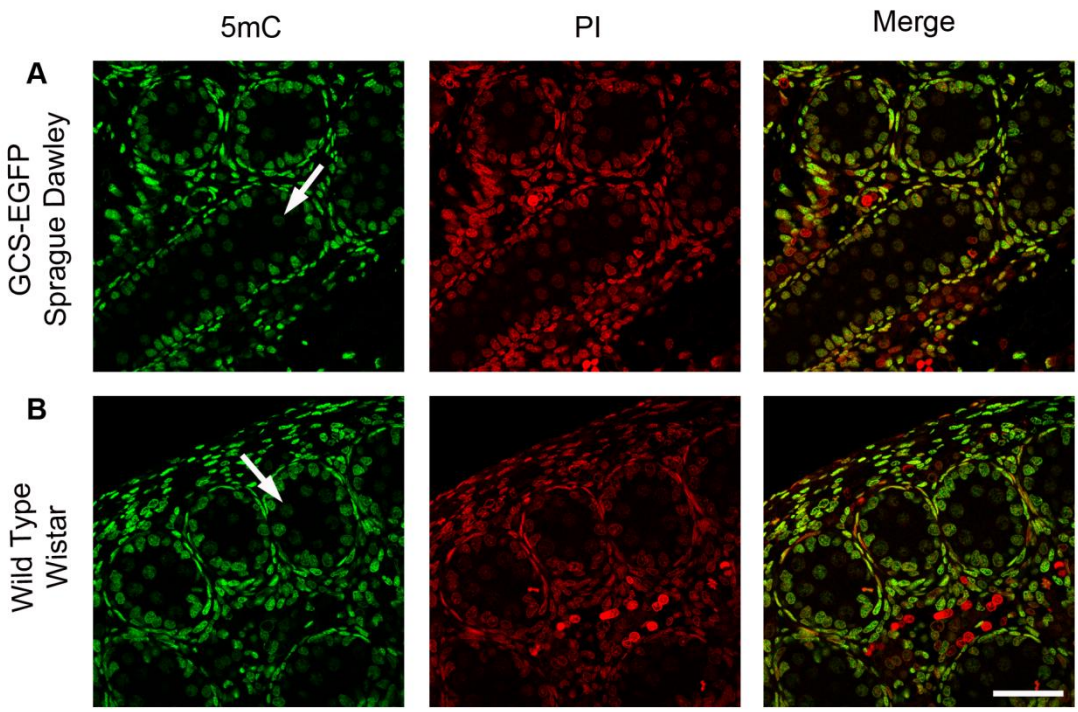

Figure 5.6. Comparing 5mC localisation in GCS-EGFP Sprague Dawley and wild-type Wistar rat testis at e20.5. 5mC (green, arrows) was identified in the somatic cells of both strains, and the germ cells of both GCS-EGFP (A) and Wistar (B) rats at e20.5. Propidium Iodide (PI) acts as a nuclear counterstain. Bar = 50µm. An enlarged version of this figure is presented in appendix Figure A3.

5.3.1.3 Confirming that GCS-EGFP Rats Show a Programmed Phenotype

Dex-exposure corresponded to a decreased pup ($p<0.01$, Figure 5.7A) and placental weight ($p<0.001$, Figure 5.7B). As a second confirmation, data was analysed by multivariate linear regression, taking into account the intra-litter association of pups. Administration of Dex was found to predict a mean decrease in pup weight (mean decrease of 0.26g, $p<0.001$) and placental weight (mean decrease of 0.09g, $p<0.001$), independently of litter and litter size. Birth weight was also significantly reduced following Dex exposure ($p<0.001$). Linear regression predicted a mean decrease of 0.73g ($p<0.001$, Figure 5.8A).

F1 offspring weight was reduced in both females ($p<0.001$) and males ($p<0.001$) at weaning (Figure 5.8B) and in males at 90 days ($p<0.001$, Figure 5.8C). However, when accounting for inter-litter association by linear regression these differences were not significant. In the second generation, offspring of Dex-exposed males and control females (SD) were significantly lighter ($p<0.001$, Figure 5.9) than controls (SS). This was confirmed by multivariate linear regression (predicted decrease 0.94g, $p<0.001$).

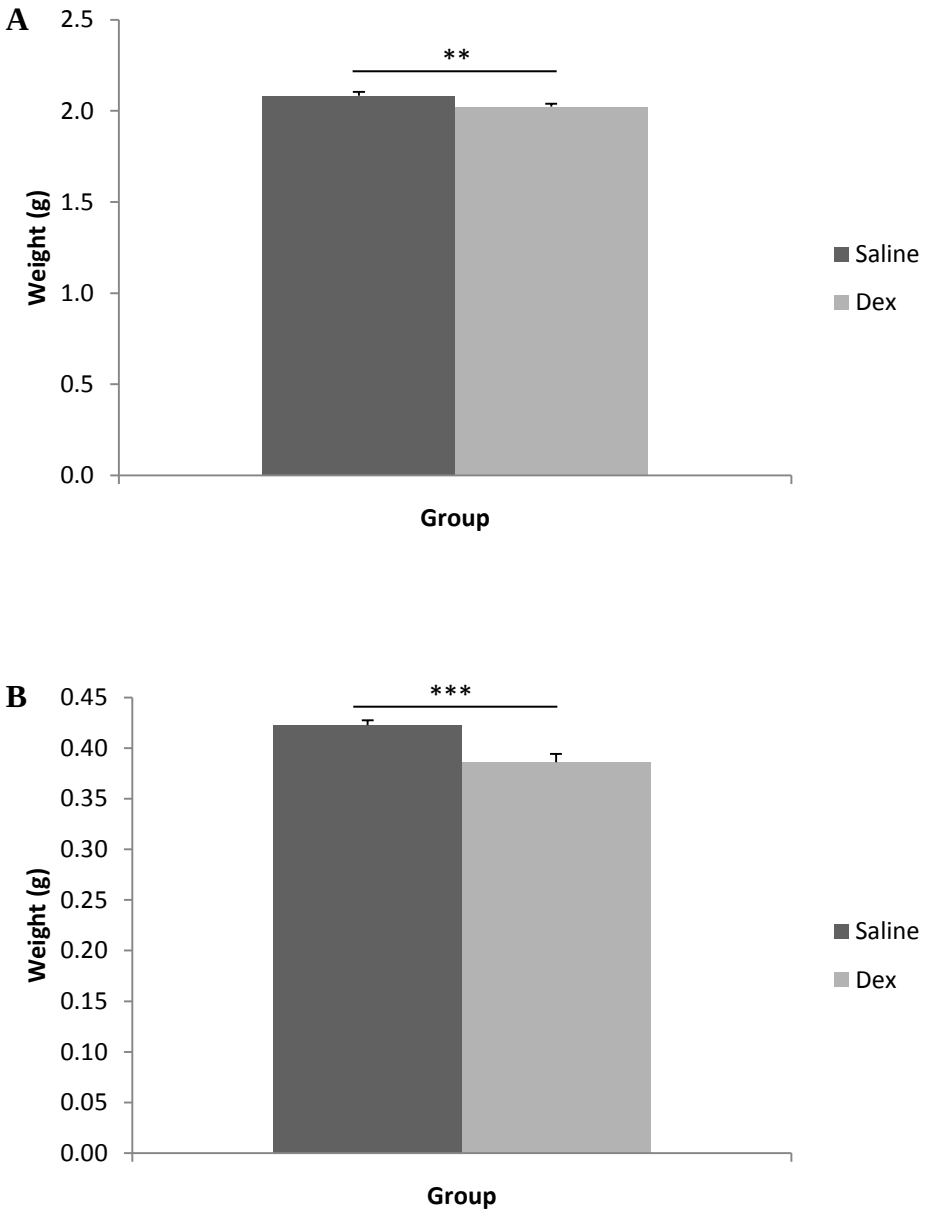

Figure 5.7. Mean pup and placental weight of F1 generation at e19.5. Pup weight (A) is decreased following Dex exposure, relative to controls (n=129 Saline, n=119 Dex, $p<0.01$). Placenta weight (B) is also decreased ($p<0.001$). Data was not normally distributed (Lilliefors $p<0.01$), and so analysed by Mann Whitney U test. Bars represent mean ± standard error. **$p<0.01$, ***$p<0.001$

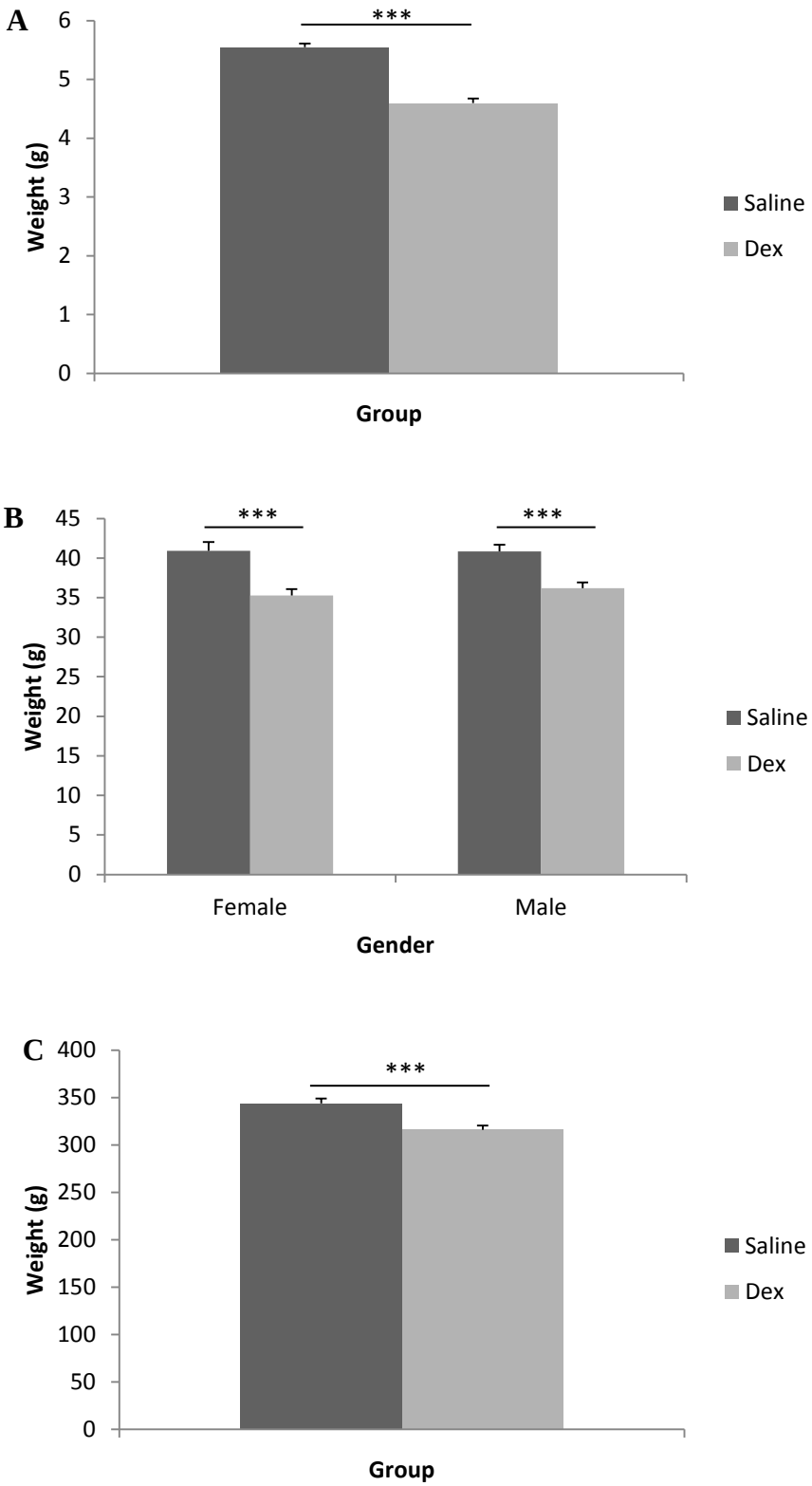

Figure 5.8. Mean weight of F1 GCS-EGFP offspring at birth, weaning and maturity. Birth weight (A) is decreased following Dex exposure, relative to controls (n=113 Saline, n=101 Dex, $p<0.001$). Weight was also decreased at weaning (B) in females (n=29 Saline, n=28 Dex, $p<0.001$) and males (n=33 Saline, n=32 Dex $p<0.001$) and in adult males (C) (n=16 Saline, n=24 Dex, $p<0.001$). Birth weight and male weaning weights were not normally distributed and so analysed by Mann Whitney U test. All other data were analysed by t-test. Bars represent mean ± standard error. ***$p<0.001$

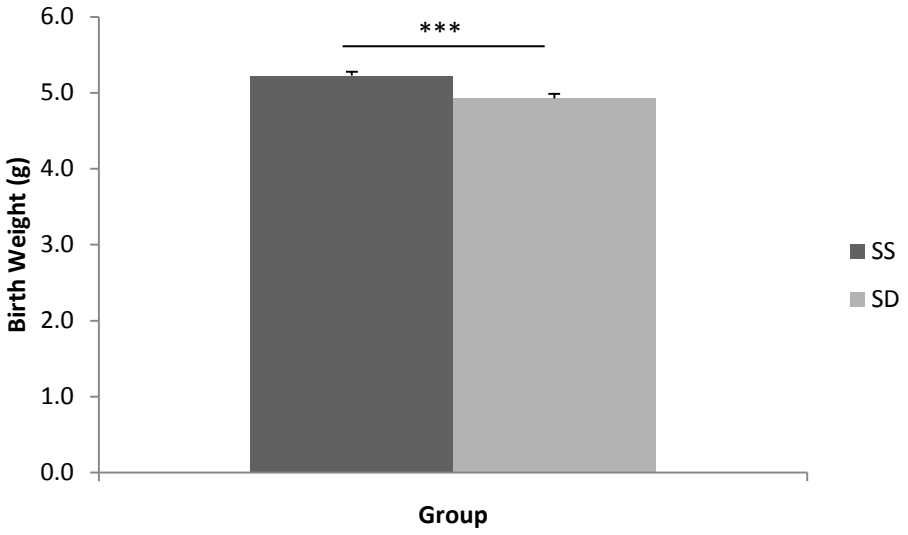

Figure 5.9. Mean weight of F2 GCS-EGFP offspring at birth. SS represents Saline mother crossed with Saline father (n=134), and SD denotes Saline mother with Dex father (n=135). The birth weight of SD pups was significantly reduced ($p<0.001$) compared to SS controls. Data was not normally distributed (Lilliefors $p<0.01$) and so analysed by Mann Whitney U test. Bars represent mean ± standard error. ***$p<0.001$

Glucose tolerance test data were not normally distributed (Lilliefors $p<0.01$ for insulin and $p<0.05$ for glucose at 30 min time-point), and so were log transformed, before performing a repeated measures ANOVA. Plasma glucose (Figure 5.10A) and insulin (Figure 5.10B) increased 30 min after glucose administration and returned to baseline after 120 min. There was no significant difference at any time-point ($p>0.05$) between Dex and Saline groups.

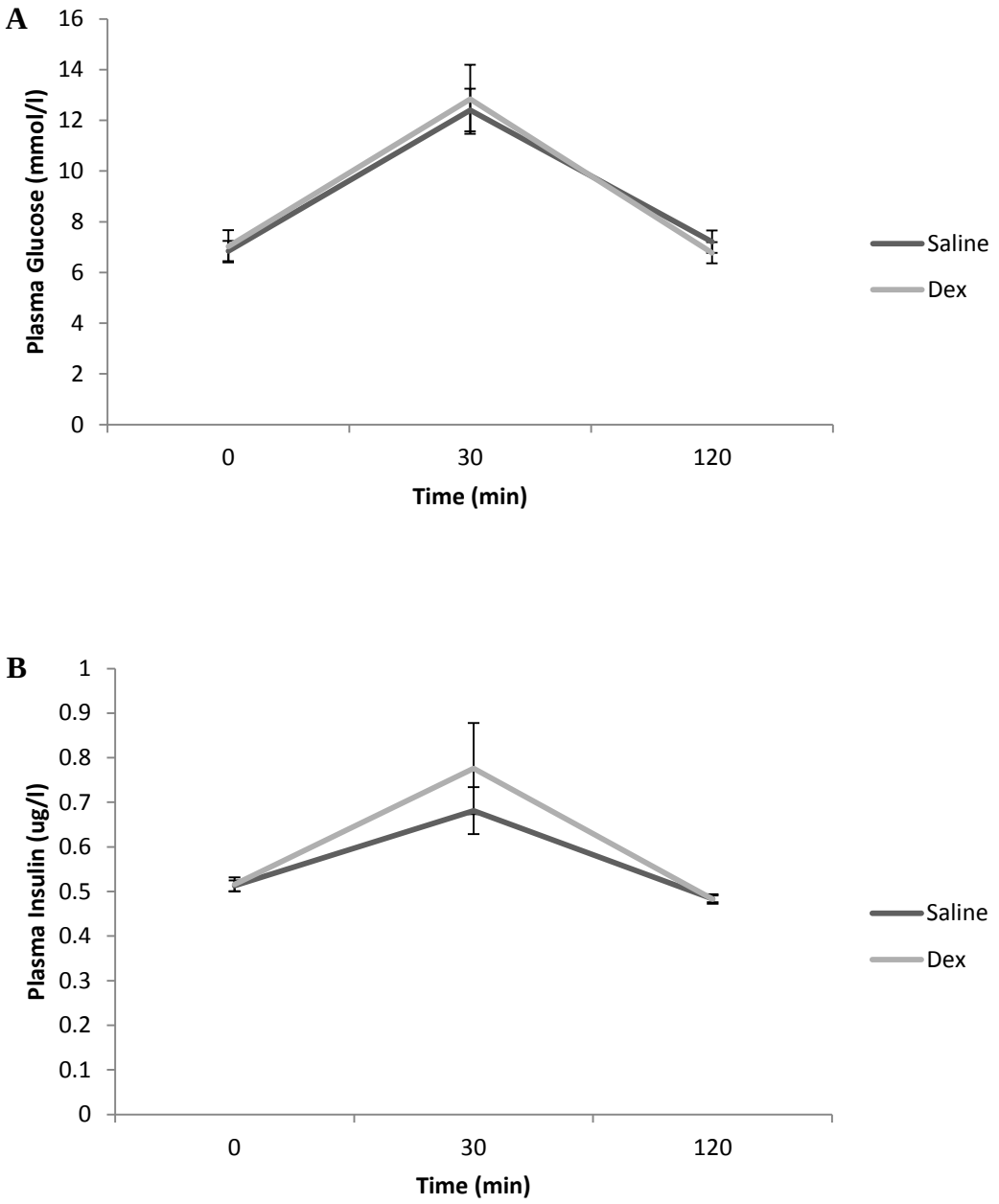

Figure 5.10. Plasma glucose and insulin levels following glucose tolerance tests. F1 Males at 90 days were taken through a glucose tolerance test, and blood taken before (Time 0) and 30 or 120 min after glucose administration. Data were not normally distributed (Lilliefors $p<0.01$ for insulin and $p<0.05$ for glucose at 30 min), and so were log transformed, before performing a repeated measures ANOVA. Plasma glucose (A) and insulin (B) had risen by 30 min and returned to baseline by 120 min. Glucose and insulin levels were not different between groups over the time-course ($p>0.05$). Values represent mean ± standard error.

5.3.2 Exploring the Effects of Dex on the Developing Germline

5.3.2.1 Descriptive Analyses of e19.5 Germ Cell ERRBS Data

Descriptive analyses of germ cell ERRBS data indicated that there was no global change in methylation between Dex and Saline samples. This was consistent both within and out with CpG islands (Pearsons R^2 values of 0.833 and 0.937 respectively) (Figure 5.11). The cytosines which were consistently differentially methylated across replicates between Dex and Saline samples were then analysed separately. Absolute difference in methylation score was calculated by subtracting the methylation score across Dex samples from that of the Saline samples, for the same DMC. The resulting value is presented as a degree of magnitude, without directionality. The vast majority (97%) of DMCs had absolute difference in methylation between Dex and Saline samples of 0.225 or less (Figure 5.12 A and B). The null hypothesis was that differentially methylated cytosines (DMCs) would show an even distribution between hyper- and hypomethylation. In DMCs with a difference of 0.225 or less between Dex and Saline groups there was a deviation from the null hypothesis. Thus there were consistently more hyper- rather than hypo-methylated DMCs with Dex exposure (Figure 5.12 A and B).

Germ cell DMCs were then grouped based on whether the corresponding e19.5 Saline liver cytosines showed high (>0.6), medium (0.5-0.6) or low (<0.5) methylation scores, with regards to ERRBS data from Chapter 6. When considering the DMCs with a difference in methylation between Dex and Saline samples of 0.225 or less; in DMCs with high corresponding liver methylation, there was a deviation from the null hypothesis, with a trend towards a predominance of hypermethylation (Figure 5.13); those with mid-range corresponding liver methylation showed little deviation from the null hypothesis (Figure 5.14); DMCs with low corresponding liver methylation deviated from the null hypothesis in the direction of hypomethylation (Figure 5.15). DMCs with a difference in methylation score of more than 0.225 showed little deviation from the null hypothesis across any of the liver methylation categories. The vast majority of germ cell DMCs were located out with CpG islands. DMCs within and out with CpG islands were consistently more hypermethylated across the majority of absolute difference categories (Figure 5.16).

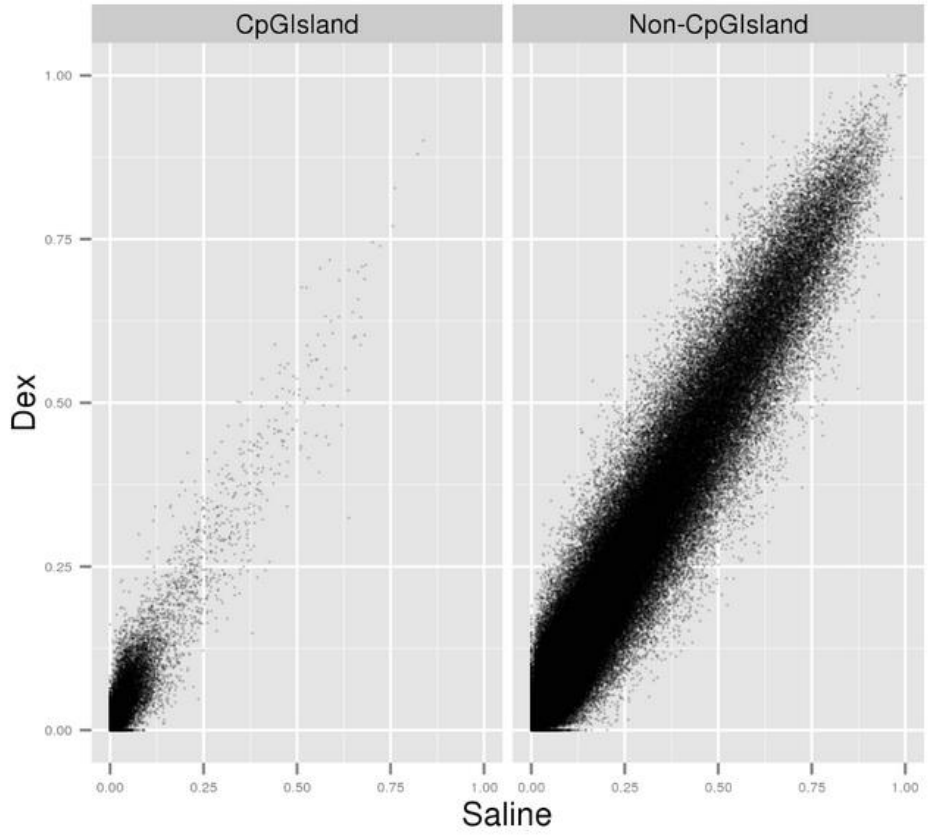

Figure 5.11. Methylation status of cytosines in Dex and Saline germ cell DNA. Each data point represents a single cytosine. The median methylation status across all reads from all samples (n=3 Dex and n=3 Saline) is given, based on 1 representing a methylated read, and 0 an unmethylated read aligning to that cytosine. Cytosines are separated into those within, and those out with CpG islands. Those with fewer than 10 repeats were excluded from the analysis.

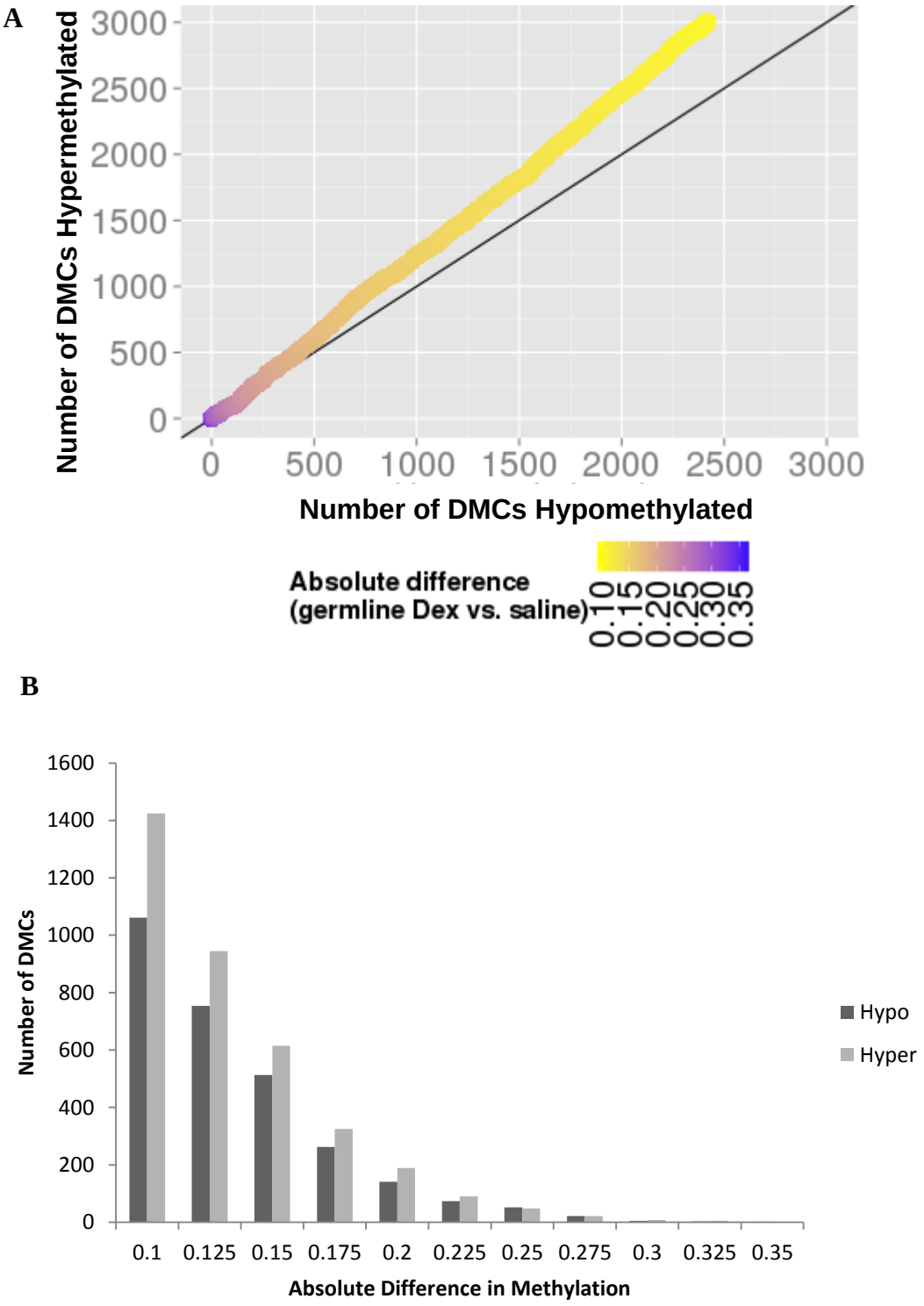

Figure 5.12. Hyper- and hypomethylation of cytosines differentially methylated between Dex and Saline germ cell DNA. DMCs consistent across all samples are plotted. Absolute difference in methylation is calculated by subtracting the methylation score across Dex samples from that for Saline samples. 97% of DMCs have an absolute difference of 0.225 or less. (A) DMCs are ranked by absolute difference between Dex and Saline samples, with yellow denoting the lowest (<0.10), and purple the highest (0.35) mean difference. The black line represents the null hypothesis, where there is no difference between hyper- and hypomethylation between DMCs. The distribution in these data therefore deviates from the null hypothesis, for DMCs with an absolute difference of 0.225 or less. (B) The number of hyper- and hypomethylated DMCs are plotted against ranges of absolute difference in methylation between Dex and Saline samples. Consistently more DMCs are hyper-methylated than hypo-methylated in Dex samples, across the majority of ranges of absolute difference.

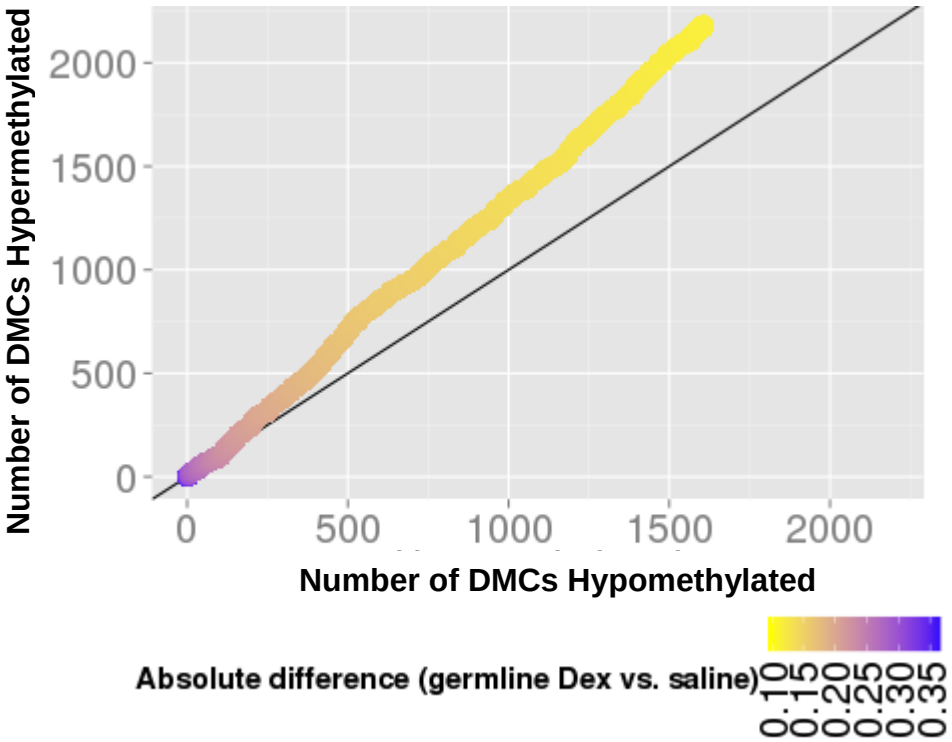

Figure 5.13. Count and absolute difference of cytosines differentially methylated in germ cell DNA and hypermethylated in control liver. Cytosines differentially methylated between Dex and Saline germ cell DNA and which exhibit high methylation (>0.6) in liver samples are plotted. Absolute difference in methylation is calculated by subtracting the germ cell DNA methylation score across Dex samples from that for Saline samples. Yellow denotes the lowest (<0.10), and purple the highest (0.35) mean difference. The black line represents the null hypothesis, where there is no difference between hyper- and hypo-methylation amongst DMCs. The distribution in these data therefore deviates from the null hypothesis, showing a shift towards hypermethylation, for DMCs with an absolute difference of 0.225 or less.

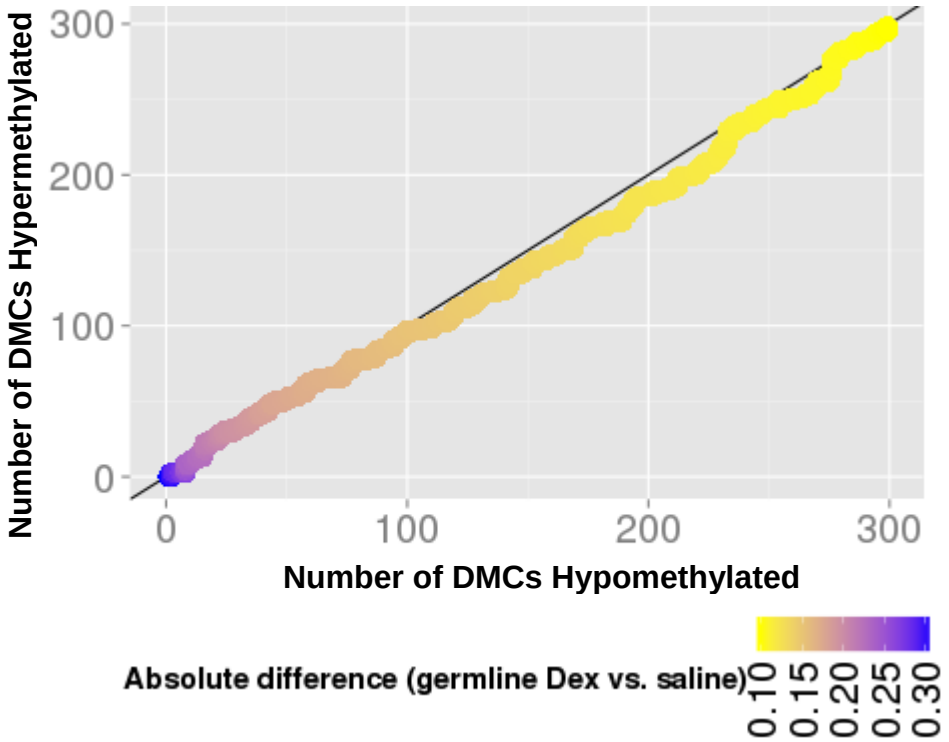

Figure 5.14. Count and absolute difference of cytosines differentially methylated in germ cell DNA exhibiting mid-level methylation in control liver. Cytosines differentially methylated between Dex and Saline germ cell DNA and which exhibit mid-level methylation (0.5-0.6) in liver samples are plotted. Absolute difference in methylation is calculated by subtracting the germ cell DNA methylation score across Dex samples from that for Saline samples. Yellow denotes the lowest (<0.10), and purple the highest (0.35) mean difference. The black line represents the null hypothesis, where there is no difference between hyper- and hypo-methylation between DMCs. The distribution in these data therefore is largely consistent with the null hypothesis.

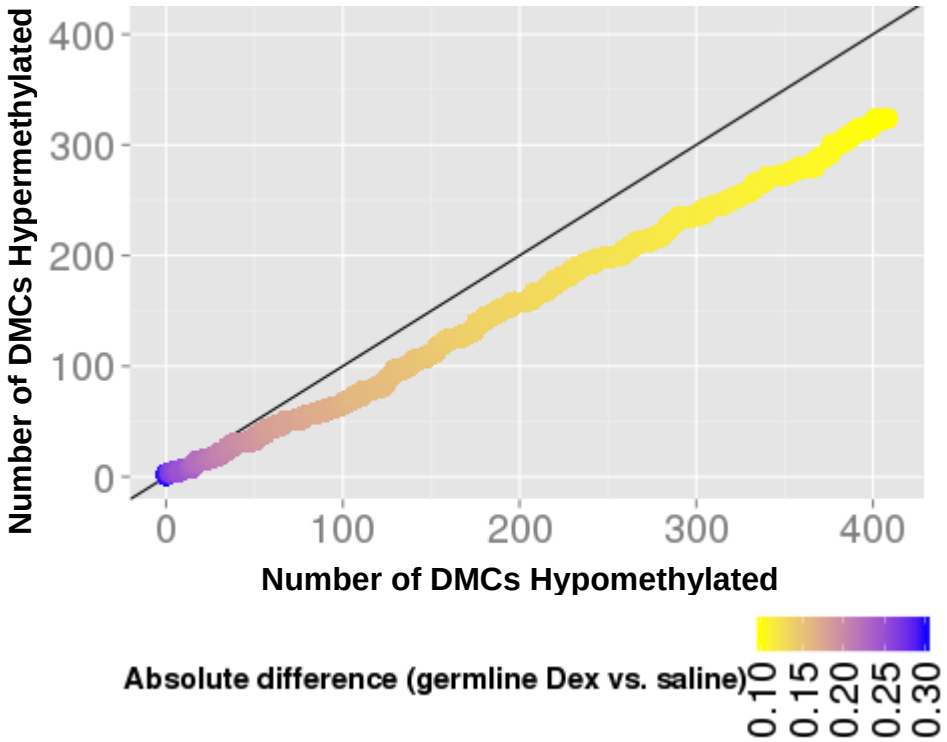

Figure 5.15. Count and absolute difference of cytosines differentially methylated in germ cell DNA exhibiting hypomethylation in control liver. Cytosines differentially methylated between Dex and Saline germ cell DNA and which exhibit low methylation (<0.5) in liver samples are plotted. Absolute difference in methylation is calculated by subtracting the germ cell DNA methylation score across Dex samples from that for Saline samples. Yellow denotes the lowest (<0.10), and purple the highest (0.35) mean difference. The black line represents the null hypothesis, where there is no difference between hyper- and hypo-methylation between DMCs. The distribution in these data therefore deviates from the null hypothesis, showing a shift towards hypomethylation, for DMCs with an absolute difference of 0.225 or less.

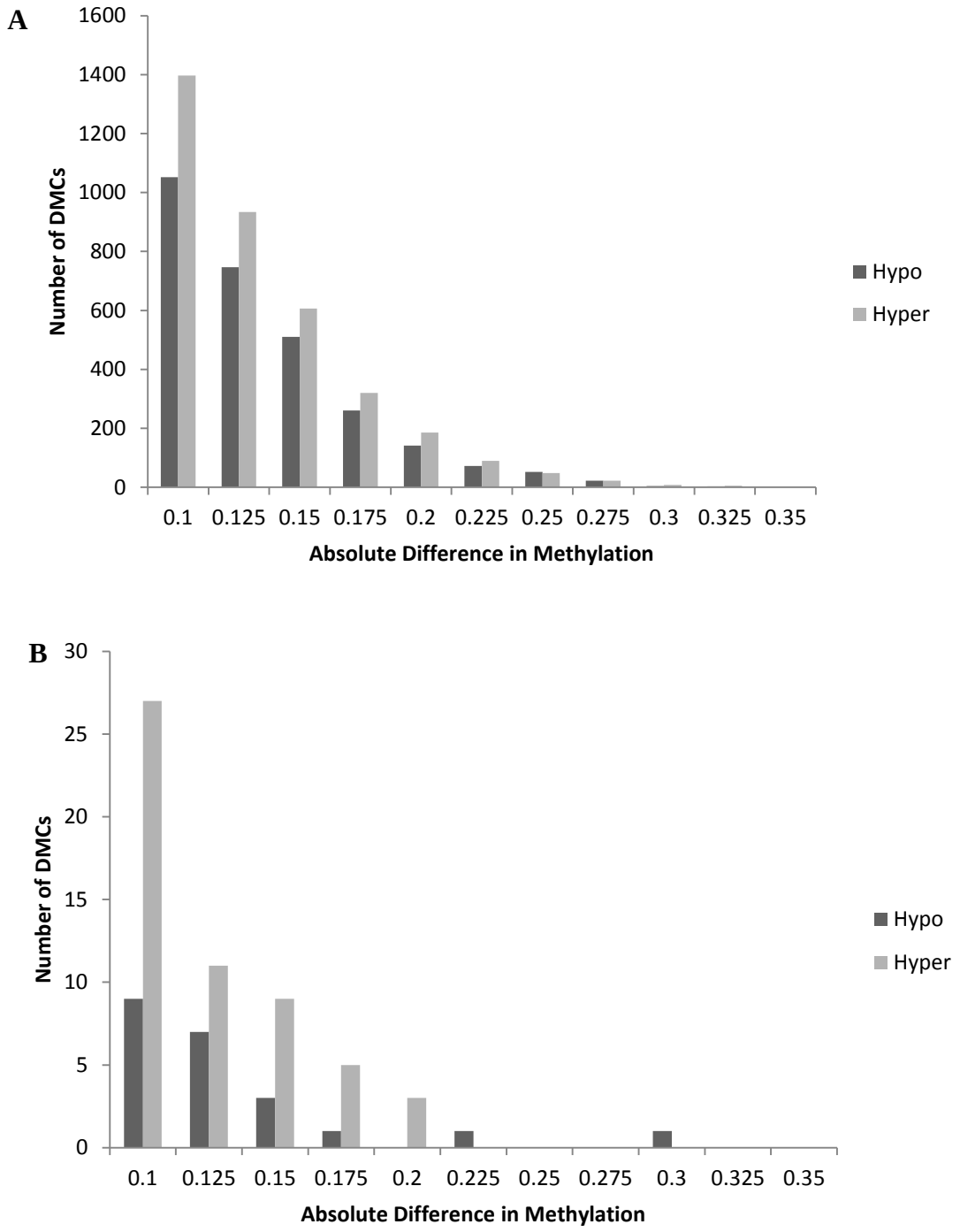

Figure 5.16. Distribution of germ cell DMCs across the genome. All cytosines which are consistently hyper- or hypo-methylated in Dex samples, relative to Saline controls are plotted. The number of hyper- and hypo-methylated cytosines are plotted against ranges of absolute difference in methylation between Dex and Saline samples. Consistently more DMCs are hypermethylated with Dex exposure both out with (A) and within (B) CpG islands. The total number of DMCs is greater out with than within CpG islands.

5.3.2.2 Biseq Analysis of e19.5 Germ Cell ERRBS Data

Biseq analysis indicated that there were 5 clusters with at least a 5% alteration in DNA methylation between Dex and Saline e19.5 germ cell samples, which were statistically significant (Table 5.1). Only one DMC (Chr6_540) was identified as having a statistically significant change in methylation of more than 10%. Methylation values represent the combined number of methylation positive (1, or 100%) and methylation negative (0, or 0%) reads across the 3 samples per treatment group. The difference in methylation between samples represents the combined methylation value for Saline samples minus that for Dex. All of the clusters corresponded to gene bodies, except Chr5_2393, which was located out with any annotated gene.

The greatest change in methylation was seen at Chr6_540, where there was a 12.2% increase in methylation with Dex exposure. An increase in methylation was also found in Chr5_2589 (7.5%), Chr5_2324 (6.2-6.3%) and Chr5_2393 (5.0-5.6%). A decrease in methylation of 5.0-6.3% was found in Chr3_2256, split across 5 DMCs.

Chromosome	Position	Cluster	Methylation difference	P Value
3	160647120	Chr3_2256	0.058	4.20E-09
	160647125		0.062	4.17E-11
	160647126		0.063	1.48E-10
	160647135		0.051	5.73E-20
	160647136		0.050	1.59E-13
5	163738989	Chr5_2324	-0.062	1.51E-21
	163738990		-0.063	4.71E-20
	165852600	Chr5_2393	-0.050	5.64E-22
	165852606		-0.054	9.61E-28
	165852611		-0.056	3.98E-18
	171668663	Chr5_2589	-0.075	1.72E-73
6	52306628	Chr6_540	-0.122	4.89E-34

Table 5.1. Biseq analysis of DMCs in F1 e19.5 germ cell DNA following Dex exposure. The position of cytosines differentially methylated between treatment groups is given in terms of chromosome (Chr), base position and cluster. The median methylation status across all reads from all samples (n=3 Dex and n=3 Saline) is given, based on 1 representing a methylated cytosine, and 0 an unmethylated cytosine. The difference in methylation represents the methylation status of the Saline group minus that of the Dex group. Positive values therefore indicate decreased methylation in Dex samples. Negative values indicate increased methylation with Dex exposure. Statistical analyses were performed using a Wald test.

5.4 Discussion

These data suggest that the GCS-EGFP rat is suitable for studying the effects of Dex programming on the male germline. EGFP expression was specific to the testis, and more specifically, the germline in males. Furthermore, immunofluorescence suggested that GCS-EGFP rats follow the same epigenetic reprogramming time-line as the Wistar rats used in previous studies. They also exhibited the characteristic programming phenotype of lower birth weight following *in utero* Dex exposure, and this was found to be transmitted through the male germline to the F2 generation. Using these rats for Dex programming studies suggested that there were no global changes in e19.5 germ cell DNA methylation as analysed by ERRBS. However DMCs identified consistently across all replicates were predominantly hypermethylated, indicating that premature remethylation may occur at a subset of cytosines with Dex exposure.

Immunofluorescence studies showed that whilst EGFP staining in adult heart, kidney, liver and spleen resembled that of the negative controls, the testis had a strongly positive detection. Furthermore, when the fetal testes of the subsequently established colony were examined under the microscope, immediately after dissection, they had a strong fluorescence. This indicated that that active EGFP was found specifically within the testes of these rats. The precise localisation of EGFP within the testis was initially explored using the Sertoli cell marker vimentin. As Sertoli cells are found within the seminiferous tubule, as for germ cells, I sought to confirm that they were not EGFP-positive, and would not therefore contaminate FACS sorted germ cell samples. Immunofluorescence with the vimentin antibody highlighted Sertoli cytoplasm, framing the nuclei. Little corresponding staining was found for EGFP, relative to the strongly positive germline cell nuclei. Upon FACS sorting of fetal testes, a very distinct population of EGFP-positive cells were visualised, not only confirming that EGFP expression was cell-specific within the testis, but indicating that a pure population of EGFP-positive cells could be isolated, with little contamination from EGFP-negative cells. A final confirmation that the cells expressing EGFP were germ cells was obtained by conducting qPCR on FACS sorted cells. The EGFP-positive cells had a significantly higher expression of the germ cell specific marker *Dazl*, than the EGFP-negative population, confirming that

this fraction consists of germ cells. Conversely the EGFP-negative population had a significantly higher expression of *Sox9*, confirming that the Sertoli cells were found within the EGFP-negative population.

This is in keeping with the results of Cronkhite *et al.* (2005), who produced the GCS-EGFP transgenic rat and supplied the founder males for the current project [92]. They show EGFP in sperm, testes and ovaries under the fluorescent microscope. This fluorescence was not visualised in the spleen, heart, liver, kidney or brain. qPCR also confirmed expression of EGFP in whole testis, epididymis and ovary, but expression in specific cells within each organ was not explored. They do, however, present images of EGFP co-staining with alkaline phosphatase, a marker of pluripotency, which can therefore identify fetal germ cells. This is, however, only shown for the epiblast and genital ridge stages during germ cell development, rather than the fetal or adult testis. Fluorescent *in situ* Hybridisation analysis (FISH), imaging the location of EGFP-specific antibody binding to isolated chromosomes, was performed on embryonic fibroblast DNA to try to identify the location of EGFP insertion in the rat genome [92]. This indicated that EGFP was inserted into chromosome 11 however the precise location or copy number of insertion was not identified [92]. The current study therefore confirms that the reported characteristics for fetal and adult testes are found within our colony. It also builds upon the work of Cronkhite *et al*. (2005) by confirming the germ cell-specific localisation of EGFP within the testis, both by immunofluorescence, and by qPCR.

Suitability of the GCS-EGFP rat for this study was further assessed in an initial comparison of their global epigenetic reprogramming time-line compared to Wistar rats. Immunofluorescence indicated that few germ cells were 5mC positive at e19.5 in both strains, however slightly more were visible in the Sprague Dawley compared to Wistar rat. As there was only 1 litter per time-point in this initial study, this could reflect a variation in exact time of implantation between the pups. However, as each germ cell identified by Propidium Iodide at e20.5 had a corresponding 5mC positive detection, it could be concluded that bulk global remethylation was occurring between e19.5-e20.5 in both strains, and therefore that they were following the same pattern of remethylation.

Further confirmation of the suitability of GCS-EGFP rats was obtained when exploring their response to *in utero* Dex exposure. A significant reduction in pup and placental weight at e19.5 and in birth weight was found following Dex treatment. This is in keeping with data from Wistar studies, both in Chapter 6 of this thesis, and in previous reports of both fetal [12] and birth weights [8,10]. Interestingly, this decrease remains at weaning in both sexes and at 90 days in males. This difference however is no longer significant if intra-litter differences are accounted for. Indeed Drake *et al*. (2005) and Nyirenda *et al*. (1998) report that Wistar pups from the Dex treatment groups exhibited 'catch up growth', with no difference in weight to controls at weaning or in adulthood. The GCS-EGFP cohort may therefore show the characteristic pattern of reduced F1 fetal and birth weight, with catch up growth.

I also sought to confirm that this phenotype would be transmitted to an F2 generation in GCS-EGFP rats. F2 pups bred from mothers exposed to Saline and fathers exposed to Dex *in utero* were significantly lighter than controls at birth, in keeping with previous studies in Wistar rats [10]. This indicates that the birth weight phenotype can be transmitted to a second generation through the male line, and therefore that it is relevant to study F1 germ cells and sperm in GCS-EGFP rats.

The phenotype of the GCS-EGFP programmed rat was further assessed by performing glucose tolerance tests in F1 males at 90 days. Plasma glucose and insulin levels were seen to rise at 30 min and return to baseline at 120 min after a glucose bolus. However there was no significant difference in response between Dex and Saline groups. This is in keeping with Drake *et al.* (2005) who found no difference in glucose or insulin response in F1 males at 6 months [10]. It is in contrast, however, with Nyirenda *et al.* (1998) who demonstrate an increase in both plasma glucose and insulin levels at 30 min following glucose load [8].

As the GCS-EGFP rats had germ cell-specific expression of EGFP, showed an intergenerational programming phenotype in response to Dex exposure, and preliminary analysis suggested that they had the same timescale for male fetal germ cell reprogramming, this strain was used for base-specific study of the germline. ERRBS of DNA from e19.5 male germ cells identified DMCs following Dex exposure, relative to Saline controls. A preliminary descriptive analysis of DMCs

was used to compare prevalence of hyper to hypo-methylation. Intriguingly, the majority of these DMCs were in the direction of hypermethylation with Dex exposure, found across a range of absolute differences in methylation between groups. This suggests there may be accelerated reprogramming of a subset of genes. To explore this possibility further, germ cell DMCs were split into three categories, dependant on the corresponding level of methylation in e19.5 control livers for that gene (based on the study conducted in Chapter 6). Intriguingly, when considering DMCs with an absolute difference of 0.225 or less, germ cell DMCs with highest liver methylation tended towards hypermethylation in Dex treatment and those with lowest liver methylation towards hypomethylation in germ cell DMCs. Thus, if we assume that methylation patterns are grossly consistent between fetal liver and germ cells, this suggests that Dex exposure may reprogram genes to their 'normal' state first. Clearly this is an imperfect comparison due to tissue specific differences in methylation profiles, however it allows preliminary conclusions can be drawn [280]. Further clarity would be achieved if the study was also conducted in germ cells from a later time-point (e20.5 or e21.5) to see if Dex exposure corresponds to a more 'mature' methylation profile at e19.5.

This prevalence of hypermethylation amongst DMCs was found both within and out with CpG islands. As CpG islands are predominantly unmethylated, it is not surprising that the majority of DMCs exist out with CpG islands [112]. However, in a previous study, CpG islands out with known transcription start sites were found to be more highly methylated, and it has been suggested that these might regulate as yet undetermined genes with particular relevance for development [112]. Thus DMCs within CpG islands, although infrequent, might be of particular relevance for further exploration.

Biseq analysis was then performed to identify which DMCs had a statistically significant difference in methylation between Dex and Saline groups, and whether these existed in clusters of DMCs within the same region. Significantly decreased methylation was identified at 5 DMCs in Chr3_2256, located within the Ral Guanosine Triphosphatase Activating Protein, Beta Subunit gene (*Ralgapb*). The corresponding protein represents the non-catalytic subunit of the RALGAP1 and

RALGAP2 complexes, which activate the RalA and RalB guanosine triphosphatases (GTPases) [281]. These GTPases exist in 2 states – their active guanosine triphosphate (GTP)-bound and inactive guanosine diphosphate (GDP)-bound forms. This alters their interaction with effector proteins and allows them to regulate cellular processes such as transcription, translation and cell survival [281]. Intriguingly Ral A has been shown to have a role in regulating glucose uptake in adipocytes in response to insulin [282,283]. Therefore, if decreased methylation of *Ralgapb* corresponded to increased gene expression, it is possible that this could have some, as yet undetermined, effect on insulin signalling.

Conversely, increased methylation was identified at Chr5_2324, corresponding to the Split Ends Family Transcriptional Repressor (*Spen*) gene. This hormone-inducible transcriptional repressor has been shown to have a role in developmental cell fate specification [284]. There are a range of proteins in the SPEN family, but all share a conserved SPEN paralog and ortholog C-terminal domain, which has been suggested to be responsible for transcriptional repression [285]. Knockout of the Msx2-Interacting Nuclear Target (MINT) protein, encoded by *Spen* in mice, was found to be embryonic lethal at e12.5-e14.5, with fetuses displaying liver, pancreas and heart abnormalities [286]. Therefore the correct regulation of the *Spen* gene may be important to development.

An increase in methylation (7.5%) was also found at Chr5_2589 in Dex-exposed germ cells. This DMC is located within the Period Circadian Clock 3 (*Per3*) gene, which is expressed in accordance with circadian rhythms. Published research predominantly focuses on the effects of polymorphisms in *Per3* in relation to disrupted sleep patterns. Intriguingly, however, these polymorphisms have been shown to have wider physiological effects, with for example, polymorphisms in *Per3* shown to associate with prognosis in patients with hepatocellular carcinoma [287]. Altered expression of *Per3*, irrespective of polymorphisms, has also been suggested to have physiological relevance, with decreased total mRNA expression of *Per3* found in hepatocellular carcinoma cells [288]. Further studies would be required to determine whether the change in methylation observed in our studies has an effect on expression of the *Per3* gene. Interestingly, a previous study suggests that Dex

exposure could influence the expression of circadian genes, with Dex found to increase the expression *Per3* in rat fibroblasts [289]. The related *Per1* gene was found to be upregulated in the livers of mice exposed to Dex postnatally [289].

The biggest increase in methylation was found at one cytosine in Chr6_540 (12.2%), corresponding to the Protein Disulphide Isomerase Family A Member 6 (*Pdia6*) gene. The PDIA6 protein exists in the endoplasmic reticulum and catalyses the formation and modification of disulfide bonds in proteins, and may have a role in protein folding [290]. PDIA6 has also been shown to have a role in maintaining calcium homeostasis within the endoplasmic reticulum [291].

Increased methylation was also seen across 3 DMCs at Chr5_2393, which does not correspond to an annotated gene. However, the closest known gene, found approximately 2880bp from the region, is Preferentially Expressed Antigen in Melanoma-like 1 (*Pramel1*). The Preferentially Expressed Antigen in Melanoma (*Prame*) gene family encodes leucine-rich repeat (LRR) proteins, which facilitate protein-protein interactions required in a range of cellular processes, such as cell adhesion, transcriptional regulation and signal transduction [292,293]. In the mouse, PRAMEL1 was identified solely in the testis, with mRNA and protein expression seen to increase postnatally. PRAMEL1 was subsequently identified in the acrosome of developing spermatids, suggesting that it might have a role in spermatogenesis and fertilisation [293]. As Chr5_2393 is located in relatively close proximity to *Pramel1*, it is possible that this represents a regulatory region for this gene, and altered methylation could ultimately influence the expression of the *Pramel1* gene.

For most of these targets it is unclear specifically what effects altered methylation, and thus potentially altered gene expression might have in the developing germline, and indeed in the next generation of pups, should these effects be carried in to the F2 generation. These changes should be validated by pyrosequencing and any corresponding effects on gene expression explored by qPCR, using primers for mRNA corresponding to the regions of differential DNA methylation. The longer term effects of these changes may also be explored by comparing to data from the ERRBS sperm study, which is pending. It should be considered that some of these sites of altered methylation correspond to changes at only one cytosine, therefore

caution should be exercised when inferring significant biological relevance. It should also be noted that many of the alterations represent relatively small changes in methylation between treatment groups, of 5-6%. This is still in keeping, however, with the liver studies in Drake *et al*. (2011), where there was a 5-6% change in methylation following Dex exposure [12]. Furthermore, previous studies report similarly modest alterations in DNA methylation with intra-uterine growth restriction [294], and variations of only 20% at the *Igf2* DMRs implicated in the growth restriction associated with Silver Russell Syndrome [295]. Thus subtle changes in DNA methylation may be expected in the Dex model, and in other examples of growth restriction, but these could potentially still have some relevance for development.

However the majority of CpGs are not differentially methylated between treatment groups, suggesting that there is not a global change in methylation at e19.5, as determined by ERRBS. This is in contrast to the immunofluorescence data in Chapter 4, which indicated that there is an increase in the number of 5mC positive germ cells at e19.5 following Dex exposure. There are a number of possible explanations for this discrepancy. The first is that ERRBS only interrogates a small portion of the genome, whereas immunofluorescence looks at the whole genome [278]. The enzymatic cleavage in ERRBS selects for CpG dinucleotides and so will capture the majority of promoters and CpG islands, but will not cover all sites of methylation throughout the genome [275]. The selection of longer MSP1 fragments in ERRBS enables capture of more regions out with CpG islands, however some DMCs will still be missed by ERRBS [278].

Differences in 5mC between treatment groups might also be missed by ERRBS as this bisulfite sequencing method cannot distinguish between 5mC and 5hmC [296]. Time-line studies in Chapters 3 and 4 indicated that little global 5hmC is detected in germ cells at e19.5 by immunofluorescence. However, as ERRBS by nature is more sensitive at detecting methylation at a base-specific level than immunofluorescence, and because the changes in methylation in this study are relatively modest (10-30%) it is possible that changes in 5hmC are making global changes in 5mC harder to detect. A major benefit in choosing ERRBS for these studies is that it can be

performed on low quantities of DNA (approximately 100ng), compared with the 5µg required for some other studies. As small quantities of DNA are obtained from FACS-sorted fetal germ cells (around 80ng per litter), this was a major consideration. ERRBS also focusses on CpG rich regions which are most likely to be methylated, reducing the cost of sequencing, whilst still giving relevant data [278]. However, further studies should also include a genome-wide technique which can distinguish between different forms of methylation. For example, Methylated DNA Immunoprecipitation (MeDIP) uses an antibody to isolate methylated DNA for subsequent sequencing [297]. An antibody specific to 5mC or 5hmC can therefore be used, distinguishing between these two forms of methylation.

It is also possible that the variation in global methylation results is due to the exact timing of fertilisation. Time-line data from Chapter 3 indicates that global remethylation is very time-specific, with the bulk occurring rapidly between e19.5 and e20.5. Although it appears that mating occurs shortly after the rats are paired (Drake *et al.*, unpublished observation), there will be variations in the exact time of fertilisation between mothers, and potentially, between different embryos in the same litter. This slight difference could impact upon the study, when global bulk global remethylation occurs rapidly. We tried to minimise this issue by performing ERRBS on 3 samples per group, each pools from 3 litters, giving 9 different litters per group. Indeed one pooled Dex sample was found to have greater global methylation than the others. Future studies could use *in vitro* fertilisation to ensure that the embryos have the same time of fertilisation, however, such intervention could potentially influence the results.

However, the main aim of experiments in Chapter 4 was to identify an interesting time-point for further study, and indeed an effect on a subset of genes was observed. These gene-specific changes will be validated by pyrosequencing, and corresponding gene expression analysed by qPCR.

It would also be informative to compare DMCs in fetal germ cells to that of mature sperm, which will be carried to the next generation. Although sperm samples were collected from F1 rats at 90 days, sequencing was unfortunately unsuccessful when DNA was first sent for RRBS (BaseClear, Belgium). The root of this issue was never

identified, however when trial sperm samples were sent to Weill Cornell for ERRBS, successful sequencing was achieved. This confirms that it is possible to perform ERRBS on these samples, but because of the delay caused by problems with the initial set of data, the full sperm study is still pending for ERRBS. Once conducted this should provide greater understanding of the relationship between alterations in germ cell methylation, and that of the resulting sperm in adulthood.

In summary these studies indicate that the GCS-EGFP rat has EGFP expression specifically in the germline, and that the global remethylation time-line and Dex programming phenotype is conserved with Wistar rats. FACS sorting of pure populations of fetal germ cells and performing ERRBS on the corresponding DNA revealed no global change in methylation between treatment groups. However of the DMCs, hypermethylation was predominant. Highly methylated genes in liver also had greater hypermethylation in fetal germ cell DMCs, whilst those of lowest methylation in the liver had prevalent hypomethylation. Taken together, this suggests that a subset of DMCs in fetal germ cells may undergo premature remethylation in association with Dex exposure. Biseq analysis indicated that clusters of statistically significant DMCs were found at *Ralgapb* and *Spen*, with significant increases of 7.5% and 12.2% found at single DMCs within the *Per3* and *Pdia6* genes respectively. Validation of these results by pyrosequencing, and an exploration of the corresponding effects on mRNA expression has yet to be performed. Pending ERRBS of sperm will also indicate whether this corresponds to DMCs in sperm, and whether these changes are likely to be transmissible to the next generation.

Chapter 6 Effects of Dex on the Liver

6.1 Introduction

As my data indicate that Dex exposure may shift the period of DNA remethylation in epigenetic reprogramming, I decided to explore what other pathways and processes may be influenced. I also sought to further compare the influence of Dex in the traditional Wistar rat programming model to that in the GCS-EGFP rat. Liver was chosen as a key organ for these studies because it is a critical regulator of metabolism [298]. Furthermore, a microarray had been performed on liver tissue from a previous programming study in the Drake lab, but had yet to be validated, giving some direction to a candidate gene approach.

Virgin Wistar females were mated with Wistar males and pregnant dams subsequently sacrificed at e20.5, and liver collected from the fetuses. I then explored gene expression in these samples, seeking firstly to examine the expression of metabolism and growth genes in the liver in response to Dex exposure, and secondly to compare gene expression in this cohort to that of previous studies. I then compared gene expression in GCS-EGFP rats to that of the Wistar cohort.

6.1.1 Glucocorticoid Regulation and Imprinted Genes

Expression of GR, the receptor through which Dex acts, was examined. Previous work indicated that the expression of *Gr* mRNA was increased at PND5 and in adulthood in the livers of F1 rats exposed to Dex *in utero* [8]. Conversely, there was no effect on *Gr* mRNA levels in liver of the Dex programmed marmoset at 24 months [75]. This indicates that altered GR expression could have relevance for the Dex programming phenotype, in a species-specific manner. Furthermore, *Gr* mRNA expression was explored in a maternal protein restriction programming model, which confers reduced birth weight and increased blood pressure in offspring from 5 weeks [299]. *Gr* mRNA expression was reported to increase in a variety of tissues, including liver, kidney and hypothalamus. This not only supports the findings of Nyirenda *et al.* (1998), but indicates that the effects on *Gr* may not necessarily be restricted to the liver. Indeed, increased glucocorticoid levels have been shown to

alter *Gr* mRNA expression in rat brains in a region-specific manner, ultimately producing more anxiety-based behaviour [300]. An increase in *Gr* mRNA expression may mediate some of the effects of Dex through its action in regulating gene expression, such as increased *Pepck* mRNA expression, first exhibited at PND5, and persistent at 8 months [8]. *Gr* mRNA expression was therefore explored because of its potential relevance in programming and development, and to provide a comparison between the current and previous cohorts.

11β-HSD1, which converts inactive glucocorticoids to their active forms (cortisone to cortisol in humans, and 11-dehydrocorticosterone to corticosterone in rodents) was then studied, as it is key in regulating the actions of glucocorticoids [41,42]. Nyirenda *et al*. (1998) show that the expression of this enzyme is not altered at PND5 or in adulthood in the liver of F1 in the Dex programming model, but fetal expression was not reported [8]. However, the authors subsequently identified an increase in the expression (at 4 and 12 months) and activity (at 12 months) of 11β-HSD1 in the liver of Dex-programmed marmosets [75]. Hepatic *11β-Hsd1* overexpression correlates with insulin resistance and hypertension in mice [301], whilst knockout mice have improved insulin sensitivity and glucose tolerance [302]. Indeed lower hepatic *11β-Hsd1* mRNA expression and enzyme activity is found in obesity, which may be a compensatory mechanism, protecting against insulin resistance [303,304]. This relevance for insulin sensitivity, regulating glucocorticoid levels and its previously identified upregulation in the Dex programming of non-human primates made it an interesting candidate gene for study.

I then explored expression of imprinted genes involved in growth and development. Imprinted genes have monoallelic expression in accordance with the parent of origin, are involved in the regulation of fetal and placental growth, and their DNA methylation is retained during zygote reprogramming [305,306]. They therefore represent suitable candidates for intergenerational inheritance of disease risk [12]. *Igf2* is a paternally imprinted gene which promotes fetal growth [307,308]. Conversely, *Cdkn1c* and *Grb10* are maternally expressed, and restrict fetal growth [305,306,309]. Drake *et al*. (2011) show an increase in the expression of these genes in F1 fetal liver at e20.0 following Dex exposure. The expression of *H19*, which is

adjacent to *Igf2* and proposed as a regulator of *Igf2* expression, was also increased [12,310,311]. The expression of these genes was therefore studied in the current cohort because they are suitable candidates for contributing to the programming phenotype, and to compare gene expression to previous work.

6.1.2 Microarray Genes

An Illumina Gene Expression Microarray was previously performed on e20.0 F1 Wistar liver tissue in the Dex programming model by the Wellcome Trust Clinical Research Facility, Edinburgh, with additional analysis by Khulan Batbayar, The University of Edinburgh. This allowed the expression of a large array of genes to be examined in parallel in Dex and control samples. A number of genes were highlighted which might be differently expressed between treatment and control groups, but required validation by qPCR. I selected some of the novel genes highlighted in the microarray for study in my cohort. Those with particular relevance for growth, development and reproduction were chosen for validation. For example, Alcohol Dehydrogenase 1 (*Adh1*) is involved in the conversion of vitamin A into its active derivatives, which in turn have many key roles in development [312,313]. Vitamin A deficiency in pregnant rats correlates with abnormal development of hindbrain in e12.5 fetuses, and fetal reabsorption by e18.5 or neonatal death [314]. Vitamin A excess has also been found to be teratogenic, correlated in particular with abnormal brain development [315]. It is therefore important that Vitamin A metabolism is correctly regulated. The ADH1 enzyme is also expressed in both the fetal and adult testis [312,316], with castration of male rats corresponding to an increased activity of liver ADH1 [317] . Its role in both fetal development and testicular function made it an interesting candidate for study in my project.

The microarray also indicated decreased expression of High Mobility Group Box 2 mRNA (*Hmgb2*) with Dex treatment. This is thought to have roles in transcriptional regulation, DNA repair and cellular differentiation [318]. HMGB2 is capable of bending DNA, thus facilitating the formation of nucleoprotein complexes [319], and inhibition of its function by RNA competition leads to a disruption of the cell cycle

[320]. A Dex-mediated change in *Hmgb2* could therefore affect chromatin compaction and repair in the developing fetus.

Gelsolin is characteristically known as an actin binding protein which helps to regulate the assembly and organisation of actin filaments [321]. Increased *Gelsolin* expression is associated with increased pathological remodelling of the heart after acute injury from myocardial infarction and heart failure, potentially through the promotion of DNAse1-mediated apoptosis [322]. Intriguingly, protein levels of Gelsolin were found to be increased in the adipose tissue of obesity-prone rats exposed to high fat diet, and the authors proposed it as a novel marker of obesity [323]. Furthermore, *Gelsolin* knockdown in adipocyte cells was associated with increased expression of the pro-inflammatory genes Tumour Necrosis Factor Alpha (*Tnfα*) and Interleukin 6 (*Il6*) [324]. This may be linked to increased *Tnfα* and *Il6* mediated lipolysis, ultimately resulting in lower triglyceride content, and therefore lower risk of heart disease [324,325]. Furthermore, Gelsolin may also have a role within the epididymis, regulating the actin cytoskeleton of sperm, and their subsequent uptake of calcium [326]. Therefore a Dex-induced alteration in *Gelsolin* expression may impede sperm maturation.

The Heat Shock 70kDa Protein 5 (*Hspa5*) gene encodes for the protein 5 of the 70kDa Heat Shock Protein (*Hsp70*) molecular chaperone family. This member facilitates the translocation of proteins into the endoplasmic reticulum, and their correct folding within [327]. As *Hspa5* knockout mice die at e3.5 due to an inhibition of cellular proliferation and increased apoptosis, a Dex-mediated alteration in this protein may result in dysregulation of cellular development [328].

Translationally-Controlled Tumour Protein (TPT1) acts as a key regulator of the p53 tumour suppressor, and of cancer stem cells [329]. It has also been implicated in fetal growth and development, with *Tpt1* knockout mice having increased apoptosis, reduced cell numbers and mortality at e9.5-e10.5 [330]. This indicates that *Tpt1* is essential for normal fetal development. Some research in drosophila has indicated that TPT1 may also be involved in growth regulation through an indirect interaction with the Mammalian Target of Rapamycin (mTOR) signalling pathway [331]. This pathway can be regulated by growth factors, stress and nutrient intake, and therefore *Tpt1* was an

interesting target for the programming model [332]. It has also been shown to be expressed in fetal germ cells and adult spermatogonia [333], and so could also be a target for germline studies.

6.1.3 Insulin Signalling Pathway Genes

The microarray also indicated increased expression of Insulin-Like Growth Factor Binding Protein 1 (*Igfbp1*). The Insulin-Like Binding Protein (IGFBP) family bind Insulin-like Growth Factors (IGF) 1 and 2 and therefore regulate their activity [334]. IGFBP1 is predominantly expressed in the liver, and binds IGFI [334,335]. Insulin down-regulates production of hepatic IGFBP1 protein, and in longitudinal studies decreased circulating IGFBP1 protein concentrations were correlated with subsequent glucose intolerance and diabetes [336,337]. Furthermore low fasting plasma IGFBP1 levels were correlated with increased cardiovascular disease risk factors, such as high blood pressure and blood triglyceride concentration [338]. Increased IGFBP1 in amniotic fluid is also associated with lower birth weight in humans [339], and expression was increased in the placentas of fetuses with intra-uterine growth restriction [340]. As these studies indicate that IGFBP1 regulates the action of the IGF1 growth factor, and is correlated with risk of diabetes and cardiovascular disease, this was an interesting target in the Dex programming model, characterised by low birth weight and subsequent cardiometabolic disease risk.

As an increase in *Igfbp1* expression with Dex exposure was indicated on the microarray, I went on to explore the expression of the serine 6 kinases, which form part of the insulin signalling pathway (see Figure 6.1). These kinases are activated by insulin-like growth factors and nutrients, and are involved in regulating transcription, through the formation of a protein synthesis pre-initiation complex [341,342]. As part of this process the RPS6 kinases phosphorylate serine 6 (RPS6) of small ribosomal subunits [342]. It also has other targets such as the Insulin Receptor Substrate 1 (IRS1) protein, which may be implicated in insulin resistance [343]. Knockout of *Rps6k1* in mice blunts responsiveness to IGF1 [342], and was shown to protect against a loss of insulin sensitivity in ageing, and to increase lifespan [344]. It also protects insulin sensitivity in mice fed a high-fat diet, potentially through

downregulation of the negative feedback loop through IRS1 [345]. Indeed therapeutic inhibition by antisense RNA in rats corresponded to decreased weight gain and food consumption, improved insulin sensitivity and a dose-dependent increase in hepatic *Igfbp1* expression [346].

A second isoform of the serine 6 kinase (RPS6K2) works with RPS6K1 to phosphorylate RPS6 [347]. Specific knockouts of *Rps6k1* or *Rps6k2* have a different phenotype, with the *Rps6k1* knockouts being significantly lighter both prenatally and postnatally, than wild-type controls, whilst *Rps6k2* weight was unaffected [347]. However, double knockouts exhibit perinatal lethality, and both isoforms appear to be required for full phosphorylation of RPS6, with potentially a more significant contribution from RPS6K2 [347].

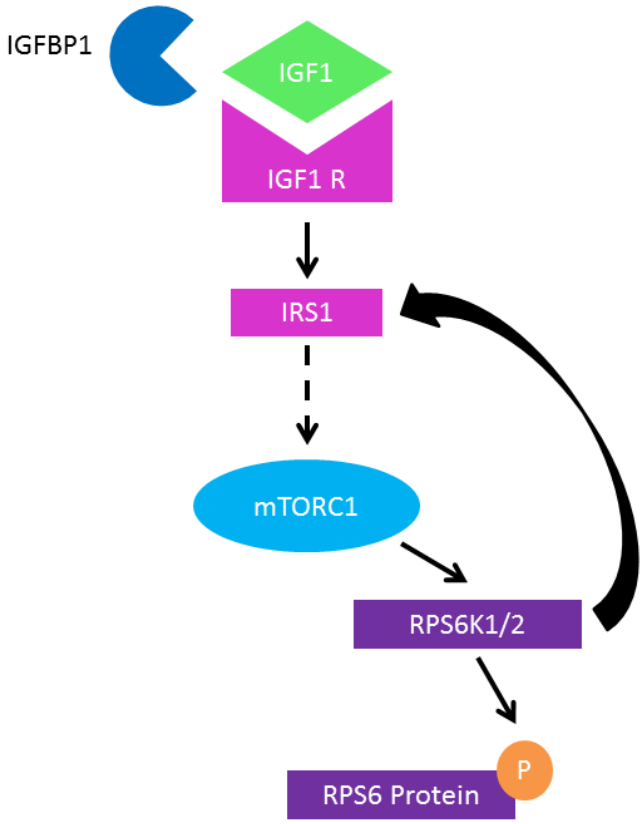

Figure 6.1. Summary of IGF1 signalling through RPS6K1. IGFBP1 competes with the IGF1 receptor (IGF1R) for interaction with IGFs [335]. Upon ligand binding, the IGF1R can interact with the Insulin Receptor Substrate 1 (IRS1) protein, which it phosphorylates [348]. This ultimately stimulates the Mammalian Target of Rapamycin C1 (mTORC1) signalling pathway [342,349]. This promotes the activity of Serine 6 Kinases 1 and 2 (RPS6K1/2) which both negatively regulate IRS1 [343], and phosphorylate the serine 6 (RPS6) ribosomal protein, ultimately promoting protein synthesis [347].

6.1.4 Exploring Gene Expression in GCS-EGFP Dex Programmed Rats

In order to confirm whether the gene changes seen in Wistar rats were conserved in GCS-EGFP rats, liver tissues collected during the F1 e19.5 germ cell study in Chapter 5 were also examined. The time-point of collection was different between the 2 strains, as I collected the Wistar tissues at the start of my PhD, and the e20.0 time-point had previously been shown to correspond to changes in pup weight and the expression of some key genes [12]. After the completion of the Wistar tissue collections, I identified the e19.5 time-point for interest in epigenetic reprogramming, and liver tissue was collected along with germ cells. Although the time-points therefore differ slightly between the 2 strains, a comparison of gene expression in fetal liver was nevertheless still likely to be informative. Therefore the expression of genes studied in the Wistar rat, as outlined above was also explored in GCS-EGFP fetal liver.

6.1.5 Exploring DNA Methylation in Liver of Dex Programmed GCS-EGFP Rats

Further understanding of the effects of Dex treatment on gene regulation in the liver was gained by studying DNA methylation. Some research has suggested that Dex programming may alter DNA methylation in the liver, with Drake *et al*. (2011) reporting a decrease in methylation at a DMR of *Igf2* in F1 liver at e20.0. An interaction of maternal and paternal Dex exposure was also found to decrease methylation at the *H19* Imprinting Control Region (ICR) in F2 e20.0 liver [12]. These were identified using a candidate rather than genome-wide approach. Glucocorticoid exposure also decreased DNA methylation of the tyrosine aminotransferase gene, involved in hepatic tyrosine metabolism, persistent in cultured rat liver cells even 3 months after exposure [267]. Maternal protein restriction was also reported to reduce methylation at the promoter of *Gr* in F1 and F2 adult rat liver [350,351]. However caution should be exercised when interpreting these studies as subsequent lab data has repeatedly indicated that the *Gr* promoter is unmethylated (Drake *et al*., unpublished data). Because DNA methylation may contribute to the regulation of gene expression directly or indirectly [352,353] these alterations could lead to changes in gene expression and ultimately have detrimental

consequences, or compensatory benefits for the programmed pup. To better understand the effects of Dex exposure on DNA methylation in the liver, I sought to identify additional sites of differential methylation, adopting a genome-wide, rather than candidate-gene approach. ERRBS was used to give a genome-wide view of specific cytosines that are differentially methylated following Dex exposure, as in Chapter 5. GCS-EGFP rats were chosen for this study, so that data could be compared with that for germline ERRBS studies.

6.2 Materials and Methods

Virgin female Wistar rats were timed-mated with stock Wistar males, and injected daily with either Dex (100µg/kg body mass) suspended in 0.9% Saline, or an equivalent volume of Saline from e15.5 until termination. Pregnant dams were sacrificed at e20.5, and all pups and placentas removed and weighed. Liver was collected from 6 pups per litter and snap frozen. Tissue was subsequently genotyped for the *Sry* gene, as outlined in Chapter 2.6.1, to identify the male pups. Livers from e19.5 GCS-EGFP rats were collected and snap frozen during the fetal germ cell study outlined in Chapter 5. They were not genotyped for *Sry*, as tissue was collected after testis isolation, and therefore the sex of the animal was known.

RNA from all samples was extracted as outlined in Chapter 2.11.3. Reverse Transcription and qPCR was then performed using the protocols outlined in Chapter 2.11.5 and 2.12 respectively.

RNA extraction from F1 e20.5 Wistar livers was performed by a masters student, Marina Mitsikakou (Centre for Reproductive Health, The University of Edinburgh), under my training and supervision. She also conducted qPCR for *H19*, *Cdkn1c* and *Igfbp1* in F1 Wistar tissues. I performed qPCR for all other genes, and extracted RNA from F1 e19.5 GCS-EGFP livers, collected in Chapter 5. I then conducted reverse transcription and qPCR on these samples, as previously. Normality of data distribution was confirmed using the Lilliefors test. Normally distributed data ($p>0.05$) was analysed by Student's t-test, and nonparametric data by Mann Whitney U test. Birth weight was analysed by both Student's t-test, as in previous studies,

and by multivariate linear regression, accounting for the intra-litter association of pups.

I also extracted DNA from F1 e19.5 GCS-EGFP livers, as outlined in Chapter 2.14.1. ERRBS was performed at Weill Cornell University Epigenetics Core, New York, USA. Bioinformatic analysis was then conducted by Dr Thomas Smith (CGAT, University of Oxford, UK).

6.3 Results

6.3.1 Effects of Dex on F1 Wistar Liver

Pup and placental weight was normally distributed (Lilliefors test $p>0.05$) and data were therefore analysed by t-test, as in previous studies [10,12]. Dex-exposure corresponded to a decrease in pup ($p<0.01$, Figure 6.2A) and placental ($p<0.001$, Figure 6.2B) weight. As a second confirmation, data was analysed by multivariate linear regression, taking into account the intra-litter association of pups. The administration of Dex was found to predict a mean decrease in pup weight (mean decrease of 0.38g, $p<0.001$) and placental weight (mean decrease of 0.07g, $p<0.01$), independently of litter and litter size.

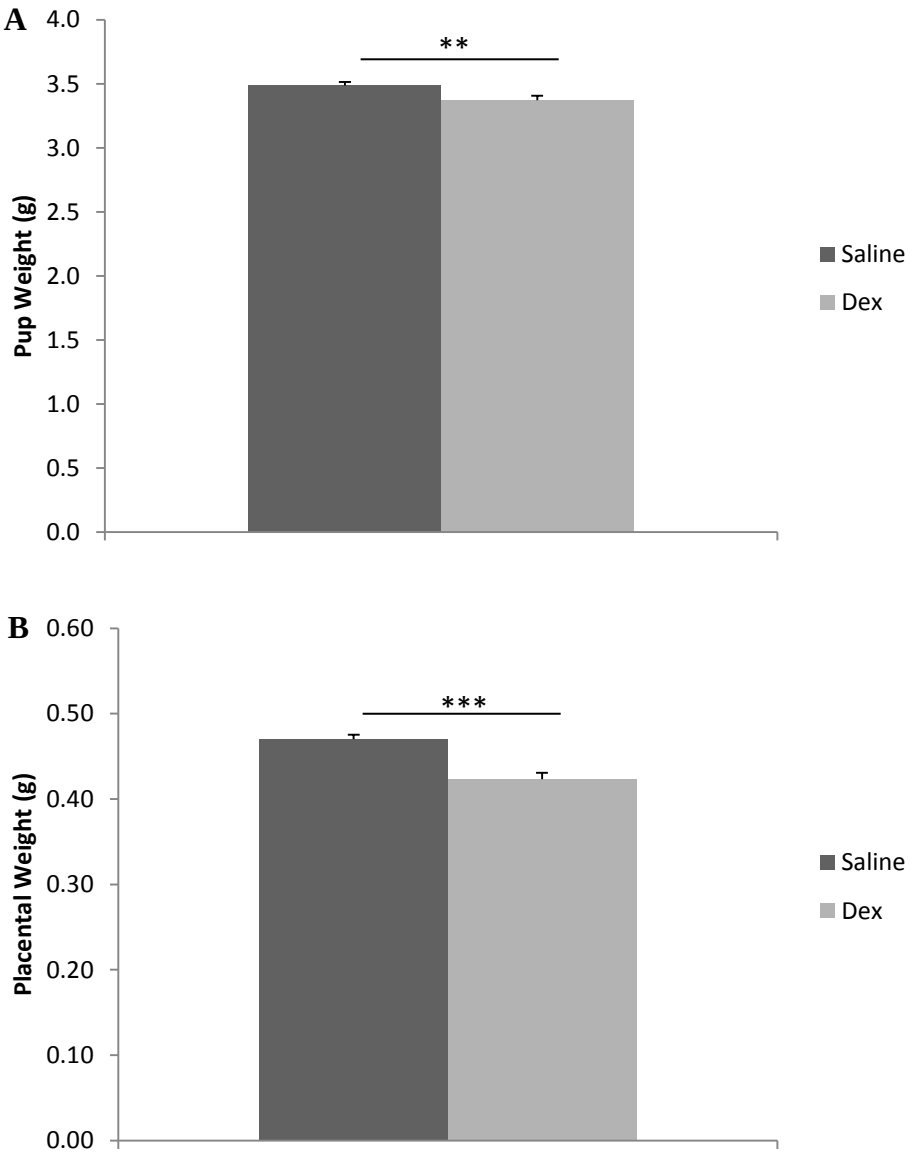

Figure 6.2. Mean pup and placenta weight of F1 Wistar rats at e20.5. Pup weight (A) was decreased following Dex exposure, relative to controls (n=112 Saline, n=87 Dex from 7 litters per group, $p<0.01$). Placental weight (B) was also decreased ($p<0.001$). Data was normally distributed ($p>0.05$) and analysed by t-test. Bars represent mean ± standard error. **$p<0.01$, ***$p<0.001$

6.3.1.1 Effects on Glucocorticoid Regulation and Imprinted Genes

The effects of Dex exposure on fetal liver gene expression in the F1 offspring were then explored by qPCR. Gene expression is expressed relative to the mean of TATA-Binding Protein (*Tbp*) and Hypoxanthine Guanine Phosphoribosyl Transferase (*Hprt*) for each sample. *Gr* expression was significantly increased ($p<0.01$) following Dex exposure in F1 liver at e20.5 (Figure 6.3). Conversely *11β-Hsd1* expression was not significantly altered between groups. The expression of *Igf2*, *H19*, *Cdkn1C* and *Grb10* was not significantly altered with Dex exposure ($p>0.05$, Figure 6.3).

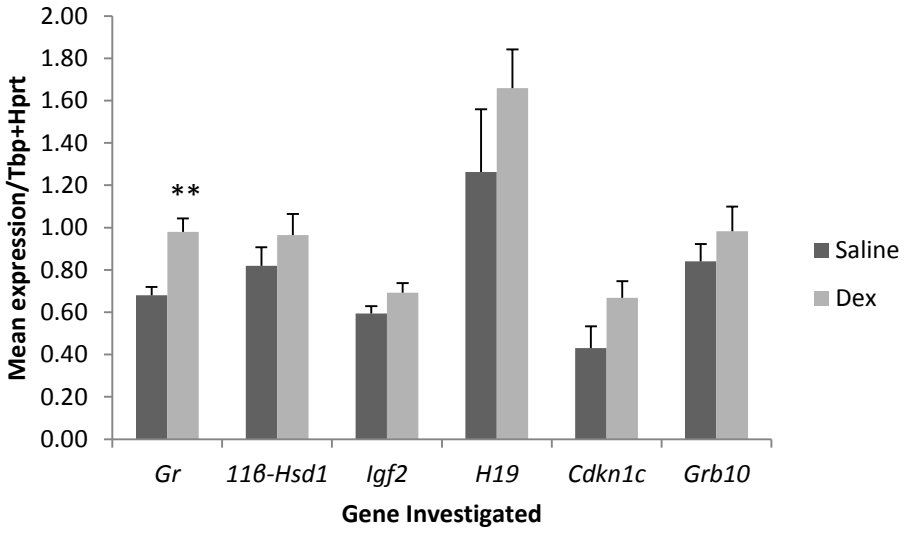

Figure 6.3. Expression of glucocorticoid regulation and imprinted genes in F1 Wistar male rat liver at e20.5. Gene expression is expressed relative to the mean of *Tbp* and *Hprt*. Mean expression of *Gr* was increased ($p<0.01$) at e20.5 following Dex exposure, relative to Saline controls. Each sample was from a male in a different litter. N=7 (for Saline and Dex samples). Data were analysed by t-test for all genes, except for *Grb10* which was not normally distributed ($p<0.01$). A Mann-Whitney U test was therefore performed. Bars represent mean ± standard error. ** $p<0.01$.

6.3.1.2 Effects on Array Genes

The expression of *Adh1* ($p<0.001$) and *Tpt1* ($p<0.01$) was significantly increased in e20.5 liver following Dex exposure (Figure 6.4). The expression of *Hmgb2*, *Gelsolin* and *Hspa5* were not significantly different between groups. All data was normally distributed ($p>0.05$) and therefore analysed by t-test.

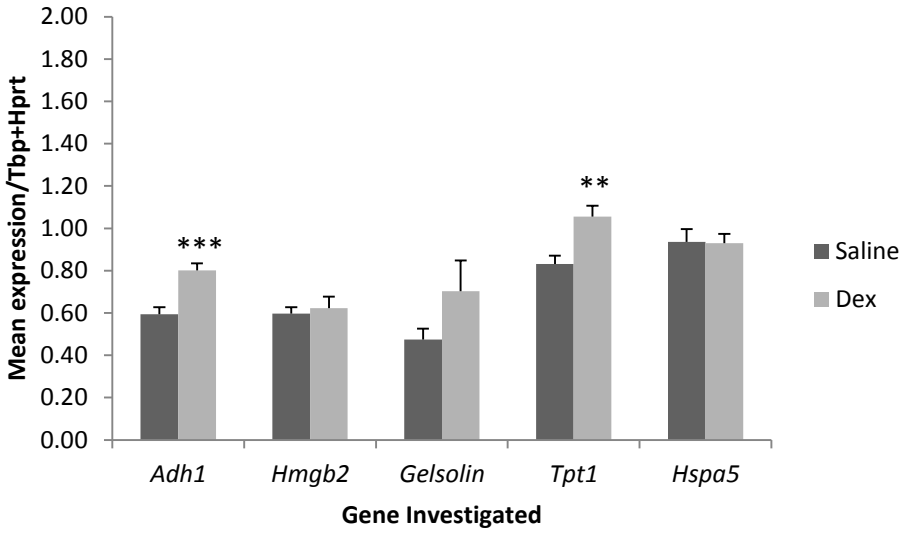

Figure 6.4. Expression of microarray genes in F1 Wistar male rat liver at e20.5. Gene expression is expressed relative to the mean of *Tbp* and *Hprt*. Mean expression was increased for *Adh1* ($p<0.001$) and *Tpt1* ($p<0.01$) at e20.5 following Dex exposure, relative to Saline controls. Each sample was from a male in a different litter. N=7 (for Saline and Dex samples). Data were analysed by t-test for all genes. Bars represent mean ± standard error. ** $p<0.01$, *** $p<0.001$.

6.3.1.3 Insulin Signalling Pathway

Igfbp1 was significantly increased ($p<0.01$) with Dex treatment (Figure 6.5). Conversely, expression of *Rps6k1* was significantly decreased ($p<0.001$) in Dex liver, whilst expression of isoform 2 (*Rps6k2*) and mRNA corresponding to the protein which these kinases act upon (*Rps6*) was not altered with treatment.

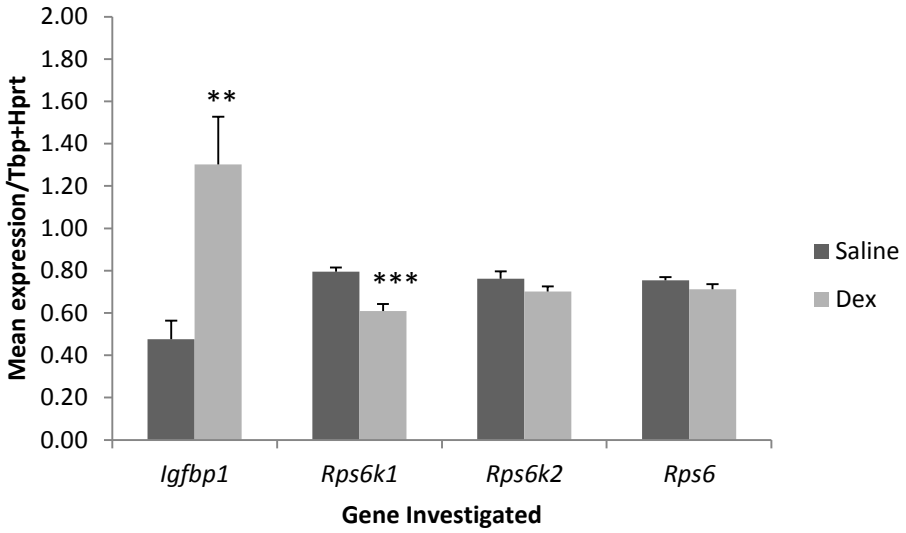

Figure 6.5. Expression of insulin signalling pathway genes in F1 Wistar male rat liver at e20.5. Gene expression is expressed relative to the mean of *Tbp* and *Hprt*. Mean expression was increased for *Igfbp1* ($p<0.01$) and decreased for *Rps6k1* ($p<0.001$) at e20.5 following Dex exposure, relative to Saline controls. Each sample was from a male in a different litter. N=7 Saline and 7 Dex. Data were analysed by t-test for all genes. Bars represent mean ± standard error. ** $p<0.01$, *** $p<0.001$.

6.3.2 Effects of Dex on F1 GCS-EGFP Sprague Dawley Liver Gene Expression

Gene expression in the F1 GCS-EGFP livers at e19.5 was investigated, to explore whether the liver phenotype was similar to that for the Wistar rat, used in previous studies. Pup and placental weights were found to be significantly reduced with Dex exposure ($p<0.01$ and $p<0.001$ respectively) in this cohort, as reported in Chapter 5.3.1.2.

6.3.2.1 Effects on Glucocorticoid Regulation and Imprinted Genes

Expression of *Gr* and *11β-Hsd1* was not altered with Dex treatment. However the expression of imprinted genes *H19* ($p<0.01$), *Cdkn1c* ($p<0.01$) and *Grb10* ($p<0.05$) was significantly increased in Dex-exposed pups (Figure 6.6). The expression of *Igf2* was not altered between groups.

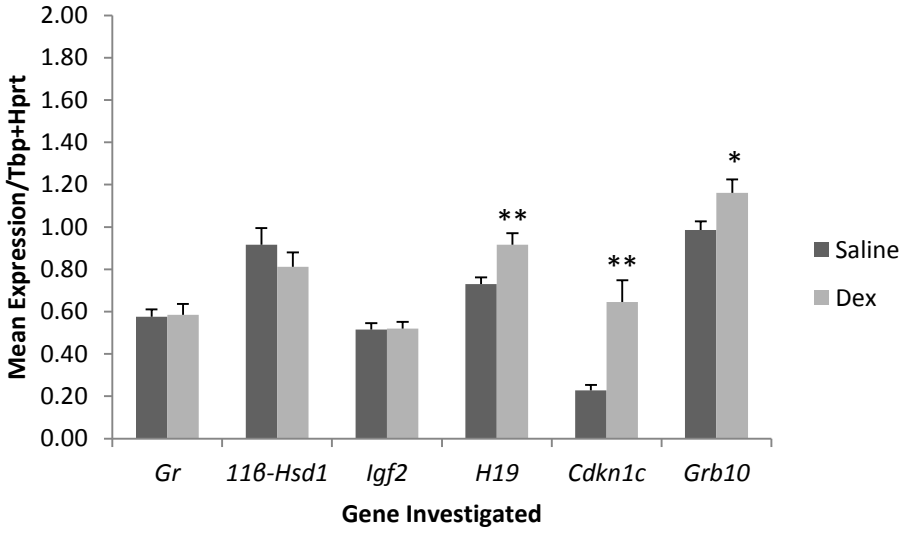

Figure 6.6. Expression of growth and imprinted genes in F1 GCS-EGFP male rat liver at e19.5. Gene expression is expressed relative to the mean of *Tbp* and *Hprt*. Mean expression was increased for *H19* ($p<0.01$), *Cdkn1c* ($p<0.01$) and *Grb10* ($p<0.05$) at e19.5 following Dex exposure, relative to Saline controls. N=9 (for Saline and Dex samples). Data were analysed by t-test for all genes, except for *Cdkn1c*, for which a Mann-Whitney U test was performed. Bars represent mean ± standard error. * $p<0.05$, ** $p<0.01$.

6.3.2.2 Effects on Array Genes

Expression of *Adh1* was increased ($p<0.05$) and *Hmgb2* and *Gelsolin* decreased ($p<0.05$ and $p<0.001$ respectively) with Dex exposure (Figure 6.7). *Tpt1* and *Hspa5* gene expression was not significantly altered between treatment groups. All data were normally distributed and analysed by t-test, except for *Adh1*, for which a Mann-Whitney U test was used.

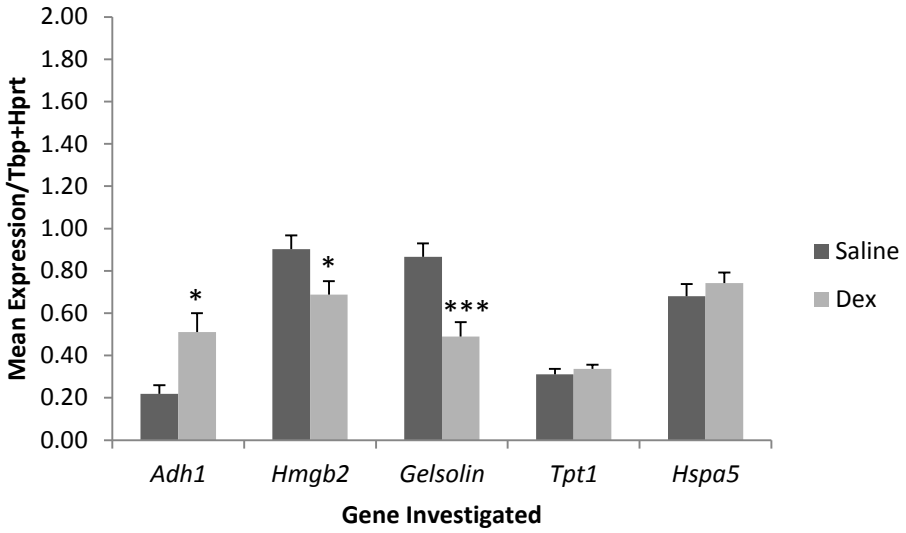

Figure 6.7. Expression of microarray genes in F1 GCS-EGFP male rat liver at e19.5. Gene expression is expressed relative to the mean of *Tbp* and *Hprt*. Mean expression was increased for *Adh1* ($p<0.05$), and decreased for *Hmgb2* ($p<0.05$) and *Gelsolin* ($p<0.001$) at e19.5 following Dex exposure, relative to Saline controls. N=9 (for Saline and Dex samples). Data were analysed by t-test for all genes, except for *Adh1*, for which a Mann-Whitney U test was performed. Bars represent mean ± standard error. * $p<0.05$, *** $p<0.001$.

6.3.2.3 Effects on Insulin Signalling Pathway Genes

As for the Wistar cohort, *Igfbp1*, found by microarray to be increased in Dex-exposed pups, was studied. An increase in *Igfbp1* expression ($p<0.001$) with Dex treatment was also seen in the livers of F1 GCS-EGFP rats at e19.5 (Figure 6.8). As in Wistar rats, the expression of *Rps6k1*, downstream of *Igfbp1* in the insulin signalling pathway, was decreased ($p<0.05$) in the Dex group, relative to Saline controls. Decreased expression was also found for the second isoform, *Rps6k2* ($p<0.05$). mRNA corresponding to the protein which RPS6K1 and 2 act upon (RPS6) was not significantly altered between treatment groups.

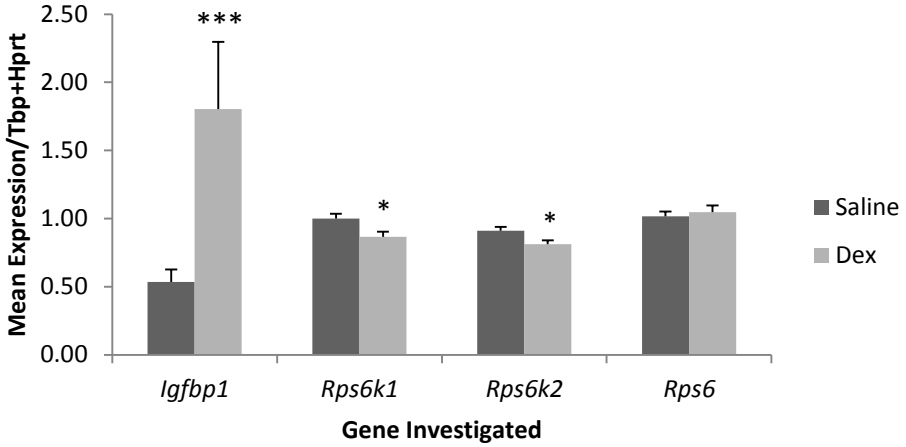

Figure 6.8. Expression of insulin signalling pathway genes in F1 GCS-EGFP male rat liver at e19.5. Gene expression is expressed relative to the mean of *Tbp* and *Hprt*. Mean expression was increased for *Igfbp1* ($p<0.001$), and decreased for *Rps6k1* ($p<0.05$) and *Rps6k2* ($p<0.05$) at e19.5 following Dex exposure, relative to Saline controls. N=9 (for Saline and Dex samples). Data were analysed by t-test for all genes, except for *Igfbp1* which was not normally distributed ($p<0.01$). A Mann-Whitney U test was therefore performed. Bars represent mean ± standard error. *$p<0.05$, *** $p<0.001$.

6.3.3 Summary of Gene Expression Results

Table 6.1 summarises the expression data for Wistar and GCS-EGFP rats, indicating whether expression was increased, decreased or unaltered with Dex treatment, relative to controls.

Gene	Expression in Wistar (e20.5)	Expression in GCS-EGFP (e19.5)	Previous Data
Gr	↑	=	↑ At PND5 – Nyirenda *et al*. (1998)
11β-Hsd1	=	=	= At PND5 – Nyirenda *et al*. (1998)
Igf2	=	=	↑ At e20.0 – Drake *et al*. (2011)
H19	=	↑	
Cdkn1c	=	↑	
Grb10	=	↑	
Adh1	↑	↑	↑ Microarray data
Hmgb2	=	⇣	⇣ Microarray data
Gelsolin	=	⇣	⇣ Microarray data
Tpt1	↑	=	⇣ Microarray data
Hspa5	=	=	↑ Microarray data
Igfbp1	↑	↑	↑ Microarray data
Rps6k1	⇣	⇣	Unknown
Rps6k2	=	⇣	Unknown
Rps6	=	=	Unknown

Table 6.1. Summary of gene expression data for F1 fetal liver in Dex programming model. Gene expression for Dex-exposed pups is shown relative to Saline controls. Expression in Wistar cohort (e20.5), GCS-EGFP cohort (e19.5) and previous studies is shown. Dex exposure corresponds to increased (upward arrow), decreased (downward dotted arrow) or unaltered (equals sign) gene expression relative to controls, based on a minimum of $p<0.05$ by t-test or Mann-Whitney U test. Blue font indicates a consistent pattern of expression between strains. All previous studies were conducted in Wistar rats.

6.3.4 Effects on GCS-EGFP DNA Methylation (ERRBS)

DNA methylation was explored at a nucleotide level in liver DNA from F1 e19.5 GCS-EGFP rats, and was highly correlated between Dex and Saline samples, both within and out with CpG islands (Pearsons R^2 values of 0.976 and 0.960 respectively) (Figure 6.9). Biseq analysis identified 9 gene clusters which had significantly different methylation scores following Dex exposure (Table 6.2), however only 2 clusters, on Chromosome 13 and 20 had a difference in methylation reads of greater than 10%. Methylation values represent the combined number of methylation positive (1) and methylation negative (0) reads across the 3 samples per treatment group.

Two clusters were identified within gene bodies – cluster 787 on chromosome 5 (denoted as Chr5_787) and cluster 284 on chromosome 7 (Chr7_284). For Chr5_787, Dex exposure gave a decrease in methylation of 6-7% methylation at 5 DMCs. At Chr7_284, 2 CpGs had a decrease in methylation of 6.2%. The greatest decreases were identified in the Dex-exposed group for Chr13_572 (12.8-13.2%) and Chr20_254 (16.6-20.2%).

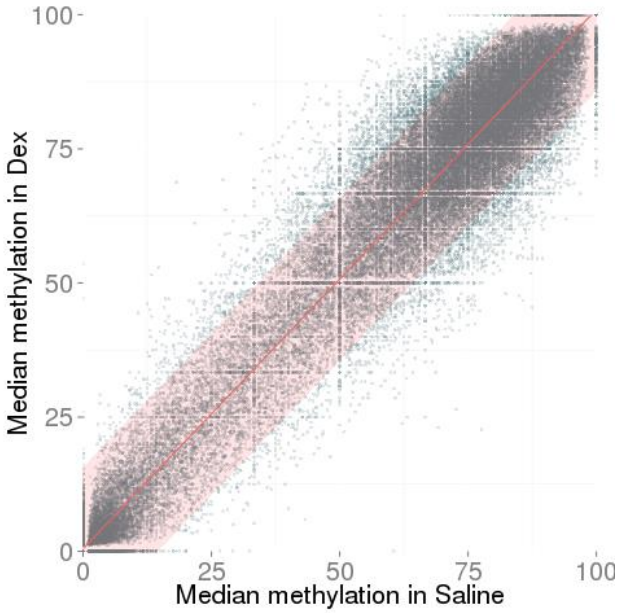

Figure 6.9. Median methylation status of cytosines in Dex and Saline liver DNA. Each data point represents a single cytosine. The median methylation status across all reads from all samples (n=3 Dex and n=3 Saline) is given, based on 100 representing a methylated read, and 0 an unmethylated read aligning to that cytosine. Cytosines with fewer than 10 repeats were excluded from the analysis. The red line indicates the linear regression of the data, and red shading the 99% prediction interval.

Chromosome	Position	Cluster	Methylation Difference	P Value
13	113187574	Chr13_572	0.132	5.92E-10
	113187590		0.128	6.71E-06
	113187591		0.128	1.21E-05
15	41652431	Chr15_282	0.052	1.11E-05
	41652434		0.051	2.12E-06
	41652435		0.051	8.90E-07
1	615737	Chr1_2	0.072	1.17E-06
	615738		0.071	1.44E-06
	615752		0.063	3.18E-06
20	10270585	Chr20_254	0.166	2.94E-08
	10270586		0.169	3.31E-08
	10270614		0.202	6.60E-16
2	115122141	Chr2_413	0.053	1.23E-05
	115122142		0.054	7.62E-06
	115122143		0.054	4.49E-06
	115122153		0.058	1.69E-08
	115122154		0.058	2.57E-08
5	144350967	Chr5_787	0.066	1.36E-12
	144350984		0.063	1.41E-07
	144350985		0.063	2.75E-07
	144350991		0.062	6.61E-06
	144350992		0.062	1.03E-05
7	13047749	Chr7_284	0.062	1.36E-22
	13047750		0.062	1.39E-24
8	117513326	Chr8_1000	0.050	1.35E-14
9	6514490	Chr9_10	0.093	8.39E-06
	6514491		0.093	8.43E-06

Table 6.2. DMCs in F1 e19.5 liver DNA following Dex exposure. The position of CpGs differentially methylated between treatment groups is given in terms of chromosome (Chr), base position and cluster. The median methylation status across all reads from all samples (n=3 Dex and n=3 Saline) is given, based on 1 representing a methylated cytosine, and 0 an unmethylated cytosine. The difference in methylation represents the methylation status of the Saline group minus that of the Dex group. Positive values therefore indicate decreased methylation in Dex samples. Statistical analyses were performed using a Wald test.

6.4 Discussion

These data indicate that Dex exposure *in utero* alters the expression of several genes across multiple pathways in fetal liver. Some of the genes had been previously researched, allowing comparison with previous cohorts. Other candidate genes were novel targets, explored to give a greater understanding of the effects of Dex on the developing fetus. Dex treatment affected gene expression in both wild-type Wistar and GCS-EGFP Sprague Dawley rats, with some changes exhibited in both strains, whilst others appeared to be strain-specific.

Expression of *Gr* was increased in Wistar rat liver at e20.5 following Dex exposure (see Table 6.1). This is in keeping with previous studies which show that the expression of *Gr* in the liver is increased at PND5 and in adulthood following in utero Dex exposure in rats [8,354]. It is also in keeping with studies that found an increase in *Gr* expression at e20.0 liver following maternal protein restriction [299]. Such an increase in *Gr* expression may mediate the effects of Dex, for example the increased *Pepck* mRNA expression, first exhibited at PND5, and persistent at 8 months, through its action in regulating gene transcription [8]. Indeed *Gr* expression has been shown to be increased in the skeletal muscle of type II diabetes patients, compared to controls, with *Gr* expression levels inversely correlated with insulin sensitivity [355]. Furthermore, administration of the insulin sensitising agent metformin abolished an increase in *Gr* with Dex programming [354].

Conversely the expression of *Gr* was not altered with Dex in the GCS-EGFP cohort, bearing similarity to the studies in Dex programmed marmosets [75]. This may represent a strain-specific difference in response to Dex. For example, strain of mouse was shown to influence the phenotype of an *11β-Hsd1* knockout [356]. This variation could also be due to the difference in time-point between GCS-EGFP (e19.5) and Wistar (e20.5) tissues. As previous studies have explored the relationship between prenatal Dex exposure and *Gr* expression postnatally [8], it is possible that a change in *Gr* expression is not established until e20.5. Indeed, the expression of *Gr* normally increases in late gestation [38], so a Dex-induced change in *Gr* expression might not be visible until later time-points.

The expression of *11β-Hsd1*, involved in the activation of corticosterone was unaltered between Dex and Saline groups in both Wistar and GCS-EGFP rats. This is in keeping with previous studies which found no change in the hepatic expression of this enzyme at PND5 or in adulthood [8]. It does however confirm a difference in response to Dex programming between rats and marmosets, where increased hepatic 11β-HSD1 was observed postnatally [75].

An increase in expression was also seen in the imprinted genes *H19, Cdkn1c* and *Grb10* in the GCS-EGFP, but not Wistar cohort (see Table 6.1). This discrepancy is likely to result from the difference in time-point between cohorts, rather than strain differences, because Drake *et al*. (2011) report an increase in the expression of these genes in Wistar rats at e20.0 [12]. Indeed, previous data indicates that fetal liver gene expression can change rapidly, within a day of gestation (Drake *et al*., unpublished data). It is fitting that *Cdkn1c* and *Grb10*, which restrict fetal growth [305,309], should be increased in the Dex model, where birth weight is decreased. It is intriguing that the expression of *H19* was also increased, whilst the expression of *Igf2*, of which it is proposed to be a negative regulator, was not altered in either Wistar or GCS-EGFP cohorts [310,311]. This may result from a complex regulation of the *H19/Igf2* locus, involving various regulatory elements, such as antisense RNA [357]. Unaltered *Igf2* expression is in contrast to the increased expression demonstrated previously [12], but may reflect a precise interaction of strain and time-point. It does however fit with the programming phenotype that *Igf2*, which is paternally imprinted to promote fetal growth [307,308], would not be increased in a model of low birth weight.

Altered expression was also seen in some of the candidate genes chosen based on a previous microarray (see Table 6.1). The significant increase in expression of *Adh1* following Dex exposure, identified on the microarray was validated in both strains. Because castration of male rats corresponds to an increase in activity of liver ADH1, I hypothesise that the Dex-induced increase in expression may be a consequence of the decreased testosterone levels which have been reported in F1 offspring of Dex-exposed dams between e19.5 and e21.5 [317,358]. As previously discussed, the importance of the correct expression of *Adh1* is evidenced by studies indicating the

detrimental effects of Vitamin A deficiency or excess in fetal development [314,315]. As knockout of *Adh1* decreases the production of active Vitamin A derivatives [359], I hypothesise that a Dex-mediated dysregulation of *Adh1* would alter Vitamin A levels, potentially promoting abnormal fetal development. If this increase in *Adh1* was also found in the testis, it might affect testicular development since research has indicated that increased Vitamin A can have a wide range of effects on the developing testis [360]. For example, retinoic acid can inhibit the pre- and early post-natal development of seminiferous tubules [361,362], and impact upon the development of cultured germ, Sertoli and Leydig cells [363]. If Dex was found to mediate changes in testicular *Adh1*, this could have longer lasting influences on spermatogenesis.

In accordance with microarray data *Hmgb2* and *Gelsolin* expression was reduced in GCS-EGFP rats. *Hmgb2* is thought to have roles in transcriptional regulation, DNA repair, extracellular signalling, and cellular differentiation [318-320]. A Dex-mediated decrease in the expression of *Hmgb2* may therefore affect chromatin compaction and repair in the developing fetus.

A decrease in *Gelsolin* mRNA expression could promote inflammation and susceptibility to insulin resistance. *Gelsolin* knockdown in adipocyte cells was associated with increased expression of the pro-inflammatory genes *TNFα* and *Il6* which may decrease triglyceride content, potentially lowering the risk of heart disease [324,325]. In this way decreased *Gelsolin* expression may be a protective, compensatory mechanism in programming. Furthermore, a Dex-induced alteration of *Gelsolin*, if also found in the epididymis, may also impede sperm maturation due to its role in regulating the actin cytoskeleton of sperm, and their subsequent uptake of calcium [326]. As a decrease in *Hmgb2* and *Gelsolin* is found in the microarray from Wistar tissues and my GCS-EGFP rats, but not the Wistar cohort, I hypothesise that these changes are time-point-specific rather than strain-specific.

The increase in expression of *Igfbp1* identified by microarray was validated in both Wistar and GCS-EGFP cohorts. As IGFBP1 binds IGF1 an increase in expression should decrease the amount of growth factor circulating. Indeed, increased IGFBP1 in amniotic fluid is also associated with lower birth weight in humans [339].

Expression was also increased in the placentas of fetuses with intra-uterine growth restriction [340]. This could also represent a compensatory mechanism, acting to protect insulin sensitivity. In longitudinal studies decreased circulating IGFBP1 levels were correlated with subsequent glucose intolerance and diabetes [336,337]. Furthermore low fasting plasma IGFBP1 levels were correlated with increased cardiovascular disease risk factors, such as high blood pressure and blood triglyceride concentration [338].

The expression of RPS6K isoforms 1 and 2 and the target of their phosphorylation RPS6 was studied. Expression of *Rps6k1* mRNA was reduced in both Wistar and GCS-EGFP cohorts, whilst *Rps6k2* was only reduced in GCS-EGFP rats. This relationship of an increase in *Igfbp1* with decrease in *Rps6k1* is consistent with antisense RNA *Rps6k1* knockdown studies, where there was a dose-dependent increase in hepatic *Igfbp1* expression [346]. This corresponded to improved insulin sensitivity. Furthermore, knockout of *Rps6k1* in mice blunts responsiveness to IGF1 [342], and was shown to protect against a loss of insulin sensitivity in ageing, and to increase lifespan [344]. It also protects insulin sensitivity in mice fed a high-fat diet, potentially through downregulation of the negative feedback loop through IRS1 [345]. A decrease in *Rps6k1* expression with Dex treatment may therefore act to counter insulin resistance.

Expression of the second isoform, *Rps6k2* was also reduced, but only in GCS-EGFP rats. This could represent either a strain-specific or a time-point-specific change. Whilst RPS6K1 and RPS6K2 work together to phosphorylate RPS6, the phenotype of specific knockouts is different. *Rps6k1* knockout mice were significantly lighter both prenatally and postnatally, than wild-type controls, whilst *Rps6k2* weight was unaffected [347]. It therefore fits that in a model of low birth weight, *Rps6k1* downregulation may be more important. Indeed if the main action of these kinases is to phosphorylate RPS6 rather than regulating its expression, it is not surprising that *Rps6* levels are not altered with changes in *Rps6k1* or *Rps6k2*. Any effect on *Rps6* might be further explored by comparing Western Blots for phosphorylated and unphosphorylated RPS6 protein.

Whilst many of the changes in gene expression proposed by the microarray were validated in either or both of my cohorts (Table 6.1), those for *Tpt1* and *Hspa5* did not. This could reflect a cohort- or specific time-point-dependent change, or indeed a false positive in the microarray.

Taken together, these data suggest that in both Wistar and GCS-EGFP rats there are changes in fetal liver gene expression with Dex exposure. Some may be a reflection of decreased birth weight and fetal growth, but also potentially promote the associated negative cardiometabolic phenotypes. Conversely, some of these and others may also form part of a compensatory mechanism, protecting insulin sensitivity. Further studies, including Western Blots, would confirm whether changes in gene expression confer changes in protein levels. Given that many of the genes studied were also explored by a microarray in Wistar rats it is possible to make educated hypotheses regarding which differences between cohorts are due to strain, and which are due to the exact time-point. However further studies with Wistar and GCS-EGFP tissues collected at exactly the same time-point, or of one strain at multiple time-points, would also confirm the basis for differences in gene expression between cohorts. These studies do however give an indication of the effects of Dex treatment on fetal liver, informing further studies.

Furthermore, ERRBS data indicated that at the sites investigated, there was no global difference in methylation between Dex and Saline groups in F1 e19.5 liver. When looking at specific cytosines however, a significant decrease in methylation status of around 13% was identified at Chr13_572, as identified by Biseq analysis. This cluster does not lie within a gene body or promoter, but exists 80kb upstream of the SET and MYND Domain Containing 2 (*Smyd2*) gene. Intriguingly, SMYD2 is an N-lysine methyltransferase which methylates H3K4 and H3K36 [364]. It can also interact with RNA polymerase II, giving another potential role in regulating gene expression [365]. SMYD2 also methylates Lysine 370 in p53, repressing the expression of this tumour suppressor, and increasing the expression of p53-regulated genes [366,367]. Indeed, inhibiting *Smyd2* expression by short interfering RNA promotes p53-induced apoptosis [366]. Combined with an ability to methylate the retinoblastoma tumour suppressor [368], this suggests that SMYD2 may therefore

have an oncogenic function [366]. Recently Sese *et al*. (2013) showed that *Smyd2* is highly expressed during human ES cell differentiation, and that knockdown in zebrafish correlates with developmental delay [369]. Therefore *Smyd2* could have an important role in cellular differentiation, and consequently early development.

It is possible that Chr13_572 could encode, for example, an enhancer for this gene, influencing its expression. Clearly, with roles in regulating gene expression, dysregulation of *Smyd2* could have a widespread impact on gene expression, although the literature does not indicate specifically what effect this might have in the liver.

Nine clusters in total had significantly altered methylation scores. Of those, only 2 were within gene bodies – cluster 787 on chromosome 5 and cluster 284 on chromosome 7. The former had 5 cytosines that were each differentially methylated by 6-7% and the latter had 2 cytosines both differentially methylated by 6.2%. Although this difference is smaller than for cluster Chr13_572, near *Smyd2*, where there was approximately 13% change in methylation score, it is still in keeping with Drake *et al*. (2011) where there was a 5-6% change in methylation in Dex-exposed liver. As previously discussed, a similarly moderate change in methylation was reported in studies of intra-uterine growth restriction [294], and 20% variations at *Igf2* DMRs implicated in the growth restriction associated with Silver-Russell syndrome [295]. It therefore appears that subtle changes in methylation may have relevance for development.

Little is known about the gene corresponding to Chr5_787, Adenylate Cyclase-Associated Protein 1 (yeast) (*Cap1*), which is related to the CAP protein in *Saccharomyces cerevisiae*, involved in the cyclic AMP pathway [370]. In humans CAP1 has been shown to interact with another member of the family, CAP2, and be involved in the recycling of actin filaments in cultured human cells [371]. Interestingly, single nucleotide polymorphisms in the *Cap1* gene have been found in association with type II diabetes [372]. It is therefore not clear exactly what effect differential methylation of *Cap1* might have in the liver, before further study of the function of the *Cap1* gene, but the literature hints that it could have some relevance for metabolic disease.

The second gene encoding cluster with differential methylation, Chr7_284 corresponds to *Basigin*. This extracellular receptor is important in a number of pathways due to its role in intracellular recognition. For example, Basigin binds Cyclophilin A acting as a mediator in the inflammatory response [373]. Knockout of *Basigin* in mice is predominantly embryonic lethal at the point of implantation, potentially due to incorrect intracellular recognition. Those mice that survived were infertile, with primary spermatocytes present, but an absence of sperm production, potentially due to the interruption of meiosis during spermatogenesis [374]. Very recently it has also been indicated that Basigin may facilitate the interaction of germ and Sertoli cells during spermatogenesis [375]. For both *Cap1* and *Basigin* it is not clear what effect a change in liver methylation might have on the developing fetus, although the literature does suggest that in other organs they do have important roles in development and metabolism.

These genes differ from previous studies where, for example, Drake *et al*. (2011) indicate a decrease in methylation at *Igf2* DMR2 in e20.0 liver with Dex exposure [12]. The fact that this was not found in the current study could reflect a difference in response to treatment between strains or cohorts. It is also possible that ERRBS is not sufficiently sensitive to detect a change in methylation reported to be approximately 4-5%. Because so many cytosines are studied in this technique, the threshold p value for statistical significance is much lower, in order to control the false discovery rate [376]. As approximately 1M cytosines are covered in our study, a standard significance threshold of $p \leq 0.05$, used in pyrosequencing would yield 50,000 false positive DMCs. As such, a lower p value threshold is calculated, which could mask subtle differences. A greater 'n' was also used in Drake *et al*. (2011), which gives a greater likelihood of detecting subtle changes. It might be necessary to perform ERRBS on more replicates to be able to detect more subtle changes in gene expression [294].

It is possible that Dex could induce larger changes in methylation, out with CpG islands, predominantly favoured by RRBS. The ERRBS technique has a greater coverage of these areas than RRBS as it characterises longer fragments from MSP1 sites, with for example a 54% increase in CpG island shore data [278]. There is

however, still a bias towards areas of high CpG density, although research has suggested that regions out with CpG islands can also be biologically relevant [113,278].

The current data could also indicate that other epigenetic mechanisms, such as histone modifications or ncRNA may be more influential than DNA methylation in mediating the observed changes in liver gene expression in Dex programming. However, caution needs to be exercised in the interpretation of this data before further validation is performed. Validation of changes in DNA methylation could be performed using pyrosequencing, with primers specific to DMRs identified by ERRBS. Any resulting effect on gene expression could then be studied using qPCR, and on protein levels, by Western Blot.

A major benefit in choosing ERRBS for these studies is that it focusses on CpG rich regions which are most likely to be methylated, reducing the cost of sequencing, whilst still giving relevant data [278]. As this technique was also initially chosen for the germline studies in Chapter 5, where cell numbers, and therefore DNA quantity was very limited, it was particularly useful that ERRBS can be performed on low quantities of DNA (approximately 100ng), compared with the 5µg required for some other studies. However, bisulfite sequencing cannot distinguish between 5hmC and 5mC, which essentially limits our interpretation and curtails our conclusions [296]. Further studies should also include a genome-wide technique which can distinguish between different forms of methylation. For example, methylated DNA immunoprecipitation (MeDIP) uses an antibody to isolate methylated DNA for subsequent sequencing [297]. An antibody specific to 5mC or 5hmC can therefore be used, distinguishing between these two forms of methylation. Our current analysis does not take into consideration the possible contribution of 5hmC and the TET family of protein dioxygenases in contributing to DNA modification profiles [377]. This may be particularly relevant as recent work demonstrates that 5hmC profiling can be used as an indicator of changes in liver cellular state. [378,379]

Taken together, these data suggest that there are alterations in gene expression in response to Dex treatment in both Wistar and GCS-EGFP fetuses, with some common and some species-specific alterations. This adds to the knowledge of the effects of Dex programming and provides direction for further study. Limited effects of treatment were seen on DNA methylation, as studied by ERRBS, although some targets were identified for further investigation.

Chapter 7 Discussion

The main aim of this thesis was to explore whether the transmission of the Dex programming phenotype through the male germline occurs through epigenetic mechanisms. Within this I aimed to confirm that epigenetic reprogramming occurs in the rat and give a timeframe for the phase of remethylation. I also explored the presence of all known forms of DNA methylation during germ cell development, both pre- and postnatally. I then sought to identify a key time-point of change in global germ cell DNA methylation during reprogramming with Dex exposure. Furthermore, I investigated the suitability of GCS-EGFP rats for Dex programming studies, and used them to explore changes in germ cell DNA methylation. I also aimed to further investigate the relationship of Dex exposure with gene expression and DNA methylation in fetal liver.

7.1 Exploring Epigenetic Reprogramming in the Rat Germline

In this thesis, I gave the first demonstration of the occurrence of epigenetic reprogramming of DNA methylation in rat fetal germ cells. Little 5mC was detected by immunofluorescence in male germ cells until e19.5 where some germ cells had a positive detection for 5mC, becoming augmented by e20.5. This indicated that an asynchronous bulk 5mC DNA remethylation phase was occurring in the rat between e19.5-e21.5. This is in keeping with mouse data, which indicates that bulk remethylation occurs prenatally in male germ cells [178,184,196]. The exact timing of demethylation was of less relevance for our studies, as bulk 5mC appeared to have been lost prior to the period of Dex exposure in the Dex-programming model. However 5mC and 5hmC were explored at e12.5 and e13.5, and whilst little 5mC was detected at either time-point, 5hmC was present. This suggested that the period of bulk demethylation occurs before e12.5 in the rat, which is again in keeping with mouse studies, reporting bulk demethylation from e11.5-e12.5 [14,177].

It was intriguing that 5hmC, 5fC and 5caC were detected in germ cells from e14.5-e16.5. This is the first report of 5fC and 5caC detection in germ cells, although 5hmC has previously been reported in mouse fetal germ cells [252]. As 5hmC, 5fC and

5caC can be produced by progressive oxidation from 5mC, and have been proposed to form part of a putative DNA demethylation pathway [149,150], it is not surprising that they are present during epigenetic reprogramming. It is however intriguing that 5fC and 5caC should be detected over a 3 day period, since previous research indicates that TET2 is capable of rapidly converting 5mC through its different methyl forms [149]. Therefore the continuing presence of 5fC and 5caC could reflect a gradual and constant removal of 5mC during e14.5-e16.5. In this case the 5fC or 5caC at any particular base may be rapidly removed, but the constant turnover might give the appearance of a more stable expression of 5fC and 5caC when assessed globally. This is supported by the identification of TDG throughout e14.5-e16.5, indicating that there is the potential for continual removal of 5fC and 5caC throughout this time period. Conversely, it could be hypothesised that there is an accumulation of these methyl forms during the period of demethylation, with bulk removal between e16.5 and e17.5. In both cases, it is possible that the continued presence of 5fC and 5caC has some functionality in germ cell development. Furthermore, the dynamic changes in detection of 5hmC, 5fC and 5caC postnatally were particularly intriguing, as bulk demethylation was not expected or detected at these time-points. Taken together, these studies suggest that 5hmC, 5fC and 5caC could have a functional role in germ cell development, in addition to forming part of a demethylation pathway. This is supported by previous work indicating that these forms may have some, as yet undetermined, role in development [157].

Clearly, there is still much to be discovered about the dynamics and potential roles of these additional forms of methylation. Performing base-pair resolution analysis of the localisation of 5fC and 5caC, such as the modified bisulfite sequencing protocol from Wang *et al*. (2014) might give greater clarity [169]. This could identify whether these modifications have a stable presence across the whole genome from e14.5-e16.5, or if they exist at different loci at different time-points, reflecting their continual removal. Identifying their localisation would also give greater insight into their potential functionality. Furthermore, studies in mice indicate that the timeframe for remethylation in epigenetic reprogramming is later in females [184,197]. It would be interesting to study this process in female rats, comparing the time-course to that

found in males and exploring whether 5hmC, 5fC and 5caC are also present in mid-gestation germ cells.

7.2 Exploring the Suitability of GCS-EGFP Rats for Dex Programming Studies

As GCS-EGFP rats were reported to have germline specific expression of EGFP, a colony was established so that pure populations of fetal germ cells and adult sperm could be isolated by FACS-sorting, and used for base-specific methylation studies. Because these rats were new to The University of Edinburgh, their use had to be optimised, and their phenotype explored. Immunofluorescence indicated that EGFP expression was tissue-specific, and germ cell-specific within the testis. A further confirmation of EGFP localisation was given by gene expression analysis of FACS-sorted cells from the fetal testis. Therefore, in keeping with Cronkhite *et al.* (2005), EGFP expression was confirmed to be germline-specific in this strain of rats, at least in the male [92]. However, whilst performing FISH identifies the genomic region of the EGFP insert, Cronkhite *et al*. (2005) did not report the exact location, or indeed copy number of EGFP. Whole genome sequencing would allow this to be identified, adding to the characterisation of this strain. If the insert is likely to affect the function of genes crucial, for example in regulating PGC development, this could influence the observed phenotype in response to Dex exposure, and should be considered when interpreting the results.

As Wistar rats had been used for the immunofluorescence studies in Chapters 3 and 4, as the GCS-EGFP colony had not yet been established, I confirmed that the time-course for epigenetic reprogramming of DNA methylation, and the Dex programming phenotype were similar in both strains of rat. Prenatal Dex exposure corresponded to reduced birth weight and e19.5 fetal and placental weight in the F1 generation. To ensure that this phenotype would be transgenerational, F1 Dex males and Saline females were bred, and had offspring with a significantly reduced birth weight compared to those whose parents had both been exposed to Saline *in utero*. Thus a low birth weight phenotype was seen to be transmitted to an F2 generation, through the male line, as previously found in Wistar rats [10].

7.3 Exploring Effects of Dex Exposure on Epigenetic Reprogramming

The effects of Dex programming on epigenetic reprogramming were explored in two different studies. In Chapter 4, the effects of Dex exposure on global 5mC remethylation were explored by immunofluorescence. At e19.5 more 5mC positive germ cells were identified with Dex exposure, relative to controls, although this difference had resolved by e20.5. I therefore hypothesised that the epigenetic reprogramming time-line might be shifted forward slightly with Dex exposure, and that e19.5 was an interesting time-point for further study. This change however did not correspond to alterations in the localisation of DNMT3a or 3b, or indeed the global time-course of DMRT1, used as a marker of testis development.

Fetal germ cells were then isolated at e19.5 by FACS sorting, DNA extracted and ERRBS performed to explore the localisation of methylation at a base-specific level. Of the DMCs, hypermethylation was more prevalent than hypomethylation, indicating that there might be accelerated remethylation in a subset of genes. To further explore this hypothesis, germ cell DMCs were grouped by whether the corresponding gene in control fetal liver had high, medium or low levels of methylation. Intriguingly, there was prevalence of hypermethylation in DMCs which had highly methylated corresponding genes in the liver, and of hypomethylation in DMCs with low liver methylation. This comparison is clearly imperfect, due to differences in the methylation profile between cell types, but gives some weight to the hypothesis that Dex may accelerate the acquisition of the completed state of remethylation in germ cells.

Biseq analysis then indicated which of these DMCs were statistically significant, and where clustering of significant DMCs occurred. 5 regions were identified as having significant DMCs with at least 5% change in methylation between Dex and Saline e19.5 germ cell samples. Chr3_2256, corresponding to the *Ralgapb* gene, had a consistent decrease in methylation across 5 DMCs. This gene is involved in regulating the action of RalA and RalB GTPases, which in turn regulate a range of cellular processes, such as transcription, translation and cell survival [281]. Intriguingly, RalA has also been shown to have a role in regulating glucose uptake in adipocytes in response to insulin [282,283].

Conversely, increased methylation was seen at Chr5_2324, Chr5_2589, and Chr6_540. The biggest increase (12.2%) was found at Chr6_540, corresponding to the *Pdia6* gene. The PDIA6 protein has a role in protein folding and the regulation of calcium homeostasis within the endoplasmic reticulum [290,291]. Chr5_2589 corresponds to the circadian clock gene *Per3*, which has been found to be upregulated in hepatocellular carcinoma, with *Per3* polymorphisms altering disease prognosis [287,288]. Any effect of decreased methylation on gene expression in our study has not yet been characterised. However, previous research indicates that Dex exposure increases the expression of *Per3* in cultured rat fibroblasts, and that it increases liver expression of the associated *Per1* gene *in vivo* [289].

Increased methylation was also seen at Chr5_2324 in Dex-exposed germ cells. This corresponds to the *Spen* gene, encoding transcriptional repressors [285]. Knockout of MINT, encoded by the *Spen* gene in mice corresponded to embryonic lethality, with liver, heart and pancreatic abnormalities in the fetus [286]. Therefore *Spen* appears to be of relevance for transcriptional regulation in development. An increase in DNA methylation was also seen at Chr5_2393. The closest annotated gene to this cluster was *Pramel1*, a member of an LRR family involved in a range of pathways through a role in facilitating protein-protein interactions [292,293]. In the mouse, expression of this gene was identified solely in the testis, and specifically in the acrosome of sperm during spermatogenesis [293].

Although there are associations with the regulation of glucose uptake, development, and transcription, the precise effect of altered methylation of these genes in the fetal germ cell is unknown. Due to a substantial delay in receipt of data following initial sequencing issues, and subsequent time constraints, validation of ERRBS data was not performed. Pyrosequencing should be conducted to confirm the base-specific changes reported for ERRBS, and qPCR should be used to compare changes in DNA methylation with gene expression. It should also be considered that in some cases, altered methylation corresponds to a single DMC, as identified by ERRBS, therefore caution should be exercised with inferring significant biological relevance. Furthermore, some of the clusters represent relatively small changes of only 5-6% with Dex exposure. This, however is in keeping with previous studies in the Dex

model, showing 5-6% changes in liver DNA methylation [12]. Indeed, subtle changes in DNA methylation have also been reported in studies of growth restriction [294,295], suggesting that small changes could still be of physiological relevance.

The effect of Dex exposure on fetal germ cell methylation has not previously been studied in any species. However this data is in keeping with Radford *et al*. (2014) who report that *in utero* undernutrition in mice corresponds to hypomethylation at some loci in adult sperm, in the absence of a global change in methylation [93]. These DMCs were also identified to be hypomethylated at e16.5, suggesting aberrant remethylation. Indeed, of the regions seen to be hypomethylated in sperm, 43% are known to be resistant to whole embryo reprogramming, suggesting that these changes could influence the phenotype of the next generation [93]. Hammoud *et al*. (2014) also demonstrated that DNA methylation profiles are strikingly conserved throughout the process of spermatogenesis [211]. This supports the theory that changes in DNA methylation in the fetal germ cells, which form the progenitors of the spermatogenic pathway, could be maintained in mature sperm and therefore transmitted to the next generation.

The predominance of hypermethylation amongst DMCs was identified both within and out with CpG islands. As CpG islands are predominantly unmethylated it was fitting that the majority of DMCs should be located out with CpG islands [112]. However, it has been suggested that orphan CpGs islands are frequently methylated during development [112], indicating that DMCs at CpG islands, although few in number, may be of particular relevance in the programming phenotype.

However, germ cell DMCs formed a small proportion of the total number of cytosines studied by ERRBS and the majority of cytosines did not show differential methylation between Dex and Saline groups. This could result from the fact that ERRBS only interrogates a small proportion of the genome. The process of enzymatic cleavage favours CpG dinucleotides, and so will capture the majority of promoters and CpG islands, but will not cover all sites of methylation [275]. ERRBS selects longer MSP1 fragments, enabling the capture of more regions out with CpG islands than in standard RRBS, however some DMCs will still be missed [278]. Furthermore, ERRBS cannot discriminate between different forms of methylation.

Whilst timeline immunofluorescence studies indicate that there is not a global prevalence of 5hmC, 5fC or 5caC at e19.5, as in mid-gestation, these forms may still have some influence on the observed methylation differences between groups, particularly as the percentage change in DMCs is relatively modest (10-30%). Data should therefore be supplemented with DNA immunoprecipitation studies, allowing the identification of individual methyl forms, particularly as they have recently been shown to be effective with 5fC and 5caC antibodies [152]. It is also possible that the differences between immunofluorescence and ERRBS data result from variation in the exact time of fertilisation. Although rats were time mated, and were previously found to mate quickly after pairing (Drake *et al*., Unpublished data), the exact time of fertilisation could vary slightly between, and even within litters. As bulk remethylation was found to occur over a short time period, between e19.5 and e20.5, it is possible that slight differences in age of the pups could have an effect on the result. The impact of this issue was reduced by performing ERRBS on three samples each pooled from three litters, giving nine different litters per group. Indeed one pooled Dex sample was found to have greater global methylation than the others. Future studies using *in vitro* fertilisation would remove this variable.

Fetal liver was used as an indicator of baseline DNA methylation and allows some reference point for DMCs in Dex-exposed germ cells at e19.5. However, a more relevant comparison could be made if a second ERRBS study were to be performed on fetal germ cells at e20.5. This would give greater clarity as to whether DMCs at e19.5 represent accelerated remethylation, and if these changes are persistent in the germline. A better understanding of the involvement of DNMTs in changes in methylation might be achieved by performing a DNMT enzyme activity assay, as in Luo *et al*. (2013) [380]. This would give a quantitative analysis of the activity of these enzymes following Dex exposure, indicating whether this might underpin a change in remethylation. A wider understanding of the effects of Dex on the developing germ cell would also be obtained by studying effects on other epigenetic mechanisms, such as ncRNA and histone modifications. Previous studies indicate that histones may be altered in the germline as a result of diet [213,214,238], and that early life stress may alter sncRNA in sperm [241]. It is therefore possible that Dex

exposure also alters these epigenetic marks, which in combination with DNA methylation allow transmission of the programming phenotype.

The studies in this thesis predominantly explore the direct effects of Dex exposure on the F1 developing pup, both in the germline and in the liver. The characteristic decrease in birth weight was found in the experiments presented in this thesis, and indeed, this was transmitted to a second generation when studied in GCS-EGFP rats. Therefore, this suggests that the previously characterised Dex programming phenotype had been replicated. Previous studies have shown that effects of Dex exposure are found in the F2, in terms of pup weight, gene expression, PEPCK expression and glucose tolerance [10,12]. We therefore hypothesise that observed effects on the F1 germline DNA methylation, if validated, may have influence on the development of the F2 offspring. Such effects on the F2, however, may not be truly inherited, in the sense that there has been some exposure, in the form of F1 germ cells, to the initial insult. Thus, whilst the experiments in this thesis, with the exception of GCS-EGFP F2 birth weight studies, look at the direct effects of Dex exposure on the liver and germ cells of the developing pup, they also explore the potential for indirect effects on the F2 generation, through alteration of the germline.

Insight into the long-term impacts of Dex exposure on germline epigenetics would also be achieved by performing ERRBS on adult sperm samples. The DNA from such samples has been prepared, and is pending sequencing. This will allow a comparison of the DMCs established in fetal germ cells, during the period of Dex exposure, with those later found in sperm, and potentially transmitted to the next generation.

7.4 Investigating the Effects of Dex Programming on Liver Gene Expression and DNA Methylation

Further insight into the effects of Dex programming in both Wistar and GCS-EGFP rats was achieved through gene expression analysis of fetal liver tissue. The expression of *Gr*, *11β-Hsd1* and imprinted genes implicated in growth and development was explored, to compare our cohorts to those of previous studies. *Gr* expression was increased in Wistar rats at e20.5, which is in keeping with studies by Nyirenda *et al*. (1998), showing increased expression shortly after birth [8]. No significant alteration in *Gr* expression was found in GCS-EGFP rats, or in *11β-Hsd1* expression in either strain. Nyirenda *et al*. (1998) similarly found no change in the expression of *11β-Hsd1* in the rat, but did report an increase in hepatic expression postnatally in the Dex programmed marmoset [8,75]. Imprinted genes *H19, Cdkn1c* and *Grb10* all had increased expression with Dex in GCS-EGFP, but not Wistar rats. Drake *et al*. (2011) had previously demonstrated an upregulation of these genes in Wistar rats, and so this discrepancy might result from a slight difference in time-point between the two cohorts [12].

A gene expression microarray had previously been performed in Wistar fetal liver, and I sought to validate some of the expression changes in the current study. Some validated in both cohorts, whilst others were only found in either Wistar or GCS-EGFP rats. These variances could result from strain-specific or time-point-specific effects on gene expression. The difference in time-point between Wistar and GCS-EGFP was a result of the Wistar cohort being collected prior to the identification of the e19.5 time-point for interest in germ cell studies. To make best use of time, resources, and animal life, these tissues were used for a comparison between strains. Although the exact cause of variation in gene expression between cohorts may not always be determined, these studies do demonstrate that Dex exposure affects gene expression in the livers of Wistar and GCS-EGFP rats, with some similarities and some differences between cohorts. However, further clarity would be achieved by studying the same time-point in both strains.

These data identified some interesting candidates for further study, such as the growth factor binding protein IGFBP1, found to have increased expression in fetal

liver of both strains following Dex exposure. This is supported by studies in humans which show an association between increased IGFBP1 protein in amniotic fluid and decreased birth weight [339]. Increased human placental *Igfbp1* mRNA expression was similarly associated with intrauterine growth restriction [340]. As low circulating IGFBP1 protein has been correlated with increased cardiovascular risk factors such as glucose intolerance, diabetes and high blood pressure [336-338], a Dex-induced increase in *Igfbp1* could represent a protective mechanism. I also explored the expression of RPS6K1, which exists downstream of IGFBP1 in the insulin signalling pathway [343]. *Rps6k1* mRNA expression was significantly decreased with Dex-exposure in the fetal livers of both wild-type Wistar and GCS-EGFP Sprague Dawley rats. This is consistent with antisense RNA *Rps6k1* knockdown studies in adult Sprague Dawley rats, which demonstrated a dose-dependent increase in hepatic *Igfbp1* mRNA expression, and improved insulin sensitivity [346]. As previous studies also suggest that *Rps6k1* knockout in mice is associated with a protection of insulin sensitivity in ageing or high-fat diet consumption [344,345], a decrease in *Rps6k1* expression with Dex-exposure may also be protective, and act to counter insulin resistance.

It would also be interesting to see if there were concurrent effects on other members of the insulin signalling pathway, such as IRS1 and members of the mTORC1 cascade. Importantly, as the actions of RPS6K1/2 involve substrate phosphorylation, this should be studied by Western Blot for phosphorylated RPS6 protein, or IRS1 [342,343]. Western Blot should also be performed for IGFBP1 and RPS6K1, and together this would confirm whether a reduction in mRNA expression reduces levels of the corresponding protein, and whether this confers a reduction in total substrate phosphorylation. The ultimate effects of Dex on this pathway could also be explored by measuring the blood pressure of the F1 adults, and insulin levels in ageing or response to high-fat diet, comparing results to *Rps6k1* knockout studies [344-346].

Some changes in DNA methylation were also identified in e19.5 GCS-EGFP liver by ERRBS. No global change in DNA methylation was exhibited, but Biseq analysis indicated that there were 9 clusters which were significantly differentially methylated. Of these, 2 aligned to annotated genes, *Cap1* and *Basigin*. The observed

changes were relatively subtle (6-7%), yet this is in keeping with a previous candidate gene study by Drake *et al*. (2011) where a 5-6% change in methylation was identified in fetal liver following Dex exposure [12]. Intriguingly, single nucleotide polymorphisms in the *Cap1* gene have been found in association with type II diabetes in human studies, suggesting it may have some, as yet undetermined, role in metabolic disease [372]. As for CAP1, the hepatic functions of Basigin have not been characterised, but it is thought to be involved in intercellular signalling, and potentially facilitates the interaction of Sertoli and germ cells during spermatogenesis [373,375]. The cluster with the most substantial difference in methylation between Dex and Saline groups did not correspond to a gene body, but was found 80kb upstream of *Smyd2*. This methyltransferase methylates H3K4 and H3K36, and can also interact with RNA polymerase II, giving another potential role in regulating gene expression [364,365]. SMYD2 has recently been suggested to have a role in development, being highly expressed during ES cell differentiation, with knockdown in zebrafish corresponding to a developmental delay [369]. I hypothesised that the cluster upstream of the *Smyd2* gene could, for example, correspond to an enhancer region, and thus Dex-mediated differential methylation might ultimately influence the regulation of the *Smyd2* gene. Clearly, with roles in regulating gene expression, dysregulation of *Smyd2* could have a widespread impact on gene expression, although the literature does not indicate specifically what effect this might have in the liver. Taken together, this study indicates that Dex exposure corresponds to DMCs at a few locations of potential relevance for development and metabolism, providing candidates for further investigation.

7.5 Relevance

This study therefore contributes to our understanding of how environmental factors can influence the developing fetus, and its offspring. Dex programming may alter remethylation at a subset of genes in the developing germ cell, and as initial research in other models indicates that this could impact upon sperm, these changes could affect the development of the next generation.

Less is known about epigenetic reprogramming in humans, due to the limited availability of fetal tissue. However infertility has been shown to correlate with alterations in sperm methylation at loci key for growth and development, therefore it appears that DNA methylation can be changed in the human germline [224,225]. I hypothesise that *in utero* exposure to environmental factors may also alter DNA methylation in the developing human fetal germ cells and subsequent sperm. Improved understanding of the potential to transmit intra-uterine exposures to the next generation emphasises the importance of a healthy *in utero* environment for the development of the fetus and the subsequent generation. A greater understanding of these mechanisms also provides the foundation for future development of therapy-based approaches. Indeed it has recently been shown that RNA targeting of DNMT1 may enable gene-specific alteration of DNA methylation [381]. Although in its infancy, this suggests that carefully targeted therapeutic approaches may be possible in the future.

7.6 Conclusion

I have demonstrated that epigenetic reprogramming of DNA methylation occurs in the rat, given a time-frame for the phase of remethylation, and explored the presence of all known forms of methylation in the developing germ cell. I also explored the effects of Dex exposure on this global remethylation timeline, and identified more 5mC positive germ cells at e19.5 following Dex exposure, relative to controls, indicating that remethylation may be accelerated. I then used GCS-EGFP rats to allow the isolation of pure populations of fetal germ cells for base-specific methylation analysis. ERRBS indicated that premature DNA remethylation may occur at a subset of loci, and future studies will explore whether these represent stable changes in germ cell methylation, and if they are transmitted to sperm. Novel changes in gene expression and methylation were also identified in the fetal liver. This study provides further insight into the transmission of the Dex programming phenotype across generations, and provides direction for further investigation.

References

1. Nichols M, Townsend N, Scarborough P, Rayner M (2014) Cardiovascular disease in Europe 2014: epidemiological update. Eur Heart J 35: 2950-2959.
2. Barker DJ, Osmond C, Golding J, Kuh D, Wadsworth ME (1989) Growth in utero, blood pressure in childhood and adult life, and mortality from cardiovascular disease. BMJ 298: 564-567.
3. Barker DJ, Gluckman PD, Godfrey KM, Harding JE, Owens JA, et al. (1993) Fetal nutrition and cardiovascular disease in adult life. Lancet 341: 938-941.
4. Roseboom TJ, van der Meulen JHP, Osmond C, Barker DJP, Ravelli ACJ, et al. (2000) Coronary heart disease after prenatal exposure to the Dutch famine, 1944-45. Heart 84: 595-598.
5. Painter RC, de Rooij SR, Roseboom TJ, Bossuyt PMM, Simmers TA, et al. (2005) Early onset of coronary heart disease after prenatal exposure to the Dutch Famine. Pediatric Research 58: 1121-1121.
6. Lederman SA, Rauh V, Weiss L, Stein JL, Hoepner LA, et al. (2004) The effects of the World Trade Center event on birth outcomes among term deliveries at three lower Manhattan hospitals. Environmental Health Perspectives 112: 1772-1778.
7. Painter RC, Roseboom TJ, Bleker OP (2005) Prenatal exposure to the Dutch famine and disease in later life: an overview. Reprod Toxicol 20: 345-352.
8. Nyirenda MJ, Lindsay RS, Kenyon CJ, Burchell A, Seckl JR (1998) Glucocorticoid exposure in late gestation permanently programs rat hepatic phosphoenolpyruvate carboxykinase and glucocorticoid receptor expression and causes glucose intolerance in adult offspring. J Clin Invest 101: 2174-2181.
9. Jimenez-Chillaron JC, Hernandez-Valencia M, Reamer C, Fisher S, Joszi A, et al. (2005) Beta-cell secretory dysfunction in the pathogenesis of low birth weight-associated diabetes: a murine model. Diabetes 54: 702-711.
10. Drake AJ, Walker BR, Seckl JR (2005) Intergenerational consequences of fetal programming by in utero exposure to glucocorticoids in rats. Am J Physiol Regul Integr Comp Physiol 288: R34-38.
11. Jimenez-Chillaron JC, Isganaitis E, Charalambous M, Gesta S, Pentinat-Pelegrin T, et al. (2009) Intergenerational Transmission of Glucose Intolerance and Obesity by In Utero Undernutrition in Mice. Diabetes 58: 460-468.
12. Drake AJ, Liu L, Kerrigan D, Meehan RR, Seckl JR (2011) Multigenerational programming in the glucocorticoid programmed rat is associated with generation-specific and parent of origin effects. Epigenetics 6: 1334-1343.
13. Xiao X, Mruk DD, Wong CKC, Cheng CY (2014) Germ Cell Transport Across the Seminiferous Epithelium During Spermatogenesis. Physiology 29: 286-298.
14. Hajkova P, Erhardt S, Lane N, Haaf T, El-Maarri O, et al. (2002) Epigenetic reprogramming in mouse primordial germ cells. Mechanisms of Development 117: 15-23.
15. Barker DJP, Osmond C, Simmonds SJ, Wield GA (1993) The Relation of Small Head Circumference and Thinness at Birth to Death from Cardiovascular-Disease in Adult Life. British Medical Journal 306: 422-426.

16. Barker DJ (1998) In utero programming of chronic disease. Clin Sci (Lond) 95: 115-128.
17. Hales CN, Barker DJ (2001) The thrifty phenotype hypothesis. Br Med Bull 60: 5-20.
18. Ravelli ACJ, van der Meulen JHP, Michels RPJ, Osmond C, Barker DJP, et al. (1998) Glucose tolerance in adults after prenatal exposure to famine. Lancet 351: 173-177.
19. Ravelli ACJ, van der Meulen JHP, Osmond C, Barker DJP, Bleker OP (1999) Obesity at the age of 50 y in men and women exposed to famine prenatally. American Journal of Clinical Nutrition 70: 811-816.
20. Stein AD, Lumey LH (2000) The relationship between maternal and offspring birth weights after maternal prenatal famine exposure: The Dutch Famine Birth Cohort Study. Human Biology 72: 641-654.
21. Boney CM, Verma A, Tucker R, Vohr BR (2005) Metabolic syndrome in childhood: association with birth weight, maternal obesity, and gestational diabetes mellitus. Pediatrics 115: e290-296.
22. Laitinen J, Power C, Jarvelin MR (2001) Family social class, maternal body mass index, childhood body mass index, and age at menarche as predictors of adult obesity. American Journal of Clinical Nutrition 74: 287-294.
23. Villamor E, Cnattingius S (2006) Interpregnancy weight change and risk of adverse pregnancy outcomes: a population-based study. Lancet 368: 1164-1170.
24. Smith J, Cianflone K, Biron S, Hould FS, Lebel S, et al. (2009) Effects of maternal surgical weight loss in mothers on intergenerational transmission of obesity. J Clin Endocrinol Metab 94: 4275-4283.
25. Gardner DS, Pearce S, Dandrea J, Walker R, Ramsay MM, et al. (2004) Peri-implantation undernutrition programs blunted angiotensin II evoked baroreflex responses in young adult sheep. Hypertension 43: 1290-1296.
26. Gardner DS, Tingey K, Van Bon BW, Ozanne SE, Wilson V, et al. (2005) Programming of glucose-insulin metabolism in adult sheep after maternal undernutrition. Am J Physiol Regul Integr Comp Physiol 289: R947-954.
27. Woods LL, Ingelfinger JR, Nyengaard JR, Rasch R (2001) Maternal protein restriction suppresses the newborn renin-angiotensin system and programs adult hypertension in rats. Pediatric Research 49: 460-467.
28. Petry CJ, Dorling MW, Pawlak DB, Ozanne SE, Hales CN (2001) Diabetes in old male offspring of rat dams fed a reduced protein diet. Int J Exp Diabetes Res 2: 139-143.
29. Fernandez-Twinn DS, Wayman A, Ekizoglou S, Martin MS, Hales CN, et al. (2005) Maternal protein restriction leads to hyperinsulinemia and reduced insulin-signaling protein expression in 21-mo-old female rat offspring. Am J Physiol Regul Integr Comp Physiol 288: R368-373.
30. Kwong WY, Wild AE, Roberts P, Willis AC, Fleming TP (2000) Maternal undernutrition during the preimplantation period of rat development causes blastocyst abnormalities and programming of postnatal hypertension. Development 127: 4195-4202.
31. Buckley AJ, Keseru B, Briody J, Thompson M, Ozanne SE, et al. (2005) Altered body composition and metabolism in the male offspring of high fat-fed rats. Metabolism 54: 500-507.

32. Khan IY, Dekou V, Douglas G, Jensen R, Hanson MA, et al. (2005) A high-fat diet during rat pregnancy or suckling induces cardiovascular dysfunction in adult offspring. Am J Physiol Regul Integr Comp Physiol 288: R127-133.
33. Bellinger L, Lilley C, Langley-Evans SC (2004) Prenatal exposure to a maternal low-protein diet programmes a preference for high-fat foods in the young adult rat. British Journal of Nutrition 92: 513-520.
34. Bayol SA, Farrington SJ, Stickland NC (2007) A maternal 'junk food' diet in pregnancy and lactation promotes an exacerbated taste for 'junk food' and a greater propensity for obesity in rat offspring. Br J Nutr 98: 843-851.
35. Nivoit P, Morens C, Van Assche FA, Jansen E, Poston L, et al. (2009) Established diet-induced obesity in female rats leads to offspring hyperphagia, adiposity and insulin resistance. Diabetologia 52: 1133-1142.
36. Reynolds RM (2010) Corticosteroid-mediated programming and the pathogenesis of obesity and diabetes. Journal of Steroid Biochemistry and Molecular Biology 122: 3-9.
37. Costa A, Rocci MP, Arisio R, Benedetto C, Fabris C, et al. (1996) Glucocorticoid receptors immunoreactivity in tissue of human embryos. J Endocrinol Invest 19: 92-98.
38. Speirs HJ, Seckl JR, Brown RW (2004) Ontogeny of glucocorticoid receptor and 11beta-hydroxysteroid dehydrogenase type-1 gene expression identifies potential critical periods of glucocorticoid susceptibility during development. J Endocrinol 181: 105-116.
39. Peltoniemi OM, Kari MA, Hallman M (2011) Repeated antenatal corticosteroid treatment: a systematic review and meta-analysis. Acta Obstet Gynecol Scand 90: 719-727.
40. Andrews RC, Walker BR (1999) Glucocorticoids and insulin resistance: old hormones, new targets. Clinical Science 96: 513-523.
41. Low SC, Chapman KE, Edwards CRW, Seckl JR (1994) Liver-Type 11-Beta-Hydroxysteroid Dehydrogenase Cdna Encodes Reductase but Not Dehydrogenase-Activity in Intact Mammalian Cos-7 Cells. J Mol Endocrinol 13: 167-174.
42. Jamieson PM, Chapman KE, Edwards CR, Seckl JR (1995) 11 beta-hydroxysteroid dehydrogenase is an exclusive 11 beta- reductase in primary cultures of rat hepatocytes: effect of physicochemical and hormonal manipulations. Endocrinology 136: 4754-4761.
43. Lindsay RS, Lindsay RM, Edwards CR, Seckl JR (1996) Inhibition of 11-beta-hydroxysteroid dehydrogenase in pregnant rats and the programming of blood pressure in the offspring. Hypertension 27: 1200-1204.
44. Lindsay RS, Lindsay RM, Waddell BJ, Seckl JR (1996) Prenatal glucocorticoid exposure leads to offspring hyperglycaemia in the rat: studies with the 11 beta-hydroxysteroid dehydrogenase inhibitor carbenoxolone. Diabetologia 39: 1299-1305.
45. Holmes MC, Abrahamsen CT, French KL, Paterson JM, Mullins JJ, et al. (2006) The mother or the fetus? 11beta-hydroxysteroid dehydrogenase type 2 null mice provide evidence for direct fetal programming of behavior by endogenous glucocorticoids. J Neurosci 26: 3840-3844.
46. Lesage J, Del-Favero F, Leonhardt M, Louvart H, Maccari S, et al. (2004) Prenatal stress induces intrauterine growth restriction and programmes

glucose intolerance and feeding behaviour disturbances in the aged rat. J Endocrinol 181: 291-296.
47. Mairesse J, Lesage J, Breton C, Bréant B, Hahn T, et al. (2007) Maternal stress alters endocrine function of the feto-placental unit in rats. Am J Physiol Endocrinol Metab 292: E1526-1533.
48. Welberg LA, Thrivikraman KV, Plotsky PM (2005) Chronic maternal stress inhibits the capacity to up-regulate placental 11beta-hydroxysteroid dehydrogenase type 2 activity. J Endocrinol 186: R7-R12.
49. Dodds HM, Taylor PJ, Johnson LP, Mortimer RH, Pond SM, et al. (1997) Cortisol metabolism and its inhibition by glycyrrhetinic acid in the isolated perfused human placental lobule. J Steroid Biochem Mol Biol 62: 337-343.
50. Raikkonen K, Pesonen AK, Heinonen K, Lahti J, Komsi N, et al. (2009) Maternal licorice consumption and detrimental cognitive and psychiatric outcomes in children. Am J Epidemiol 170: 1137-1146.
51. Raikkonen K, Seckl JR, Heinonen K, Pyhala R, Feldt K, et al. (2010) Maternal prenatal licorice consumption alters hypothalamic-pituitary-adrenocortical axis function in children. Psychoneuroendocrinology 35: 1587-1593.
52. Strandberg TE, Jarvenpaa AL, Vanhanen H, McKeigue PM (2001) Birth outcome in relation to licorice consumption during pregnancy. Am J Epidemiol 153: 1085-1088.
53. Albiston AL, Obeyesekere VR, Smith RE, Krozowski ZS (1994) Cloning and tissue distribution of the human 11 beta-hydroxysteroid dehydrogenase type 2 enzyme. Mol Cell Endocrinol 105: R11-17.
54. Ghaemmaghami P, Dainese SM, La Marca R, Zimmermann R, Ehlert U (2014) The Association Between the Acute Psychobiological Stress Response in Second Trimester Pregnant Women, Amniotic Fluid Glucocorticoids, and Neonatal Birth Outcome. Dev Psychobiol 56: 734-747.
55. Kenny L, Everard C, Khashan A (2014) Maternal Stress and in Utero Programming. In: Seckl JR, Christen Y, editors. Hormones, Intrauterine Health and Programming: Springer International Publishing. pp. 41-55.
56. Berkowitz GS, Wolff MS, Janevic TM, Holzman IR, Yehuda R, et al. (2003) The World Trade Center disaster and intrauterine growth restriction. Jama-Journal of the American Medical Association 290: 595-596.
57. Diederich S, Eigendorff E, Burkhardt P, Quinkler M, Bumke-Vogt C, et al. (2002) 11 beta-hydroxysteroid dehydrogenase types 1 and 2: An important pharmacokinetic determinant for the activity of synthetic mineralo- and glucocorticoids. Journal of Clinical Endocrinology & Metabolism 87: 5695-5701.
58. Dalziel SR, Walker NK, Parag V, Mantell C, Rea HH, et al. (2005) Cardiovascular risk factors after antenatal exposure to betamethasone: 30-year follow-up of a randomised controlled trial. Lancet 365: 1856-1862.
59. Finken MJ, Keijzer-Veen MG, Dekker FW, Frolich M, Walther FJ, et al. (2008) Antenatal glucocorticoid treatment is not associated with long-term metabolic risks in individuals born before 32 weeks of gestation. Arch Dis Child Fetal Neonatal Ed 93: F442-447.
60. Davis EP, Waffarn F, Sandman CA (2011) Prenatal treatment with glucocorticoids sensitizes the hpa axis response to stress among full-term infants. Dev Psychobiol 53: 175-183.

61. Friedman JE, Yun JS, Patel YM, Mcgrane MM, Hanson RW (1993) Glucocorticoids Regulate the Induction of Phosphoenolpyruvate Carboxykinase (Gtp) Gene-Transcription during Diabetes. Journal of Biological Chemistry 268: 12952-12957.
62. Benediktsson R, Lindsay RS, Noble J, Seckl JR, Edwards CR (1993) Glucocorticoid exposure in utero: new model for adult hypertension. Lancet 341: 339-341.
63. Sugden MC, Langdown ML, Munns MJ, Holness MJ (2001) Maternal glucocorticoid treatment modulates placental leptin and leptin receptor expression and materno-fetal leptin physiology during late pregnancy, and elicits hypertension associated with hyperleptinaemia in the early-growth-retarded adult offspring. Eur J Endocrinol 145: 529-539.
64. Drake AJ, Raubenheimer PJ, Kerrigan D, McInnes KJ, Seckl JR, et al. (2010) Prenatal dexamethasone programs expression of genes in liver and adipose tissue and increased hepatic lipid accumulation but not obesity on a high-fat diet. Endocrinology 151: 1581-1587.
65. Cleasby ME, Kelly PA, Walker BR, Seckl JR (2003) Programming of rat muscle and fat metabolism by in utero overexposure to glucocorticoids. Endocrinology 144: 999-1007.
66. O'Regan D, Kenyon CJ, Seckl JR, Holmes MC (2004) Glucocorticoid exposure in late gestation in the rat permanently programs gender-specific differences in adult cardiovascular and metabolic physiology. American Journal of Physiology-Endocrinology and Metabolism 287: E863-E870.
67. Hadoke PW, Lindsay RS, Seckl JR, Walker BR, Kenyon CJ (2006) Altered vascular contractility in adult female rats with hypertension programmed by prenatal glucocorticoid exposure. J Endocrinol 188: 435-442.
68. Berry LM, Polk DH, Ikegami M, Jobe AH, Padbury JF, et al. (1997) Preterm newborn lamb renal and cardiovascular responses after fetal or maternal antenatal betamethasone. Am J Physiol 272: R1972-1979.
69. Tangalakis K, Lumbers ER, Moritz KM, Towstoless MK, Wintour EM (1992) Effect of cortisol on blood pressure and vascular reactivity in the ovine fetus. Exp Physiol 77: 709-717.
70. Roghair RD, Segar JL, Sharma RV, Zimmerman MC, Jagadeesha DK, et al. (2005) Newborn lamb coronary artery reactivity is programmed by early gestation dexamethasone before the onset of systemic hypertension. American Journal of Physiology-Regulatory Integrative and Comparative Physiology 289: R1169-R1176.
71. Molnar J, Howe DC, Nijland MJM, Nathanielsz PW (2003) Prenatal dexamethasone leads to both endothelial dysfunction and vasodilatory compensation in sheep. Journal of Physiology-London 547: 61-66.
72. Sloboda DM, Newnham JP, Challis JRG (2002) Repeated maternal glucocorticoid administration and the developing liver in fetal sheep. Journal of Endocrinology 175: 535-543.
73. Koenen SV, Mecenas CA, Smith GS, Jenkins S, Nathanielsz PW (2002) Effects of maternal betamethasone administration on fetal and maternal blood pressure and heart rate in the baboon at 0.7 of gestation. American Journal of Obstetrics and Gynecology 186: 812-817.

74. de Vries A, Holmes MC, Heijnis A, Seier JV, Heerden J, et al. (2007) Prenatal dexamethasone exposure induces changes in nonhuman primate offspring cardiometabolic and hypothalamic-pituitary-adrenal axis function. J Clin Invest 117: 1058-1067.
75. Nyirenda MJ, Carter R, Tang JI, de Vries A, Schlumbohm C, et al. (2009) Prenatal Programming of Metabolic Syndrome in the Common Marmoset Is Associated With Increased Expression of 11 beta-Hydroxysteroid Dehydrogenase Type 1. Diabetes 58: 2873-2879.
76. Long NM, Shasa DR, Ford SP, Nathanielsz PW (2012) Growth and insulin dynamics in two generations of female offspring of mothers receiving a single course of synthetic glucocorticoids. Am J Obstet Gynecol 207: 203 e201-208.
77. Iqbal M, Moisiadis VG, Kostaki A, Matthews SG (2012) Transgenerational effects of prenatal synthetic glucocorticoids on hypothalamic-pituitary-adrenal function. Endocrinology 153: 3295-3307.
78. Zambrano E, Martinez-Samayoa PM, Bautista CJ, Deas M, Guillen L, et al. (2005) Sex differences in transgenerational alterations of growth and metabolism in progeny (F2) of female offspring (F1) of rats fed a low protein diet during pregnancy and lactation. J Physiol 566: 225-236.
79. Benyshek DC, Johnston CS, Martin JF (2006) Glucose metabolism is altered in the adequately-nourished grand-offspring (F-3 generation) of rats malnourished during gestation and perinatal life. Diabetologia 49: 1117-1119.
80. Kaati G, Bygren LO, Edvinsson S (2002) Cardiovascular and diabetes mortality determined by nutrition during parents' and grandparents' slow growth period. Eur J Hum Genet 10: 682-688.
81. Pembrey ME, Bygren LO, Kaati G, Edvinsson S, Northstone K, et al. (2006) Sex-specific, male-line transgenerational responses in humans. Eur J Hum Genet 14: 159-166.
82. Painter RC, Osmond C, Gluckman P, Hanson M, Phillips DI, et al. (2008) Transgenerational effects of prenatal exposure to the Dutch famine on neonatal adiposity and health in later life. BJOG 115: 1243-1249.
83. Weber JE, Russell LD, Wong V, Peterson RN (1983) Three-dimensional reconstruction of a rat stage V Sertoli cell: II. Morphometry of Sertoli--Sertoli and Sertoli--germ-cell relationships. Am J Anat 167: 163-179.
84. Russell L (1977) Movement of spermatocytes from the basal to the adluminal compartment of the rat testis. Am J Anat 148: 313-328.
85. Hess RA, Renato de Franca L (2008) Spermatogenesis and cycle of the seminiferous epithelium. Adv Exp Med Biol 636: 1-15.
86. Ruwanpura SM, McLachlan RI, Meachem SJ (2010) Hormonal regulation of male germ cell development. Journal of Endocrinology 205: 117-131.
87. Zambrano E, Rodriguez-Gonzalez GL, Guzman C, Garcia-Becerra R, Boeck L, et al. (2005) A maternal low protein diet during pregnancy and lactation in the rat impairs male reproductive development. J Physiol 563: 275-284.
88. Ward IL, Ward OB, Affuso JD, Long WD, 3rd, French JA, et al. (2003) Fetal testosterone surge: specific modulations induced in male rats by maternal stress and/or alcohol consumption. Horm Behav 43: 531-539.
89. Ward IL, Stehm KE (1991) Prenatal stress feminizes juvenile play patterns in male rats. Physiol Behav 50: 601-605.

90. Hines M, Johnston KJ, Golombok S, Rust J, Stevens M, et al. (2002) Prenatal stress and gender role behavior in girls and boys: a longitudinal, population study. Horm Behav 42: 126-134.
91. Drake AJ, van den Driesche S, Scott HM, Hutchison GR, Seckl JR, et al. (2009) Glucocorticoids Amplify Dibutyl Phthalate-Induced Disruption of Testosterone Production and Male Reproductive Development. Endocrinology 150: 5055-5064.
92. Cronkhite JT, Norlander C, Furth JK, Levan G, Garbers DL, et al. (2005) Male and female germline specific expression of an EGFP reporter gene in a unique strain of transgenic rats. Dev Biol 284: 171-183.
93. Radford EJ, Ito M, Shi H, Corish JA, Yamazawa K, et al. (2014) In utero undernourishment perturbs the adult sperm methylome and intergenerational metabolism. Science 345.
94. Waddington CH (1952) The Epigenetics of Birds. Cambridge: At the University Press.
95. Berger SL, Kouzarides T, Shiekhattar R, Shilatifard A (2009) An operational definition of epigenetics. Genes & Development 23: 781-783.
96. Luger K, Mader AW, Richmond RK, Sargent DF, Richmond TJ (1997) Crystal structure of the nucleosome core particle at 2.8 angstrom resolution. Nature 389: 251-260.
97. Mcghee JD, Felsenfeld G (1980) Nucleosome Structure. Annual Review of Biochemistry 49: 1115-1156.
98. Beaujean N (2013) Histone post-translational modifications in preimplantation mouse embryos and their role in nuclear architecture. Mol Reprod Dev 81: 100-112.
99. Barski A, Cuddapah S, Cui K, Roh TY, Schones DE, et al. (2007) High-resolution profiling of histone methylations in the human genome. Cell 129: 823-837.
100. Allegrucci C, Thurston A, Lucas E, Young L (2005) Epigenetics and the germline. Reproduction 129: 137-149.
101. Esteller M (2011) Non-coding RNAs in human disease. Nature Reviews Genetics 12: 861-874.
102. Wheeler HLJTB (1904) 5-Methylcytosine. American Chemical Journal 31: 591-606.
103. Johnson TB, Coghill RD (1925) Researches on pyrimidines. CIII. The discovery of 5-methyl-cytosine in tuberculinic acid, the nucleic acid of the tubercle bacillus. Journal of the American Chemical Society 47: 2838-2844.
104. Hotchkiss RD (1948) The quantitative separation of purines, pyrimidines, and nucleosides by paper chromatography. J Biol Chem 175: 315-332.
105. Holliday R, Pugh JE (1975) DNA modification mechanisms and gene activity during development. Science 187: 226-232.
106. Riggs AD (1975) X inactivation, differentiation, and DNA methylation. Cytogenet Cell Genet 14: 9-25.
107. Capuano F, Mulleder M, Kok R, Blom HJ, Ralser M (2014) Cytosine DNA Methylation Is Found in Drosophila melanogaster but Absent in Saccharomyces cerevisiae, Schizosaccharomyces pombe, and Other Yeast Species. Analytical Chemistry 86: 3697-3702.

108. Lorincz MC, Dickerson DR, Schmitt M, Groudine M (2004) Intragenic DNA methylation alters chromatin structure and elongation efficiency in mammalian cells. Nat Struct Mol Biol 11: 1068-1075.
109. Fuks F, Hurd PJ, Wolf D, Nan XS, Bird AP, et al. (2003) The Methyl-CpG-binding protein MeCP2 links DNA methylation to histone methylation. Journal of Biological Chemistry 278: 4035-4040.
110. Wu SC, Zhang Y (2010) Active DNA demethylation: many roads lead to Rome. Nat Rev Mol Cell Biol 11: 607-620.
111. Deaton AM, Bird A (2011) CpG islands and the regulation of transcription. Genes Dev 25: 1010-1022.
112. Illingworth RS, Gruenewald-Schneider U, Webb S, Kerr AR, James KD, et al. (2010) Orphan CpG islands identify numerous conserved promoters in the mammalian genome. PLoS Genet 6: e1001134.
113. Irizarry RA, Ladd-Acosta C, Wen B, Wu ZJ, Montano C, et al. (2009) The human colon cancer methylome shows similar hypo- and hypermethylation at conserved tissue-specific CpG island shores. Nature Genetics 41: 178-186.
114. Ji H, Ehrlich LI, Seita J, Murakami P, Doi A, et al. (2010) Comprehensive methylome map of lineage commitment from haematopoietic progenitors. Nature 467: 338-342.
115. Ziller MJ, Muller F, Liao J, Zhang YY, Gu HC, et al. (2011) Genomic Distribution and Inter-Sample Variation of Non-CpG Methylation across Human Cell Types. Plos Genetics 7: e1002389.
116. Lister R, Pelizzola M, Dowen RH, Hawkins RD, Hon G, et al. (2009) Human DNA methylomes at base resolution show widespread epigenomic differences. Nature 462: 315-322.
117. Fouse SD, Shen Y, Pellegrini M, Cole S, Meissner A, et al. (2008) Promoter CpG methylation contributes to ES cell gene regulation in parallel with Oct4/Nanog, PcG complex, and histone H3 K4/K27 trimethylation. Cell Stem Cell 2: 160-169.
118. Sharp AJ, Stathaki E, Migliavacca E, Brahmachary M, Montgomery SB, et al. (2011) DNA methylation profiles of human active and inactive X chromosomes. Genome Res 21: 1592-1600.
119. Bala Tannan N, Brahmachary M, Garg P, Borel C, Alnefaie R, et al. (2014) DNA methylation profiling in X;autosome translocations supports a role for L1 repeats in the spread of X chromosome inactivation. Hum Mol Genet 23: 1224-1236.
120. Hellman A, Chess A (2007) Gene body-specific methylation on the active X chromosome. Science 315: 1141-1143.
121. Ollinger R, Reichmann J, Adams IR (2010) Meiosis and retrotransposon silencing during germ cell development in mice. Differentiation 79: 147-158.
122. Walsh CP, Chaillet JR, Bestor TH (1998) Transcription of IAP endogenous retroviruses is constrained by cytosine methylation. Nat Genet 20: 116-117.
123. Karimi MM, Goyal P, Maksakova IA, Bilenky M, Leung D, et al. (2011) DNA methylation and SETDB1/H3K9me3 regulate predominantly distinct sets of genes, retroelements, and chimeric transcripts in mESCs. Cell Stem Cell 8: 676-687.
124. Arnaud P (2010) Genomic imprinting in germ cells: imprints are under control. Reproduction 140: 411-423.

125. Haig D, Westoby M (1989) Parent-Specific Gene-Expression and the Triploid Endosperm. American Naturalist 134: 147-155.
126. Haig D (2004) Genomic imprinting and kinship: How good is the evidence? Annual Review of Genetics 38: 553-585.
127. Smits G, Mungall AJ, Griffiths-Jones S, Smith P, Beury D, et al. (2008) Conservation of the H19 noncoding RNA and H19-IGF2 imprinting mechanism in therians. Nat Genet 40: 971-976.
128. Haig D, Graham C (1991) Genomic imprinting and the strange case of the insulin-like growth factor II receptor. Cell 64: 1045-1046.
129. Haig D (2014) Coadaptation and conflict, misconception and muddle, in the evolution of genomic imprinting. Heredity 113: 96-103.
130. Arand J, Spieler D, Karius T, Branco MR, Meilinger D, et al. (2012) In Vivo Control of CpG and Non-CpG DNA Methylation by DNA Methyltransferases. Plos Genetics 8: e1002750.
131. Sharif J, Muto M, Takebayashi SI, Suetake I, Iwamatsu A, et al. (2007) The SRA protein Np95 mediates epigenetic inheritance by recruiting Dnmt1 to methylated DNA. Nature 450: 908-U925.
132. Li E, Bestor TH, Jaenisch R (1992) Targeted mutation of the DNA methyltransferase gene results in embryonic lethality. Cell 69: 915-926.
133. Howell CY, Bestor TH, Ding F, Latham KE, Mertineit C, et al. (2001) Genomic imprinting disrupted by a maternal effect mutation in the Dnmt1 gene. Cell 104: 829-838.
134. Mertineit C, Yoder JA, Taketo T, Laird DW, Trasler JM, et al. (1998) Sex-specific exons control DNA methyltransferase in mammalian germ cells. Development 125: 889-897.
135. Li E, Beard C, Jaenisch R (1993) Role for DNA methylation in genomic imprinting. Nature 366: 362-365.
136. Tahiliani M, Koh KP, Shen Y, Pastor WA, Bandukwala H, et al. (2009) Conversion of 5-methylcytosine to 5-hydroxymethylcytosine in mammalian DNA by MLL partner TET1. Science 324: 930-935.
137. Ito S, D'Alessio AC, Taranova OV, Hong K, Sowers LC, et al. (2010) Role of Tet proteins in 5mC to 5hmC conversion, ES-cell self-renewal and inner cell mass specification. Nature 466: 1129-1133.
138. Wyatt GR, Cohen SS (1952) A new pyrimidine base from bacteriophage nucleic acids. Nature 170: 1072-1073.
139. Penn NW, Suwalski R, O'Riley C, Bojanowski K, Yura R (1972) The presence of 5-hydroxymethylcytosine in animal deoxyribonucleic acid. Biochem J 126: 781-790.
140. Kothari RM, Shankar V (1976) 5-Methylcytosine content in the vertebrate deoxyribonucleic acids: species specificity. J Mol Evol 7: 325-329.
141. Kriaucionis S, Heintz N (2009) The nuclear DNA base 5-hydroxymethylcytosine is present in Purkinje neurons and the brain. Science 324: 929-930.
142. Moricova P, Ondrej V, Navratilova B, Luhova L (2013) Changes of DNA methylation and hydroxymethylation in plant protoplast cultures. Acta Biochim Pol 60: 33-36.
143. Yao Q, Song CX, He C, Kumaran D, Dunn JJ (2012) Heterologous expression and purification of Arabidopsis thaliana VIM1 protein: in vitro evidence for

its inability to recognize hydroxymethylcytosine, a rare base in Arabidopsis DNA. Protein Expr Purif 83: 104-111.
144. Erdmann RM, Souza AL, Clish CB, Gehring M (2015) 5-Hydroxymethylcytosine Is Not Present in Appreciable Quantities in Arabidopsis DNA. G3-Genes Genomes Genetics 5: 1-8.
145. Nestor CE, Ottaviano R, Reddington J, Sproul D, Reinhardt D, et al. (2012) Tissue type is a major modifier of the 5-hydroxymethylcytosine content of human genes. Genome Research 22: 467-477.
146. Williams K, Christensen J, Pedersen MT, Johansen JV, Cloos PA, et al. (2011) TET1 and hydroxymethylcytosine in transcription and DNA methylation fidelity. Nature 473: 343-348.
147. Ficz G, Branco MR, Seisenberger S, Santos F, Krueger F, et al. (2011) Dynamic regulation of 5-hydroxymethylcytosine in mouse ES cells and during differentiation. Nature 473: 398-402.
148. Dawlaty MM, Breiling A, Le T, Raddatz G, Barrasa MI, et al. (2013) Combined Deficiency of Tet1 and Tet2 Causes Epigenetic Abnormalities but Is Compatible with Postnatal Development. Developmental Cell 24: 310-323.
149. Ito S, Shen L, Dai Q, Wu SC, Collins LB, et al. (2011) Tet Proteins Can Convert 5-Methylcytosine to 5-Formylcytosine and 5-Carboxylcytosine. Science 333: 1300-1303.
150. He YF, Li BZ, Li Z, Liu P, Wang Y, et al. (2011) Tet-Mediated Formation of 5-Carboxylcytosine and Its Excision by TDG in Mammalian DNA. Science 333: 1303-1307.
151. Maiti A, Drohat AC (2011) Thymine DNA glycosylase can rapidly excise 5-formylcytosine and 5-carboxylcytosine: potential implications for active demethylation of CpG sites. J Biol Chem 286: 35334-35338.
152. Shen L, Wu H, Diep D, Yamaguchi S, D'Alessio AC, et al. (2013) Genome-wide Analysis Reveals TET- and TDG-Dependent 5-Methylcytosine Oxidation Dynamics. Cell 153: 692-706.
153. Nabel CS, Jia H, Ye Y, Shen L, Goldschmidt HL, et al. (2012) AID/APOBEC deaminases disfavor modified cytosines implicated in DNA demethylation. Nat Chem Biol 8: 751-758.
154. Penterman J, Zilberman D, Huh JH, Ballinger T, Henikoff S, et al. (2007) DNA demethylation in the Arabidopsis genome. Proceedings of the National Academy of Sciences of the United States of America 104: 6752-6757.
155. Tang Y, Xiong J, Jiang HP, Zheng SJ, Feng YQ, et al. (2014) Determination of oxidation products of 5-methylcytosine in plants by chemical derivatization coupled with liquid chromatography/tandem mass spectrometry analysis. Analytical Chemistry 86: 7764-7772.
156. Rose CM, van den Driesche S, Meehan RR, Drake AJ (2013) Epigenetic reprogramming: preparing the epigenome for the next generation. Biochem Soc Trans 41: 809-814.
157. Inoue A, Shen L, Dai Q, He C, Zhang Y (2011) Generation and replication-dependent dilution of 5fC and 5caC during mouse preimplantation development. Cell Research 21: 1670-1676.
158. Metivier R, Gallais R, Tiffoche C, Le Peron C, Jurkowska RZ, et al. (2008) Cyclical DNA methylation of a transcriptionally active promoter. Nature 452: 45-U42.

159. Bhutani N, Brady JJ, Damian M, Sacco A, Corbel SY, et al. (2010) Reprogramming towards pluripotency requires AID-dependent DNA demethylation. Nature 463: 1042-U1057.
160. Rai K, Huggins IJ, James SR, Karpf AR, Jones DA, et al. (2008) DNA Demethylation in Zebrafish Involves the Coupling of a Deaminase, a Glycosylase, and Gadd45. Cell 135: 1201-1212.
161. Hendrich B, Hardeland U, Ng HH, Jiricny J, Bird A (1999) The thymine glycosylase MBD4 can bind to the product of deamination at methylated CpG sites. Nature 401: 301-304.
162. Hashimoto H, Liu Y, Upadhyay AK, Chang Y, Howerton SB, et al. (2012) Recognition and potential mechanisms for replication and erasure of cytosine hydroxymethylation. Nucleic Acids Res 40: 4841-4849.
163. Bennett MT, Rodgers MT, Hebert AS, Ruslander LE, Eisele L, et al. (2006) Specificity of human thymine DNA glycosylase depends on N-glycosidic bond stability. Journal of the American Chemical Society 128: 12510-12519.
164. Guo JU, Su Y, Zhong C, Ming GL, Song H (2011) Hydroxylation of 5-methylcytosine by TET1 promotes active DNA demethylation in the adult brain. Cell 145: 423-434.
165. Boorstein RJ, Cummings A, Marenstein DR, Chan MK, Ma YL, et al. (2001) Definitive identification of mammalian 5-hydroxymethyluracil DNA N-glycosylase activity as SMUG1. Journal of Biological Chemistry 276: 41991-41997.
166. Popp C, Dean W, Feng SH, Cokus SJ, Andrews S, et al. (2010) Genome-wide erasure of DNA methylation in mouse primordial germ cells is affected by AID deficiency. Nature 463: 1101-1105.
167. Inoue A, Zhang Y (2011) Replication-Dependent Loss of 5-Hydroxymethylcytosine in Mouse Preimplantation Embryos. Science 334: 194-194.
168. Iqbal K, Jin SG, Pfeifer GP, Szabo PE (2011) Reprogramming of the paternal genome upon fertilization involves genome-wide oxidation of 5-methylcytosine. Proceedings of the National Academy of Sciences of the United States of America 108: 3642-3647.
169. Wang L, Zhang J, Duan J, Gao X, Zhu W, et al. (2014) Programming and Inheritance of Parental DNA Methylomes in Mammals. Cell 157: 979-991.
170. Gu TP, Guo F, Yang H, Wu HP, Xu GF, et al. (2011) The role of Tet3 DNA dioxygenase in epigenetic reprogramming by oocytes. Nature 477: 606-612.
171. Raiber EA, Beraldi D, Ficz G, Burgess HE, Branco MR, et al. (2012) Genome-wide distribution of 5-formylcytosine in embryonic stem cells is associated with transcription and depends on thymine DNA glycosylase. Genome Biol 13: R69.
172. Lane N, Dean W, Erhardt S, Hajkova P, Surani A, et al. (2003) Resistance of IAPs to methylation reprogramming may provide a mechanism for epigenetic inheritance in the mouse. Genesis 35: 88-93.
173. De Felici M (2011) Nuclear reprogramming in mouse primordial germ cells: epigenetic contribution. Stem Cells Int 2011: 425863.
174. Saitou M, Barton SC, Surani MA (2002) A molecular programme for the specification of germ cell fate in mice. Nature 418: 293-300.

175. Molyneaux KA, Stallock J, Schaible K, Wylie C (2001) Time-lapse analysis of living mouse germ cell migration. Dev Biol 240: 488-498.
176. Shovlin TC, Durcova-Hills G, Surani A, McLaren A (2008) Heterogeneity in imprinted methylation patterns of pluripotent embryonic germ cells derived from pre-migratory mouse germ cells. Dev Biol 313: 674-681.
177. Lee J, Inoue K, Ono R, Ogonuki N, Kohda T, et al. (2002) Erasing genomic imprinting memory in mouse clone embryos produced from day 11.5 primordial germ cells. Development 129: 1807-1817.
178. Yamazaki Y, Mann MR, Lee SS, Marh J, McCarrey JR, et al. (2003) Reprogramming of primordial germ cells begins before migration into the genital ridge, making these cells inadequate donors for reproductive cloning. Proc Natl Acad Sci U S A 100: 12207-12212.
179. Hackett JA, Reddington JP, Nestor CE, Dunican DS, Branco MR, et al. (2012) Promoter DNA methylation couples genome-defence mechanisms to epigenetic reprogramming in the mouse germline. Development 139: 3623-3632.
180. Guibert S, Forne T, Weber M (2012) Global profiling of DNA methylation erasure in mouse primordial germ cells. Genome Research 22: 633-641.
181. Seki Y, Hayashi K, Itoh K, Mizugaki M, Saitou M, et al. (2005) Extensive and orderly reprogramming of genome-wide chromatin modifications associated with specification and early development of germ cells in mice. Developmental Biology 278: 440-458.
182. Hajkova P, Jeffries SJ, Lee C, Miller N, Jackson SP, et al. (2010) Genome-Wide Reprogramming in the Mouse Germ Line Entails the Base Excision Repair Pathway. Science 329: 78-82.
183. Hackett JA, Sengupta R, Zylicz JJ, Murakami K, Lee C, et al. (2013) Germline DNA Demethylation Dynamics and Imprint Erasure Through 5-Hydroxymethylcytosine. Science 339: 448-452.
184. Lees-Murdock DJ, De Felici M, Walsh CP (2003) Methylation dynamics of repetitive DNA elements in the mouse germ cell lineage. Genomics 82: 230-237.
185. Cortellino S, Xu J, Sannai M, Moore R, Caretti E, et al. (2011) Thymine DNA glycosylase is essential for active DNA demethylation by linked deamination-base excision repair. Cell 146: 67-79.
186. Kagiwada S, Kurimoto K, Hirota T, Yamaji M, Saitou M (2013) Replication-coupled passive DNA demethylation for the erasure of genome imprints in mice. Embo Journal 32: 340-353.
187. Seisenberger S, Andrews S, Krueger F, Arand J, Walter J, et al. (2012) The Dynamics of Genome-wide DNA Methylation Reprogramming in Mouse Primordial Germ Cells. Mol Cell 48: 1-14.
188. Messerschmidt DM, Knowles BB, Solter D (2014) DNA methylation dynamics during epigenetic reprogramming in the germline and preimplantation embryos. Genes & Development 28: 812-828.
189. Quenneville S, Verde G, Corsinotti A, Kapopoulou A, Jakobsson J, et al. (2011) In embryonic stem cells, ZFP57/KAP1 recognize a methylated hexanucleotide to affect chromatin and DNA methylation of imprinting control regions. Mol Cell 44: 361-372.

190. Li XJ, Ito M, Zhou F, Youngson N, Zuo XP, et al. (2008) A Maternal-Zygotic Effect Gene, Zfp57, Maintains Both Maternal and Paternal Imprints. Developmental Cell 15: 547-557.
191. Qin CH, Wang ZB, Shang J, Bekkari K, Liu R, et al. (2010) Intracisternal A Particle Genes: Distribution in the Mouse Genome, Active Subtypes, and Potential Roles as Species-Specific Mediators of Susceptibility to Cancer. Molecular Carcinogenesis 49: 54-67.
192. Reichmann J, Crichton JH, Madej MJ, Taggart M, Gautier P, et al. (2012) Microarray Analysis of LTR Retrotransposon Silencing Identifies Hdac1 as a Regulator of Retrotransposon Expression in Mouse Embryonic Stem Cells. Plos Computational Biology 8: 1-21.
193. Lopes SMCD, Hayashi K, Shovlin TC, Mifsud W, Surani MA, et al. (2008) X chromosome activity in mouse XX primordial germ cells. Plos Genetics 4: e30.
194. Seki Y, Yamaji M, Yabuta Y, Sano M, Shigeta M, et al. (2007) Cellular dynamics associated with the genome-wide epigenetic reprogramming in migrating primordial germ cells in mice. Development 134: 2627-2638.
195. Tachibana M, Matsumura Y, Fukuda M, Kimura H, Shinkai Y (2008) G9a/GLP complexes independently mediate H3K9 and DNA methylation to silence transcription. EMBO J 27: 2681-2690.
196. Li JY, Lees-Murdock DJ, Xu GL, Walsh CP (2004) Timing of establishment of paternal methylation imprints in the mouse. Genomics 84: 952-960.
197. Lucifero D, Mertineit C, Clarke HJ, Bestor TH, Trasler JM (2002) Methylation dynamics of imprinted genes in mouse germ cells. Genomics 79: 530-538.
198. Davis TL, Yang GJ, McCarrey JR, Bartolomei MS (2000) The H19 methylation imprint is erased and re-established differentially on the parental alleles during male germ cell development. Human Molecular Genetics 9: 2885-2894.
199. Kaneda M, Sado T, Hata K, Okano M, Tsujimoto N, et al. (2004) Role of de novo DNA methyltransferases in initiation of genomic imprinting and X-chromosome inactivation. Cold Spring Harb Symp Quant Biol 69: 125-129.
200. Kato Y, Kaneda M, Hata K, Kumaki K, Hisano M, et al. (2007) Role of the Dnmt3 family in de novo methylation of imprinted and repetitive sequences during male germ cell development in the mouse. Human Molecular Genetics 16: 2272-2280.
201. Gowher H, Liebert K, Hermann A, Xu GL, Jeltsch A (2005) Mechanism of stimulation of catalytic activity of Dnmt3A and Dnmt3B DNA-(cytosine-C5)-methyltransferases by Dnmt3L. Journal of Biological Chemistry 280: 13341-13348.
202. Niles KM, Chan D, La Salle S, Oakes CC, Trasler JM (2011) Critical period of nonpromoter DNA methylation acquisition during prenatal male germ cell development. PLoS One 6: 1-11.
203. La Salle S, Mertineit C, Taketo T, Moens PB, Bestor TH, et al. (2004) Windows for sex-specific methylation marked by DNA methyltransferase expression profiles in mouse germ cells. Dev Biol 268: 403-415.
204. Lucifero D, La Salle S, Bourc'his D, Martel J, Bestor TH, et al. (2007) Coordinate regulation of DNA methyltransferase expression during oogenesis. Bmc Developmental Biology 7: 36.

205. Kaneda M, Hirasawa R, Chiba H, Okano M, Li E, et al. (2010) Genetic evidence for Dnmt3a-dependent imprinting during oocyte growth obtained by conditional knockout with Zp3-Cre and complete exclusion of Dnmt3b by chimera formation. Genes Cells 15: 169-179.
206. Hyldig SMW, Croxall N, Contreras DA, Thomsen PD, Alberio R (2011) Epigenetic reprogramming in the porcine germ line (vol 11, 11, 2011). Bmc Developmental Biology 11: 1-11.
207. Almstrup K, Nielsen JE, Mlynarska O, Jansen MT, Jorgensen A, et al. (2010) Carcinoma in situ testis displays permissive chromatin modifications similar to immature foetal germ cells. Br J Cancer 103: 1269-1276.
208. Sonne SB, Almstrup K, Dalgaard M, Juncker AS, Edsgard D, et al. (2009) Analysis of Gene Expression Profiles of Microdissected Cell Populations Indicates that Testicular Carcinoma In situ Is an Arrested Gonocyte. Cancer Research 69: 5241-5250.
209. Wermann H, Stoop H, Gillis AJ, Honecker F, van Gurp RJ, et al. (2010) Global DNA methylation in fetal human germ cells and germ cell tumours: association with differentiation and cisplatin resistance. J Pathol 221: 433-442.
210. Molaro A, Hodges E, Fang F, Song Q, McCombie WR, et al. (2011) Sperm methylation profiles reveal features of epigenetic inheritance and evolution in primates. Cell 146: 1029-1041.
211. Hammoud SS, Low DH, Yi C, Carrell DT, Guccione E, et al. (2014) Chromatin and transcription transitions of mammalian adult germline stem cells and spermatogenesis. Cell Stem Cell 15: 239-253.
212. Yamaguchi S, Shen L, Liu YT, Sendler D, Zhang Y (2013) Role of Tet1 in erasure of genomic imprinting. Nature 504: 460-464.
213. Lambrot R, Xu C, Saint-Phar S, Chountalos G, Cohen T, et al. (2013) Low paternal dietary folate alters the mouse sperm epigenome and is associated with negative pregnancy outcomes. Nature Communications 4: e2889.
214. Carone BR, Fauquier L, Habib N, Shea JM, Hart CE, et al. (2010) Paternally Induced Transgenerational Environmental Reprogramming of Metabolic Gene Expression in Mammals. Cell 143: 1084-1096.
215. Anway MD, Cupp AS, Uzumcu M, Skinner MK (2005) Epigenetic transgenerational actions of endocrine disruptors and male fertility. Science 308: 1466-1469.
216. Anway MD, Memon MA, Uzumcu M, Skinner MK (2006) Transgenerational effect of the endocrine disruptor vinclozolin on male spermatogenesis. J Androl 27: 868-879.
217. Anway MD, Leathers C, Skinner MK (2006) Endocrine disruptor vinclozolin induced epigenetic transgenerational adult-onset disease. Endocrinology 147: 5515-5523.
218. Anway MD, Rekow SS, Skinner MK (2008) Transgenerational epigenetic programming of the embryonic testis transcriptome. Genomics 91: 30-40.
219. Guerrero-Bosagna C, Settles M, Lucker B, Skinner MK (2010) Epigenetic Transgenerational Actions of Vinclozolin on Promoter Regions of the Sperm Epigenome. PLoS One 5: e13100.
220. Guerrero-Bosagna C, Covert TR, Haque MM, Settles M, Nilsson EE, et al. (2012) Epigenetic transgenerational inheritance of vinclozolin induced mouse

adult onset disease and associated sperm epigenome biomarkers. Reprod Toxicol 34: 694-707.
221. Schneider S, Kaufmann W, Buesen R, van Ravenzwaay B (2008) Vinclozolin--the lack of a transgenerational effect after oral maternal exposure during organogenesis. Reprod Toxicol 25: 352-360.
222. Wei YC, Yang CR, Wei YP, Zhao ZA, Hou Y, et al. (2014) Paternally induced transgenerational inheritance of susceptibility to diabetes in mammals. Proceedings of the National Academy of Sciences of the United States of America 111: 1873-1878.
223. Franklin TB, Russig H, Weiss IC, Graff J, Linder N, et al. (2010) Epigenetic Transmission of the Impact of Early Stress Across Generations. Biological Psychiatry 68: 408-415.
224. Boissonnas CC, Abdalaoui HE, Haelewyn V, Fauque P, Dupont JM, et al. (2010) Specific epigenetic alterations of IGF2-H19 locus in spermatozoa from infertile men. Eur J Hum Genet 18: 73-80.
225. Poplinski A, Tuttelmann F, Kanber D, Horsthemke B, Gromoll J (2010) Idiopathic male infertility is strongly associated with aberrant methylation of MEST and IGF2/H19 ICR1. International Journal of Andrology 33: 642-649.
226. Hammoud SS, Purwar J, Pflueger C, Cairns BR, Carrell DT (2010) Alterations in sperm DNA methylation patterns at imprinted loci in two classes of infertility. Fertility and Sterility 94: 1728-1733.
227. Marques CJ, Costa P, Vaz B, Carvalho F, Fernandes S, et al. (2008) Abnormal methylation of imprinted genes in human sperm is associated with oligozoospermia. Mol Hum Reprod 14: 67-74.
228. El Hajj N, Pliushch G, Schneider E, Dittrich M, Muller T, et al. (2013) Metabolic programming of MEST DNA methylation by intrauterine exposure to gestational diabetes mellitus. Diabetes 62: 1320-1328.
229. Bliek J, Terhal P, van den Bogaard MJ, Maas S, Hamel B, et al. (2006) Hypomethylation of the h19 gene causes not only Silver-Russell syndrome (SRS) but also isolated asymmetry or an SRS-like phenotype. American Journal of Human Genetics 78: 604-614.
230. Marcon L, Boissonneault G (2004) Transient DNA strand breaks during mouse and human spermiogenesis new insights in stage specificity and link to chromatin remodeling. Biology of Reproduction 70: 910-918.
231. Rathke C, Baarends WM, Awe S, Renkawitz-Pohl R (2014) Chromatin dynamics during spermiogenesis. Biochim Biophys Acta 1839: 155-168.
232. Balhorn R, Gledhill BL, Wyrobek AJ (1977) Mouse sperm chromatin proteins: quantitative isolation and partial characterization. Biochemistry 16: 4074-4080.
233. Bench GS, Friz AM, Corzett MH, Morse DH, Balhorn R (1996) DNA and total protamine masses in individual sperm from fertile mammalian subjects. Cytometry 23: 263-271.
234. Erkek S, Hisano M, Liang CY, Gill M, Murr R, et al. (2013) Molecular determinants of nucleosome retention at CpG-rich sequences in mouse spermatozoa. Nat Struct Mol Biol 20: 868-875.
235. Hammoud SS, Nix DA, Zhang H, Purwar J, Carrell DT, et al. (2009) Distinctive chromatin in human sperm packages genes for embryo development. Nature 460: 473-478.

236. Carone BR, Hung JH, Hainer SJ, Chou MT, Carone DM, et al. (2014) High-resolution mapping of chromatin packaging in mouse embryonic stem cells and sperm. Dev Cell 30: 11-22.
237. Samans B, Yang Y, Krebs S, Sarode GV, Blum H, et al. (2014) Uniformity of nucleosome preservation pattern in Mammalian sperm and its connection to repetitive DNA elements. Dev Cell 30: 23-35.
238. Palmer NO, Fullston T, Mitchell M, Setchell BP, Lane M (2011) SIRT6 in mouse spermatogenesis is modulated by diet-induced obesity. Reproduction Fertility and Development 23: 929-939.
239. Ostermeier GC, Dix DJ, Miller D, Khatri P, Krawetz SA (2002) Spermatozoal RNA profiles of normal fertile men. Lancet 360: 772-777.
240. Kawano M, Kawaji H, Grandjean V, Kiani J, Rassoulzadegan M (2012) Novel Small Noncoding RNAs in Mouse Spermatozoa, Zygotes and Early Embryos. PLoS One 7: e44542.
241. Gapp K, Jawaid A, Sarkies P, Bohacek J, Pelczar P, et al. (2014) Implication of sperm RNAs in transgenerational inheritance of the effects of early trauma in mice. Nat Neurosci 17: 667-669.
242. Grandjean V, Gounon P, Wagner N, Martin L, Wagner KD, et al. (2009) The miR-124-Sox9 paramutation: RNA-mediated epigenetic control of embryonic and adult growth. Development 136: 3647-3655.
243. Rassoulzadegan M, Grandjean V, Gounon P, Vincent S, Gillot I, et al. (2006) RNA-mediated non-mendelian inheritance of an epigenetic change in the mouse. Nature 441: 469-474.
244. Wagner KD, Wagner N, Ghanbarian H, Grandjean V, Gounon P, et al. (2008) RNA induction and inheritance of epigenetic cardiac hypertrophy in the mouse. Dev Cell 14: 962-969.
245. Wurster B, Hess B (1973) The reaction of hexokinase with equilibrated D-glucose. Eur J Biochem 36: 68-71.
246. Fleige S, Pfaffl MW (2006) RNA integrity and the effect on the real-time qRT-PCR performance. Mol Aspects Med 27: 126-139.
247. Griffin J (2013) Methods of Sperm DNA Extraction for Genetic and Epigenetic Studies. In: Carrell DT, Aston KI, editors. Spermatogenesis: Humana Press. pp. 379-384.
248. Weyrich A (2012) Preparation of genomic DNA from mammalian sperm. Curr Protoc Mol Biol Chapter 2: Unit 2 13 11-13.
249. Rose CM, van den Driesche S, Sharpe RM, Meehan RR, Drake AJ (2014) Dynamic changes in DNA modification states during late gestation male germ line development in the rat. Epigenetics & Chromatin 7: 1-15.
250. Hefler LA, Tempfer CB, Moreno RM, O'Brien WE, Gregg AR (2001) Endothelial-derived nitric oxide and angiotensinogen: blood pressure and metabolism during mouse pregnancy. Am J Physiol Regul Integr Comp Physiol 280: R174-182.
251. Kafri T, Ariel M, Brandeis M, Shemer R, Urven L, et al. (1992) Developmental pattern of gene-specific DNA methylation in the mouse embryo and germ line. Genes Dev 6: 705-714.
252. Nakashima H, Kimura T, Kaga Y, Nakatani T, Seki Y, et al. (2013) Effects of dppa3 on DNA methylation dynamics during primordial germ cell development in mice. Biology of Reproduction 88: 1-9.

253. Iurlaro M, Ficz G, Oxley D, Raiber EA, Bachman M, et al. (2013) A screen for hydroxymethylcytosine and formylcytosine binding proteins suggests functions in transcription and chromatin regulation. Genome Biol 14: R119.
254. Hutchison GR, Scott HM, Walker M, McKinnell C, Ferrara D, et al. (2008) Sertoli cell development and function in an animal model of testicular dysgenesis syndrome. Biology of Reproduction 78: 352-360.
255. Sharpe RM, McKinnell C, Kivlin C, Fisher JS (2003) Proliferation and functional maturation of Sertoli cells, and their relevance to disorders of testis function in adulthood. Reproduction 125: 769-784.
256. Kimmins S, Sassone-Corsi P (2005) Chromatin remodelling and epigenetic features of germ cells. Nature 434: 583-589.
257. Okano M, Bell DW, Haber DA, Li E (1999) DNA methyltransferases Dnmt3a and Dnmt3b are essential for de novo methylation and mammalian development. Cell 99: 247-257.
258. Hata K, Okano M, Lei H, Li E (2002) Dnmt3L cooperates with the Dnmt3 family of de novo DNA methyltransferases to establish maternal imprints in mice. Development 129: 1983-1993.
259. Jobling MS, Hutchison GR, van den Driesche S, Sharpe RM (2011) Effects of di(n-butyl) phthalate exposure on foetal rat germ-cell number and differentiation: identification of age-specific windows of vulnerability. International Journal of Andrology 34: E386-E396.
260. Kaneda M, Okano M, Hata K, Sado T, Tsujimoto N, et al. (2004) Essential role for de novo DNA methyltransferase Dnmt3a in paternal and maternal imprinting. Nature 429: 900-903.
261. Weber MA, Groos S, Hopfl U, Spielmann M, Aumuller G, et al. (2000) Glucocorticoid receptor distribution in rat testis during postnatal development and effects of dexamethasone on immature peritubular cells in vitro. Andrologia 32: 23-30.
262. Levy FO, Ree AH, Eikvar L, Govindan MV, Jahnsen T, et al. (1989) Glucocorticoid receptors and glucocorticoid effects in rat sertoli cells. Endocrinology 124: 430-436.
263. Hazra R, Upton D, Jimenez M, Desai R, Handelsman DJ, et al. (2014) In vivo actions of the Sertoli cell glucocorticoid receptor. Endocrinology 155: en20131940.
264. Li L, Wong CK (2008) Effects of dexamethasone and dibutyryl cAMP on stanniocalcin-1 mRNA expression in rat primary Sertoli and Leydig cells. Mol Cell Endocrinol 283: 96-103.
265. Lim K, Yoon S, Lee M, Byun S, Kweon G, et al. (1996) Glucocorticoid regulation of androgen binding protein expression in primary sertoli cell cultures from rats. Biochem Biophys Res Commun 218: 490-494.
266. Gluckman PD, Hanson MA, Buklijas T, Low FM, Beedle AS (2009) Epigenetic mechanisms that underpin metabolic and cardiovascular diseases. Nat Rev Endocrinol 5: 401-408.
267. Thomassin H, Flavin M, Espinas ML, Grange T (2001) Glucocorticoid-induced DNA demethylation and gene memory during development. EMBO J 20: 1974-1983.
268. Ollinger R, Childs AJ, Burgess HM, Speed RM, Lundegaard PR, et al. (2008) Deletion of the pluripotency-associated Tex19.1 gene causes activation of

endogenous retroviruses and defective spermatogenesis in mice. PLoS Genet 4: e1000199.
269. Okano M, Takebayashi S, Okumura K, Li E (1999) Assignment of cytosine-5 DNA methyltransferases Dnmt3a and Dnmt3b to mouse chromosome bands 12A2-A3 and 2H1 by in situ hybridization. Cytogenet Cell Genet 86: 333-334.
270. Sharma D, Bhave S, Gregg E, Uht R (2013) Dexamethasone induces a putative repressor complex and chromatin modifications in the CRH promoter. Mol Endocrinol 27: 1142-1152.
271. Schmidt M, Sangild PT, Blum JW, Andersen JB, Greve T (2004) Combined ACTH and glucocorticoid treatment improves survival and organ maturation in premature newborn calves. Theriogenology 61: 1729-1744.
272. Roberts D, Dalziel SR (2006) Antenatal corticosteroids for accelerating fetal lung maturation for women at risk of preterm birth. Cochrane Database Syst Rev 3: CD004454.
273. Neves FM, Paccola CC, Miraglia SM, Cipriano I (2013) Morphometric evaluation of the fetal rat liver after maternal dexamethasone treatment: effect on the maturation of erythroid and megakaryocytic cells. Vet Clin Pathol 42: 483-489.
274. Meissner A, Gnirke A, Bell GW, Ramsahoye B, Lander ES, et al. (2005) Reduced representation bisulfite sequencing for comparative high-resolution DNA methylation analysis. Nucleic Acids Res 33: 5868-5877.
275. Gu H, Smith ZD, Bock C, Boyle P, Gnirke A, et al. (2011) Preparation of reduced representation bisulfite sequencing libraries for genome-scale DNA methylation profiling. Nat Protoc 6: 468-481.
276. Guo JU, Su Y, Shin JH, Shin J, Li H, et al. (2014) Distribution, recognition and regulation of non-CpG methylation in the adult mammalian brain. Nat Neurosci 17: 215-222.
277. Herman JG, Graff JR, Myohanen S, Nelkin BD, Baylin SB (1996) Methylation-specific PCR: A novel PCR assay for methylation status of CpG islands. Proceedings of the National Academy of Sciences of the United States of America 93: 9821-9826.
278. Akalin A, Garrett-Bakelman FE, Kormaksson M, Busuttil J, Zhang L, et al. (2012) Base-pair resolution DNA methylation sequencing reveals profoundly divergent epigenetic landscapes in acute myeloid leukemia. PLoS Genet 8: e1002781.
279. Hebestreit K, Dugas M, Klein HU (2013) Detection of significantly differentially methylated regions in targeted bisulfite sequencing data. Bioinformatics 29: 1647-1653.
280. Shiota K, Kogo Y, Ohgane J, Imamura T, Urano A, et al. (2002) Epigenetic marks by DNA methylation specific to stem, germ and somatic cells in mice. Genes Cells 7: 961-969.
281. Shirakawa R, Fukai S, Kawato M, Higashi T, Kondo H, et al. (2009) Tuberous Sclerosis Tumor Suppressor Complex-like Complexes Act as GTPase-activating Proteins for Ral GTPases. Journal of Biological Chemistry 284: 21580-21588.

282. Chen XW, Leto D, Xiong T, Yu G, Cheng A, et al. (2011) A Ral GAP complex links PI 3-kinase/Akt signaling to RalA activation in insulin action. Molecular Biology of the Cell 22: 141-152.
283. Karunanithi S, Xiong T, Uhm M, Leto D, Sun J, et al. (2014) A Rab10:RalA G protein cascade regulates insulin-stimulated glucose uptake in adipocytes. Molecular Biology of the Cell 25: 3059-3069.
284. Kuang B, Wu SC, Shin Y, Luo L, Kolodziej P (2000) split ends encodes large nuclear proteins that regulate neuronal cell fate and axon extension in the Drosophila embryo. Development 127: 1517-1529.
285. Ariyoshi M, Schwabe JW (2003) A conserved structural motif reveals the essential transcriptional repression function of Spen proteins and their role in developmental signaling. Genes Dev 17: 1909-1920.
286. Kuroda K, Han H, Tani S, Tanigaki K, Tun T, et al. (2003) Regulation of marginal zone B cell development by MINT, a suppressor of Notch/RBP-J signaling pathway. Immunity 18: 301-312.
287. Zhao B, Lu J, Yin J, Liu H, Guo X, et al. (2012) A functional polymorphism in PER3 gene is associated with prognosis in hepatocellular carcinoma. Liver Int 32: 1451-1459.
288. Lin YM, Chang JH, Yeh KT, Yang MY, Li TC, et al. (2008) Disturbance of Circadian Gene Expression in Hepatocellular Carcinoma. Molecular Carcinogenesis 47: 925-933.
289. Balsalobre A, Brown SA, Marcacci L, Tronche F, Kellendonk C, et al. (2000) Resetting of circadian time in peripheral tissues by glucocorticoid signaling. Science 289: 2344-2347.
290. Kikuchi M, Doi E, Tsujimoto I, Horibe T, Tsujimoto Y (2002) Functional analysis of human P5, a protein disulfide isomerase homologue. J Biochem 132: 451-455.
291. Groenendyk J, Peng ZL, Dudek E, Fan X, Mizianty MJ, et al. (2014) Interplay Between the Oxidoreductase PDIA6 and microRNA-322 Controls the Response to Disrupted Endoplasmic Reticulum Calcium Homeostasis. Science Signaling 7.
292. Epping MT, Wang LM, Edel MJ, Carlee L, Hernandez M, et al. (2005) The human tumor antigen repressor of retinoic acid PRAME is a dominant receptor signaling. Cell 122: 835-847.
293. Mistry BV, Zhao Y, Chang TC, Yasue H, Chiba M, et al. (2013) Differential expression of PRAMEL1, a cancer/testis antigen, during spermatogenesis in the mouse. PLoS One 8: e60611.
294. Einstein F, Thompson RF, Bhagat TD, Fazzari MJ, Verma A, et al. (2010) Cytosine methylation dysregulation in neonates following intrauterine growth restriction. PLoS One 5: e8887.
295. Murrell A, Ito Y, Verde G, Huddleston J, Woodfine K, et al. (2008) Distinct Methylation Changes at the IGF2-H19 Locus in Congenital Growth Disorders and Cancer. PLoS One 3: e1849.
296. Nestor C, Ruzov A, Meehan R, Dunican D (2010) Enzymatic approaches and bisulfite sequencing cannot distinguish between 5-methylcytosine and 5-hydroxymethylcytosine in DNA. Biotechniques 48: 317-319.
297. Weber M, Davies JJ, Wittig D, Oakeley EJ, Haase M, et al. (2005) Chromosome-wide and promoter-specific analyses identify sites of

differential DNA methylation in normal and transformed human cells. Nat Genet 37: 853-862.
298. Bechmann LP, Hannivoort RA, Gerken G, Hotamisligil GS, Trauner M, et al. (2012) The interaction of hepatic lipid and glucose metabolism in liver diseases. J Hepatol 56: 952-964.
299. Bertram C, Trowern AR, Copin N, Jackson AA, Whorwood CB (2001) The maternal diet during pregnancy programs altered expression of the glucocorticoid receptor and type 2 11beta-hydroxysteroid dehydrogenase: potential molecular mechanisms underlying the programming of hypertension in utero. Endocrinology 142: 2841-2853.
300. Welberg LA, Seckl JR, Holmes MC (2000) Inhibition of 11beta-hydroxysteroid dehydrogenase, the foeto-placental barrier to maternal glucocorticoids, permanently programs amygdala GR mRNA expression and anxiety-like behaviour in the offspring. Eur J Neurosci 12: 1047-1054.
301. Paterson JM, Morton NM, Fievet C, Kenyon CJ, Holmes MC, et al. (2004) Metabolic syndrome without obesity: Hepatic overexpression of 11 beta-hydroxysteroid dehydrogenase type 1 in transgenic mice. Proceedings of the National Academy of Sciences of the United States of America 101: 7088-7093.
302. Morton NM, Holmes MC, Fievet C, Staels B, Tailleux A, et al. (2001) Improved lipid and lipoprotein profile, hepatic insulin sensitivity, and glucose tolerance in 11beta-hydroxysteroid dehydrogenase type 1 null mice. J Biol Chem 276: 41293-41300.
303. Livingstone DE, Jones GC, Smith K, Jamieson PM, Andrew R, et al. (2000) Understanding the role of glucocorticoids in obesity: tissue-specific alterations of corticosterone metabolism in obese Zucker rats. Endocrinology 141: 560-563.
304. Prasad SSSV, Prashanth A, Kumar CP, Reddy SJ, Giridharan NV, et al. (2010) A novel genetically-obese rat model with elevated 11beta-hydroxysteroid dehydrogenase type 1 activity in subcutaneous adipose tissue. Lipids in Health and Disease 9: 1-6.
305. Andrews SC, Wood MD, Tunster SJ, Barton SC, Surani MA, et al. (2007) Cdkn1c (p57Kip2) is the major regulator of embryonic growth within its imprinted domain on mouse distal chromosome 7. BMC Dev Biol 7: 53.
306. Charalambous M, Cowley M, Geoghegan F, Smith FM, Radford EJ, et al. (2010) Maternally-inherited Grb10 reduces placental size and efficiency. Dev Biol 337: 1-8.
307. DeChiara TM, Efstratiadis A, Robertson EJ (1990) A growth-deficiency phenotype in heterozygous mice carrying an insulin-like growth factor II gene disrupted by targeting. Nature 345: 78-80.
308. DeChiara TM, Robertson EJ, Efstratiadis A (1991) Parental imprinting of the mouse insulin-like growth factor II gene. Cell 64: 849-859.
309. Charalambous M, Smith FM, Bennett WR, Crew TE, Mackenzie F, et al. (2003) Disruption of the imprinted Grb10 gene leads to disproportionate overgrowth by an Igf2-independent mechanism. Proc Natl Acad Sci U S A 100: 8292-8297.

310. Li YM, Franklin G, Cui HM, Svensson K, He XB, et al. (1998) The H19 transcript is associated with polysomes and may regulate IGF2 expression in trans. Journal of Biological Chemistry 273: 28247-28252.
311. Tran VG, Court F, Duputie A, Antoine E, Aptel N, et al. (2012) H19 Antisense RNA Can Up-Regulate Igf2 Transcription by Activation of a Novel Promoter in Mouse Myoblasts. PLoS One 7: e37923.
312. Vonesch JL, Nakshatri H, Philippe M, Chambon P, Dolle P (1994) Stage and Tissue-Specific Expression of the Alcohol-Dehydrogenase 1 (Adh-1) Gene during Mouse Development. Developmental Dynamics 199: 199-213.
313. Zile MH (2001) Function of vitamin A in vertebrate embryonic development. Journal of Nutrition 131: 705-708.
314. White JC, Shankar VN, Highland M, Epstein ML, DeLuca PF, et al. (1998) Defects in embryonic hindbrain development and fetal resorption resulting from vitamin A deficiency in the rat are prevented by feeding pharmacological levels of all-trans-retinoic acid. Proceedings of the National Academy of Sciences of the United States of America 95: 13459-13464.
315. Rothman KJ, Moore LL, Singer MR, Nguyen USDT, Mannino S, et al. (1995) Teratogenicity of High Vitamin-a Intake. New England Journal of Medicine 333: 1369-1373.
316. Estonius M, Svensson S, Hoog JO (1996) Alcohol dehydrogenase in human tissues: Localisation of transcripts coding for five classes of the enzyme. Febs Letters 397: 338-342.
317. Aasmoe L, Aarbakke J (1999) Sex-dependent induction of alcohol dehydrogenase activity in rats. Biochemical Pharmacology 57: 1067-1072.
318. Pallier C, Scaffidi P, Chopineau-Proust S, Agresti A, Nordmann P, et al. (2003) Association of chromatin proteins high mobility group box (HMGB) 1 and HMGB2 with mitotic chromosomes. Molecular Biology of the Cell 14: 3414-3426.
319. Thomas JO, Travers AA (2001) HMG1 and 2, and related 'architectural' DNA-binding proteins. Trends in Biochemical Sciences 26: 167-174.
320. Yamazaki F, Nagatsuka Y, Shirakawa H, Yoshida M (1995) Repression of Cell-Cycle Progression by Antisense Hmg2 Rna. Biochem Biophys Res Commun 210: 1045-1051.
321. Li GH, Arora PD, Chen Y, McCulloch CA, Liu P (2012) Multifunctional roles of gelsolin in health and diseases. Medicinal Research Reviews 32: 999-1025.
322. Li GH, Shi Y, Chen Y, Sun M, Sader S, et al. (2009) Gelsolin Regulates Cardiac Remodeling After Myocardial Infarction Through DNase I-Mediated Apoptosis. Circulation Research 104: 896-U131.
323. Joo JI, Oh TS, Kim DH, Choi DK, Wang X, et al. (2011) Differential expression of adipose tissue proteins between obesity-susceptible and -resistant rats fed a high-fat diet. Proteomics 11: 1429-1448.
324. Mukherjee R, Yun JW (2012) Long chain acyl CoA synthetase 1 and gelsolin are oppositely regulated in adipogenesis and lipogenesis. Biochem Biophys Res Commun 420: 588-593.
325. Jeppesen J, Hein HO, Suadicani P, Gyntelberg F (1998) Triglyceride concentration and ischemic heart disease: an eight-year follow-up in the Copenhagen Male Study. Circulation 97: 1029-1036.

326. Beaulieu V, Da Silva N, Pastor-Soler N, Brown CR, Smith PJS, et al. (2005) Modulation of the actin cytoskeleton via gelsolin regulates vacuolar H+-ATPase recycling. Journal of Biological Chemistry 280: 8452-8463.
327. Daugaard M, Rohde M, Jaattela M (2007) The heat shock protein 70 family: Highly homologous proteins with overlapping and distinct functions. Febs Letters 581: 3702-3710.
328. Luo SZ, Mao CH, Lee B, Lee AS (2006) GRP78/BiP is required for cell proliferation and protecting the inner cell mass from apoptosis during early mouse embryonic development. Molecular and Cellular Biology 26: 5688-5697.
329. Amson R, Pece S, Lespagnol A, Vyas R, Mazzarol G, et al. (2012) Reciprocal repression between P53 and TCTP. Nature Medicine 18: 91-99.
330. Chen SH, Wu PS, Chou CH, Yan YT, Liu H, et al. (2007) A knockout mouse approach reveals that TCTP functions as an essential factor for cell proliferation and survival in a tissue- or cell type-specific manner. Molecular Biology of the Cell 18: 2525-2532.
331. Hsu YC, Chern JJ, Cai Y, Liu MY, Choi KW (2007) Drosophila TCTP is essential for growth and proliferation through regulation of dRheb GTPase. Nature 445: 785-788.
332. Laplante M, Sabatini DM (2012) mTOR signaling in growth control and disease. Cell 149: 274-293.
333. Guillaume E, Pineau C, Evrard B, Dupaix A, Moertz E, et al. (2001) Cellular distribution of translationally controlled tumor protein in rat and human testes. Proteomics 1: 880-889.
334. Duan CM, Xu QJ (2005) Roles of insulin-like growth factor (IGF) binding proteins in regulating IGF actions. General and Comparative Endocrinology 142: 44-52.
335. Rajwani A, Ezzat V, Smith J, Yuldasheva NY, Duncan ER, et al. (2012) Increasing Circulating IGFBP1 Levels Improves Insulin Sensitivity, Promotes Nitric Oxide Production, Lowers Blood Pressure, and Protects Against Atherosclerosis. Diabetes 61: 915-924.
336. Lewitt MS, Hilding A, Ostenson CG, Efendic S, Brismar K, et al. (2008) Insulin-like growth factor-binding protein-1 in the prediction and development of type 2 diabetes in middle-aged Swedish men. Diabetologia 51: 1135-1145.
337. Sandhu MS, Heald AH, Gibson JM, Cruickshank JK, Dunger DB, et al. (2002) Circulating concentrations of insulin-like growth factor-I and development of glucose intolerance: a prospective observational study. Lancet 359: 1740-1745.
338. Heald AH, Cruickshank JK, Riste LK, Cade JE, Anderson S, et al. (2001) Close relation of fasting insulin-like growth factor binding protein-1 (IGFBP-1) with glucose tolerance and cardiovascular risk in two populations. Diabetologia 44: 333-339.
339. Tisi DK, Liu XJ, Wykes LJ, Skinner CD, Koski KG (2005) Insulin-like growth factor II and binding proteins 1 and 3 from second trimester human amniotic fluid are associated with infant birth weight. Journal of Nutrition 135: 1667-1672.

340. Okamoto A, Endo H, Kalionis B, Shinya M, Saito M, et al. (2006) IGFBP1 and Follistatin-like 3 genes are significantly up-regulated in expression profiles of the IUGR placenta. Placenta 27: 317-321.
341. Holz MK, Ballif BA, Gygi SP, Blenis J (2005) mTOR and S6K1 mediate assembly of the translation preinitiation complex through dynamic protein interchange and ordered phosphorylation events. Cell 123: 569-580.
342. Ohanna M, Sobering AK, Lapointe T, Lorenzo L, Praud C, et al. (2005) Atrophy of S6K1(-/-) skeletal muscle cells reveals distinct mTOR effectors for cell cycle and size control. Nature Cell Biology 7: 286-294.
343. Tremblay F, Brule S, Um SH, Li Y, Masuda K, et al. (2007) Identification of IRS-1 Ser-1101 as a target of S6K1 in nutrient- and obesity-induced insulin resistance. Proceedings of the National Academy of Sciences of the United States of America 104: 14056-14061.
344. Selman C, Tullet JMA, Wieser D, Irvine E, Lingard SJ, et al. (2009) Ribosomal Protein S6 Kinase 1 Signaling Regulates Mammalian Life Span. Science 326: 140-144.
345. Um SH, Frigerio F, Watanabe M, Picard F, Joaquin M, et al. (2004) Absence of S6K1 protects against age- and diet-induced obesity while enhancing insulin sensitivity. Nature 431: 200-205.
346. Younis HS, Hirakawa B, Scott W, Tran P, Bhat G, et al. (2011) Antisense Inhibition of S6 Kinase 1 Produces Improved Glucose Tolerance and Is Well Tolerated for 4 Weeks of Treatment in Rats. Pharmacology 87: 11-23.
347. Pende M, Um SH, Mieulet V, Sticker M, Goss VL, et al. (2004) S6K1(-/-)/S6K2(-/-) mice exhibit perinatal lethality and rapamycin-sensitive 5'-terminal oligopyrimidine mRNA translation and reveal a mitogen-activated protein kinase-dependent S6 kinase pathway. Mol Cell Biol 24: 3112-3124.
348. Araki E, Lipes MA, Patti ME, Bruning JC, Haag B, 3rd, et al. (1994) Alternative pathway of insulin signalling in mice with targeted disruption of the IRS-1 gene. Nature 372: 186-190.
349. Schiaffino S, Mammucari C (2011) Regulation of skeletal muscle growth by the IGF1-Akt/PKB pathway: insights from genetic models. Skelet Muscle 1: 1-14.
350. Burdge GC, Slater-Jefferies J, Torrens C, Phillips ES, Hanson MA, et al. (2007) Dietary protein restriction of pregnant rats in the F0 generation induces altered methylation of hepatic gene promoters in the adult male offspring in the F1 and F2 generations. Br J Nutr 97: 435-439.
351. Lillycrop KA, Slater-Jefferies JL, Hanson MA, Godfrey KM, Jackson AA, et al. (2007) Induction of altered epigenetic regulation of the hepatic glucocorticoid receptor in the offspring of rats fed a protein-restricted diet during pregnancy suggests that reduced DNA methyltransferase-1 expression is involved in impaired DNA methylation and changes in histone modifications. British Journal of Nutrition 97: 1064-1073.
352. Reddington JP, Pennings S, Meehan RR (2013) Non-canonical functions of the DNA methylome in gene regulation. Biochem J 451: 13-23.
353. Meng HX, Hackett JA, Nestor C, Dunican DS, Madej M, et al. (2011) Apoptosis and DNA methylation. Cancers (Basel) 3: 1798-1820.
354. Cleasby ME, Livingstone DEW, Nyirenda MJ, Seckl JR, Walker BR (2003) Is programming of glucocorticoid receptor expression by prenatal

dexamethasone in the rat secondary to metabolic derangement in adulthood? European Journal of Endocrinology 148: 129-138.
355. Vestergaard H, Bratholm P, Christensen NJ (2001) Increments in insulin sensitivity during intensive treatment are closely correlated with decrements in glucocorticoid receptor mRNA in skeletal muscle from patients with Type II diabetes. Clinical Science 101: 533-540.
356. Carter RN, Paterson JM, Tworowska U, Stenvers DJ, Mullins JJ, et al. (2009) Hypothalamic-Pituitary-Adrenal Axis Abnormalities in Response to Deletion of 11 beta-HSD1 is Strain-Dependent. Journal of Neuroendocrinology 21: 879-887.
357. Berteaux N, Aptel N, Cathala G, Genton C, Coll J, et al. (2008) A novel H19 antisense RNA overexpressed in breast cancer contributes to paternal IGF2 expression. Mol Cell Biol 28: 6731-6745.
358. Lalau JD, Aubert ML, Carmignac DF, Gregoire I, Dupouy JP (1990) Reduction in Testicular Function in Rats .2. Reduction by Dexamethasone in Fetal and Neonatal Rats. Neuroendocrinology 51: 289-293.
359. Molotkov A, Deltour L, Foglio MH, Cuenca AE, Duester G (2002) Distinct retinoid metabolic functions for alcohol dehydrogenase genes Adh1 and Adh4 in protection against vitamin A toxicity or deficiency revealed in double null mutant mice. Journal of Biological Chemistry 277: 13804-13811.
360. Livera G, Rouiller-Fabre V, Pairault C, Levacher C, Habert R (2002) Regulation and perturbation of testicular functions by vitamin A. Reproduction 124: 173-180.
361. Cupp AS, Dufour JM, Kim G, Skinner MK, Kim KH (1999) Action of retinoids on embryonic and early postnatal testis development. Endocrinology 140: 2343-2352.
362. Marinos E, Kulukussa M, Zotos A, Kittas C (1995) Retinoic Acid Affects Basement-Membrane Formation of the Seminiferous Cords in 14-Day Male-Rat Gonads in-Vitro. Differentiation 59: 87-94.
363. Livera G, Rouiller-Fabre V, Durand P, Habert R (2000) Multiple effects of retinoids on the development of Sertoli, germ, and Leydig cells of fetal and neonatal rat testis in culture. Biology of Reproduction 62: 1303-1314.
364. Abu-Farha M, Lambert JP, Al-Madhoun AS, Elisma F, Skerjanc IS, et al. (2008) The tale of two domains - Proteomics and genomics analysis of SMYD2, a new histone methyltransferase. Molecular & Cellular Proteomics 7: 560-572.
365. Diehl F, Brown MA, van Amerongen MJ, Novoyatleva T, Wietelmann A, et al. (2010) Cardiac Deletion of Smyd2 Is Dispensable for Mouse Heart Development. PLoS One 5: e9748.
366. Huang J, Perez-Burgos L, Placek BJ, Sengupta R, Richter M, et al. (2006) Repression of p53 activity by Smyd2-mediated methylation. Nature 444: 629-632.
367. Wang L, Li L, Zhang H, Luo X, Dai J, et al. (2011) Structure of human SMYD2 protein reveals the basis of p53 tumor suppressor methylation. J Biol Chem 286: 38725-38737.
368. Saddic LA, West LE, Aslanian A, Yates JR, 3rd, Rubin SM, et al. (2010) Methylation of the retinoblastoma tumor suppressor by SMYD2. J Biol Chem 285: 37733-37740.

369. Sese B, Barrero MJ, Fabregat MC, Sander V, Belmonte JCI (2013) SMYD2 is induced during cell differentiation and participates in early development. International Journal of Developmental Biology 57: 357-364.
370. Matviw H, Yu G, Young D (1992) Identification of a Human Cdna-Encoding a Protein That Is Structurally and Functionally Related to the Yeast Adenylyl Cyclase-Associated Cap Proteins. Molecular and Cellular Biology 12: 5033-5040.
371. Moriyama K, Yahara I (2002) Human CAP1 is a key factor in the recycling of cofilin and actin for rapid actin turnover. Journal of Cell Science 115: 1591-1601.
372. Ban HJ, Heo JY, Oh KS, Park KJ (2010) Identification of Type 2 Diabetes-associated combination of SNPs using Support Vector Machine. Bmc Genetics 11: 1-11.
373. Yurchenko V, Zybarth G, O'Connor M, Dai WW, Franchin G, et al. (2002) Active site residues of cyclophilin A are crucial for its signaling activity via CD147. J Biol Chem 277: 22959-22965.
374. Igakura T, Kadomatsu K, Kaname T, Muramatsu H, Fan QW, et al. (1998) A null mutation in basigin, an immunoglobulin superfamily member, indicates its important roles in peri-implantation development and spermatogenesis. Developmental Biology 194: 152-165.
375. Bi JJ, Li YF, Sun FY, Saalbach A, Klein C, et al. (2013) Basigin null mutant male mice are sterile and exhibit impaired interactions between germ cells and Sertoli cells. Developmental Biology 380: 145-156.
376. Wang HQ, Tuominen LK, Tsai CJ (2011) SLIM: a sliding linear model for estimating the proportion of true null hypotheses in datasets with dependence structures. Bioinformatics 27: 225-231.
377. Laird A, Thomson JP, Harrison DJ, Meehan RR (2013) 5-hydroxymethylcytosine profiling as an indicator of cellular state. Epigenomics 5: 655-669.
378. Thomson JP, Lempiainen H, Hackett JA, Nestor CE, Muller A, et al. (2012) Non-genotoxic carcinogen exposure induces defined changes in the 5-hydroxymethylome. Genome Biol 13: R93.
379. Thomson JP, Hunter JM, Lempiainen H, Muller A, Terranova R, et al. (2013) Dynamic changes in 5-hydroxymethylation signatures underpin early and late events in drug exposed liver. Nucleic Acids Res 41: 5639-5654.
380. Luo SH, Zhang XM, Yu M, Yan H, Liu H, et al. (2013) Folic Acid Acts Through DNA Methyltransferases to Induce the Differentiation of Neural Stem Cells into Neurons. Cell Biochemistry and Biophysics 66: 559-566.
381. Di Ruscio A, Ebralidze AK, Benoukraf T, Amabile G, Goff LA, et al. (2013) DNMT1-interacting RNAs block gene-specific DNA methylation. Nature 503: 371-376.

Appendix

An enlarged version of two figures is provided, to make the localisation of immunofluorescence more visible. Images originally displayed in Figure 3.3, presenting the localisation of 5mC and 5hmC in the fetal testis during mid gestation, are given in Figures A1 (e14.5-e15.5) and A2 (e16.5-e17.5). An enlarged version of Figure 5.6, comparing 5mC localisation in GCS-EGFP Sprague Dawley and wild-type Wistar rat testis at e20.5, is presented in Figure A3.

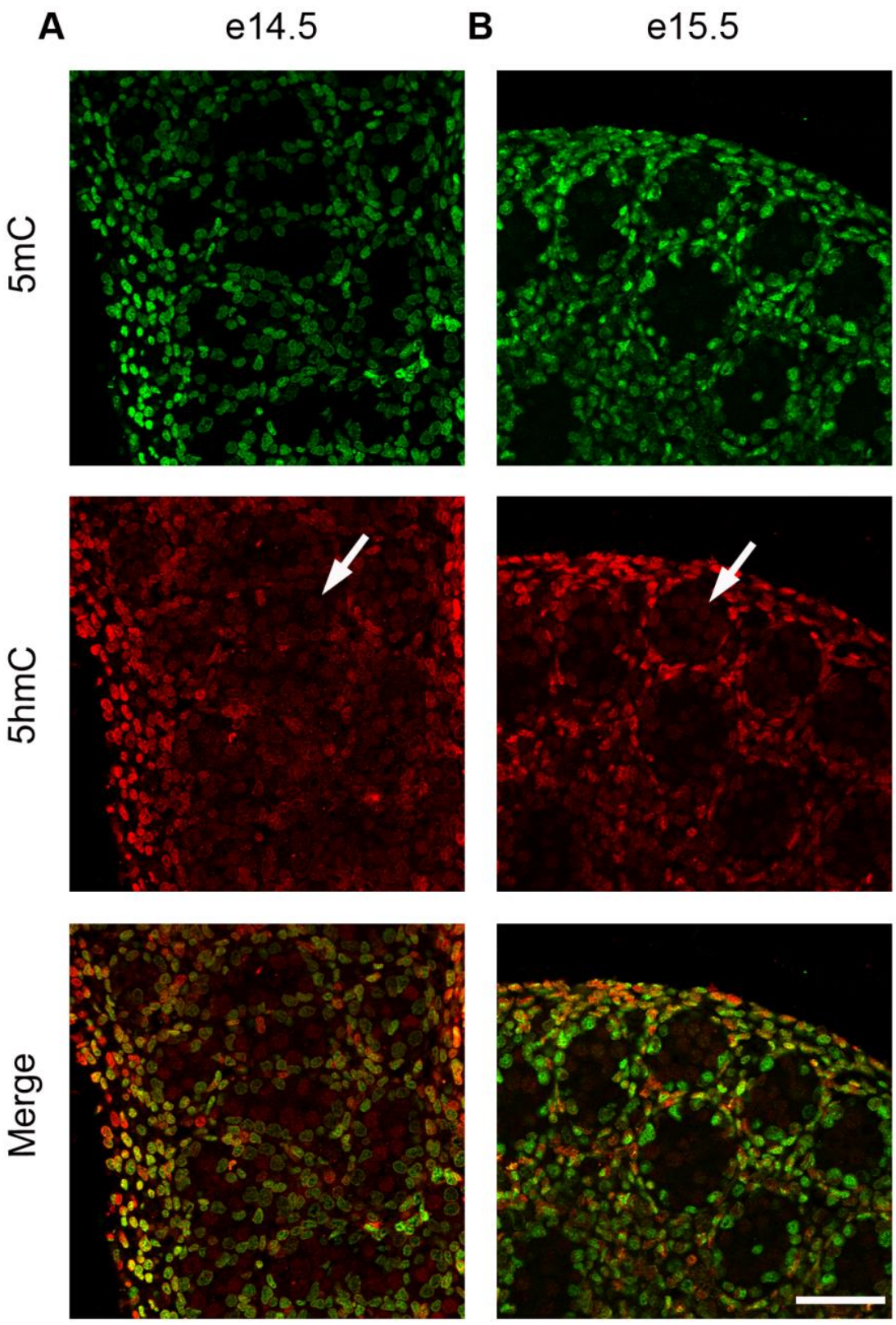

Figure A1 – Enlargement of Figure 3.3 Part 1 - Localisation of 5mC and 5hmC during mid gestation. Images of immunostained testis show 5hmC localisation in germ cells between e14.5-e15.5 (A-B) (red, arrows). Some 5mC is also weakly detectable. Both 5mC and 5hmC are detectable in somatic cells throughout the time course. Bar = 50µm.

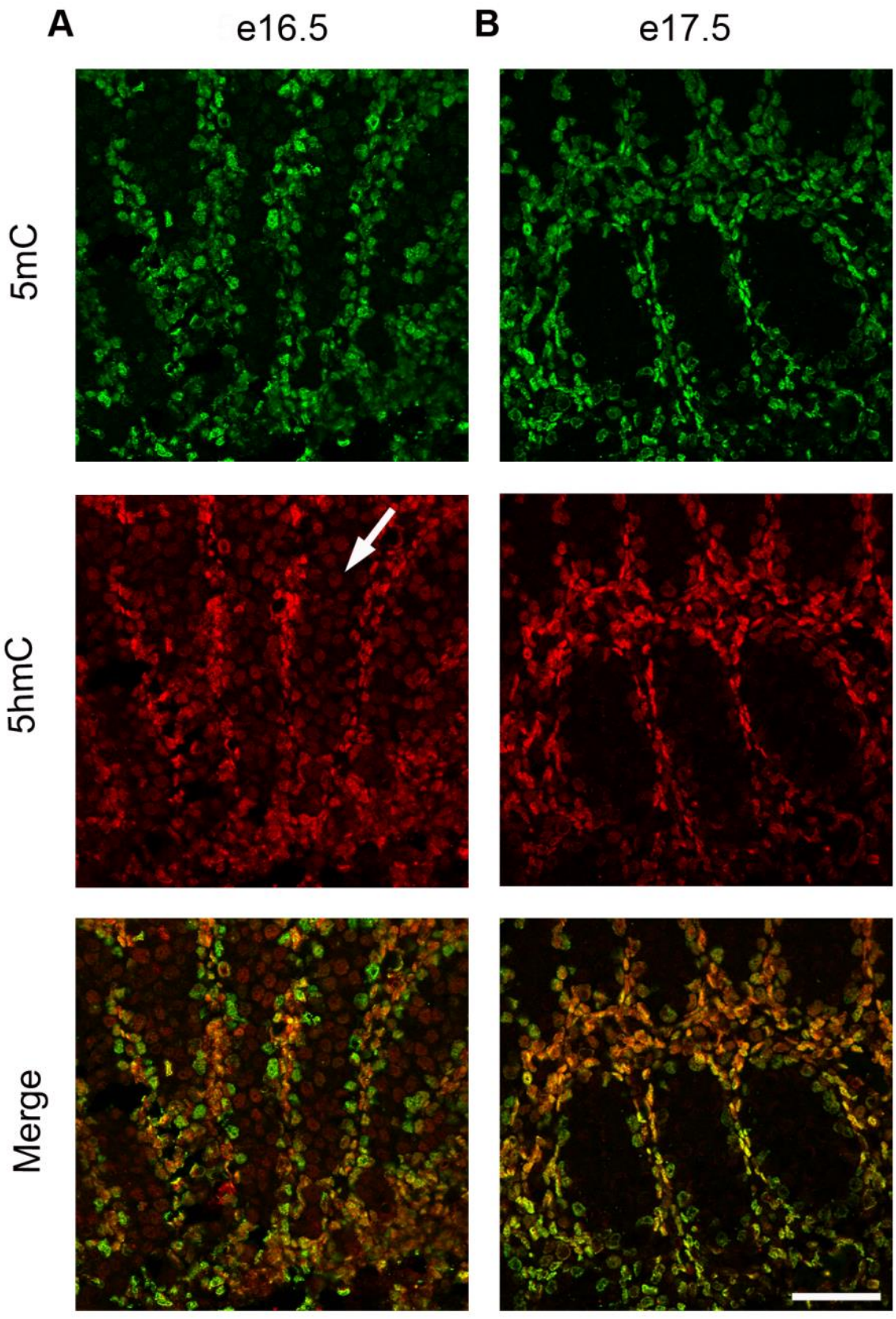

Figure A2 – Enlargement of Figure 3.3 Part 2 - Localisation of 5mC and 5hmC during mid gestation. Images of immunostained testis show 5hmC localisation in germ cells at e16.5 (A) (red, arrows). Some 5mC is also weakly detectable. Neither forms of methylation are detectable in germ cells at e17.5 (B). Both 5mC and 5hmC are detectable in somatic cells throughout the time course. Bar = 50μm.

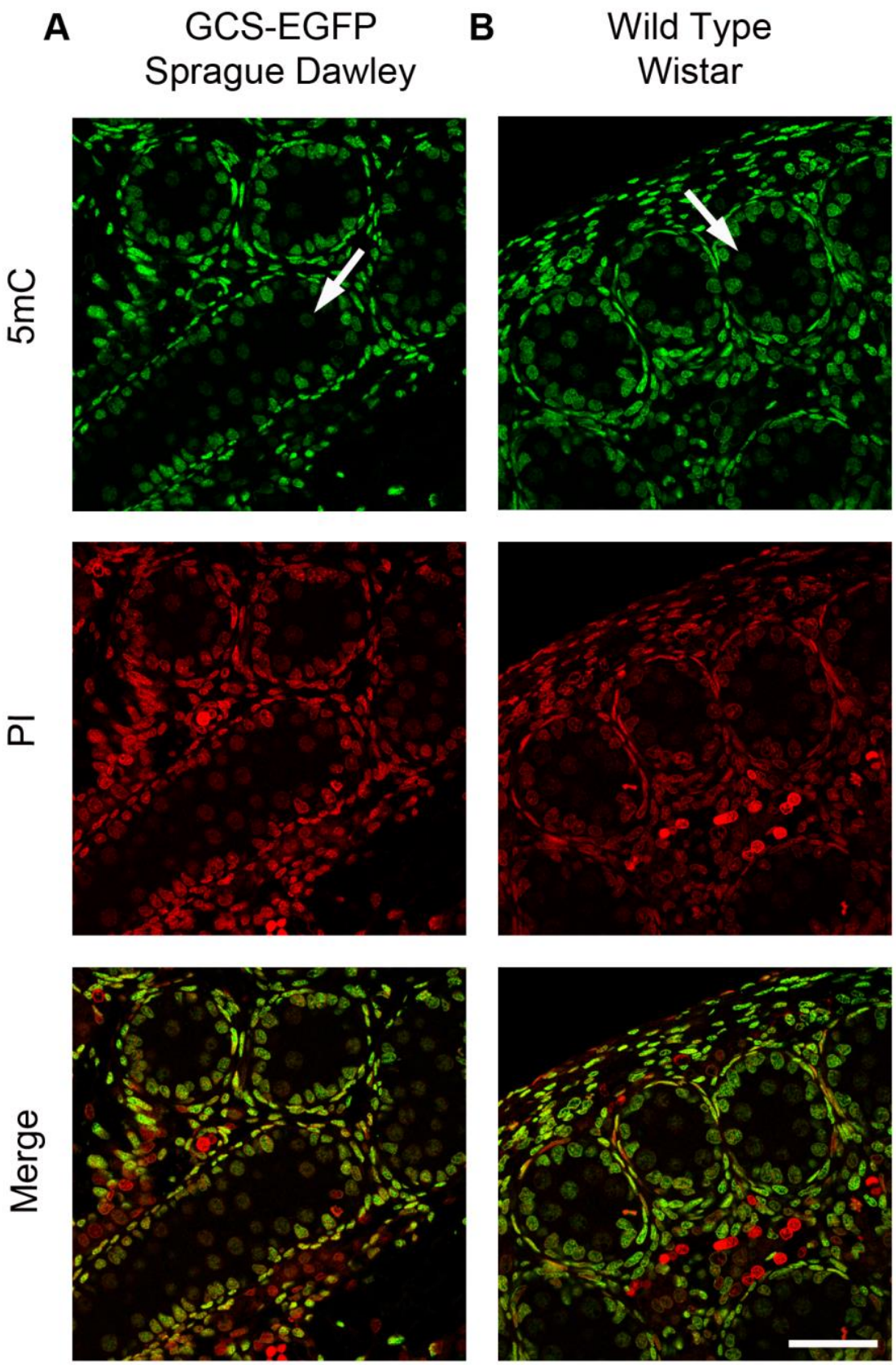

Figure A3 – Enlargement of Figure 5.6 - Comparing 5mC localisation in GCS-EGFP Sprague Dawley and wild-type Wistar rat testis at e20.5. 5mC (green, arrows) was identified in the somatic cells of both strains, and the germ cells of both GCS-EGFP (A) and Wistar (B) rats at e20.5. Propidium Iodide (PI) acts as a nuclear counterstain. Bar = 50µm.